

Optimized Green Walls

Study of Vertical Green Systems' Performance in an Urban Setting

Francisco Guzmán

Optimized Green Walls

Study of Vertical Green Systems' Performance in an Urban Setting

by

Francisco Guzmán Sáenz

In partial fulfilment of the requirements for the degree of

Master of Science in Civil Engineering

Track: Building Engineering

Specialization: Building Physics and Technology

At Delft University of Technology,

to be defended publicly on Thursday July 25th, 2019 at 14:30.

Student number: 4710487
Project duration: December, 2018 – July, 2019
Thesis committee: Prof. ir. P. Luscuere, Committee Chairman
Dr. ir. M. Ottelé, Supervisor
Dr. ir. M. Turrin, Supervisor
Dr. ir. R. Schipper, Graduation Coordinator

An electronic version of this thesis is available at <http://repository.tudelft.nl/>

Cover image: Treehouse, ADDP Architects LLP



Abstract

The construction, operation and maintenance of buildings consume more than 40% of primary energy in most countries. Out of this 40%, a large portion is related to the operational phase involving heat losses through a buildings envelope. To reduce this loss, several materials have been developed to reduce the thermal transmittance through a façade, even though they carry a heavy environmental burden. Furthermore, the unregulated and rapid expansion of urban environments led to a considerable amount of problems. Among them, the urban heat island effect demands special attention as it has been responsible for an increase of the energy consumption to higher mortality rates. In part, the use of materials with high thermal admittance is responsible for these effects. Vertical green systems have shown to be a potential solution to improve, among others, the thermal demands of buildings and to mitigate the urban heat island effect. However, due to the uncertainty associated with their design process and operation, the implementation of vegetation as a construction material in an urban setting is often overlooked. Therefore, an in-depth study of their performance under different configurations and climate conditions is needed.

The optimization study was based on the parametrization of a green façade and a living wall system which aimed to identify their response under variable initial conditions. A analysis of the essential parameters in the vegetation model was performed. Consequently, the leaf area index showed the highest effect, followed by the substrate thickness, leaf angle distribution, leaf surface albedo and finally by the moisture content of the substrate layer. Furthermore, a state-of-the-art computational work flow was developed through the integration of ENVI_met, Rhino/Grasshopper and modeFRONTIER, in combination with Python 3 scripting, to evaluate the performance of vertical greenery systems. The evaluation focused on the heat transmission through the façade of a single building, in comparison to a reference model. The work flow allowed the study of the impact of each parameter in the behavior of the system and led to the development of several design guidelines. The optimized result was tested in an urban setting to evaluate its potential as a mitigation strategy for the urban heat island effect.

The largest reduction in thermal transmission took place in equatorial, fully humid climate due to the low vapor pressure deficit; while the lowest in a temperate climate during winter conditions, suggesting the lower efficiency of the systems under cold weather. Furthermore, living wall systems have a significantly higher performance in comparison to green façades. On the other hand, the latent heat release associated with the evapotranspiration process has a strong correlation with the leaf area index, given the simultaneous action of the aerodynamic and bulk surface resistance. The optimized configuration of the vegetation was then derived based partly on this correlation. Moreover, the leaf angle distribution displayed a high correlation with the solar zenith angle and the leaf surface albedo with the intensity of the solar radiation and the ambient temperature. Additionally, among the substrate properties, the substrate thickness indicated a large potential in reducing heat transmission.

The effects of vertical green systems in an urban setting suggested an improvement of the environmental conditions. While the leaf area index is directly related to the decrease of wind speed and evaporative cooling, the leaf surface albedo influenced the amount of reflected shortwave radiation in a façade. Furthermore, the highest cooling potential was observed in desert climates as a result of the high vapor pressure deficit with temperature drops of up to 0.25 °C.

The outcome of this research indicates that an optimized vertical greenery system is a suitable replacement for artificial insulating materials as a passive alternative to reduce energy demands in buildings. Indicating a decrease in heat transmission from 8% to 50% of the original heat flux. Furthermore, the findings of the urban study suggests that a decrease in the ambient temperature and an overall reduction of the negative impacts related to the urban heat island effect is possible.

Acknowledgements

I would like to express my gratitude to my entire thesis committee: Peter Luscuere, Marc Ottel , Michela Turrin and Roel Schipper, whose supervision, insight and expertise led me to successfully complete this project under the highest standards.

Additionally, I like to thank Eva Stache, Marjolein Pijpers-van Esch, Daniela Maiullari and Tatiana Armijos for sharing their support and time during the conception of the computational models.

Furthermore, I would like to express my profound gratitude to my grandparents, who have provided me with much more than they can imagine. To my parents, Francisco and Esther for their unfailing support, encouragement and love throughout my entire life.

Finally, special thanks goes to Melanie, whose patience, advice and guidance pushed me to become better each day. This accomplishment would not have been possible without you.

*Francisco Guzm n S enz
Delft, July 2019*

Contents

List of Figures	xi
List of Tables	xv
Acronyms	xvii
1 Introduction	1
2 Problem Context	3
2.1 Climate change	3
2.2 Urbanization	3
2.2.1 Urban heat island effect	4
2.2.2 Air pollution	5
2.2.3 Noise pollution	5
2.2.4 Biodiversity	6
2.3 Energy demands	6
2.3.1 Bio-climatic Design	7
2.4 Summary	8
3 Research Definition	9
3.1 Problem statement	9
3.2 Aims and focus of this research	9
3.3 Research questions	10
3.4 Methodology and chapter scheme.	10
4 Greenery Systems in the Built Environment	13
4.1 General introduction	13
4.1.1 Historical overview	14
4.1.2 Greenery system typologies	15
4.2 Vertical green	19
4.2.1 Effects of vertical green	19
4.2.2 Risks of vertical green	22
4.2.3 Implementation and feasibility	23
4.3 Summary	23
5 Physical and Thermal Aspects of Vertical Greenery Systems	25
5.1 Analysis cases	26
5.2 Vertical green energy balance	28
5.2.1 Parameter overview	28
5.2.2 Shortwave radiation, E	28
5.2.3 Long wave radiation, R.	31
5.2.4 Convective heat transfer, C_v	31
5.2.5 Evapotranspiration	32
5.3 Substrate thermal and physical properties	33
5.3.1 Moisture related properties.	33
5.3.2 Influence of density and moisture content on soil thermal properties	33
5.3.3 Thermal mass	33
5.4 Summary	34

6	Computational Workflow and Model Definition	37
6.1	Parametric modelling	37
6.2	Computational workflow	38
6.2.1	Software packages	38
6.2.2	Integration	38
6.3	Model definition	40
6.3.1	Urban street canyon	40
6.3.2	Additional modelling considerations	41
6.4	Climate conditions	42
6.4.1	Climate zones	43
6.4.2	Weather data selection	44
6.5	Summary	46
7	Impact of Vertical Greenery Systems on Heat Transmission	47
7.1	Introduction	47
7.2	Parameter variability on thermal demands	47
7.3	Living wall system	48
7.3.1	Leaf area index	48
7.3.2	Leaf angle distribution	51
7.3.3	Leaf surface albedo	53
7.3.4	Substrate properties	54
7.4	Green façade	55
7.4.1	Leaf area index	55
7.4.2	Leaf angle distribution	57
7.4.3	Albedo	58
7.5	Optimal vertical green system configuration	58
7.5.1	Economic feasibility of vertical green systems	59
7.5.2	Plant layer parametrization	60
7.6	Summary	61
8	Impact of Vertical Green Systems on an Urban Setting	63
8.1	Introduction	63
8.2	Wind speed	63
8.3	Ambient temperature	66
8.3.1	Living wall systems	66
8.3.2	Green façades	68
8.3.3	Observations regarding the ambient temperature	70
8.4	Reflected short wave and emitted long wave radiation	70
8.4.1	Living wall systems	71
8.4.2	Green façades	72
8.5	Mitigation of the urban heat island effect	73
8.6	Summary	74
9	Conclusion	75
9.1	Conclusions	75
9.2	Limitations	78
9.3	Recommendations & Future work	78
	Bibliography	81
A	Grid Size Study	87
B	Computational Optimization Process	91
B.1	Optimization algorithms	91
B.1.1	Direct search	91
B.1.2	Metaheuristics	91
B.1.3	Model-based methods	92
B.2	Tools	92

C Optimization and Urban Study Results	93
C.1 Reference grey model	93
C.1.1 Group A: Singapore	93
C.1.2 Group B: Phoenix.	95
C.1.3 Group C: Amsterdam.	96
C.2 Optimization results living wall system	98
C.2.1 Group A: Singapore	98
C.2.2 Group B: Phoenix.	100
C.2.3 Group C: Amsterdam.	102
C.3 Optimization results green façade	104
C.3.1 Group A: Singapore	104
C.3.2 Group B: Phoenix.	106
C.3.3 Group C: Amsterdam.	108
C.4 Optimized single green building model	110
C.4.1 Singapore	110
C.4.2 Group B: Phoenix.	112
C.4.3 Group C: Amsterdam.	113
C.5 Optimized full green building model	115
C.5.1 Singapore	115
C.5.2 Group B: Phoenix.	116
C.5.3 Group C: Amsterdam.	118
D Grasshopper Component Scripts	121
D.1 Adding input to ENVI_met database.	121
D.2 Checking model completion for data processing	123
D.3 ENVI_met data processing.	126

List of Figures

2.1	Causes of urban heat island effect	4
2.2	Noise levels	6
2.3	Bio-climatic design approach	7
3.1	Overview of research outline	11
4.1	M&S Greenery shopping store in Newcastle, UK	14
4.2	Bosco Verticale, residential building in Milan, Italy	14
4.3	Types of building integrated vegetation	15
4.4	Green wall classification according to their construction characteristics	17
4.5	Classification of vertical greenery systems: (a) Direct green façade (b) Indirect green façade (c) Continuous Living wall system (d) Modular Living wall system (e) Linear Living wall system	17
4.6	Typical configuration of living wall system	18
4.7	Factors involved in the generation of the urban heat island effect	21
4.8	Temperature and wind speed profiles for a living wall system	22
5.1	Givoni diagram. Bio-climatic interpretation of a psychometric chart for thermal comfort	26
5.2	Schematic representation of the model for the analysis of a green façade	27
5.3	Schematic representation of the model for the analysis of a living wall system	27
5.4	Transmissivity coefficient as a function of LAI and κ	29
5.5	Varying levels of leaf area index in a vegetation layer	30
5.6	Solar zenith angle (θ_z), the altitude angle (α) and the azimuth angle (A_z) of the sun when viewed from point P	30
5.7	Thermal conductivity as a function of soil density and moisture content for sandy loam soil type	34
5.8	Temperature increase as a function of soil density and moisture content during 60 minutes	35
6.1	Definition of the ENVI_met model in Grasshopper in combination with Python	39
6.2	Overview of the integrated work-flow for the optimization of the greenery system	39
6.3	Schematic representation of an urban street canyon	40
6.4	3D view of the urban street canyon	40
6.5	modeFRONTIER simulations work-flow for LWS	43
6.6	Temperature and relative humidity during 01/04/1989 in Singapore, Singapore	44
6.7	Temperature and relative humidity during 01/08/1988 in Phoenix, AZ, USA	45
6.8	Temperature and relative humidity during 06/01/1995 (winter conditions) in Amsterdam, NL	45
6.9	Sun path diagrams for (a) Singapore, (b) Phoenix and (c) Amsterdam	45
7.1	Effects of relative humidity (a) and stomatal resistance (b) on latent heat release	49
7.2	Heating and cooling demands as a function of LAI for (a) Singapore $\overline{RH} = 87.9\%$, (b) Phoenix $\overline{RH} = 18.3\%$, (c) Amsterdam $\overline{RH} = 94.2\%$ in a LWS	50
7.3	Leaf area index and leaf angle distribution effects on heating and cooling demands for (a) Singapore, (b) Phoenix, (c) Amsterdam in a LWS	52
7.4	Transmissivity of a vegetation later as a function of solar zenith angle θ_z	53
7.5	Varying albedo effects on normalized heating and cooling demands for a LWS	53

7.6	Substrate thickness effect on heating and cooling demands on (a) Singapore, (b) Phoenix, (c) Amsterdam	54
7.7	Water coefficient of substrate for plant effect on heating and cooling demands on (a) Singapore, (b) Phoenix, (c) Amsterdam for a LWS	55
7.8	Heating and cooling effects as a function of LAI for (a) Singapore $\overline{RH} = 87.9\%$, (b) Phoenix $\overline{RH} = 18.3\%$, (c) Amsterdam $\overline{RH} = 94.2\%$ in a GF	56
7.9	Leaf area index and leaf angle distribution effects on heating and cooling demands for (a) Singapore, (b) Phoenix, (c) Amsterdam in a GF	57
7.10	Varying albedo effects on normalized heating and cooling demands for a GF	58
8.1	Wind speed as a function of LAI in each climate group and vector direction. (a) Living wall system south, (b) Living wall system west, (c) Green façade south, (d) Green façade west	64
8.2	Polynomial regression between initial wind speed and leaf area index for a VGS	65
8.3	Effects of LAI in wind speed and surface heat resistance in a VGS	65
8.4	Cases for evaluation of the ambient temperature in varying urban conditions	66
8.5	Effects of the implementation of a LWS on (a) single and (b) multiple buildings during an hour period in Singapore	67
8.6	Effects of the implementation of LWS on (a) single and (b) multiple buildings during an hour period in Phoenix, Az	67
8.7	Effects of the implementation of LWS on (a) single and (b) multiple buildings during an hour period in Amsterdam	68
8.8	Effects of the implementation of a GF on (a) single and (b) multiple buildings during an hour period in Singapore	69
8.9	Effects of the implementation of a GF on (a) single and (b) multiple buildings during an hour period in Phoenix, Az	69
8.10	Effects of the implementation of a GF on (a) single and (b) multiple buildings during an hour period in Amsterdam	69
8.11	(a) Reflected short wave radiation and (b) emitted long wave radiation for vertical wall systems during April 1 st 1989 for Singapore	72
8.12	(a) Reflected short wave radiation and (b) emitted long wave radiation for vertical wall systems during August 1 st 1988 for Phoenix	72
8.13	(a) Reflected short wave radiation and (b) emitted long wave radiation for vertical wall systems during January 6 th 1988 for Amsterdam	73
A.1	Computational time trend	88
A.2	Geometrical configuration of the base model with different grid sizes. From Top left to bottom right: 2m, 3m, 5m, 6m, 7m, 10m	89
C.1	Air temperature at 14:00 on April 1 st 1989, for Singapore grey model	93
C.2	Wind speed at 14:00 on April 1 st 1989 for Singapore grey model	94
C.3	Wind orientation at 14:00 on April 1 st 1989 for Singapore grey model	94
C.4	Air temperature at 17:00 on August 1 st 1988, for Phoenix grey model	95
C.5	Wind speed at 17:00 on August 1 st 1988, for Phoenix grey model	95
C.6	Wind orientation at 17:00 on August 1 st 1988, for Phoenix grey model	96
C.7	Air temperature at 7:00 on January 6 th 1995, for Amsterdam grey model	96
C.8	Wind speed at 7:00 on January 6 th 1995, for Amsterdam grey model	97
C.9	Wind orientation at 7:00 on January 6 th 1995, for Amsterdam grey model	97
C.10	Correlation matrix for all parameters analyzed in the optimization for Group A: Singapore	98
C.11	Parallel coordinates from optimization study for Group A: Singapore	98
C.12	Bubble plot showing the relation between substrate thickness, water coefficient and cooling demands for Group A: Singapore	99
C.13	Bubble plot showing the relation between LAI, χ and wind speed in south and west directions in Singapore	99

C.14	Correlation matrix for all parameters analyzed in the optimization for Group B: Phoenix	100
C.15	Parallel coordinates from optimization study for Group B: Phoenix	100
C.16	Bubble plot showing the relation between substrate thickness, water coefficient and cooling demands for Group B: Phoenix	101
C.17	Bubble plot showing the relation between LAI, <i>chi</i> and wind speed in south and west directions in Phoenix, AZ	101
C.18	Correlation matrix for all parameters analyzed in the optimization for Group C: Amsterdam	102
C.19	Parallel coordinates from optimization study for Group C: Amsterdam	102
C.20	Bubble plot showing the relation between substrate thickness, water coefficient and cooling demands for Group C: Amsterdam	103
C.21	Bubble plot showing the relation between LAI, <i>chi</i> and wind speed in south and west directions in Amsterdam	103
C.22	Correlation matrix for all parameters analyzed in the optimization for Group A: Singapore	104
C.23	Parallel coordinates from optimization study for Group A: Singapore	104
C.24	Bubble plot showing the relation between LAI, cooling demands, <i>chi</i> and Albedo in Singapore	105
C.25	Bubble plot showing the relation between LAI, <i>chi</i> and wind speed in south and west directions in Singapore	105
C.26	Correlation matrix for all parameters analyzed in the optimization for Group B: Phoenix	106
C.27	Parallel coordinates from optimization study for Group B: Phoenix	106
C.28	Bubble plot showing the relation between LAI, cooling demands, <i>chi</i> and Albedo in Phoenix	107
C.29	Bubble plot showing the relation between LAI, <i>chi</i> and wind speed in south and west directions in Phoenix, AZ	107
C.30	Correlation matrix for all parameters analyzed in the optimization for Group C: Amsterdam	108
C.31	Parallel coordinates from optimization study for Group C: Amsterdam	108
C.32	Bubble plot showing the relation between LAI, cooling demands, <i>chi</i> and Albedo in Amsterdam	109
C.33	Bubble plot showing the relation between LAI, <i>chi</i> and wind speed in south and west directions in Amsterdam	109
C.34	Air temperature at 14:00 on April 1 st 1989, for Singapore single green building model	110
C.35	Wind speed at 14:00 on April 1 st 1989 for Singapore single green building model	110
C.36	Wind orientation at 14:00 on April 1 st 1989 for Singapore single green building model	111
C.37	Air temperature at 17:00 on August 1 st 1988, for Phoenix single green building model	112
C.38	Wind speed at 17:00 on August 1 st 1988, for Phoenix single green building model	112
C.39	Wind orientation at 17:00 on August 1 st 1988, for Phoenix single green building model	113
C.40	Air temperature at 7:00 on January 6 th 1995, for Amsterdam single green building model	113
C.41	Wind speed at 7:00 on January 6 th 1995, for Amsterdam single green building model	114
C.42	Wind orientation at 7:00 on January 6 th 1995, for Amsterdam single green building model	114
C.43	Air temperature at 14:00 on April 1 st 1989, for Singapore full green building model	115
C.44	Wind speed at 14:00 on April 1 st 1989 for Singapore full green building model	115
C.45	Wind orientation at 14:00 on April 1 st 1989 for Singapore full green building model	116

C.46	Air temperature at 17:00 on August 1 st 1988, for Phoenix full green building model	116
C.47	Wind speed at 17:00 on August 1 st 1988, for Phoenix full green building model	117
C.48	Wind orientation at 17:00 on August 1 st 1988, for Phoenix full green building model	117
C.49	Air temperature at 7:00 on January 6 th 1995, for Amsterdam full green building model	118
C.50	Wind speed at 7:00 on January 6 th 1995, for Amsterdam full green building model	118
C.51	Wind orientation at 7:00 on January 6 th 1995, for Amsterdam full green building model	119

List of Tables

5.1	Parameter table used for green wall energy balance	28
6.1	Variable values, boundaries and constraints used for simulations	41
6.2	Criteria used to categorize climate conditions based on temperature and precipitation amount	43
7.1	Correlation factors for thermal demands in green façades and living wall systems	48
7.2	Water coefficient of substrate for plant and its corresponding value of moisture content in the substrate layer.	55
7.3	Optimal parameter configuration for living wall systems for different climate conditions	59
7.4	Energy savings caused by the reduction in transmissive heat transfer and equivalent performance offered by a single Rockwool layer for an optimized vertical green system in each climate condition	59
8.1	Solar Zenith angles for Singapore, Phoenix and Amsterdam weather condition	71
8.2	Decrease of incoming short wave radiation due to shading effect caused by the vegetation layer	74
9.1	Design strategies for vertical green systems	75
9.2	Percentual reduction of heat transmission due to the leaf area index	77
9.3	Percentual reduction of heat transmission due to the thickness and moisture content of the substrate layer	77
A.1	Computational time required for grid size alternatives	87
A.2	Results for Air Temperature [°C] at SW corner of central building	88

Acronyms

CDC	Cooling dominated climates
FAO	Food and agricultural organization
GF	Grasshopper
GF	Green façade(s)
HDC	Heating dominated climates
LAD	Leaf angle distribution
LAI	Leaf area index
LCA	Life cycle analysis
LWS	Living wall system(s)
mF	modeFRONTIER
MC	Moisture content
NZEB	Near-zero energy building
PAR	Photosynthetically active radiation
UHI	Urban heat island
VGS	Vertical greenery system(s)
VPD	Vapor pressure deficit
WC	Water coefficient of substrate for plant

1

Introduction

In the last 40 years, the consumption of earth's natural resources has tripled. This increasing trend is seen worldwide without any restrictions regarding industrial sectors [45]. Nevertheless, the building sector is considered as one of the largest energy consumers as well as responsible for the release of considerable amounts of green house gases [22]. The increase in resource demand has many origins, among them a rising amount of people in urban areas. Population worldwide is moving towards cities drastically increasing the population density creating a highly complex system of resource supply and demand in a very limited space. In order to compensate for this increasing demand, many alternatives have been successfully used. However, at a great cost. Highly polluting industrial processes, environmentally unfriendly products and non-renewable energy sources, have been cities main sources of goods and services in the last decades. Thankfully, this trend is changing due to a more conscious environmental approach for both a city's management and an individual's personal lifestyle. The building sector is following the same trend, for both the design and construction process, which has to a much larger attention to the performance of buildings and the development of "green" or sustainable alternatives to meet all of the markets demands.

Innovative technologies and energy efficiency measures are known widely across the building sector. Photo-voltaic panels, wind turbines and highly efficient synthetic insulation materials have been developed as a response to current demands. However, under a life cycle assessment, they have a heavy environmental toll, e.g. photo-voltaic panels have a large carbon footprint due to their manufacturing procedure and raw materials. Even though they have a considerable impact during the operation phase, they take a prominent role in the overall environmental impact of a building. Additionally, most of these currently developed alternatives are limited, providing benefits only to an individual project or building. They are unable to deal with problems that come with the rapid expansion rate of cities such as air and noise pollution, industrial waste, urban heat island effect among others. Several options must be considered and implemented to tackle these effects while taking into account that a building has a clear influence on its environment as well. One of which, although quite popular, has often been overlooked in a buildings design process: greenery systems.

The use of greenery in buildings is not a new concept and its benefits have been documented for several decades now. The employment of greenery in buildings does not alter only the interior conditions of a building, but also has a contribution on psychological effects, such as stress reduction, increase in social behavior, productivity and stimulation of creativity [48]; as well as an improvement of unfavorable micro-climatic conditions in its immediate surroundings [38]. Green systems, including green façades, roofs and balconies, sky-gardens and living walls; could provide a solution to the problems created by the aggressive and sometimes unrestricted expansion of cities.

Besides all the proven benefits, greenery systems come with a downfall. The high dependency of the weather conditions on a buildings energy demand define the efficiency of the system. Therefore, there is not a single ideal system that can be applied to all conditions. The variability of local weather, as well as the diversity of plants available to a specific loca-

tion may cause a highly complex design problem. This complexity could not only reduce the performance of the systems, but negate their application completely due to an unfavorable economic result. Despite the large applicability of greenery systems throughout cities, further study is still required to identify the optimal configuration of the greenery system while considering the influence of different climate types [69].

It is the goal and purpose of this MSc. thesis to increase the knowledge regarding greenery systems as well as to push their implementation to create a more sustainable, healthy and comfortable living environment.

2

Problem Context

This chapter analyzes the major problems associated with this research project, including those related to climate change, large scale urbanization and energy demands for buildings.

2.1. Climate change

Due to anthropogenic causes, global temperatures are continuously rising. The impacts of man-made climate change are slowly becoming more present, manifesting themselves in extreme weather conditions. If left unchecked, global temperature rise can lead to dangerous conditions for people, economies and ecosystems. An increase in summer temperatures, precipitation seasonality, weather patterns and a rise of sea level are few of the possible implications that climate change can have on a worldwide scale. Therefore, mitigation or adaptation strategies must be taken into action in order to prevent irreversible damage to both human societies and environment. In particular when efforts must be double due to the recent reduction of global temperature rise from 2°C to 1.5°C as stated by the IPCC. Although difficult to achieve in such a limited time frame, climate change must be dealt with accordingly and will require a larger commitment from policymakers to meet environmental goals.

The building sector is responsible for a large amount of global energy consumption and resources. Considerable actions must be taken to reduce the overall impact of this sector in the emission of harmful gases. However, a reduction of the emission of green house gases will not prevent the effects of climate change. Due to their long shelf life, in particular carbon dioxide, the high concentration present in the atmosphere has already defined its composition for the next decades[28]. The effects that we will observe in the next decades have already been defined by the excessive release of green house gases in the last century.

In order to create a positive contribution, the building sector can adopt several strategies to reduce the high concentrations of CO₂ currently in the atmosphere. These strategies can range from the utilization of structural timber, to greenery systems to more advanced technological techniques to allow direct carbon sequestration. Applying them can cause a large influence in moderating the impacts of climate change in urban areas.

2.2. Urbanization

The population density in the world has been increasing through the last century. Currently, close to 50% of the world's population live in urban areas that occupy approximately 2.8% of the total land of the planet [80]. With more and more people migrating towards urban areas, an increasing amount of resources will be needed in order to maintain acceptable living conditions. The arrangement of space within a city greatly influences the way that a city is perceived and used by its inhabitants. An appropriate urban design can lead to better quality of life as well as keeping the delicate balance between our society and the environment.

The significant effects of these aspects will have an increasing role in shaping the design process of individual buildings. Urban areas can be seen as artificial environments with

complex interactions between all actors within it. Therefore, the choices made in the design stage for each of them can have deep implications on the behavior of the entire system. The complex nature of urban areas, coupled with an increase in the urbanization rate and industrialization has led to the rise of several problems that can affect the performance of cities as well as causing harmful conditions for its inhabitants.

Among these problems, several stand out. Urban heat island effect, air and noise pollution and a lack of biodiversity causes the complexity of the interactions between all actors to escalate. Due to the added difficulty of creating a balanced environment, satisfying the minimum requirements for long term health and comfort for human and wildlife alike will become a challenging task.

2.2.1. Urban heat island effect

One of the most critical and know problems in cities is the urban heat island (UHI) effect. This refers to the phenomenon that the urban air temperature rises to a point which exceeds its surrounding rural environment. The UHI has many causes in an urban environment [46], among them:

1. Absorption of short-wave radiation from the sun in low albedo materials
2. Air pollution in the atmosphere absorbs long-wave radiation
3. Obstruction of the sky by buildings traps long wave radiation by being reflected back to the urban environment
4. Storage of anthropogenic heat released by combustion processes
5. Increased heat storage by buildings with large thermal admittance
6. Larger energy input to sensible heat and less into latent heat.
7. The turbulent heat transport from within streets is decreased by a reduction of wind speed

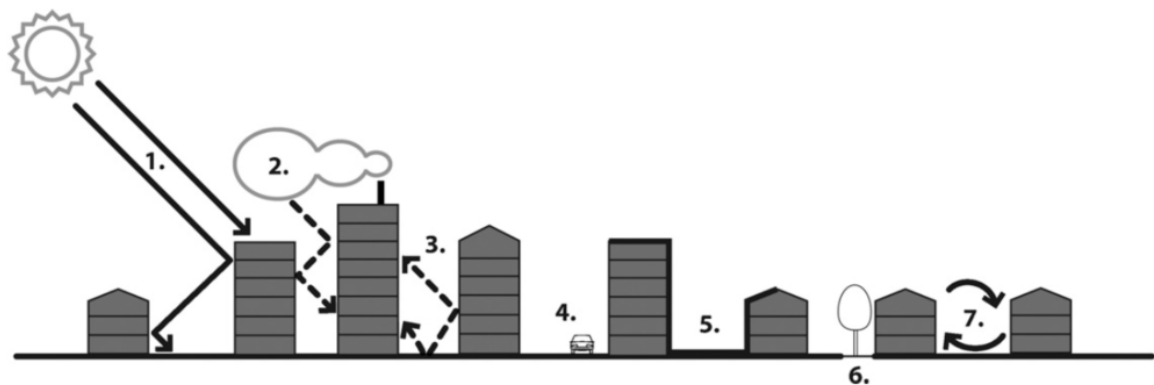


Figure 2.1: Causes of urban heat island effect [46]

Its effects can range from the deterioration of the living environment, an increase in energy consumption, elevation in ground-level ozone and larger mortality rates [72]. As seen in Figure 2.1, several parameters cannot be controlled, nevertheless, many of the causes can be associated with the configuration, materials and surface of the envelope of buildings. A proper design, considering not only the individual requirements of a project, can lead to a mitigation of the effects of UHI and an increase in the environmental and physical quality of an urban space.

The potential measures to reduce the impact of UHI can be categorized into a reduction of anthropogenic heat release, an efficient roof design and other factors such as the albedo,

humidification potential, etc. Applying greenery systems in buildings is a widely accepted mitigation strategy for UHI, since it, directly or indirectly, involves all described measures [72]. When comparing a green façade to a non-greened one, a green façade has a much lower heat absorption which ends up in a less heat irradiated back into the atmosphere during the evening and at night. This is one way greenery systems can contribute to the mitigation of the urban heat island effect [57]. Nevertheless, these systems have a seasonal behavior, i.e. lower biological activity during heating season [80]. The efficiency of vegetation layers in reducing ambient temperatures is higher during summer than in winter leading to a design problem which should aim to balance its effects to achieve the best overall behavior throughout the year.

2.2.2. Air pollution

A substantial amount of air pollution sources comes from man-made activities and derives from combustion of biomass or fossil fuel. Due to the magnitude of urban areas, these emissions greatly influence the air quality and climate change from local up to global scales. Their effects go over the health risks commonly associated with them, but can also lead to a decrease of economic output and a diversion of resources [43]. Nonetheless, air pollution is hardly an exclusive man-made problem. Natural events such as volcanic eruptions, forests fires, among others; have led to the release of many pollutants into the atmosphere like SO₂, H₂S and CO. However, health concerns due to air pollution has become a significant issue in the last century mostly due to human unrestrained industrial activity [7].

The rapid growth of cities has led to an intensive use of energy coming from non-renewable sources. Transportation, industrial processes and energy production take a prominent role in the emission of pollutants in the atmosphere, such as CO₂, CH₄, N₂O, halocarbons and particulate matter. Among them, fine particulate matter (PM_{2.5}) is mostly associated to health effects. However, air pollution as a whole can lead to visibility impairment, ecosystem degradation and health risks such as asthma, cardiovascular, respiratory diseases and even cancer [7, 43].

Many strategies can improve air quality and reduce pollution in urban areas. Policy measures promoting clean energy and replacements for combustible fuel sources can greatly reduce the concentration of pollutants continuously added to the atmosphere, reducing harmful emissions and guaranteeing minimum levels of air quality in cities [7]. Nevertheless, the amount of atmospheric pollution present in several mega-cities around the world require additional measures that go beyond just the reduction of emissions. Active measures must be taken to remove the concentration of pollutants in highly contaminated air. Vegetation, such as trees, can provide an effective solution for this problem. They can directly remove air pollutants and intercept particulate matters in the air. Indirectly, they are also capable of reducing the air temperature through shading and evapotranspiration, reducing the energy demands for cooling in summer and decreasing the amount of pollutants from energy production [93]. It should be noted however, that trees can also produce air pollutants, as is the case of pollen that can have serious health consequences on people allergic to them.

2.2.3. Noise pollution

Noise pollution is one of the four major pollution sources in the world, harming more than 80 million people only in the European Union [24]. Due to the high density of transportation services, industries and construction sites in urban environments, there is a significant contribution from noise pollution to an urban lifestyle. Depending on the magnitude of the noise level, a person might be subjected to different levels of risk as seen on Figure 2.2. Long exposure to these sound levels can have mild to severe effects on health from sleep disturbances to cardiovascular problems [25].

Besides the associated health risks, noise can create additional problems. Even if certain noise events do not cause permanent damage they can be responsible for substantial losses to the public. These losses can range from a simple disturbance in the neighborhood to a decrease in property values [40].

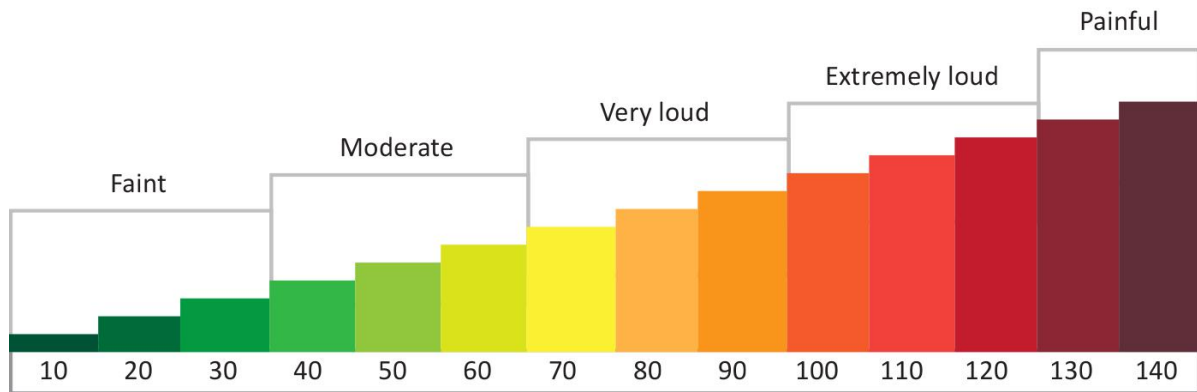


Figure 2.2: Noise levels adapted from [36]

2.2.4. Biodiversity

The conservation of biodiversity can be seen as both a global and local issue, since it plays a fundamental role in the protection of local species as well as governing human sustainability processes [37]. The aggressive expansion and use of artificial materials in cities during the last decades has led to a significant decrease in the amount of greenery within cities, replacing it by concrete or asphalt surfaces. This has been accompanied by a direct reduction in the amount of animal species present in the urban environment, forcing them to find alternative sources of shelter and food.

While it has been stated that biodiversity has a paramount role in the long-term functionality of ecosystems as well as providing shelter from the environment for endangered species, its importance in urban environments has been pushed into the background in the development of cities[4]; favoring economic growth over sustainable development. Greenery in buildings has the option to counter the increasing grey context of cities, providing diverse environments for both fauna and flora. Nevertheless, the use of vernacular plant life is highly recommended due to their intrinsic capacity to adjust to local climate conditions.

Even though the benefit of biodiversity focuses on the conservation of different species, its importance has a broader range, from the provision of ecosystem services to positive impacts on the quality of life and human health [31]. A greener urban environment will not only improve the quality of living conditions for its populace, but the increase of the amount of plant and animal species can provide a closer and more balanced relationship between nature and cities.

2.3. Energy demands

With the current energy trends, several policies have been placed into account to limit the energy consumption for buildings. Nevertheless, with increasing environmental performance benchmarks energy efficiency standards will not be sufficient to achieve international goals [89]. Even though there is a high importance and interest in applying principles that would reduce the impact of the operation of buildings to the environment, the dependency in local climate raises the complexity of the problem. As every solution must be tailored for each project, the amount of resources required during the design phase is increased as no large scale standardization is possible. Nonetheless, much research has taken place to identify the parameters and possible strategies to improve the energy performance of buildings.

Due to the variability of climate, particularly in the 21st century as a result of climate change, more extreme climatic conditions will be present. Analyzing a single aspect namely the variation in heating and cooling demands will lead to a different building behavior. Research done in this field shows that for the period between 1975 and 2085, the heating degree days (DD_H) will decrease by an estimated 13% to 87% but the cooling degree days (DD_C) can increase between 0% to 2500% [88]. This will lead to a substantial impact on the energy demands of buildings and will create additional challenges for future generations. Nonetheless,

due to the long service life of buildings, the design decisions taken during its conception will have to consider the climate conditions throughout its entire lifespan. It should be noted that even after the implementation of the most effective free-cooling techniques, there is a clear overheating problem that will be only compensated by mechanical cooling [88]. As stated in the previous sections, climate change and urbanization, specifically UHI; can cause major disruptions in the environment. Solutions will need to be developed and implemented to counteract these negative effects.

In practice, passive and active measures are used to counter the environmental impacts of the building sector. However, when considering the optimal balance between costs and benefits, focusing on energy savings, passive measures overtake active ones. Thermal insulation should be first priority, with high performance glazing and heating systems coming next and finally the implementation of solar collectors and PV-panels [70].

In order to fully optimize the energy demands of a building, an integrated design approach is a promising alternative. The relationship between the exterior climate and the interior conditions is highly connected and several tools such as building information modelling and bio-climatic design can provide the integrated design that buildings desperately need in order to reduce their impact on the environment.

2.3.1. Bio-climatic Design

Bio-climatic architecture is a design approach meant to reduce the environmental impact of the construction sector by using passive design techniques taking into account the local climate of the project. This design offers cheap, adequate and sustainable solutions to problems that may increase energy demands or hinder healthy living conditions [50, 84]. Figure 2.3 shows the design approach taken using passive methods. A clever use of geometry, orientation and vegetation can greatly reduce a buildings demands to satisfy both thermal comfort and energy requirements.

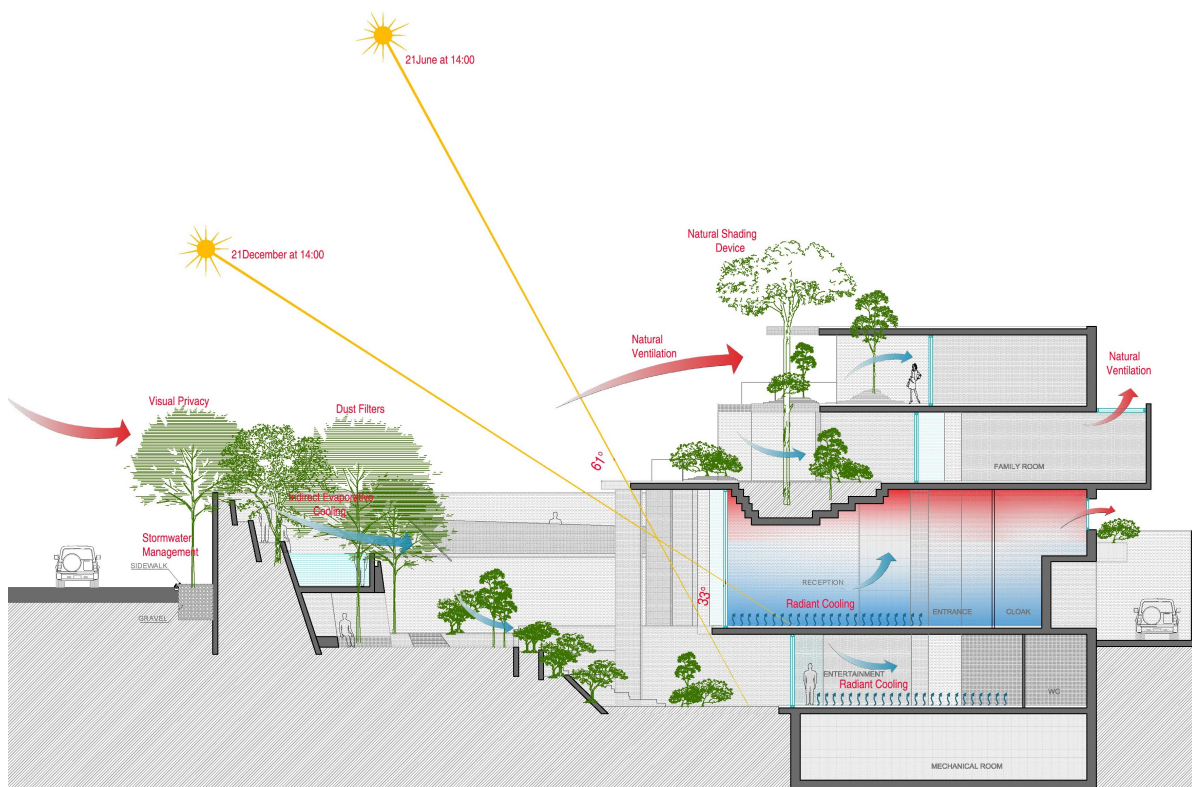


Figure 2.3: Bio-climatic design approach, adapted from [47]

The application of passive measures avoids the present day dependency on mechanical systems which can represent major investment and operation costs during the lifetime of

the building. Currently, heating, ventilation and air conditioning are the largest energy consumers in buildings. The principles governing bio-climatic design aim to provide harmony between the built environment and its natural surroundings. Its goal aims to use as many of the site characteristics as possible, leading to a reduction of the energy demands and of the amount of active systems needed to maintain a comfort levels. These benefits translate into economic savings, protection from and to the environment and an increase of indoor living conditions [16].

Achieving adequate comfort levels can turn to be a daunting task, in particular when considering the variability of external conditions. Analyzing a psychometric chart detailing levels of comfort can define the ranges which determines human comfort [50]. However, small variations can lead to a high percentage of dissatisfied people. Nevertheless, several alternatives can be used in order to achieve these levels. Depending on the conditions, many correction strategies can be applied, which range from conventional heating measures through air conditioning to evaporative cooling. It is desirable to provide this adequate level of comfort with the use of passive techniques that will consume no additional energy. In case they are needed, active measures should be used to compensate for any drawbacks in the bio-climatic design though, their dependency should be minimized.

A complete bio-climatic design is a complex task. Therefore, this research proposal will focus on the inclusion of vegetation on a buildings envelope and how can they improve a buildings performance.

2.4. Summary

Ever-increasing urbanization rates have led to the development of city wide problems. Problems such as noise and air pollution, an increasing demand of resources, urban heat island effect and a diminishing amount of green spaces and biodiversity within cities have caused an array of issues that directly affect adequate health and sustainable living conditions. Even though many sustainable approaches have been taken into consideration on an urban scale, greenery systems in the envelope of buildings have proven to show good results to tackle most of the problems that cities are currently facing. Vegetation in buildings can reduce the amount of resources required for a buildings operation, as well as creating an extra layer of protection and improving both air and noise quality and temperature ranges around its immediate surroundings. It has been proven that green envelopes can significantly improve the current state of urban environments while simultaneously creating a larger connection between human society and nature. Although their implementation on a large scale is increasing, it is still limited when analyzing the scope of the problem.

3

Research Definition

3.1. Problem statement

With an increasing trend in resource demand worldwide, sustainable solutions are stepping up. Local solutions such as the implementation of vegetation in the building industry (greenery systems) can provide an efficient way to solve global problems. Despite the fact that it has proven to provide substantial benefits to a buildings performance, greenery systems are still developing in both literature and practice. The capacity to reduce energy demands while improving its surroundings are unmatched by any other system, as shown by many authors and research on the topic. However, greenery in buildings have not reached large scale implementation in the building sector due to conditions such as lack of knowledge, higher initial cost, or technical difficulties.

3.2. Aims and focus of this research

Aims

This research aims to determine the efficiency of greenery systems in different climate conditions while proving that, when designed properly, they are a passive, eco-friendly and feasible solution to reduce energy demands in buildings. It aims to identify the most relevant parameters influencing the behavior of greenery systems to enable the creation of a targeted system for different climatic conditions.

Focus

The optimization of the energy performance of buildings is no simple task. A building by itself, is a large system with multiple factors interacting with each other. Even without the inclusion of greenery systems, finding the optimal solution for this problem requires significant involvement and knowledge of the design and construction process.

The inclusion of greenery systems into such a system, further increases its complexity. As it involves additional parameters, although independent, there is a direct effect on the overall performance in regards to energy consumption. The behavior and performance of any greenery system depends on a large number of parameters, nevertheless, the focus of this analysis and optimization procedures will be grouped into to: vegetation properties and soil substrate properties.

Among the vegetation properties, the focus will be on the effects of the leaf area index (LAI), radiation attenuation coefficient (κ) and the leaf stomatal conductance (g_s). While for the soil substrate properties, the influence of soil density, moisture content and thickness will be taken into account. Greenery systems have the advantage of providing a passive alternative to improve a buildings energy efficiency for both heating and cooling seasons and to reduce the dependency on mechanical systems or artificial products while providing a better environment for the people in its surroundings.

3.3. Research questions

Main research question

How can vertical green systems be optimized to improve the performance of a building for different climate types?

Sub-research questions

- Which are the parameters with the highest influence on the performance of vertical green systems?
- To what extent is evapotranspiration capable of reducing a building's energy demand?
- How large is the influence of the soil substrate layer for the performance of the system?
- How does a vertical green system respond under the urban heat island effect in an urban environment?
- How does the leaf area index influence wind velocity in the surroundings of the vegetation layer?

3.4. Methodology and chapter scheme

This section will detail the methodology that will be the basis for the definition of the research and the steps taken to answer the questions posed in the previous chapter. The research done within this thesis can be divided in the following steps:

Part I introduces the topic and provides the relevant background information that led to the development of this project. It describes the aims, focus and research questions for this research. The methodology is detailed showing the procedure that the investigation will follow, including the scope and limitations in the project. Includes Chapters 1, 2 and 3.

Part II shows the theoretical framework. A literature review from the historical development, classification and characteristics of greenery system will be performed. Additionally, a review on the energy balance of both green façades and living wall systems is done to identify the relevant parameters governing their performance. Includes Chapters 4 and 5.

Part III applies the knowledge gathered in Part II on an experimental setup. A simplified analytic model and analysis is created to show the effects of these systems in the energy demands of a building. Further on, higher complexity models will be defined in ENVI_met software package. Finally, the optimization procedure for both the green façade and living wall system will be performed with modeFRONTIER to identify the most optimal configuration of the systems for different climate types and sensitivity to local climatic conditions. Includes Chapters 6 and 7.

Part IV will state the answers for the research questions, conclusions, recommendations and final remarks, while discussing further research on the topic. Includes Chapter 8.

The outline for this thesis is shown in Figure 3.1.

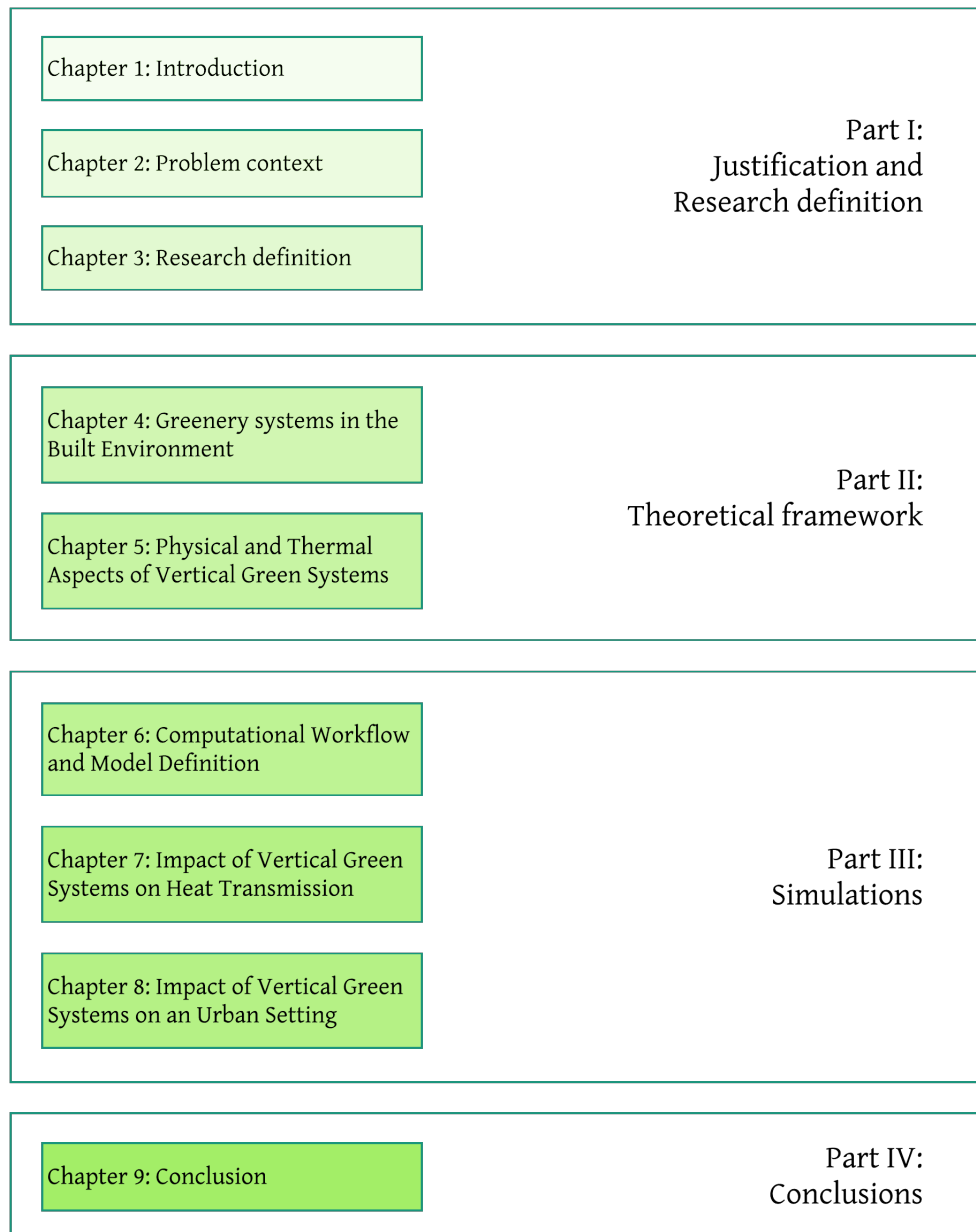


Figure 3.1: Overview of research outline

4

Greenery Systems in the Built Environment

This chapter provides an overview of the existing forms of greenery systems that will be used in this research. It focuses on their characteristics, typologies, benefits, drawbacks and illustrates their application in real life projects.

4.1. General introduction

Urban greening can improve the environment of urban areas and is turning into a key design consideration in modern building envelopes [57]. Greenery systems are becoming more common due to their aesthetic influence on buildings and their countless benefits at both building and urban scales. Among these the reduction of energy demands and ambient temperatures as well as the mitigation of the urban heat island effect stand out [62]. Additionally they present the added benefit of contributing to the insertion of vegetation in cities without taking any valuable space on street level while increasing urban biodiversity, storm water management, air quality, etc [49]. Even though vegetation in the built environment has been used for hundreds of years, they became less common during the last century due to rising architectural styles during the 1900's. However, an emerging trend in sustainability worldwide paired with a focus on environmental care has led to their reappearance in the construction industry furthering the green building movement.

Green buildings nowadays are designed in order to provide sustainable solutions for mitigation of hazardous impacts of the building stock on the environment, society and economy [53]. Projects including vegetation are becoming more common and are seamlessly being integrated into the urban canopy. Buildings like the ones shown in Figures 4.1 and 4.2 have exhibited the benefits and the feasibility of implementing these systems. However, several drawbacks associated with vegetation in buildings such as a higher initial investment, maintenance costs and their unpredictable behavior over time [62], have kept the development of these systems idle.



Figure 4.1: M&S Greenery shopping store in Newcastle, UK [5]



Figure 4.2: Bosco Verticale, residential building in Milan, Italy [79]

4.1.1. Historical overview

The first description of greenery in an urban environment comes from the depiction of the Hanging Gardens of Babylon built by King Nebuchadnezzar for his wife Amystis around 600 B.C. [20]. Further development of vertical and horizontal greenery systems came from humanity's needs for survival, using natural materials to create an enclosure for protection from the environment and harsh weather conditions such as simple earth shelter which provided

adequate thermal protection. However, the cooling effect of earth sheltered roofs was significantly smaller than the one of a vegetated roof, suggesting that important role of a plant layer [75, 91]. The combined use of soil and vegetation provided excellent insulating qualities allowing heat retention in cold climates and cooling effect in warm ones [60].

Further use of vegetation came throughout the centuries. Greenery systems were implemented in Mediterranean countries during the first century for shading, cooling and fruit production in the façades [51]. Vertical gardens were used as hanging gardens from the 16th to 17th century in India, Spain and Mexico; in 18th century France and 20th century Russia [60]. Modern developments of these systems came from contemporary architecture with architects such as Le Corbusier and Frank Lloyd Wright who used green roofs extensively in their projects focusing on the harmony between nature and humans. Le Corbusier even included green roofs in his vision of urban areas, making them his fifth point in *A New Architecture*[18].

Currently, the market of greenery systems is growing due to the implementation of government policies and support for sustainable building alternatives, creating a new vision for urban environments. The increasing amount of inspiration taken from nature follows a bio-climatic or even bio-mimicry design approach which are defining the modern urban landscape. Also, the fundamental importance of human-nature interaction has already been proven in countries such as Germany, France, Norway, Switzerland and Singapore which have began implementing measures to create cleaner and greener cities, as seen by the allocation of land and resources for this goal [82].

4.1.2. Greenery system typologies

From the use of green alternatives to create suitable enclosures in the past, current methods used to implement greenery in the built environment have grown and led to the development of many different types of building integrated vegetation. The five main concepts will be further defined in this section and are green roofs, green balconies, sky gardens, indoor sky gardens, and green walls; shown schematically in Figure 4.3.

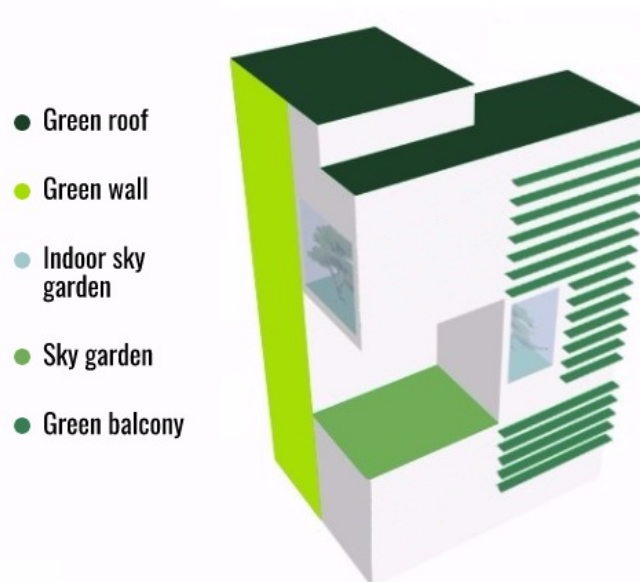


Figure 4.3: Types of building integrated vegetation. Adapted from [69]

Green roofs

Green roofs are the most commonly used greenery system and have been largely implemented in European, North American and tropical Asian countries. They are composed of several layers which include vegetation, growing medium, filter, drainage, root barrier and a water-

proofing membrane. Green roofs can be classified either as extensive or intensive, depending on their use, maintenance and construction process. Extensive green roofs are characterized by a thin soil substrate, low maintenance and a limited selection of plant species, whereas intensive green roofs allow more flexibility in the choice of plant species. This increased flexibility leads to higher maintenance costs due to the requirements of a deeper substrate layer and irrigation system.

As rooftops can represent up to 32% of the horizontal space in urban areas [55], they cause a significant impact in a buildings performance as well as in the micro-climate conditions of its surroundings. More precisely, green roofs are associated with the following benefits [69]: larger roof service life by diminishing the deteriorating effects of UV light and temperature fluctuations, mitigation of the UHI by the change of the urban surfaces albedo, noise reduction, storm water management, increased biodiversity, enhanced thermal performance and building energy efficiency as they provide acceptable insulating properties with as little as 10cm of soil layer [35].

Furthermore, green roofs can be a suitable retrofitting alternative for energy savings in buildings. Additional considerations needed for the retrofit, for example measuring the existing structural capacity, could counter the benefits of this type of retrofitting. However, Castleton et. al [11] found that the additional loads associated with extensive green roofs, in general, do not require additional structural support.

Sky gardens

Sky gardens are defined as a green space on the rooftop or intermediate floors characterized by an indirect connection to the buildings envelope [51], which reduces efficiency as a thermal barrier. Nonetheless, several macro scale environmental benefits like the mitigation of UHI, enhanced biodiversity, aesthetic view and air pollutant removal can still be achieved.

Even if there are no direct thermal benefits, sky gardens can have indirect energy benefits by cooling the air temperature around them, reducing the requirements of HVAC systems [69]. Although they have similar benefits as other greenery typologies, sky gardens are designed especially as recreational areas to improve social interaction. Thereby, indoor sky gardens provide the additional benefit of providing a comfortable environment independent of outdoor weather conditions [51]. They also have a direct effect on indoor air quality, as they remove high concentrations of air pollutants that can not only cause health problems to the occupants of a building but can also lead to a reduction of working productivity [48].

Green balconies

The main purpose of Balconies is to create a connection between indoor and outdoor environments [69]. As several studies have shown, green balconies have similar beneficial effects as sky gardens and can significantly increase the property value of a building in comparison to similar ones without any green balconies [67]. Nevertheless, there is still a lack of research in the overall impact of green balconies on the micro-climate of buildings, but promising results were presented by Marugg [51], in a research performed on the effects of green balconies on the micro climate by solar shading, evapotranspiration and wind flow change. However, green balconies can lead to a negative impact in winter conditions increasing energy demands, although they can provide cooling benefits during summer.

Green walls

Vertical greenery systems (VGS) can provide the same benefits as all the other building integrated vegetation systems described in the previous section considering both macro and micro scales. However, they have the potential to create a larger impact due to a much bigger surface area in comparison to green roofs [57, 69]. They are seen as a promising alternative to make high density urban areas more sustainable, in particular when used on high-rise buildings.

There are two main groups of VGS, green façades (GF) and living wall systems (LWS) as seen in Figure 4.4. The main differences between the two categories are based on their rooting systems, the suitability of plant species, plant irrigation and the existence of a cavity between the vegetation and the façade [57].

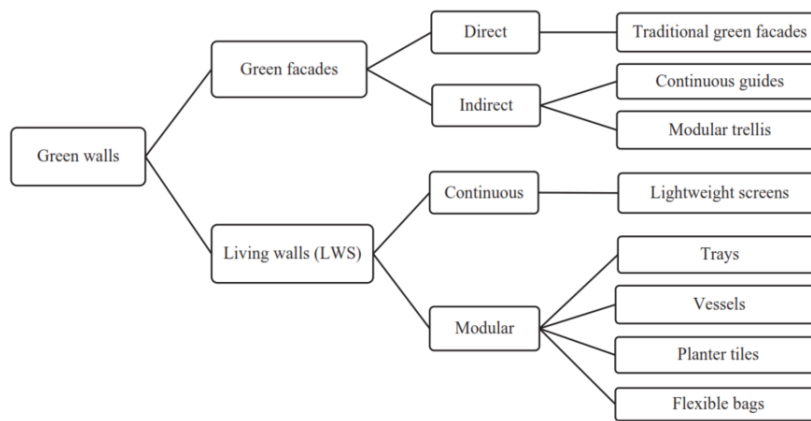


Figure 4.4: Green wall classification according to their construction characteristics [49]

Green façades, referring to systems with direct ground rooting (Figure 4.5), have their own design considerations. For example, one restriction is the selection of suitable plant species for this system, which is quite limited as they have to reach high altitudes. Therefore, climbing plants are usually used in these systems although, they are limited to a maximum height of 25 meters [49]. There are two categories of green façades, direct or indirect greening. In direct façades, plants are attached to the wall, adhering to the surface through aerial roots, suction or by adhesive root structures [53, 57]. Whereas indirect façades use a supporting structure in order to facilitate the growth of the vegetation layer. This structure consists of cables, meshes or nets made from stainless, coated or galvanized steel or from hard wood, aluminum or plastic. Therefore, climber plant species are more suited for this application. The inclusion of an air gap between the vegetation layer and the façade in indirect greening systems changes their performance, as an additional layer is created improving the thermal resistance of the façade as a whole. Furthermore, the air gap allows for air to flow freely thus creating a natural ventilation system which removes moisture, coming from the environment or from the vegetation layer, therefore preventing damage to the rest of the building.

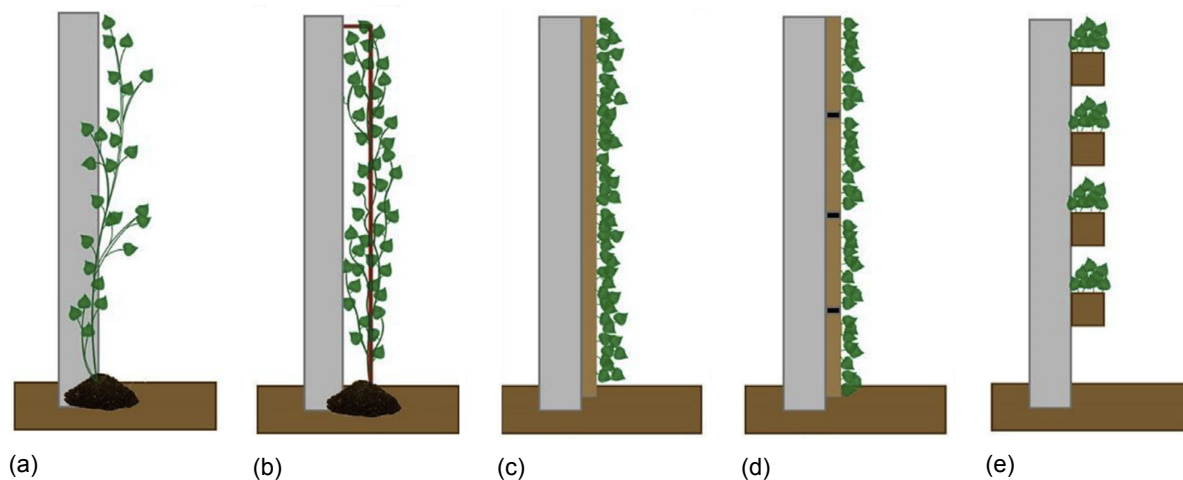


Figure 4.5: Classification of vertical greenery systems: (a) Direct green façade (b) Indirect green façade (c) Continuous LWS (d) Modular LWS (e) Linear (LWS) [53]

Both systems, direct and indirect, have advantages and disadvantages regarding their construction, maintenance and performance. A full, comprehensive table has been developed by Manso et al. [49], and is summarized in the following points:

Advantages

- No additional supporting structure (direct façade) or irrigation system is needed

- Low cost and water consumption
- High accessibility for maintenance
- Easy and accessible plant replacement

Disadvantages

- Limited plant selection
- Slow growth rate and surface coverage
- Possibility of plant detachment from façade or guides

Unlike green façades, living wall systems are not directly rooted into the ground (Figure 4.5) and are therefore not limited by any height constraints. In exchange, an artificial growing medium is required to allow proper plant growth and root attachment. This layer, from here on referred to as substrate layer, varies per manufacturer although common substrates are planter boxes (1), foams (2), laminar layers of felt sheets (3) or mineral wool (4), shown in Figure 4.6.

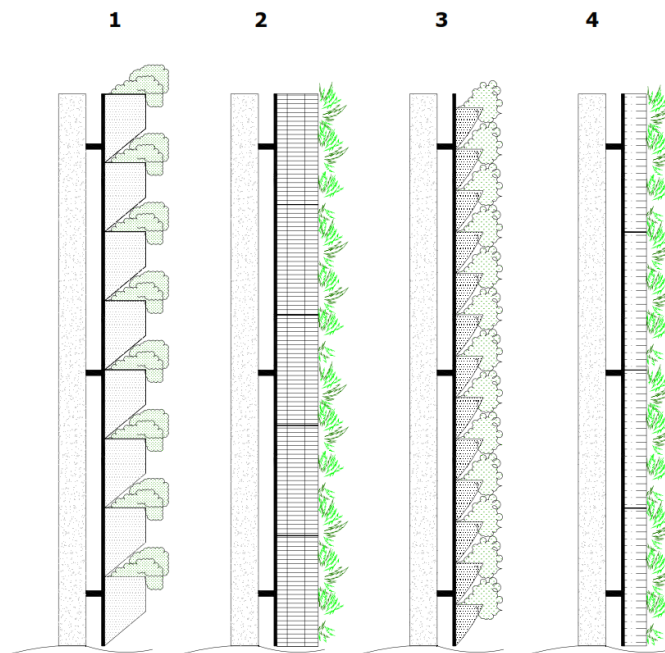


Figure 4.6: Typical configuration of living wall system [57]

Similar to green façades, there are direct and indirect systems available for living walls with the following associated advantages and disadvantages summarized from Manso et. al [49]:

Advantages

- Controlled irrigation and drainage
- More efficient growth due to their pre-cultivation potential [69]
- Storm water management due to the water retention capacity of the substrate layer[80]

Disadvantages

- Higher installation and maintenance cost
- Complex implementation
- Heavy solution, limited to the structure's load bearing capacity
- Limited space for root growth

Although based on a similar concept, the design and construction process of a GF or a LWS varies significantly as they involve different components, creating a unique approach for each system. For instance, in the case of LWS, the additional requirements of structural supports, drainage and irrigation systems, etc; are some of the aspects that must be analyzed in the design of a LWS that are not present in a GF. Caution must be taken when designing all these elements to guarantee proper function during operation and minimize maintenance to keep investment costs to a minimum, since these components can become a significant part of the initial investment.

4.2. Vertical green

Building integrated vegetation has a large number of effects that can be seen in projects taking place all over the world. Nonetheless, there are still barriers slowing down their implementation in a large scale, among them social and economic factors, lack of knowledge, shortage of public and private incentives, technical issues, uncertainty in design due to modelling software and the intrinsic uncertainty associated with a plant's performance.

Nevertheless, the wide range of benefits that are associated with building integrated vegetation has the potential to close the gap between theoretical analysis and real life implementation. Therefore, the positive effects as well as the associated risks of VGS are analyzed and discussed.

4.2.1. Effects of vertical green

Aesthetic appearance

Government policies and new trends in building design have led to the inclusion of greenery in urban areas in order to counter the negative effects of rapid urbanization. Research in the field of environmental psychology has shown that people favor areas with vegetation over those without [90], and alternative research found that indoor use of vegetation has a significant effect on the comfort and productivity of people [48]. Furthermore, a survey conducted by White and Gatersleben [90] involving 188 participants determined that the integration of vegetation in the built environment helps to satisfy the human need for aesthetics and restoration, favoring a more natural landscape look over well kept, human influenced vegetation. In all cases, the survey showed that vegetation increases the aesthetic appraisal of buildings compared to those without and exhibiting a clear preference of green façades over green roofs.

Sound absorption and insulation

Davis et al. [21] performed an evaluation of the sound absorption properties of a vertical garden considering the effects of the substrate layer as well as the plants. Their results showed that the thickness of the substrate is proportional to the absorption of low frequency sound waves. While moisture content has its own effect, with higher values leading to a decrease in the sound absorption coefficient. Vegetation on the other hand has a minimal influence on the sound absorption of the system in low frequencies, but providing a much larger influence on frequencies higher than 400 Hz. This knowledge allows a dynamic design of the greenery system as it can be targeted to counter urban noise sources such as ground traffic or air travel, which can be useful as a sustainable tool to tackle noise pollution in urban environments.

So far, there is no clear consensus on the sound insulation properties of green walls, as just a small amount of research has taken place. Nonetheless, an investigation performed

by Azkorra et al. [6] identified that while the sound reduction indexes from a green wall are relatively small in comparison with traditional construction materials, small changes in the configuration of the VGS could increase its acoustic properties. This leads to the conclusion that a targeted design for sound insulation can increase the efficiency of VGS for acoustic purposes.

Biodiversity

The conservation of biodiversity in cities is a global issue that plays an important role in the protection of local and regional species as well as providing a stronger connection to nature through an understanding of the elaborate processes governing global and human sustainability [37]. During the last century, rapid urban expansion and limited conservation of natural areas has forced many animal species to find alternative sources of food and shelter, leading to a direct reduction of the amount of fauna present in the urban environment. The diminishing levels of biodiversity present in cities decrease the resilience of a functioning ecosystem in the long term [4]. Moreover, design for biodiversity in the built environment can lead to additional benefits to the local ecosystem like buffering of population of different species, as well as providing gene banks and ecological corridors [48].

Although there is a lot of research still needed to understand and exploit the effects of building integrated vegetation on urban biodiversity, current research has shown that the implementation of these systems can effectively increase biodiversity and be used as a safe haven for endangered species to recover.

Psychological benefits

Mangione [48] researched the effects of micro forests on the performance of their occupants. His results are taken as an indication and extrapolated to understand the full effects that outdoor greenery systems can have on the population in their vicinity. For example, regarding psychological benefits, working performance substantially increased when employees were in contact with innovative office spaces, such as a forest space type.

Moreover, plants in the work environment had a significant effect on the thermal comfort of the occupants in a building, without any seasonal influence. The psychological effects caused by the perception of a physical environment, has a direct relation on a person's thermal comfort which is highly influenced by their environment, establishing a relationship with the overall energy consumption of buildings [48].

External shading

By intercepting short wave radiation, a layer of vegetation can create a significant shading effect. Its extent depends highly on the foliage density and leaf orientation of the plant which are described by the leaf area index (LAI) and the leaf angle distribution (LAD) respectively. Sun-shading provided by vegetation can be a efficient and natural measure to counter high temperatures during summer conditions as Abkari et al. [3] has shown that the shadowing effect of trees could lead to cooling energy savings up to 30%, while also decreasing peak energy demands. Thereby, the choice of plant species plays a pivotal role in the design of a green wall. During heating season the use of evergreen plant species can be detrimental to the system, as the favorable solar radiation incident in the façade can be considerably reduced, limiting the possibility to heat the building through natural processes. In contrast, the selection of deciduous species could prove to be more beneficial as the foliage is reduced in winter allowing solar radiation to directly heat the façade.

In addition, the shadowing effect caused by the foliage also reduces the damaging effects of UV radiation and thermal stress on the building due to lower temperature fluctuations [57].

Mitigation of the urban heat island effect

The emergence of the urban heat island effect is complex and is related to several aspects briefly shown in Figure 4.7, that go beyond the scope of this thesis. However, the impacts and dangers it presents to cities are quantifiable and highly relevant for today's society.

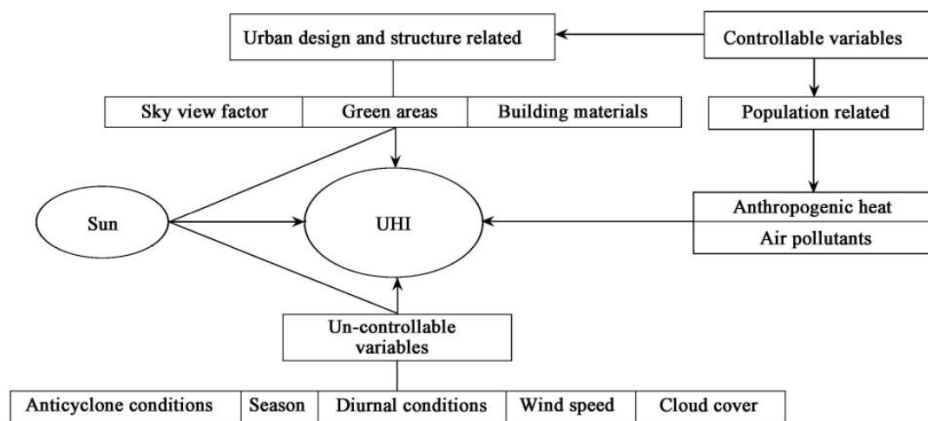


Figure 4.7: Factors involved in the generation of the urban heat island effect [72]

The cooling effect of vegetation on a building through shading and evapotranspiration is not just limited to the reduction of the façades temperature, but can also have a significant impact outside of the building, which can lead to a decrease in the air temperature of a whole urban street canyon [23]. Large scale changes in the albedo of surfaces have a large impact in the local peak ambient temperature [74]. The change in the surfaces albedo caused by a greenery system paired with the limited amount of heat that can be stored in vegetation, leads to a reduction of the total amount of solar radiation absorbed and later released by a grey urban canopy. Additionally, many studies have proven that the mitigation potential of greenery systems is much higher in urban areas including them than in those without [74]. This shows that building integrated vegetation can be considered as an efficient alternative to weaken the hazardous effects of the UHI.

Effects on wind speed

Using green walls can also result in a reduction of the wind speed in the underlying exterior construction material [65]. According to several authors [32, 57], foliage of plants can create an almost stagnant air layer or at least, significantly reduce the wind speed, although there is limited information regarding this effect. Such a stagnant air layer largely reduces the convective heat transfer through a cavity affecting directly the insulating properties of a façade.

The relationship between the foliage density of a vegetation layer and the wind speed in close proximity has been experimentally defined by Perini et al. [65]. It shows a clear trend in the reduction of wind speed close to a vegetation layer, which has been verified by the development of air flow profiles created by Grabowiecki [32].

Further results have also shown that although both wind speed and temperature can be modified by a vegetation layer, there is no significant difference found in either of them at a distance of 1 m away from the façade. While the most significant effects are seen in close proximity to the foliage layer [65] as seen on Figure 4.8.

Air pollution

Additionally, vegetation has the capacity to reduce the amount of air pollution caused by PM_x , CO_2 and acidifying substances. Plants can use these pollutants by means of photosynthesis for plant growth and capture them on their leaves surfaces. The amount of pollutant absorption by a plant depends on its leaf stomatal conductance which is responsible for the regulation of photosynthesis and transpiration rates [59]. Furthermore, pollutant capture depends on the roughness and hairiness of a leaf's surface, for example, the atmospheric concentration of particulate matter ($PM_{2.5}$ and PM_{10}) can be reduced by its capture and adhesion to leaves and plant stems, whereupon it can be washed away by rain and deposited into the soil below [57].

Besides that, several other factors alter the rate at which a plant can capture air pol-

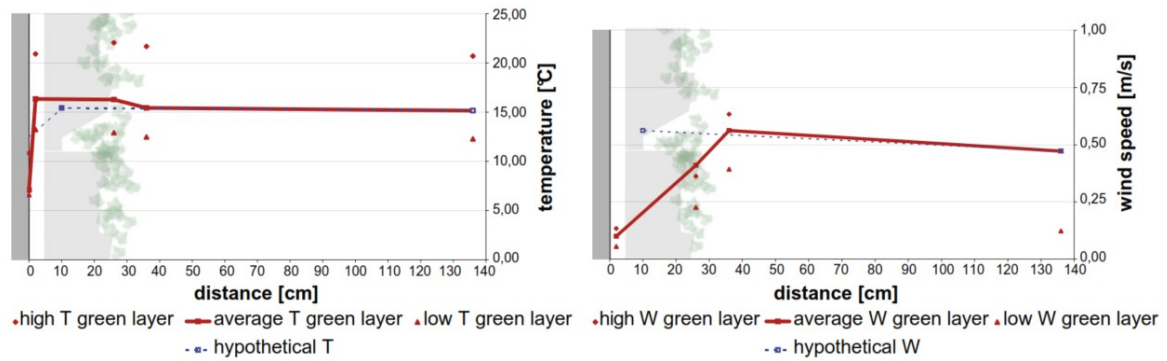


Figure 4.8: Temperature and wind speed profiles for a living wall system [65]

lutants, among them the leaf surface moisture, stickiness and electrical charge. Although many alternatives to reduce atmospheric pollution exist, for instance catalytical processes and electrical precipitation, vegetation provides a natural and efficient alternative to drastically improve air quality.

Storm water management

Aside from the energy and thermal benefits that greenery systems can provide, their water retention capacity is of high importance. More precisely, their to store water proved to be an effective solution for storm-water management [80]. By reducing the water flow into existing sewer systems, the demand on these systems can be reduced, improving their service life and allowing for a better control of water flow through an urban environment.

4.2.2. Risks of vertical green

Among all the benefits related to VGS, several risks associated with their implementation are also possible. This section will provide an overview of the different ways that VGS could lead to problems within the urban environment.

Moisture

In general, VGS can reduce the amount of moisture problems present in a building's enclosure since the additional vegetation and substrate (in the case of LWS) layers can effectively stop water and moisture from reaching the façade. Thicker vegetation layers also serve, to a certain point, as a water proof membrane protecting the façade from water and moisture damage from external sources. However, the reduction of water and moisture transfer works reciprocally. Due to a large decrease in the wind speed behind the vegetation close to the façade and a minimum amount of solar radiation coming through, any moisture introduced into the cavity between a vertical greenery system and a building can lead to moisture problems as there are no counter measures to remove it from there.

Although this type of moisture problems can easily be avoided with proper façade design as well as adequate water and moisture barriers, attention must be placed when the retrofitting of a façade will take place. Enclosing moisture in a cavity can lead to several service problems in a building, therefore proper measures must be taken to ensure a dry and well ventilated cavity before the installation of a VGS. Even though the evapotranspiration process of a vegetation layer constantly releases moisture through evapotranspiration, covering a façade with vegetation does not raise the moisture content of the façade [57].

Deterioration

In the case of green façades, direct greening systems attach to the surface of stony materials on the façade. Thereby, their roots anchor themselves on the façade's surface and have a minimum to negligible impact on the integrity of the wall. As long as the cladding is in good condition, plants do not cause any damage to the façade. However, if cracks are present and have a considerable width, roots can find themselves digging into the cracks furthering the

deterioration of the material [9].

Therefore, the use of self clinging plants should be avoided when mortar joints are soft or have a high porosity [57]. While the damage that can be caused by self clinging plants is comparatively minimal, root growth from woody species (mostly used in LWS) is much larger and can lead to significant damage to the façade.

Although green walls can cause deterioration due to plant growth and water leakage, proper design of the system can prevent this damage, allowing the building to take full advantage of the benefits green walls can offer.

Maintenance

Depending on the complexity of the system, regular maintenance should be properly scheduled. Required maintenance work varies depending on the type of greenery system used. In the case of green walls, maintenance just consists of simple trimming and pruning of climbers to prevent the plant from tampering with openings or windows. Whereas for living walls, maintenance labor has a higher degree of complexity due to the larger care required for the vegetation. Besides proper trimming and pruning, plants might need replacement and checking of irrigation systems ensuring that an adequate water supply is being provided [33]. Additionally, in winter conditions whenever frost damage is a possibility, the irrigation system must be emptied and replaced with a suitable system to provide the plants with the nutrients they require.

4.2.3. Implementation and feasibility

Buildings account for a large portion of the total energy use worldwide. Therefore, more sustainable and feasible alternatives are under research, development and implementation with the goal of reducing the impact the building sector has on the demand of resources from the planet. Thereby, among all building integrated vegetation systems, green façades have shown the most promising results leading to the largest energy savings due to their larger area of application.

But, as complex systems, green façades come with additional design considerations as well as expenses. A study performed by Perini et al. [64] evaluated the cost-benefit of the application of green walls in the built environment, and stated that green façades can be economically sustainable, considering only the air purification and carbon reduction capacity of the system. Whereas LWS, the study concluded that they are not economically sustainable when considering only these factors, as their larger investment and maintenance costs significantly surpasses the ones for green façades.

Even though LWS carry a much larger economic weight (around 350 - 1200€/m² depending on the growing medium, maintenance, materials and design complexity [57]), their social benefits should not be disregarded since they could increase the properties value, possibly countering their high initial costs. Although the value of the social benefits generated by building integrated vegetation is known, the systems have a larger influence in its surroundings, besides the ones providing to the building where its implemented. Therefore, requiring more research to fully understand their effects. Therefore, economic incentives should be provided to promote the installation of vegetation throughout the urban canopy. Initial investment costs should be reduced to take full advantage of a thorough implementation in an urban setting; as the effects of a single green wall does not constitute major changes in a larger scale [64].

4.3. Summary

This chapter showed the literature study performed on the origins, use, benefits and risks of VGS in the urban environment. It details the potential of these systems to improve the living conditions of the environment and gives an overview of the different types that will be analyzed in this research project. Due to its larger area of implementation, vertical green systems were chosen to be the subject for the analysis as they provide a significant amount of benefits, for example: aesthetic appearance, sound absorption and insulation, biodiversity, psychological benefits, external sun-shading, mitigation of the UHI effect, reduction of

wind speed and storm water management to name a few. Additionally, the risks involved in the installation and maintenance of these systems were analyzed where it was concluded that although they can cause damage in existing buildings, adequate design, proper care and regular maintenance can completely eliminate all the risks associated with the use of vegetation in the built environment.

5

Physical and Thermal Aspects of Vertical Greenery Systems

This chapter will analyze the physical processes involved in the the energy balance of the relevant greenery systems. It describes the parametrization approach taken to simplify the problem and the mathematical interpretation of the behavior of vegetation as a construction element for the built environment.

The Energy Performance of Buildings Directive of European Commission has stated that all new public buildings must be near zero-energy (NZEB) by 2018 and by December 2020 for private ones [15]. This is a daunting task and requires the implementation of several techniques, guidelines and adoption of sustainable principles to significantly decrease the energy and raw material demand of the building sector. However, new and better solutions are needed to counter the effects of man made climate change as well as to enhance the energy efficiency of the built environment and meet climate policy targets [26]. The NZEB status must be reached for new projects, nevertheless, the current building stock is filled with old buildings, characterized by their low insulation and zero to no regard to thermal comfort and energy efficiency. As the application of new sustainable policies include the entire building stock, a considerable investment of both time and resources is needed to comply with target demands. The evident dangers posed by unsustainable industry and construction practices have led to consequences represented, to a certain extent, by climate change. Therefore, the sustainable trend has flooded almost every industry, and architecture is not an exception. Sustainable designs, i.e. green or natural buildings, have taken the front row of modern architectural styles, taking inspiration from nature with leading concepts such as bio-mimicry or bio-climatic design.

As seen on many projects where sustainability is a priority, the application of bio-climatic strategies is a critical factor in the reduction of energy consumption and CO₂ emissions from the construction sector [50]. These strategies intend to minimize the environmental footprint through the use of passive design techniques that take advantage of local weather conditions. Nonetheless, one of the main constraints in the pursue of NZEB is the indoor thermal comfort requirements. To put into perspective, according to Perini et al. [65] a change in the internal ambient air temperature of 0.5°C can reduce air conditioning demands for up to 8%. Although thermal comfort has a direct relation to the energy efficiency as well as service requirements of a building, the influence of external vegetation in internal comfort will not be analyzed as the topic is outside the scope of this thesis. Nevertheless, as a reference, Figure 5.1 indicates the acceptable comfort zones based on dry and wet bulb temperatures as well as relative humidity of the indoor space. It shows the range and application of bio-climatic strategies that can be used to increase thermal comfort and limit the need for mechanical support and equipment under a particular set of conditions. The set of conditions shown in Figure 5.1, indicate the relevance of passive strategies to obtain a NZEB, which can be obtained with the proper configuration of a vertical greenery system (VGS). For a more detailed review of bio-climatic strategies and principles refer to [19, 50, 84]

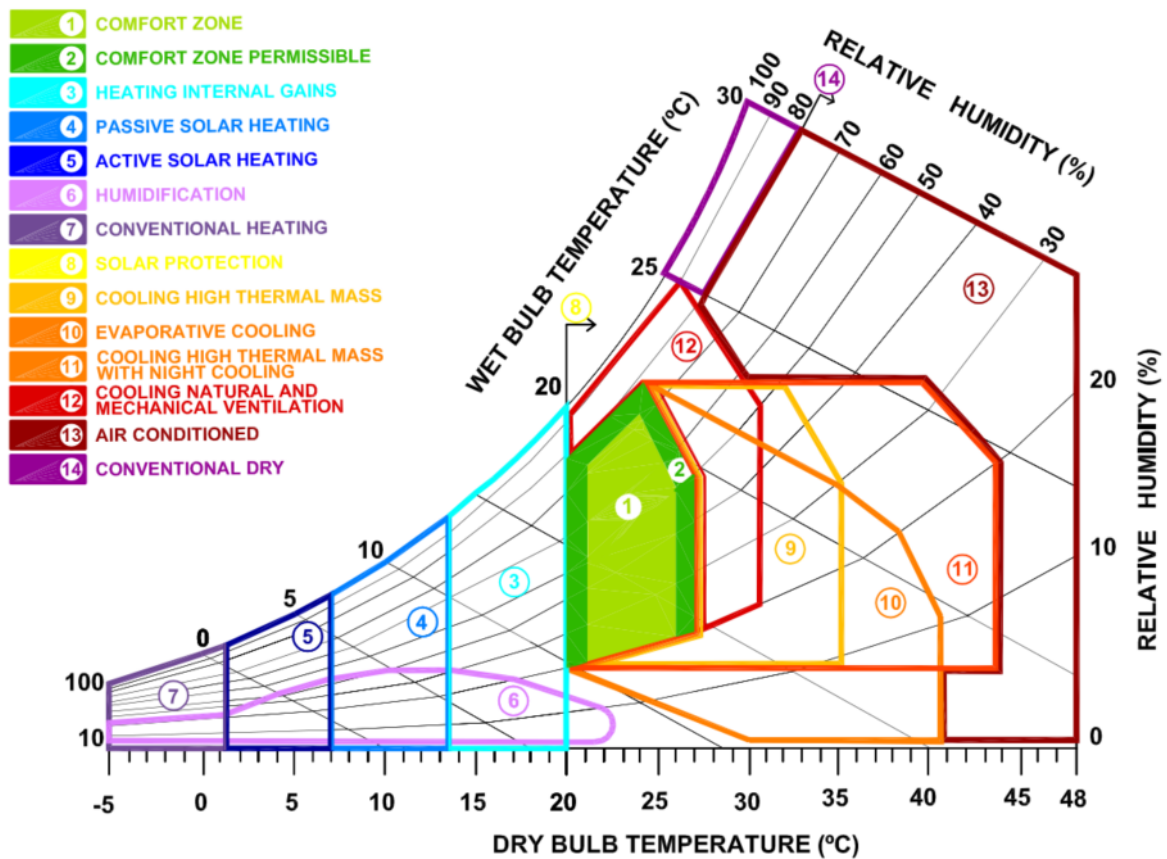


Figure 5.1: Givoni diagram. Bio-climatic interpretation of a psychometric chart for thermal comfort [50]

The energy performance of a buildings is a complex topic as it includes a wide array of interrelated aspects such as lighting, ventilation, internal heat gains, thermal insulation, etc. It is in the early design phases that decisions have the largest impact on energy performance. For example, the adequate building orientation or used ventilation systems can lead to a multitude of benefits in later stages of a project[8]. Further research made by Raji et al.[71] identified that the plan shape, depth, orientation and window-to-wall ratio together with the general design of the envelope are the main areas of interest when aiming for a design focused on minimizing energy demands.

Chapter 4 develops the benefits of building integrated vegetation. When VGS are used as a building's envelope, heating demands can be reduced by up to 25% during cold weather conditions [52] as they provide the same function as an artificial insulation such as Rock-wool. Nevertheless, unlike artificial insulating materials, VGS provides external shading and a cooling effect caused by the evapotranspiration process which greatly increases the energy efficiency during hot weather conditions. All in all, VGS are a proven alternative to create an environmentally friendly approach for a buildings design. However, the uncertainty associated with their performance raises their complexity and can even limit their application as a construction material. In order to fully understand its behavior, the following sections will detail the physical processes taking place within the different components of a VGS. The analysis is broken down into the heat balance of the vegetation layer, and the influence of moisture content and density on the thermal properties of the soil substrate.

5.1. Analysis cases

The information described in Chapter 4 shows the wide range of benefits associated with VGS, proving their potential when implemented in the urban environment. Therefore, an independent analysis of green façades and living wall systems will take place in order to de-

termine their most optimal configuration in a variety of climate conditions. Even though the benefits of greenery systems in warm climates have been proven, their effects on cold weather conditions require further research [14]. The evaluation of these models seen in Figure 5.2 and 5.3, provide a better insight into their behavior, creating a better understanding of the optimal configuration and its effect in micro and macro scales.

Case I: Green façade Consists of an indirect green wall rooted in an artificial substrate. Takes into account the heat transfer through a façade consisting of a vegetation layer, an air cavity, a building and the indoor air. Considered heat transfer mechanisms include short and long wave radiative transfer, convection, evapotranspiration from the vegetation layer, conduction and heat storage through and within the external building wall. This model will consider the effect of a vegetation layer on a bare façade wall.

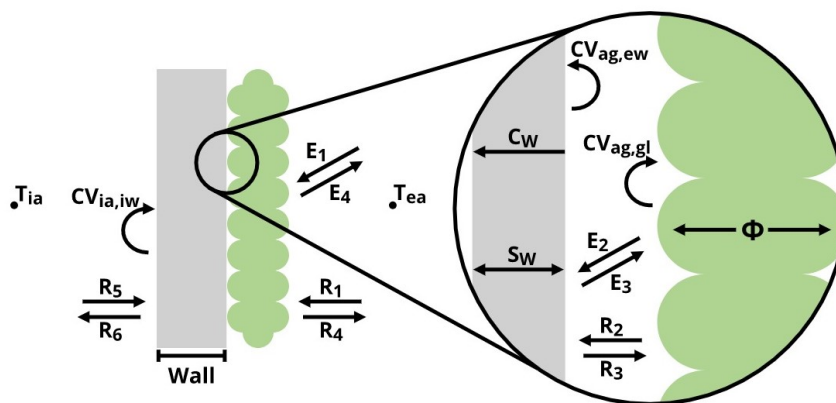


Figure 5.2: Schematic representation of the model for the analysis of a green façade

Case II: Living wall system Consists of a continuous living wall. Similar to Case I, all previous heat transfer mechanisms are considered with the inclusion of the transfer between the vegetation and the substrate layers, as well as conduction and heat storage through and in the soil. This model, besides analyzing the effects of a vegetation layer considers the influence of the addition of a soil substrate, which has the potential to increase the heat transfer resistance through the façade as well as serving as thermal mass to regulate indoor ambient temperature.

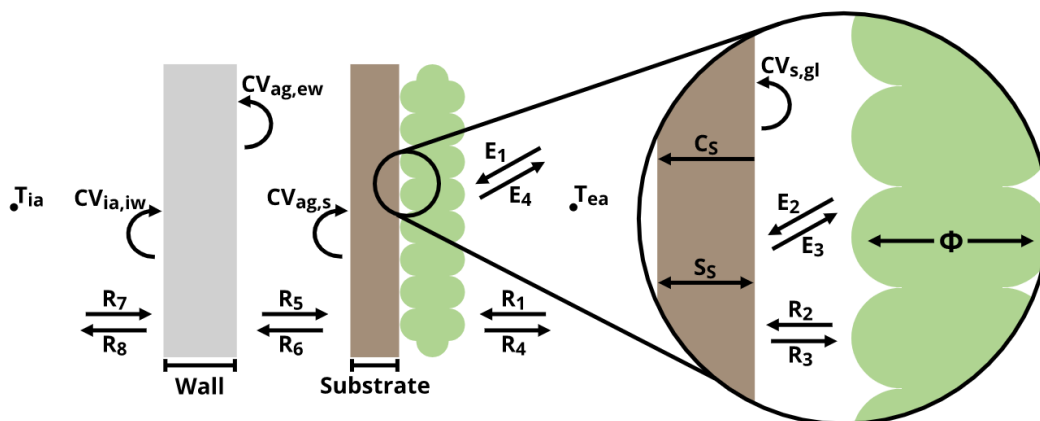


Figure 5.3: Schematic representation of the model for the analysis of a living wall system

5.2. Vertical green energy balance

The heat balance of the green layer [17, 81] can be described by Equation 5.1.

$$\sum E + \varepsilon_i * \sum R + \sum C_V - \phi = 0 \quad (5.1)$$

Where,

E : Short wave radiation:

R : Long wave radiation:

C_V : Convection

ϕ : Evapotranspiration

The following sections describe the components for each section of Equation 5.1.

5.2.1. Parameter overview

To simplify the understanding of the physical processes that govern the behavior of plants, the energy balance has been parametrized in order to create a quantifiable mathematical model. The parameters used on the definition of the energy balances of a green wall are described in Table 5.1. Additional information can be found in [17, 81].

Variable	Description	Units
E_1	solar radiation on green layer	W/m^2
ε_w	wall emissivity	%
ε_{gl}	green layer emissivity	%
LAI	leaf area index	-
κ	extinction coefficient	-
τ	solar transmissivity	-
R_{sky}	radiation coming from the sky	W/m^2
R_{gr}	radiation coming from the ground	W/m^2
T_{sky}	sky temperature	K
T_{gr}	ground temperature	K
T_{gl}	green layer temperature	K
σ	Stephan-Boltzmann constant	W/m^2k^4
ρ_a	air density	kg/m^3
C_{pa}	specific heat capacity of air	J/kgK
T_{ea}	exterior air temperature	K
T_{ag}	air gap temperature	K
r_e	aerodynamic resistance	s/m
h_e	combined heat transfer coefficient	W/m^2K
$e_s(T)$	air vapor pressure at saturation	Pa
e_a	partial air vapor pressure	Pa
γ	psychometric constant	Pa/K
r_s	bulk surface resistance	s/m
η_l	bulk stomatal resistance of the well-illuminated leaf	s/m

Table 5.1: Parameter table used for green wall energy balance

5.2.2. Shortwave radiation, E

Incoming radiation from the sun has a significant effect in our climate. The total amount of radiation coming through the light spectrum is defined as the solar constant and has a value of $1353 W/m^2$ [73]. This total energy is classified as short wave radiation which takes part in the visible part of the spectrum, and long wave radiation on the infrared side addressed in the following section.

The vegetation layer in a VGS has a considerable effect in shielding surfaces from short wave radiation (E, see Eq. 5.2). This shadowing effect is caused by the foliage which reduces the amount of transmitted radiation through the canopy. It is determined by the solar

transmissivity which is a function of the leaf area index, extinction coefficient and leaf angle distribution.

$$E_2 = \tau * E_1 \quad (5.2)$$

Where τ is the solar transmissivity. The remaining energy associated with short wave radiation is a portion of the value E_2 seen in Figure ??, caused by the different absorption and reflectivity coefficients of the façade and vegetation surfaces.

Solar transmissivity (τ) Refers to the ratio of transmitted photosynthetically active radiation (PAR) and incident PAR above the canopy [63], which shows the effects of leaf area index (LAI) and extinction coefficient (κ) on the amount of solar radiation going through a vegetation layer as seen on Figure 5.4. The solar transmissivity can then be calculated through the relationship developed by Monsi and Saeki in 1953 shown in Eq. 5.3.

$$\tau = \exp(-\kappa LAI) \quad (5.3)$$

Figure 5.4 shows the behavior of the transmissivity coefficient with varying values of both LAI and κ . For both variables, higher values lead to a decrease of the solar radiation through the vegetation layer representing its shadowing effect.

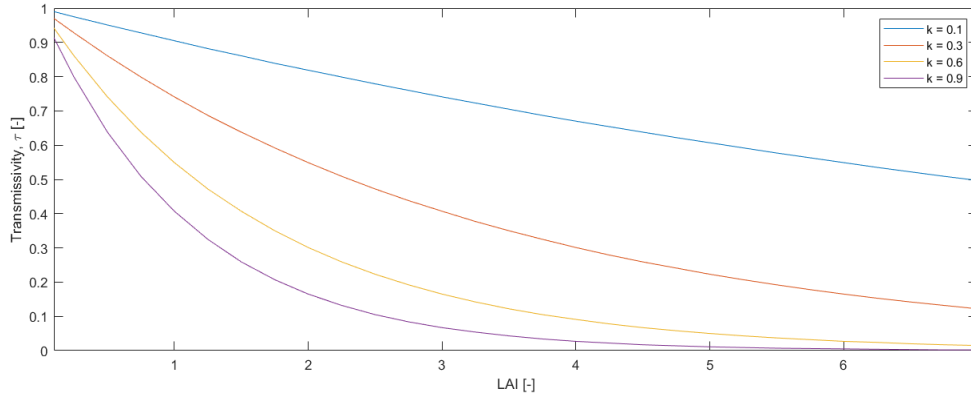


Figure 5.4: Transmissivity coefficient as a function of LAI and κ [81]

Leaf Area Index The leaf area index (LAI) is an indirect measurement of the foliage density of a vegetation layer. It is defined as the ratio between the leaf area and the square meters of façade or roof below it. Although it has a defining role in a plants behavior, there is no defined relation between it and its potential for energy savings [63].

The LAI can be determined either directly or indirectly. The direct approach consists of measuring the area of each leaf in a square meter, while the indirect one evaluates the amount of light transmitted or reflected by the plants canopy through the PAR inversion technique. Nevertheless, for a numerical estimation of the value of the LAI, Eq. 5.4 can be used [63].

$$LAI = \frac{\left[\left(1 - \frac{1}{2\kappa}\right) f_b - 1 \right] \ln(\tau)}{A(1 - 0.47f_b)} \quad (5.4)$$

Where A is leaf absorptivity taken as 0.9 for healthy green foliage, f_b is the beam fraction calculated as the ratio between diffuse and direct radiation, τ is the total transmissivity through a plant layer and κ is the extinction coefficient. To better understand the physical representation and the range of values of the LAI in a façade, Figure 5.5 shows an example of various values of LAI and their associated foliage density, where Figure 5.5a has a coverage of 25% of the surface area.

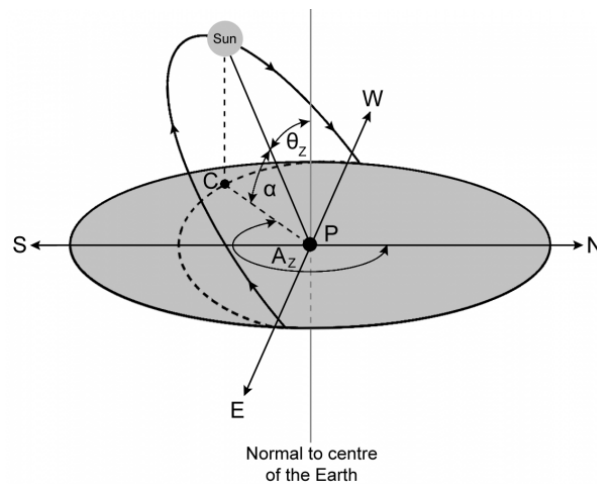
(a) LAI ≈ 0.25 (b) LAI ≈ 0.75 (c) LAI ≈ 1.50

Figure 5.5: Varying levels of leaf area index in a vegetation layer [81]

Extinction coefficient (κ) The extinction coefficient represents the amount of radiation that is absorbed by the canopy at a given solar zenith angle and canopy leaf area angle distribution as seen in Figure 5.6. It can be computed through Eq. 5.5[63].

$$\kappa = \frac{\sqrt{\chi^2 + \tan^2(\theta_z)}}{\chi + 1.744(\chi + 1.182)^{-0.733}} \quad (5.5)$$

Where θ_z is the solar zenith angle and χ the leaf angle distribution.

Figure 5.6: Solar zenith angle (θ_z), the altitude angle (α) and the azimuth angle (A_z) of the sun when viewed from point P [41]

Leaf Angle Distribution, χ The leaf angle distribution (LAD), describes the projection of leaf area into a horizontal surface. Depending on the plant species, it can take the following values [63]:

- $\chi < 1$ for canopies with predominately vertical orientations
- $\chi = 1$ for a mixture of orientations
- $\chi > 1$ for canopies with predominately horizontal orientations

5.2.3. Long wave radiation, R

Long wave solar radiation is the low energy counterpart of short wave radiation. It represents the infrared part of the spectrum and its emission is based on the Stephan-Boltzmann law $R = \sigma T^4$, which consists of emitted short wave radiation proportional to the temperature of the body [83]. Therefore, the emission of long wavelengths is not directly altered by the implementation of greenery systems, but is indirectly controlled by the modification of the surface properties and their temperature.

The amount of long wave radiation emitted from buildings is directly related to the surfaces albedo. The albedo of a surface represents the fraction of incident light that the surface can reflect and is an intrinsic material property which plays a pivotal role in maintaining the earth-atmosphere energy balance [13]. In general, the higher the surface albedo, the larger the amount of sunlight reflected of the surface. The albedo of different surfaces can vary significantly, however, in the case of urban surfaces like concrete it can go up to 0.55 while vegetation's albedo is commonly found in the lower range from 0.10 to 0.20.

The average albedo present in the urban environment is partly responsible for the UHI effect and its impact on the ambient temperature is discussed in Chapter 8.

5.2.4. Convective heat transfer, C_v

Convection is the mechanism responsible for heat transfer through a medium and is affected by, among other things, the speed of the air flow over a surface [86]. The amount of convective heat transfer is defined by the temperature difference as well as the heat transfer coefficient for convection α_c . For common construction materials, these values have been standardized for indoor and outdoor environments. Nevertheless, convective heat transfer between a vegetation layer and external air is more complex. According to Convertino et al. [17], this heat exchange is based on a pure forced flow model (See Eq. 5.6), which depends on the medium properties as well as the aerodynamic resistance of the plant. This resistance defines the transfer of heat and water vapor from an evaporating surface into the ambient air, involving air friction from a vegetation surface [27]. It is a function of the wind speed and the height of where measurements are taken, and varies per plant species. Reference values are taken for a grass surface following a simplified expression Eq. 5.7, which can then be converted into different plant species through constants specific to each one.

All other convective heat transfer mechanisms taking place in the façade follows the basic expression as shown in Eq. 5.8

$$CV_{ea,gl} = \rho_a * C_{p_a} * (T_{ea} - T_{gl}) * r_e^{-1} \quad (5.6)$$

$$r_e = \frac{208}{v_w} \quad (5.7)$$

$$CV_{ag,gl} = h_{ag} * (T_{ag} - T_{gl}) \quad (5.8)$$

Wind effects VGS act as a wind barrier and therefore, blocks the effect of high wind speed on a building's façade [61]. As stated in Chapter 4, Grabowiecki et al. and Perini et al. [32, 65] determined an empirical relation between a vegetation layer and wind speed, although there is limited research involving this effect. Lower wind speeds can increase the thermal resistance in a façade; therefore, the capacity of a vegetation layer to alter wind speed will be further analyzed in the following chapters.

5.2.5. Evapotranspiration

Evapotranspiration plays a monumental role in the behavior of a plant layer but relies heavily on local climate conditions and availability of water [35]. It is defined as the sum of evaporation of water from the soil surface and transpiration from plants. The concept was first developed by Howard Penmann in 1948 and defines the latent heat flux from vegetation [27], which led to the development of the Penmann-Monteith equation in 1965 (See Eq. 5.9).

$$\lambda ET = \frac{\Delta(R_n - G) + \rho_a * C_{pa} * \frac{(e_s - e_a)}{r_a}}{\Delta + \gamma \left(1 + \frac{r_s}{r_e}\right)} \quad (5.9)$$

Where R_n is the net radiation, G the soil energy flux and Δ the slope of the saturation vapor pressure-temperature.

As both soil evaporation and plant transpiration take place simultaneously, it is complicated to make a clear distinction. However, when a plant has a lower coverage or foliage density, soil evaporation is predominant. The opposite leads to higher levels of transpiration which is regulated by the total water coefficient of substrate for plant [51]. To measure the effects of the evapotranspiration process for the heat flux through a façade, an estimation of the latent heat release associated with this process is commonly used. The rate of latent heat release was adapted from Eq. 5.9 in Convertino's [17] thermal model which is shown in Eq. 5.10.

$$\Phi = \rho_a * C_{pa} * \frac{(e_s - e_a)}{\gamma * (r_s + r_e)} \quad (5.10)$$

Where ρ_a and C_{pa} are the density and specific heat of air respectively, e_s the air vapor pressure at saturation, e_a the partial air vapor pressure, γ the psychrometric constant, r_s the build surface resistance and r_e the aerodynamic resistance of the vegetation layer.

Leaf energy balance The energy balance of a vegetation layer relies on the internal processes of its basic component: leaves. A typical leaf is commonly represented as a flat, thin plate with radiative and convective heat exchange with its surroundings¹. To obtain the amount of heat transfer between a leaf and its environment, the leaf surface temperature can be obtained using the method developed by Campbell [10], which shows the complexity of the leaf functions as well as the large amount of factors involved in its estimation, for example: solar radiation, air humidity, wind speed and internal CO₂ concentration and stomatal conductance.

Among these factors, the stomatal conductance g_l , is of particular interest. It provides an indication of the rate of water vapor that is leaving the plants surface through its pores during transpiration, and measures the degree of stomatal opening which can be used to determine the plant water status [29]. The rate of water vapor leaving the plants depends on the amount (0.2-2%) and pore size as well as their location on the leaf's surface. Pore size regulates the gas exchange between the plant and its environment which adjusts to the temperature and humidity conditions depending on the plants requirements and atmospheric conditions [81]. Based on their morphology, leaves can be classified as either amphistomatous which have pores on both sides of a leaf, or as hypostomatous with pores only on the lower surface of the leaf.

The effects of stomatal conductance on the energy balance of a leaf are highly dynamic and depend on the plant species. In general, lower values of stomatal conductance decrease the latent heat release from evapotranspiration. However, the full effects of the stomatal conductance on the energy balance of a VGS are outside of the scope of this thesis.

FAO adaptation of the Penmann-Monteith equation Identifying the water requirements for proper plant growth is particularly relevant for the agricultural sector. These requirements can be obtained through the estimation of the evapotranspiration rate which allows an accurate prediction of water use [51]. As these requirements are specific to each plant species,

¹Conductive heat transfer is often neglected due to its minimal contribution [81]

the Food and Agricultural Organization of the United Nations (FAO) developed a simplified method to determine the evapotranspiration rate of any plant based on a reference crop. The evapotranspiration rate incorporates factors specific to the plant species K_c , which contains the effects of individual crop characteristics and soil evaporation; and K_s which considers the water stress due to droughts. Nevertheless, as long as the moisture level in a soil does not go below the management allowable depletion, no permanent wilting should take place in the plant [66].

5.3. Substrate thermal and physical properties

The substrate layer on a VGS, besides serving as a growing medium for the vegetation, serves a dual purpose of insulating the building. Soil properties, such as moisture content, density, thickness, among others; define its thermal properties which can be modified in order to obtain an efficient design. Therefore, the influence of these properties and their effects on the soil's behavior must be understood. This section will analyze the effects of moisture content and density on a substrate layer; which as been taken as a sandy loam soil type due to the optimal growing conditions it gives to vegetation [2].

5.3.1. Moisture related properties

The amount of moisture present in a substrate layer is crucial in determining a plant's growth. Therefore, several limits exist in order to guarantee that enough moisture will be present in the soil to allow proper plant growth but not low enough so that wilting will take place. These limits are related to the soil type and have no relation to the amount of moisture required by plants, they are simply an indication of the soil's capacity to absorb and retain water. For these reasons, the following parameters have been defined [85]:

Field capacity Amount of water that is remaining on the soil after a few days after being wet and free drainage has ceased.

Permanent wilting point Water content of a soil when most plants wilt and fail to recover.

Water coefficient of substrate for plant (WC) Amount of water that can be effectively absorbed by plant roots. It is the amount of available water, stored or released between the field capacity and the permanent wilting point.

For the case of sandy loam soil types, the field capacity is approximately 20% and the permanent wilting point ranges from 10 to 15%. Based on these values, the water coefficient of substrate for plant can be defined. It has been defined in a range varying from 0.60 to 1.00, indicating that in this soil type, plants can absorb a minimum of 60% to 100% of the moisture left in the soil once it has naturally drained.

5.3.2. Influence of density and moisture content on soil thermal properties

As stated before, density, moisture content and substrate thickness are directly related to the thermal conductivity of the material, which can change its insulating properties [1, 2]. As seen on Figure 5.7 there is a directly proportional relation between the density and the thermal conductivity λ , and the moisture content and the thermal conductivity, lowering the insulation effect provided by the layer. This effect is caused by a reduction of the porosity of the substrate, which is replaced by either soil or water allowing an easier movement of heat due to a lower thermal conductivity when compared to the previously air filled pores.

5.3.3. Thermal mass

In many countries worldwide, vernacular architecture principles include heavy building materials to control extreme temperature fluctuations. Their capacity to store and release heat has been invaluable to create comfortable living conditions in a variety of weather conditions. For example the use of thermal mass has been implemented in projects for centuries in Gothic style architecture. The full effects of thermal mass in a building are a dynamic

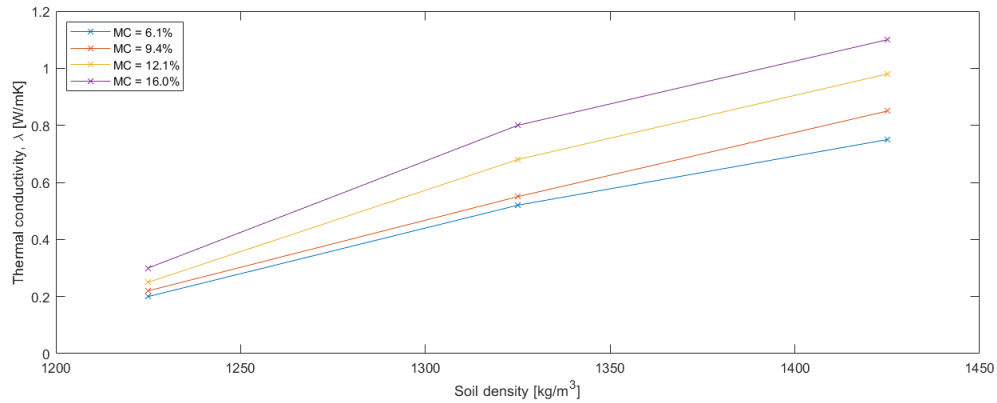


Figure 5.7: Thermal conductivity as a function of soil density and moisture content for sandy loam soil type [2]

problem involving material properties as well as time, which has been formulated by Fourier in his heat equation (Eq. 5.11).

$$\frac{\partial T}{\partial t} = D \frac{\partial^2 T}{\partial z^2} \quad (5.11)$$

However, due to variable moisture levels in a VGS, a simplified analysis was carried out. The amount of heat stored in the substrate layer was calculated as a function of the specific heat capacity for a particular density and moisture content, which is represented by the wet density seen in Eq. 5.12, and by the volumetric heat capacity seen in Eq. 5.13.

$$\rho = \frac{\rho_d}{1 + w} \quad (5.12)$$

$$c = \rho \frac{c_s + w c_w}{1 + w} \quad (5.13)$$

The volumetric heat capacity can then be used to determine the temperature increase of the sample. Considering that $Q = C_v * \Delta T$ and $Q = P * t$, with $P = E_1$, the following expression is derived:

$$\Delta T = \frac{t * E_1}{C_v} \quad (5.14)$$

Eq. 5.14 shows the increase of temperature caused by the solar radiation incident on the bare surface of the substrate as a function of the density and moisture content during 60 minutes. Results obtained from this analysis are presented in Figure 5.8².

5.4. Summary

A description of all the components involved in a vertical green system was performed. Two analysis cases are taken into account: a direct green wall and an indirect continuous living wall system meant to understand the different physical phenomena associated with their behavior. Furthermore, the energy balance of the systems were broken down and each component analyzed individually to create a parametric approach of the problem which allows the creation of a quantifiable mathematical model. The effects of short wave radiation, long wave radiation, convective heat transfer, evapotranspiration and substrate insulation identified the main variables responsible for the behavior of the system showing the potentially large effects that changes in the composition of VGS can have on their thermal performance.

²Solar radiation is assumed as 800 W/m² and substrate thickness as 15 cm

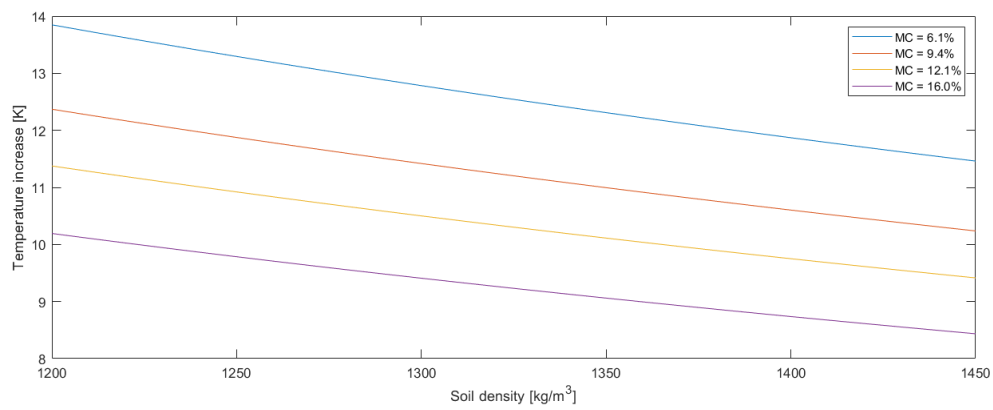


Figure 5.8: Temperature increase as a function of soil density and moisture content during 60 minutes

6

Computational Workflow and Model Definition

This chapter will detail the definition of the parametrized mathematical model, its conception, software formulation and boundary conditions used for the evaluation of the VGS described in Chapter 5.

6.1. Parametric modelling

Parametric design is a fascinating tool based on algorithmic thinking that allows the expression of complex problems through the use of parameters and rules that create a design when bound together [42]. It allows for a geometrical representation of entities with editable attributes and relationships. Attributes, or design variables, can be expressed as independent values serving as inputs for the model that lead to different solutions. Every solution obtained from a parametric definition is generated respecting the previously defined relationships between the design variables.

A parametric approach has the capacity of generating high flexibility in the design process which allows an exploration of different configurations and geometries for a better perception of the end result. The design exploration process can significantly increase the efficiency of the design process as a multitude of solutions can be evaluated for a particular objective. Based on the specific constraints of the problem, the optimal solution can be found in the design landscape that fits the objective function while respecting the boundary conditions.

In the case of architectural or engineering design processes, parametrization is highly beneficial as it is suited for the integration of different disciplines. For the optimization problem tackled in this research, parametrization allows the creation of a continuous workflow meant to test and evaluate several configurations of vertical greenery systems (VGS), by means of the mathematical relationships that represent the physical processes governing their behavior.

Although parametric modelling is mostly associated with architectural projects or geometry related problems, its potential to break down complex problems and analyze the relationship between its building blocks can be applied to an endless number of projects. As detailed in Chapter 5, the performance of a vegetation layer depends on several individual variables. Although many aspects influence the performance of a VGS under a particular set of boundary conditions, the dominant variables were studied to obtain a better understanding of the system's behavior. This led to the development of design considerations, or rules of thumb which can be used for a large scale implementation of VGS in urban areas. Parametric design tools are used to define the basis for the computational workflow of this research, which has shown its potential for the definition of complex problems and to increase efficiency by reducing computational time and resources.

6.2. Computational workflow

Due to the bulky computational component in this research, this section will go over model definition and the workflow created meant to ensure an automatic simulation process.

6.2.1. Software packages

The workflow conceived to simulate the micro-climate conditions created by a greenery system, takes full advantage of several software packages. The optimization study is based on an integration of these software packages which allowed the evaluation of the VGS effects in a smooth workflow with an efficient simulation time. To do so, three different software packages and an additional programming language were used. A brief description is shown in the next list:

- ENVI_met: holistic three dimensional non-hydrostatic model used for the simulation of surface-plant-air interactions often used to simulate urban environments and to assess the effects of green architecture. (<https://www.envi-met.com/>)
- Rhino/Grasshopper (GH): graphical algorithm editor tightly integrated with Rhino's 3-D modeling tools, allowing for design exploration using generative algorithms. (<https://www.grasshopper3d.com/>)
- modeFRONTIER (mF): modular environment for process automation and optimization in the engineering design process. (<https://www.esteco.com/modelfrontier>)
- Python 3: programming language optimized for quick and effective integration between systems. (<https://www.python.org/>)

6.2.2. Integration

The integrated workflow used several features of each software combining them to achieve the objectives set for this research. The models were simulated parametrically and aimed to analyze the micro-climate conditions generated by a VGS. The combination of different software packages led to the development of a new workflow that can be used as the basis for further research involving optimization of the atmospheric conditions in an urban setting.

The model definition uses GH as its design environment with the Dragonfly component developed by Chris Mackey and Antonello Di Nunzio which supports large-scale climate and urban heat island simulation¹. The plugin allows the creation of the entire ENVI_met workflow, from the definition of the model space, materials, weather forcing and simulation configuration directly into the GH canvas. Nevertheless, as the plugin was recently released, several features were missing which were needed for the proposed workflow. These components were scripted with the use of GHPython and GH_cPython² to allow a higher flexibility and control of the model inputs and results. Among them, the components allowed the initialization of the model, defining the materials used for the VGS, calculation of the transmissivity τ , based on the LAI, χ and θ_z ; recognition of the simulation's completion, and automatic data post-processing used for the optimization study as seen in Figure 6.1.

Once the entire model definition is completed the analysis starts following the workflow seen in Figure 6.2. With the source model defined in GH, mf is used to launch the simulations. Modifications in the input variables are given from mF to the GH canvas and processed through Dragonfly. The output is created through predefined components³ and given as an input to mF which then uses them for further post-processing. Once the simulation is finished, a new set of input variables is given and the process starts over. In general, to complete an optimization process, a predefined criteria is used to determine the point at which the optimization will end. This is usually taken as an increase in the performance of the model which guarantees convergence. Nevertheless, due to the large computational

¹For more information about this plugin and all its components see <https://github.com/chriswmackey/Dragonfly>

²Both plugins are Python interpreters for GH. Nevertheless, GHPython is an embedded plugin able to run basic Python scripts optimized for the Rhino environment, while GH_cPython implements CPython codes inside GH allowing access all Python scientific libraries.

³All component scripts are detailed in Appendix D

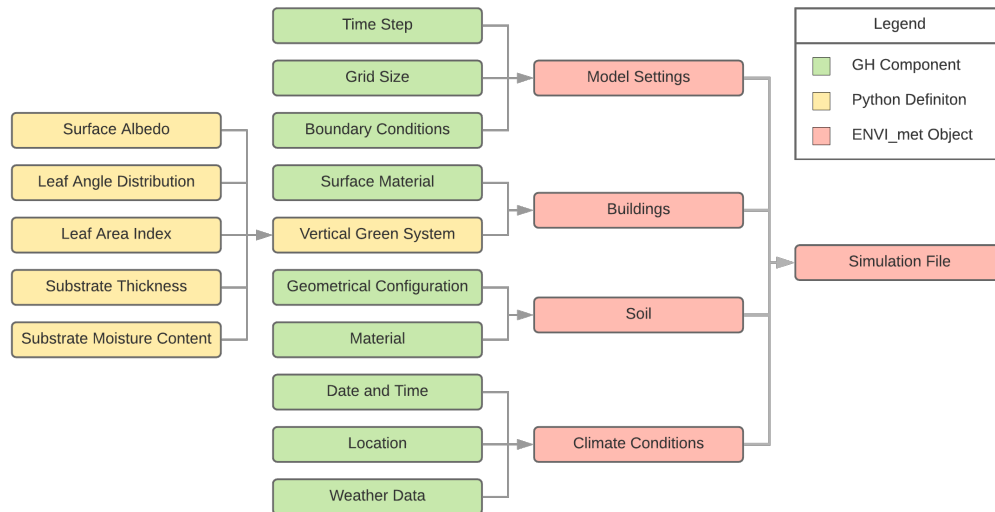


Figure 6.1: Definition of the ENVI_met model in Grasshopper in combination with Python

times associated with this simulations, a fixed amount of 60 loops was assumed to be sufficient to create a meaningful representation of the design landscape. The 60 simulations indicate the behavior of the system with different initial conditions as well as an approximation of the optimal configuration of the VGS. With the optimization process taking place in mF, 30 simulations were performed as a design of experiments (DOE) based on a uniform latin hypercube sampling to obtain an initial understanding of the design landscape. The additional 30 simulations were performed with the piLOPT blackbox optimization algorithm⁴, which draws information from the DOE and uses it as an first "generation" (as an analogy with genetic algorithms) for the optimization process, further increasing the overall speed and performance of the optimization algorithm.

Nevertheless, to reduce the large computational times mentioned before, commonly associated with similar optimization studies, a computational time study was made to determine the optimal grid size and time step of the model in ENVI_met without major accuracy loss. The study concluded that a grid size of five meters in X, Y and Z directions was ideal, while respecting the geometrical configuration of the model. Additionally, the changes in time steps were minimally influential in the computational times, therefore the default values recommended by ENVI_met were kept for all simulations⁵.

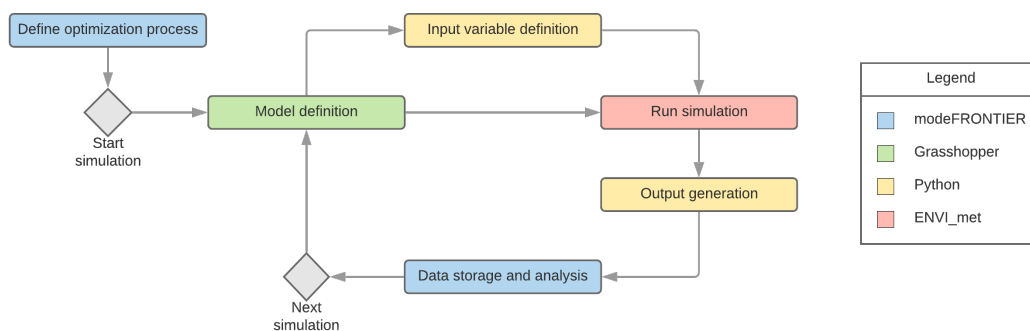


Figure 6.2: Overview of the integrated work-flow for the optimization of the greenery system

⁴More information regarding the definition and analysis of suitable algorithms for the optimization process is shown in Appendix B

⁵The computational time study definition and results are shown in Appendix A

6.3. Model definition

6.3.1. Urban street canyon

The impact of VGS can not only be observed in the building where it is installed, but it has an important effect in its surroundings. This study of environmental changes aims to identify the extent of the effects of urban vegetation on the ambient temperature magnitude and distribution. To do so, an urban context was conceived to accurately resemble the UHI effect and all the phenomena associated with wind fluid dynamics, temperature distribution, heat transfer, among others.

The theoretical concept of an urban canyon came from T.R. Oke in 1976 as there was a need to adequately define the energy balance of an urban environment. Urban street canyons are used to represent an urban setting comprising of narrow streets with buildings lined up on both sides with a predefined aspect ratio H/W^6 , as seen in Figure 6.3. It is a simplification of the complex configuration of an urban area and allows the representation of the three-dimensional nature of an urban canopy through the repetition of standardized units [54]. This repetition creates a portrayal of an urban area which simplifies the mathematical representation and computational analysis performed in this research. Due to the crucial importance of an urban canyon's geometry on air flow and temperature distribution [56], a symmetric street canyon with a N-S orientation and an aspect ratio of 1.0 has been taken for the base geometrical definition of the model. The $H/W = 1.0$ aspect ratio represent a regular street canyon [87], frequently found in urban settings.

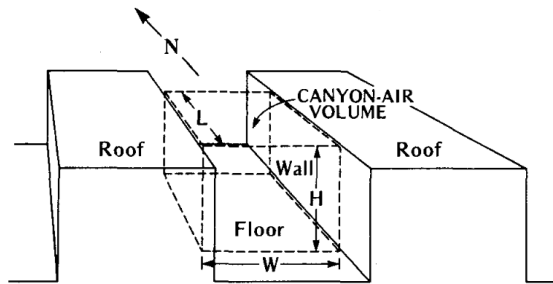


Figure 6.3: Schematic representation of an urban street canyon [54]

Furthermore, the aspect ratio of the urban canyon was extrapolated to fit a symmetrical 3D space of nine buildings. The buildings width is 30 meters in X and Y directions with a height of 15 meters same as the width of the street. Nevertheless, the latter is broken down in a three meter yard next to the buildings, and a nine meter asphalt road representing sidewalk and vehicle roads. Figure 6.4 details the measurements⁷ and configuration of the urban street canyon used for this research.

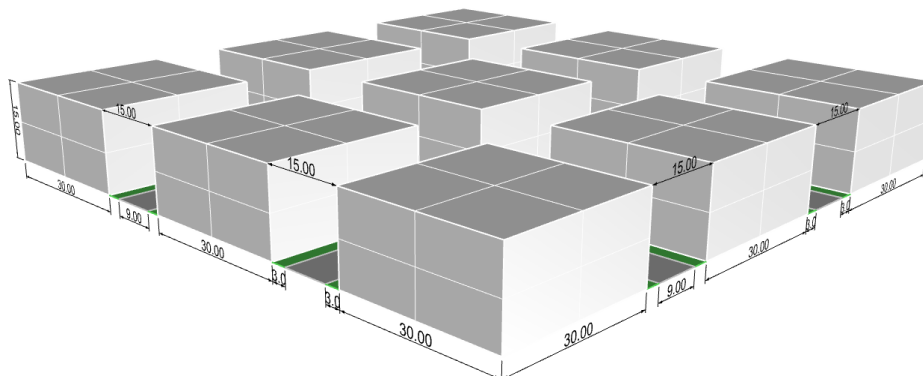


Figure 6.4: 3D view of the urban street canyon

⁶Height over Width

⁷Measurements are in meters

Albedo	Adapted	0	1	2	3	4		
	Real	0.09	0.12	0.15	0.18	0.21		
Leaf Area Index	Adapted	0	1	2	3	4	5	6
	Real	0.1	0.4	0.7	1	1.3	1.6	1.9
	Adapted	7	8	9	10	11	12	13
	Real	2.2	2.5	2.8	3.1	3.4	3.7	4.0
Leaf Angle Distribution	Adapted	1	2	3				
	Real	0.5	1.0	1.5				
Substrate Thickness	Adapted	0	1	2	3	4		
	Real	0.6	0.7	0.8	0.9	1.0		
Moisture content	Adapted	0	1	2	3			
	Real	0.15	0.20	0.25	0.30			

Table 6.1: Variable values, boundaries and constraints used for simulations

Nine buildings are considered in the whole urban setting, using the exterior eight to create a buffer zone around the central building to accurately represent the real conditions in its surroundings. Enabling the evaluation of the full effects of building integrated vegetation on the performance of a building regarding its heating and cooling demands. To fully understand the effects of VGS, a reference model consisting of nine concrete buildings, was used as a benchmark for the project. This model was used throughout all the simulations regardless of climate conditions and type of VGS, setting a frame of reference to easily interpret the changes caused by the alteration of the initial conditions of the system.

6.3.2. Additional modelling considerations

Rhino/Grasshopper A considerable amount of adaptations had to be done to the predefined work-flow in Dragonfly plug-in for GH. As detailed before, auxiliary components had to be scripted to compensate the lack of functions required for the research project. Although new components are currently under development to complement the existing library in Dragonfly, by the time this research took place they were not available to the general public.

The auxiliary components took advantage of the built-in scripting capabilities existing in Grasshopper. Although several Python libraries are included in the embedded Python component in GH, additional functions were needed. Therefore, to access all the libraries required from Python, GH_CPython, a Grasshopper component developed by Mahmoud Abdel Rahman [68] whose idea is to provide a component that implements CPython codes inside Grasshopper was used which allowed access to libraries such as Numpy and Pandas. This libraries work with fast numeric array computations which were required to read the EDX/EDT file formats used by ENVI_met to store all simulation results⁸.

During the optimization study, each VGS had a different set of variables that controlled its performance. For LWS, three variables detailing the vegetation layer and two detailing the substrate layer performance were used, while GF only considered the variables influencing the vegetation layer. To simplify the process and reduce optimization times, constraints were placed on the variables to reduce its range and control their step limiting the large amount of possible combinations in the configuration of the systems. The constraints defined for each parameter were based on a literature review which identified the values commonly found in practice. As seen on Table 6.1, Adapted values relate to the values in the computational (GH/mF) definition while Real ones correspond to the true values used in the simulations which effectively represent the configuration of both the vegetation and substrate layers.

ENVI_met The ENVI_met model definition follows a straightforward process. The software creates a three-dimensional space comprised by blocks whose size are based on the grid def-

⁸Full scripts are shown in Appendix D

inition. These blocks can be used to create countless geometrical typologies however, they are limited when dealing with curved geometries. Therefore a regular, rectangular and symmetrical configuration is used for all nine buildings in the models to reduce computational times and simplify the post-processing of results.

The benchmark model consists of a similar material configuration for all elements. The offset of three meters around the buildings are modelled as a grass layer (0000XX⁹), while the rest of the roads and sidewalks are modelled as asphalt road surfaces (0000ST⁹). The rest of the surfaces in the envelope of the buildings are assigned as heavy concrete (0100C1⁹) with $\lambda = 1.30 \text{ W/m}^2\text{K}$ and a wall thickness of 0.30 meters. Furthermore, it should be noted that no ventilation nor fenestration is considered to purely analyze the heat flux through the facade and a constant indoor temperature of 20°C has been set for both heating and cooling dominated climates, and the vegetation layer was assumed to have a stomatal resistance r_s , of 200 s/m.

To aid with the simulation process, ENVI_met possesses two additional configurations. The option to create a telescoping grid and the use of nesting grids. Nesting grids are used to create more reliable results in the edges of the model. As the model definition extends to little over the edges of the buildings, a nesting grid of 3 additional cells was defined to improve the stability of the model. Telescoping on the other hand, allows the creation of larger separations of individual grid cells after a defined point. It allows a coarser definition were results do not require to be as detailed. Therefore, for all models, the telescoping distance was taken at three meters above the highest building point (18 meters) with a growing percentage of 50% until a maximum height of 30 meters is reached. The maximum height in an ENVI_met model must be at least twice the height of the highest building as it aids in the calculation of computational fluid dynamics and in the convergence of the simulation, as stated by the software's developers.

modeFRONTIER The optimization process is meant to try different configurations of the VGS to minimize heating and cooling demands for each weather conditions. The process takes the input and interprets the results from GH to understand the relations governing its behavior. An example of the work flow used for the optimization study of the LWS is shown in Figure 6.5, showing the input and output variables, as well as conditions for the termination of the simulation in case of unexpected errors. This condition was required due to the errors that arose during the testing period, which led the the simulations in ENVI_met and the entire workflow, to crash. Therefore, a condition that recognize this error was created that allowed a continuous and automatic workflow, skipping faulty simulations and finalizing the optimization study without interruptions or unexpected crashes.

6.4. Climate conditions

In problems related to energy efficiency within the built environment, weather is of paramount importance. As stated in Chapter 2 and 5, passive energy reduction techniques provided by bio-climatic strategies are highly sensitive to the climate they are working on. VGS are a passive energy saving tool used for several purposes, however, their biological component suggests that they are highly sensitive to atmospheric boundary conditions. For example, the weather's effect in plant growth, and on their physiological responses such as transpiration, needs to be considered [62] to fully determine the effects of a vegetation layer in an urban environment and on a building's thermal performance. Therefore, a diverse group of climate conditions has been considered for the analysis. Climate conditions ranging from sub zero temperatures to 40+ °C with varying relative humidity are used aiming to understand the influence of different temperatures and relative humidity levels in the performance of a VGS. Furthermore, to create a reliable and theoretical sound analysis, the Köppen-Geiger climate classification system is used to set a foundation for the climate conditions used in the simulations.

⁹Refers to the ENVI_met material code predefined in the database manager



Figure 6.5: modeFRONTIER simulations work-flow for LWS

6.4.1. Climate zones

The Köpper-Geiger climate classification was developed by Wladimir Köppen in 1900 and was updated by Rudolf Geiger in 1961. It took Köppen’s experience as a botanist which allowed him to identify the pivotal role plants have as climate indicators [62]. The Köpper-Geiger classification identifies five main climate types, each with its own sub-categorization. This sub-categorization is based on temperature ranges and the amount of precipitation that is taking place in a particular location. The criteria used for it is shown in Table 6.2.

Type	Description	Criterion
A	Equatorial climates	$T_{min} \geq + 18 \text{ }^\circ\text{C}$
Af	Equatorial rainforest, fully humid	$P_{min} \geq 60 \text{ mm}$
Am	Equatorial monsoon	$P_{min} \geq 25 (100 - P_{min})$
As	Equatorial savannah with dry summer	$P_{min} < 60 \text{ mm in summer}$
Aw	Equatorial savannah with dry winter	$P_{min} < 60 \text{ mm in winter}$
B	Arid climates	$P_{ann} < 10P_{th}$
BS	Steppe climate	$P_{ann} > 5P_{th}$
BW	Desert climate	$P_{ann} \leq 10P_{th}$
C	Warm temperate climates	$-3 \text{ }^\circ\text{C} < T_{min} < + 18 \text{ }^\circ\text{C}$
Cs	Warm temp. climate with dry summer	$P_{smin} < P_{wmin}, P_{wmax} > 3P_{smin}, P_{smin} < 40 \text{ mm}$
Cw	Warm temp. climate with dry winter	$P_{wmin} < P_{smin} \text{ and } P_{smax} > 10P_{wmin}$
Cf	Warm temp. climate, fully humid	Neither Cs nor Cw
D	Snow climates	$T_{min} \leq -3 \text{ }^\circ\text{C}$
Ds	Snow climate with dry summer	$P_{smin} < P_{wmin}, P_{wmax} > 3P_{smin}, P_{smin} < 40 \text{ mm}$
Dw	Snow climate with dry winter	$P_{wmin} < P_{smin} \text{ and } P_{smax} > 10P_{wmin}$
Df	Snow climate, fully humid	Neither Ds nor Dw
E	Polar climates	$T_{max} < + 10 \text{ }^\circ\text{C}$
ET	Tundra climate	$0 \text{ }^\circ\text{C} \leq T_{max} < +10 \text{ }^\circ\text{C}$
EF	Frost climate	$T_{max} < 0 \text{ }^\circ\text{C}$

Table 6.2: Criteria used to categorize climate conditions based on temperature and precipitation amount

6.4.2. Weather data selection

Three independent weather conditions have been considered for this research based on the Köppen-Geiger climate classification. The selection of these weather conditions aim to obtain a wide overview of climate conditions where VGS have shown to have positive benefits, having temperature and relative humidity as the principal considerations due to their considerable influence in a vegetation's layer behavior. Additionally, different locations worldwide were chosen to examine the effects of sun inclination or solar zenith angles θ_z as seen in Figure 5.6. Chapter 5, shows the significant relation between the leaf angle orientation χ , and the transmissivity of the vegetation layer which has a dominant role in the amount of short wave radiation effectively transmitted through the vegetation layer. The combination of different weather conditions regarding temperature and relative humidity levels, paired with locations with different solar zenith angles give an understanding of the response of VGS in any climate condition worldwide and has the additional benefit of allowing an accurate extrapolation of results for climate conditions and locations that are not directly considered in this research.

Therefore, three individual cities have been selected, each with a different latitude, and temperature and corresponding relative humidity. The following list details the characteristics of each selected climate condition, and their corresponding category in the climate classification¹⁰:

1. Group Af: equatorial rainforest, fully humid. Characterized by an average temperature of over 18°C with a minimum precipitation of $P_{min} \geq 60\text{mm}$. For this case the City of Singapore (1.3521°N , 103.8198°E) is considered due to its close proximity to the equator (See Figure 6.9a). The hottest day in the year was considered for the analysis, with a temperature and relative humidity as shown in Figure 6.6.

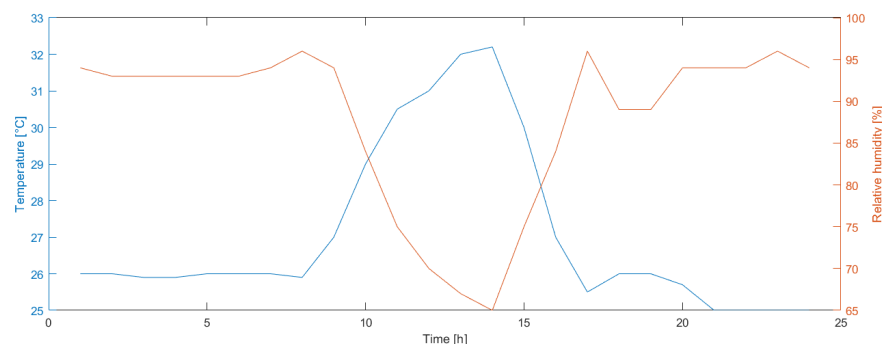


Figure 6.6: Temperature and relative humidity during 01/04/1989 in Singapore, Singapore

2. Group BW: desert climate. Characterized by $P_{ann} \leq 5P_{th}$. For this case the city of Phoenix, AZ (33.4484°N , 112.0740°W) is taken due to its high temperature and low relative humidity during the hottest day of the year. Its location in the middle latitudes of the globe is also taken advantage as the zenith angle changes in comparison with Group A (See Figure 6.9b). The temperature and relative humidity weather data are shown in Figure 6.7.

¹⁰Full weather files can be downloaded from <http://www.ladybug.tools/epwmap/>

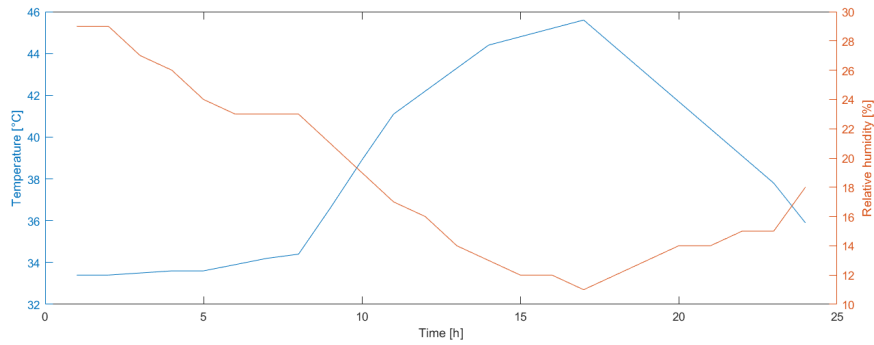


Figure 6.7: Temperature and relative humidity during 01/08/1988 in Phoenix, AZ, USA

3. Group Cf: warm, temperate, fully humid climate. Characterized by having an average temperature between -3°C and 18°C with high humidity levels throughout the year. For this case the city of Amsterdam, NL (52.3680°N , 4.9036°E) is used. In contrast with the previous groups, the coldest day in the year was considered as seen on Figure 6.8.

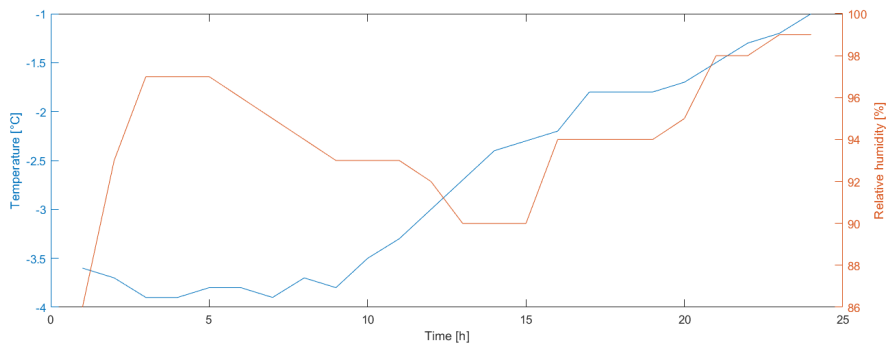


Figure 6.8: Temperature and relative humidity during 06/01/1995 (winter conditions) in Amsterdam, NL

Furthermore, Figure 6.9 shows the clear difference in the sun paths for each selected location. The variation in the solar zenith angle from Singapore to Amsterdam provides the analysis of intermediate locations where results and conclusions can be derived. The influence of sunlight orientation has a considerable effect when bio-climatic strategies are in use, as they significantly reduce heating and cooling demands in buildings as well as daylight and visual comfort, nevertheless, the latter will not be considered in this research.

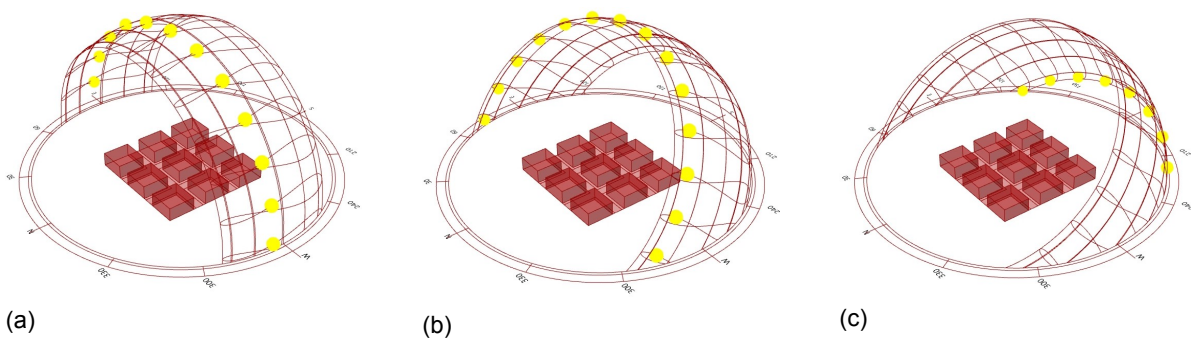


Figure 6.9: Sun path diagrams for (a) Singapore, (b) Phoenix and (c) Amsterdam

6.5. Summary

The parametric approach used for the definition of the computational model is described in this chapter. The integrated workflow uses ENVI_met, Grasshopper and modeFRONTIER in combination with Python scripts to create a smooth and automatic workflow used for the evaluation of the performance of the VGS in an urban setting. Additionally, the urban geometry is defined based on the urban street canyon definition created by T.R. Oke with a height to width ratio of 1.0. Furthermore, an overview of the climate conditions used in the simulations is presented. They include a wide array of conditions in different locations worldwide ranging from equatorial climate (Singapore), desert climate (Phoenix) and temperate climate (Amsterdam).

Impact of Vertical Greenery Systems on Heat Transmission

This chapter will present the results obtained from the optimization study regarding their performance as an insulation material by limiting the heat transmission through the façade in each of the three climate conditions defined in Chapter 6.

7.1. Introduction

The heating and cooling demand calculations are based on the energy flow through the façade of the reference buildings due to heat transmission through the façade. To do so, the full effects of the analyzed VGS are represented by the change in the temperature of the outer layer of the building's wall, which can be analyzed through the wall model used in ENVI_met. This multi-node model approach provides a clear grasp on the heat flow through different materials in a wall and allows the calculation of the outside surface temperature based on the façade's energy budget [77]. This calculation follows the transmission heat transfer equation (Eq. 7.1) through a solid medium [86] under each hour during a one day period. Furthermore, the individual heat transferred in each grid-cell of the model's façade was calculated and summed to obtain the total heating or cooling demands for the building. Apart from heat resistance provided by the thermal conductivity of the façade, no additional resistances, e.g. surface air resistance, are taken into account in the calculations.

$$Q_{trans} = U * A * (T_o - T_{in}) \quad (7.1)$$

Where U is the thermal transmittance of the façade, calculated by $U = 1/R = \lambda/d$ with R as the thermal resistance, λ as the thermal conductivity of the material and d as the wall thickness; A is the façade's surface area, T_o the outer surface temperature of the wall and T_{in} the indoor building temperature.

As a result, negative values of Q_{trans} indicate that the building requires heating while positive values indicate cooling requirements. Furthermore, the results of the optimization study presented in this research are verified by simple calculations based on Convertino's thermal model for a vegetation layer [17]. Whereby, the result show an interdependent relationship between heating and cooling demands and the latent heat transfer associated to the evapotranspiration process of a VGS.

7.2. Parameter variability on thermal demands

Every parameter included in the definition of a VGS has an influence on the performance of the system as a whole. Nevertheless, some have a much larger effect on controlling the heat transmission flux and therefore on reducing the heating or cooling demands in a building. The preliminary study performed in Chapter 5 showed that some factors have a predominant role in the heat transfer properties of the system, such as the relative humidity, the stomatal

conductance and the bulk and aerodynamic resistance. However, the optimization study gave a deeper understanding of the influence of the different factors on the design landscape due to the insight of the relations existing within the system. Although both VGS under consideration have a similar composition, their unique characteristics have a direct relation to the thermal properties of the system. For a better understanding, Table 7.1¹ shows the correlation factors obtained from green façades (GF) and from living wall systems (LWS) for each parameter, together with their respective impact on cooling dominated climates (CDC) and heating dominated climates (HDC).

	Green Façade		Living Wall System	
	CDC	HDC	CDC	HDC
Albedo	-0.254 to -0.360	0.207	0.058 to 0.234	0.159
LAD	-0.120 to 0.034	0.007	-0.179 to 0.176	-0.238
LAI	-0.585 to -0.958	-0.977	-0.400 to -0.432	-0.870
Thickness	-	-	-0.407 to -0.342	-0.724
WC	-	-	0.002 to -0.102	-0.114

Table 7.1: Correlation factors for thermal demands in green façades and living wall systems

The correlation factors show a higher influence of the LAI and albedo on the performance of a GF when compared to a LWS. More precisely, in the case of a GF, the LAI has the highest effect on the thermal behavior of both GF and LWS, followed by the albedo and by a lower extent the leaf angle distribution (LAD). These correlations allowed a deeper understanding of the system which proves to be useful for its design. Furthermore, it can also be seen that the performance of the VGS depends on the weather conditions, thus indicating the importance of the boundary conditions, which will be the focus of further analysis in this research.

On the other hand, for a LWS, the LAI has the largest contribution towards the the reduction of both heating and cooling demands, followed by the substrate thickness, the leaf surface albedo and lastly by the water content in the substrate layer. Additionally, further analysis showed that the effects of the LAI and the substrate thickness are higher in HDC than in CDC, proving the importance of the boundary conditions, i.e. weather conditions. The remainder of the parameters which includes the albedo, the LAD and the water coefficient have a lesser contribution to the heating and cooling demands through heat transmission.

Although the correlation matrix shown in Table 7.1 offers a reliable insight into the performance of both VGS, it is however, not enough to fully understand the intricate relations present in this problem. Hence the following sections will show a detailed analysis of the effects of each parameter in the transmission heat flux of the systems.

7.3. Living wall system

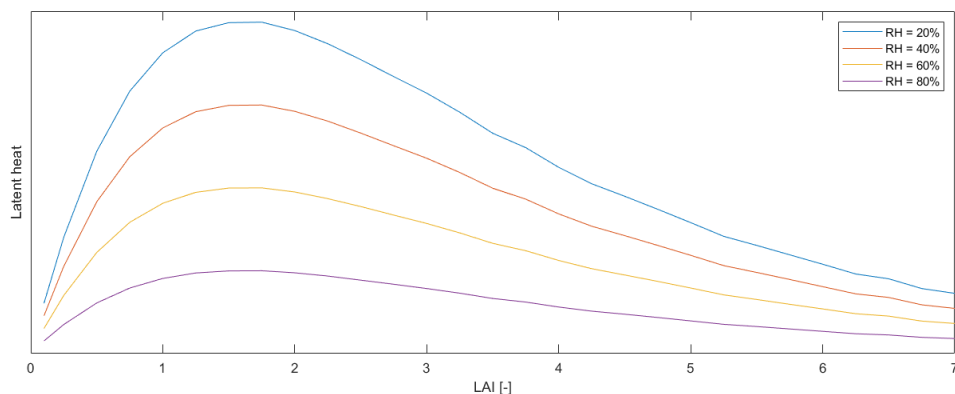
In this section the results obtained from the simulations defined in Chapter 6 of the living wall system are shown. Afterwards, the outcome of the optimization process on the heat transmission through the façade is presented².

7.3.1. Leaf area index

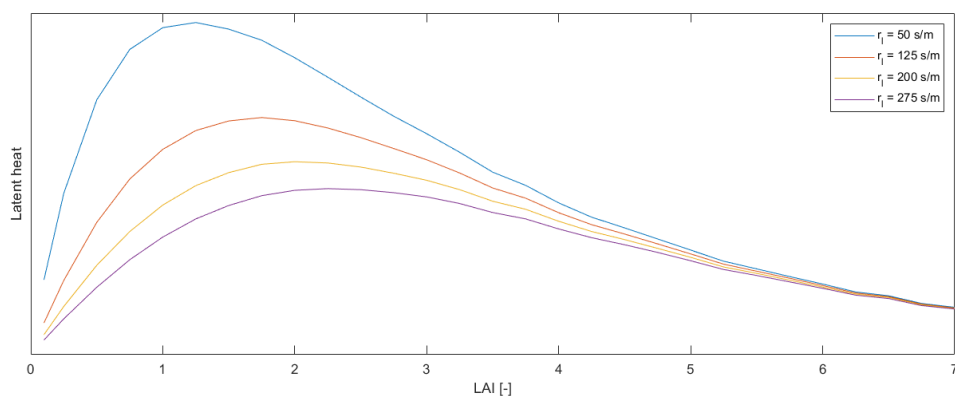
As already described in Section 7.2, the LAI has a dominant role in the performance of both types of VGS. Nevertheless, several aspects need to be understood first to fully explain the results obtained from the optimization study. Among them, the influence of the relative humidity in the ambient air can drastically affect the evapotranspiration process. More precisely, based on the vegetation thermal model [17] the latent heat release and therefore, the effective temperature in the façade's surface, is minimal with a high relative humidity and

¹The value ranges shown for cooling dominated climates refer to the results for the Singapore and Phoenix weather conditions respectively

²Appendix C, shows the full simulation results for the living wall systems in every climate condition obtained from the optimization study



(a)



(b)

Figure 7.1: Effects of relative humidity (a) and stomatal resistance (b) on latent heat release

reaches a maximum with low relative humidity as seen in Figure ??³. This behavior is caused by its proximity to the water vapor saturation of the ambient air, which reduces the amount of moisture that can be released by the plant through its stomata. Furthermore, as dry climates are characterized by low relative humidity, the effect of the evapotranspiration process is significantly higher as there is a higher gas exchange between the ambient air and the plant in order to create an equilibrium in the system. Alternatively, this can be understood by the vapor pressure deficit (VPD), which is a measurement of the drying power of the atmosphere [51] and is responsible for the amount of moisture that can effectively leave the plant.

As stated in Chapter 5, the stomatal resistance is responsible for the gas exchange between the leaves and the atmosphere. Furthermore, the degree of stomata opening is one of the defining factors in the evapotranspiration rate. As seen on Figure 7.1b, the stomatal resistance controls the peak value of the latent heat release due to the dominant role of the bulk surface resistance, which describes resistance of vapor flow through the transpiration effects of the vegetation layer as well as the evaporation from the soil surface [27]. Therefore, due to a low leaf coverage, soil evaporation is mainly responsible for the evapotranspiration rate, while both the transpiration effects and aerodynamic resistance of the vegetation layer can be considered negligible. Nonetheless, in denser canopy layers, the contribution from soil evaporation is significantly lower due to the transmissivity degree of the vegetation layer (See Eq. 5.3 and Figure 5.4), as plant transpiration increases due to more energy intercepted by the canopy. As a result, the reduction of heat flux reaches a minimum due to the varying contribution of the soil and vegetation layers, which indicates the relevance of the relative

³No numerical scale is shown for the latent heat axis, as it was constructed with arbitrary values and is meant to show the trend due to the variation of relative humidity and stomatal resistance as a function of LAI

humidity as well as the growth stage of a plant in moderating the heat transmission through a LWS. A full analysis of this parameter could lead to a more precise comprehension of the behavior of a plant, but, due to its innate botanical background, the full effects of the stomatal resistance are outside of the scope of this thesis.

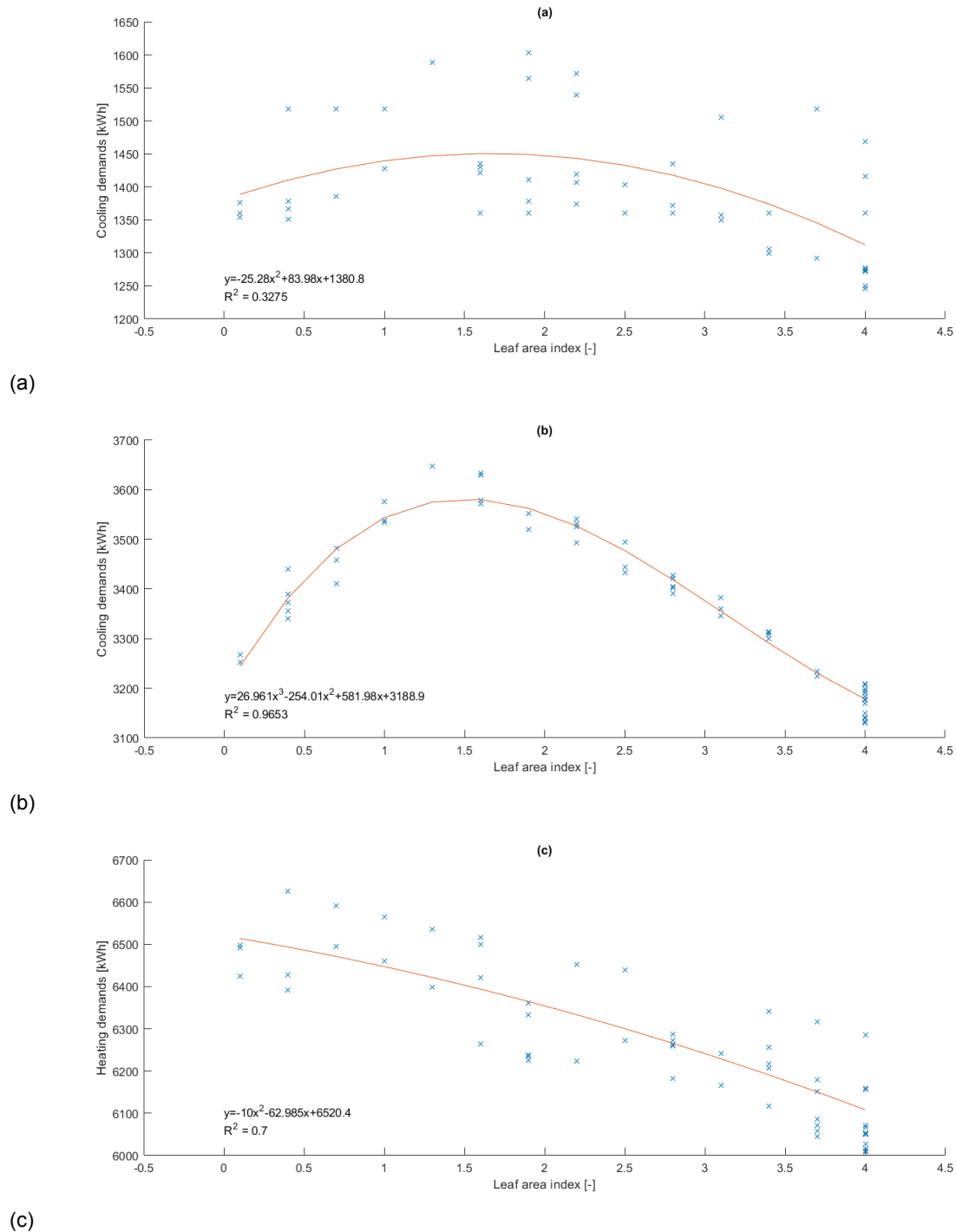


Figure 7.2: Heating and cooling demands as a function of LAI for (a) Singapore $\overline{RH} = 87.9\%$, (b) Phoenix $\overline{RH} = 18.3\%$, (c) Amsterdam $\overline{RH} = 94.2\%$ in a LWS

The beginning of this section gives an overview of the effects of varying foliage densities on the performance of a LWS. Furthermore, Figure 7.2 shows the different effects of the LAI and the evapotranspiration on heating and cooling demands obtained in the optimization study

under atmospheric conditions with variable humidity and temperature. Due to the large scattering of the simulation results, a polynomial regression was made to better understand the latent heat release associated with the evapotranspiration process as a function of the LAI. As a result, a high correlation between the data for Phoenix and Amsterdam is observed while a low correlation is present for Singapore, caused by the large irregularity of the simulation results.

Furthermore, the relation between the LAI and the evapotranspiration process can be explained through the collaboration between the aerodynamic resistance and bulk surface resistance which regulates the rate at which this process takes place. Nevertheless, the regressions on Figure 7.2 shows that, when searching for the optima, either the lowest or highest values of LAI cause a lower energy flux through the building façade, effectively reducing the buildings thermal loads. With low leaf coverage, the bulk surface resistance governs the evapotranspiration process creating a higher cooling effect. But, with increasing levels of LAI, the effects of the bulk surface resistance are decreased and the aerodynamic resistance of the vegetation layer is raised. This increase in the aerodynamic resistance does not compensate for the loss of the substrate evaporation, which leads to a lower heat transmission through the façade. Once the vegetation canopy becomes denser, i.e. ($LAI \leq 4.0$), the bulk surface resistance becomes negligible and the aerodynamic resistance becomes the governing factor in the evapotranspiration process, further decreasing the heat transmission through the LWS as confirmed by He et al. [35].

In the case of weather conditions with high relative humidity the relation is more direct, indicating a minor relevance of the VPD. However, with low relative humidity as is the case of Phoenix, a clear maximum on the heat transfer of the LWS is obtained where LAI takes a value of approximately 1.5^4 .

All in all, the results from the optimization showed that the LAI has a significant contribution to reduce the heat flux through as a façade, increasing the insulating capacity of a LWS. In general, the lower the of relative humidity of the environment, the more dynamic the behaviour of the system as it adapts to the climate conditions through the leaf's stomata. However, an increase of efficiency in the system can be obtained by the proper selection of the vegetation's canopy density. An increase of the leaf area index from 0.1 to a value of 4, can lead to a decrease in thermal demands of 8.09% in hot and humid weather (Singapore), 3.63% in hot and dry conditions (Phoenix) and by up to 6.46% in cold and humid climates (Amsterdam).

7.3.2. Leaf angle distribution

Unlike the LAI, the LAD has no relation with the climate conditions where the LWS is used but responds directly to its geographical location. As seen on Figure 7.3, different values of LAD can have a positive or negative influence on the thermal performance of a LWS. In contrast to the LAI, the values of LAD are less widespread, varying from 0.5 to 1.5 indicating whether the leaf canopy has a predominantly vertical or horizontal orientation, respectively, while LAD values of 1.0 represent canopies with a mixture of orientations [63]. Although their effect is subtle, locations with low zenith angles such as Singapore and Phoenix (see Figure 6.9), show that a mixture of leaf orientations within the canopy is detrimental to the performance of the system. Therefore, either vertical or horizontal leaf orientations provide a better coverage and insulation to a building as they limit the effects of short wave radiation in a building's façade. On the other hand, due to the high zenith angles in the case of Amsterdam, there is no preferable orientation as the extinction coefficient depends less on the LAD and more on the solar zenith angle.

⁴The peak shown in Figure 7.2 is specific to this case and to a fixed stomatal resistance assumed for this research

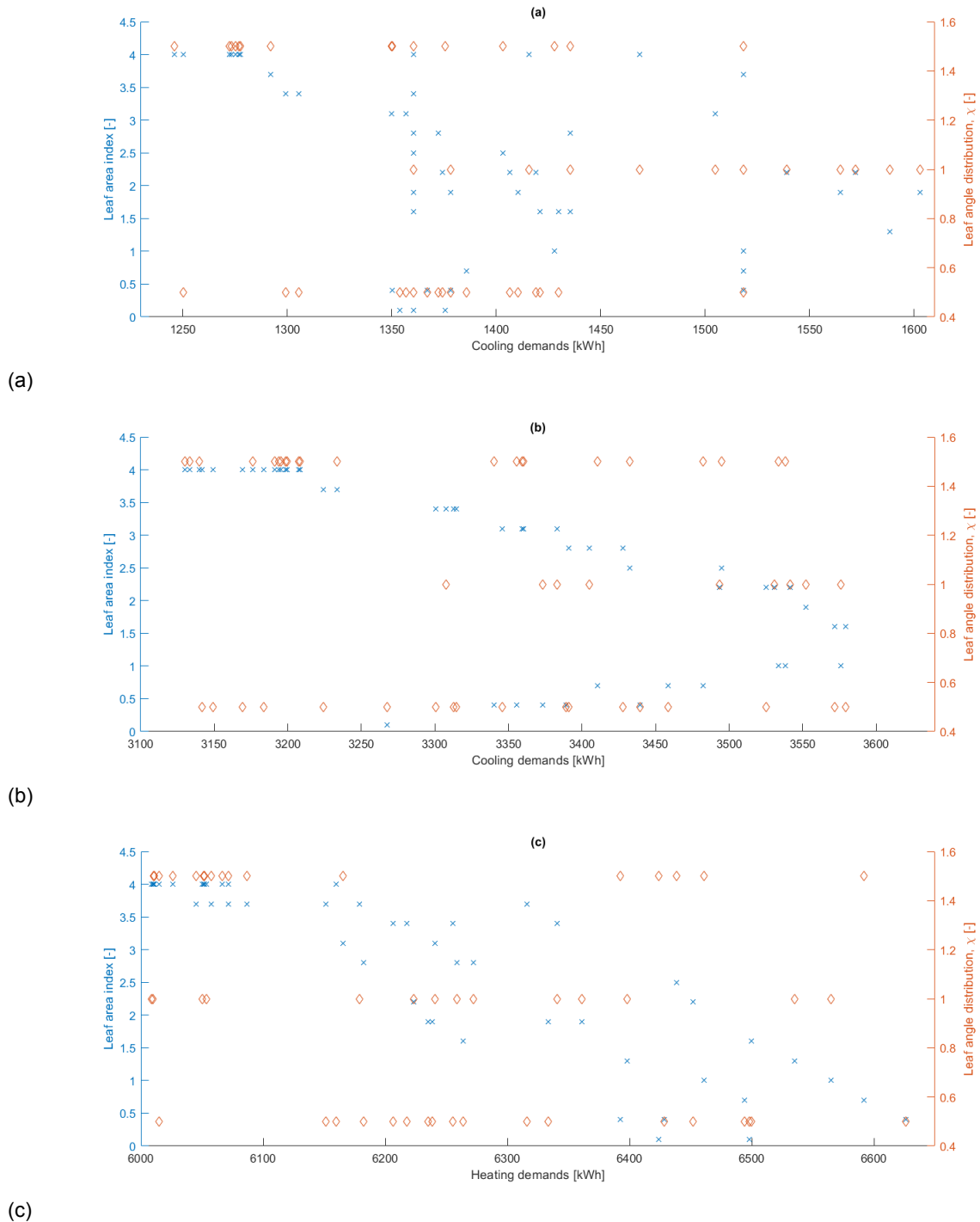


Figure 7.3: Leaf area index and leaf angle distribution effects on heating and cooling demands for (a) Singapore, (b) Phoenix, (c) Amsterdam in a LWS

This results have been further confirmed by the independent analysis of the solar zenith angle (θ_z) in the transmissivity of the vegetation layer, τ . Figure 7.4 shows the ever-decreasing effects of the LAD on τ with increasing solar zenith angles, indicating the lower relevance of the LAD in high latitudes.

Therefore, based on the optimization study results, the influence of the LAD is independent of the temperature and relative humidity of the VGS location. Nevertheless, it is directly related to the solar zenith angle obtained from the geographical location of the VGS. Furthermore, in low latitude locations such as Singapore, a particularly high affinity between

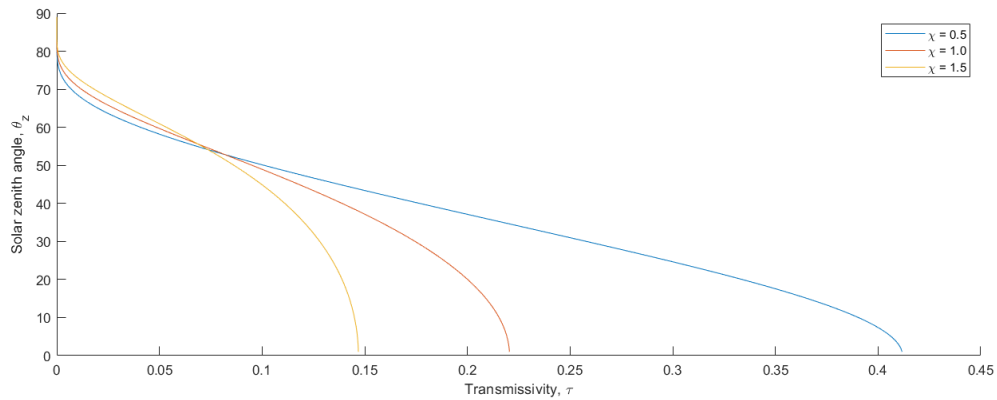


Figure 7.4: Transmissivity of a vegetation later as a function of solar zenith angle θ_z

the optimal LAD and the heat transmission through the system was found. An increase the of performance of the VGS by 8.41% was found; whereas in medium latitudes such as Phoenix a performance increase of 1.48% can be obtained. On the contrary, the LAD has a negligible impact in the thermal performance of a building in high latitude locations such as Amsterdam.

7.3.3. Leaf surface albedo

The albedo of a surface is defined as the amount of sunlight that can be reflected off a surface. As stated in Chapter 5, it is a crucial aspect of the earth-atmosphere energy balance and is directly related to the amount of long wave radiation emitted from buildings in an urban environment. However, although the surface albedo has is paramount for the atmospheric balance, it has a lesser role in the heat transmission through a LWS. The effects of the leaf surface albedo have a higher correlation with the urban scale effects, which will be discussed in Chapter 8. Nonetheless, the contribution and influence in the heat flux through a LWS will be analyzed.

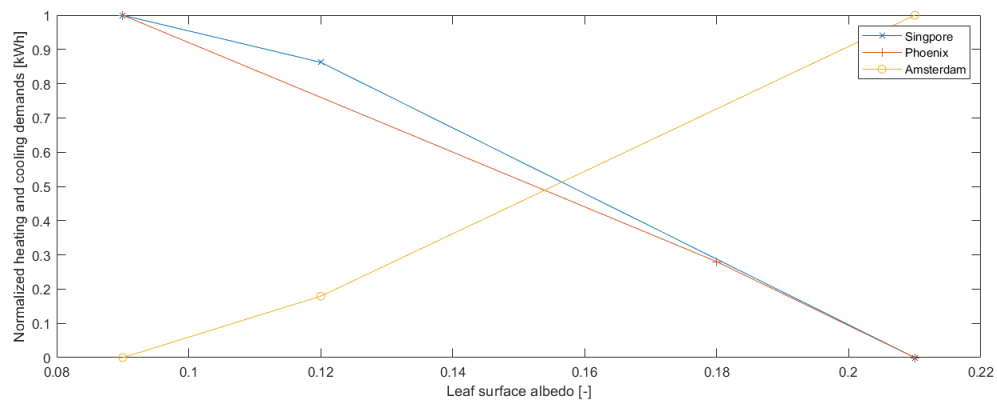


Figure 7.5: Varying albedo effects on normalized heating and cooling demands for a LWS

As seen in Figure 7.5, lower heating and cooling demands are associated with higher values of surface albedo for hot climate conditions like Singapore and Phoenix, while increasing values are preferred for cold conditions. As a result of hot climate conditions, the higher albedo of a leaf surface reduces a large portion of the incoming short wave radiation; therefore, decreasing the amount of energy absorbed in the system and subsequently, the temperature of the façade. By comparison, in the case of Amsterdam, the opposite is seen. Due to the lower ambient temperatures, lower values of surface albedo provide a larger absorption of the short wave radiation, increasing the energy in the system effectively increasing

the façade's temperature and reducing heating demands.

Even though the albedo has an effect on the heat flux of a LWS, compared to the LAI and the LAD, its influence in the thermal performance of the VGS is lower as it can only increase its efficiency by 2.53%, 0.37% and 0.08% for Singapore, Phoenix and Amsterdam respectively. This efficiency increase is caused by a change of the leaf albedo from 0.09 to 0.21; or in other words, lighter vegetation shades are more efficient for cooling-dominated climates and darker ones are preferred for heating-dominated ones.

7.3.4. Substrate properties

The insulation properties of the sandy loam soil substrate, is highly dependent on the moisture content and thickness of the substrate. Consequently, the results obtained from the various simulations in each climate condition are shown in this section.

Substrate thickness As expected, the heat flux resistance of the substrate later is directly proportional to the thickness of the substrate layer as seen on the results from the simulations in Figure 7.6. A change in the substrate thickness from 15 to 30 cm was considered, which took into account the minimal thickness required for plant growth in a LWS and a practical limitation to avoid overbearing the building's structure. Although higher thickness decreases heat flux, in the case of Amsterdam, a higher effect represented by the slope of the linear regression is present. It indicates the higher efficiency of the substrate layer as an insulation layer since it provides additional thermal mass for the building. Furthermore, this additional thermal mass aims to close the gap between available and required heat in the system by the storage of energy in materials with high thermal admittance.

All in all, the savings of heating and cooling demands provided by the VGS can decrease by up to 8.09% for Singapore, 2.16% for Phoenix and 4.29% for Amsterdam by increasing the substrate thickness from 15 cm to 30 cm.

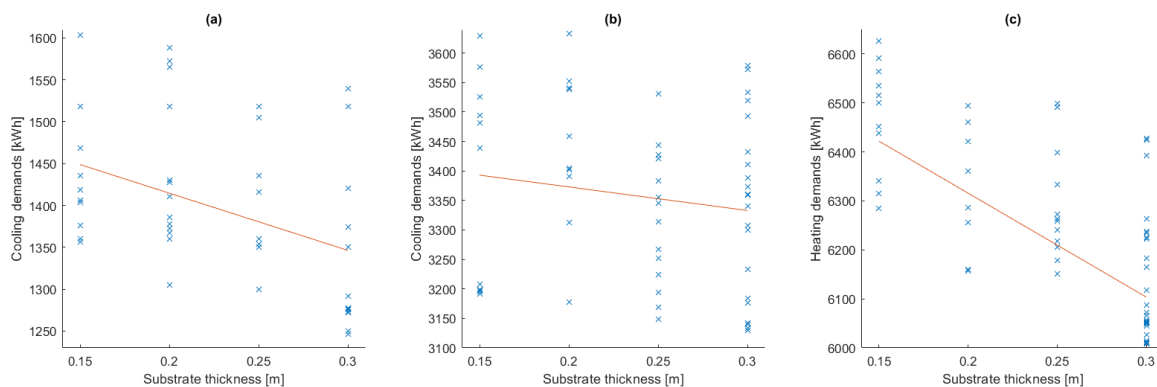


Figure 7.6: Substrate thickness effect on heating and cooling demands on (a) Singapore, (b) Phoenix, (c) Amsterdam

Moisture content Although there is a clear effect of the moisture content (MC) in the thermal performance of the substrate layer, see Section 5.3, the results from the optimization study showed that it is mostly represented by the evapotranspiration rate in a LWS. Therefore, changes in the mechanical properties of the substrate are secondary to the effects provided by the rate of evaporation. Nevertheless, having an adequate water supply for the vegetation stored in the substrate layer is required to allow proper vegetation growth and; furthermore, increases the performance of the evapotranspiration process which creates a much more effective barrier against heat flux through a façade. In this research, the amount of moisture present in the substrate was considered constant through the simulation period and is one of the driving factors of the evapotranspiration process. However, it has a significant contribution in the condition of the surrounding environment explained in Chapter 8.

The water coefficient defined in Chapter 5, is based on the field capacity and the permanent wilting point for this type of soil. Table 7.2 shows the corresponding moisture content

in the substrate for each value of water coefficient of substrate for plant.

Water coefficient	0.6	0.7	0.8	0.9	1.0
Moisture content	11.7%	13.65%	15.60%	17.55%	19.5%

Table 7.2: Water coefficient of substrate for plant and its corresponding value of moisture content in the substrate layer.

The effect that the moisture content has on the thermal properties of the substrate layer in different climate conditions seen in Figure 7.7, shows that lower thermal demands are associated with higher moisture contents with the lowest effect seen in weather conditions with high relative humidity. On the contrary, equatorial climate types such as Singapore show a negligible effect of the MC in the cooling demands while Amsterdam's temperate conditions can increase the performance of the LWS by 0.93% when increasing the MC from 11.7% to 19.5%.

Nevertheless, further study is required in cold weather conditions, as the possibility of freezing temperatures can completely alter the thermal behavior of the substrate layer as well as causing irreparable damage to the vegetation layer. Finally, in arid climates, the moisture content can significantly decrease the energy demands of the building when compared to Group A and Group B climate types. The highest amount of water available in the substrate, 19.5%, can reduce the heat flux through it by a maximum of 1.45% from a substrate layer with an MC of 11.7%.

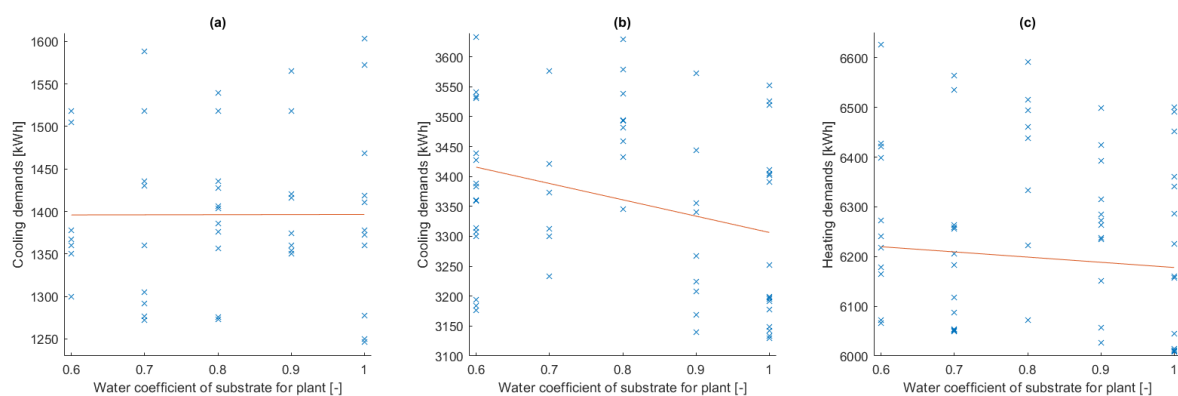


Figure 7.7: Water coefficient of substrate for plant effect on heating and cooling demands on (a) Singapore, (b) Phoenix, (c) Amsterdam for a LWS

7.4. Green façade

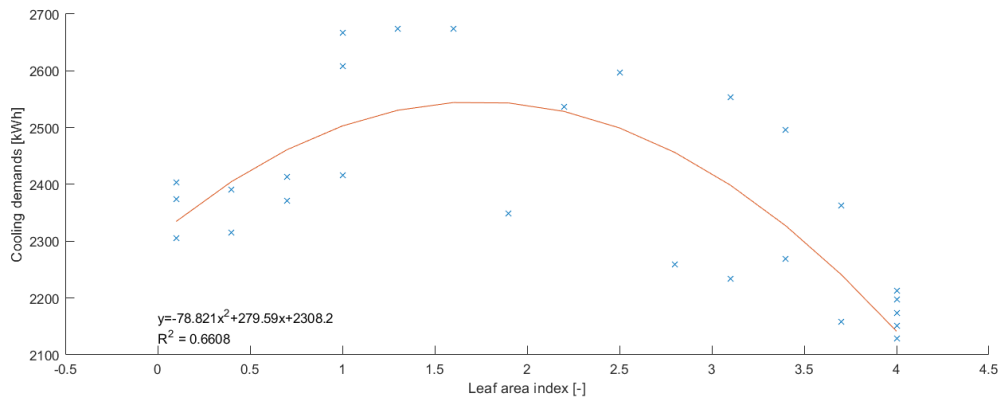
This section analyses the results obtained from the simulation of the green façade. Therefore, it presents the outcome of the optimization process on heat transmission through a façade due to the inclusion of a direct green system in a building⁵.

7.4.1. Leaf area index

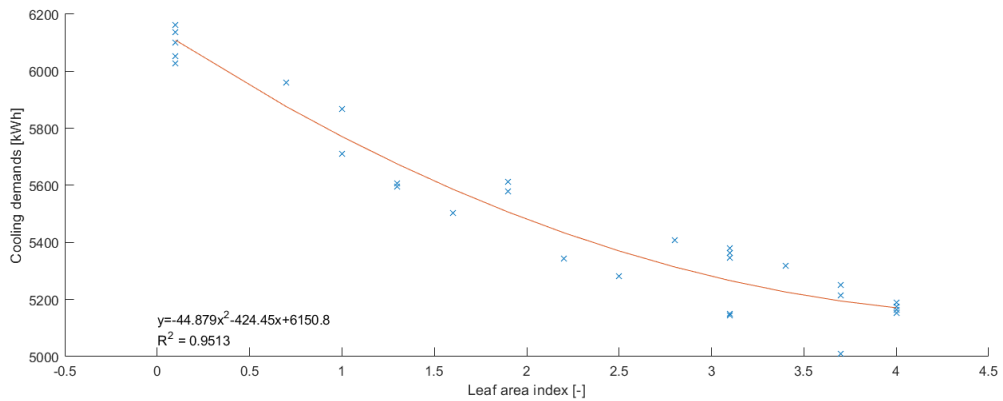
As seen in Section 7.3.1, the foliage density represented by the LAI has a dominant effect in the performance of a VGS. The cooling or heating effect of the evapotranspiration process is controlled in part by the combination of the bulk surface resistance and the aerodynamic resistance of the vegetation layer. Nevertheless, the bulk surface resistance is significantly decreased in a GF as there is no evaporation taking place from the substrate layer. Therefore, only the plant transpiration component from the evapotranspiration process and the aerodynamic resistance remains. As the transpiration process relies heavily on the aerodynamic resistance, higher foliage densities increase the aerodynamic resistance which lowers

⁵Appendix C, shows the full simulation results for the living wall systems in every climate condition obtained from the optimization study

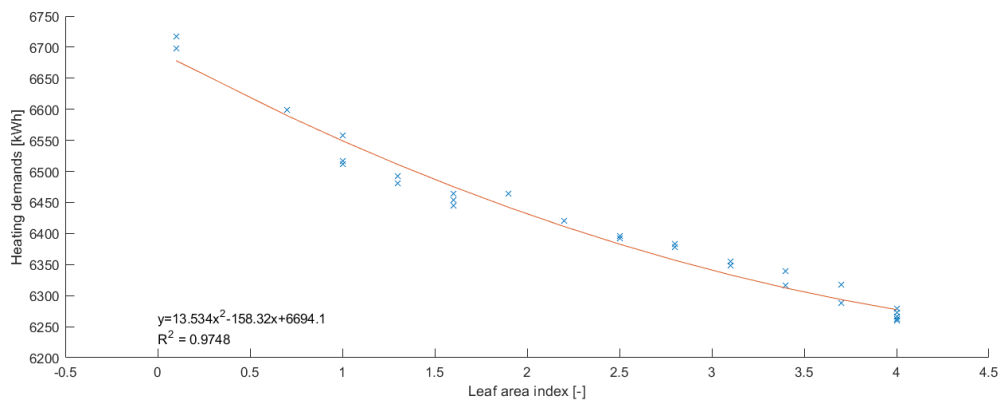
the heat and water vapor transfer in the plant layer [27]. Therefore, as seen in Figure 7.8, the higher the LAI the largest the reduction of heat transmission through the GF, being able to decrease the cooling demands by 18.67% in Phoenix and the heating demands by 6.81% in Amsterdam.



(a)



(b)



(c)

Figure 7.8: Heating and cooling effects as a function of LAI for (a) Singapore $\overline{RH} = 87.9\%$, (b) Phoenix $\overline{RH} = 18.3\%$, (c) Amsterdam $\overline{RH} = 94.2\%$ in a GF

The polynomial regressions seen in Figure 7.8 show that there is a strong correlation between all results and the expected behavior for this system based on the analysis of Conventino's thermal model [17]. Although, the bulk surface resistance is minimal in a GF,

results from Singapore show that the transpiration effect of the vegetation layer has a considerable effect in the performance of this system under these weather conditions; as a reduction of more than 20% of the cooling demands can be obtained with the optimal value of the LAI in a GF.

7.4.2. Leaf angle distribution

Similar to the LWS, the leaf angle distribution influences the performance of a GF depending its geographical location. The LAD has the highest effect on low and middle latitudes while in high latitudes, the transmissivity of the vegetation layer is governed mostly by the high solar zenith angles, making the contribution from the LAD negligible, as seen in Figure 7.4.

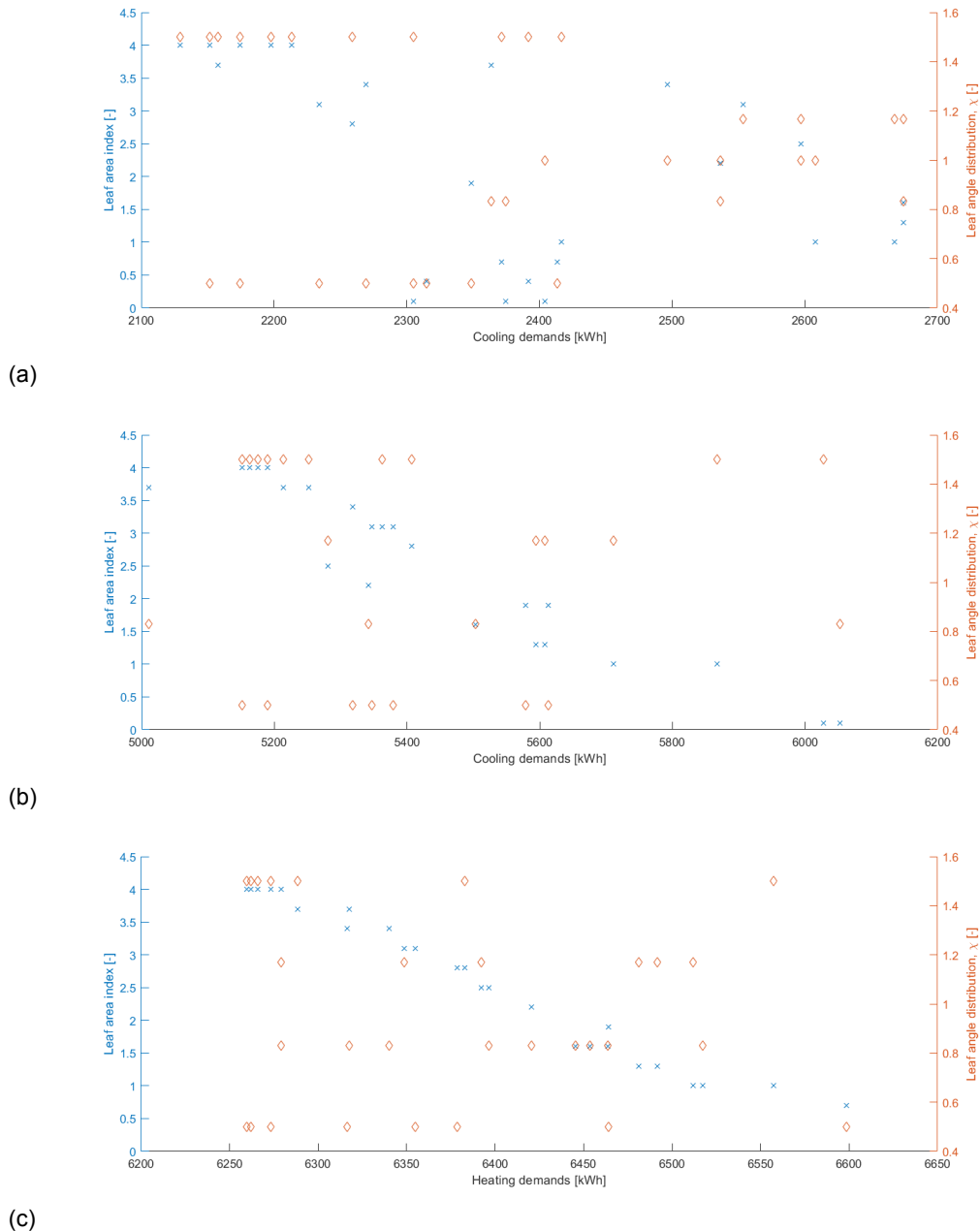


Figure 7.9: Leaf area index and leaf angle distribution effects on heating and cooling demands for (a) Singapore, (b) Phoenix, (c) Amsterdam in a GF

Additionally, Figure 7.9 shows that the effects of the LAD in heat transmission are inde-

pendent from the climate conditions, nevertheless, either vertical or horizontal leaf orientations can decrease the heat flux through the system by up to 4% in low latitudes and 3% in middle ones. In the case of Amsterdam, due to the high solar zenith angle, the LAD has a negligible influence in the heat transfer through the façade. Therefore, there is a larger freedom in the design for the system as a wider variety of plant species can be selected for the same purpose. In other words, as long as the rest of the parameters have been considered and optimized for the performance of a GF, the LAD is irrelevant.

7.4.3. Albedo

Compared to the importance of the albedo in the energy balance of the planet, its weight in the insulating properties of a vegetation layer is minimal. Although the albedo has a predominant role in the energy balance an urban environment, its influence in the analysis of a façade should not be neglected as it has the potential to further minimize heating or cooling demands in buildings.

Subsequently, Figure 7.10 shows the normalized effects of the albedo in the heat transmission through the GF. In the cases of CDC, the lower albedo decreases the cooling demands as there is a higher percentage of reflected short wave radiation and consequently lower absorption leading to the reduction of heat gains in the system. However, in the case of HDC, larger values of the surface albedo increases energy absorption, raising the temperature of the system thus decreasing the heating demands. This behavior matches the results obtained from the LWS study and proves the influence of the albedo in the performance of a GF. All in all, the variation of leaf surface albedo from 0.09 to 0.21 is not overly significant as it can only decrease cooling demands by 3.81% in Singapore and 2.18% in Phoenix and decrease heating demands by 0.22% in Amsterdam but is representative of the effects of a vegetation layer on the energy performance in a building.

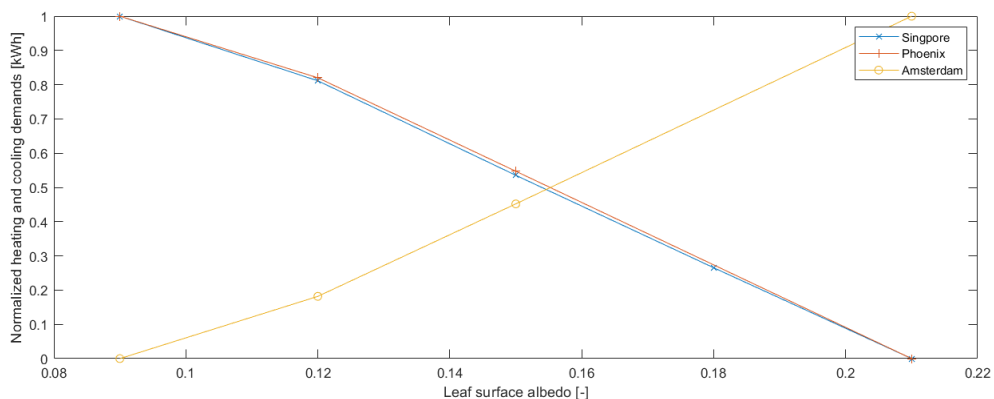


Figure 7.10: Varying albedo effects on normalized heating and cooling demands for a GF

7.5. Optimal vertical green system configuration

The results of this study showed the optimization potential for both GF and LWS aiming to improve their thermal insulation capacity and therefore, decrease the energy demands of a building. The optimal choice of the vegetation and the substrate parameters can lead to significant reductions of the heating and cooling demands in a variety of climates as seen in Table 7.3 by decreasing the heat transmission through the façade. Nevertheless, due to the dynamic behavior of the vegetation layer, especially considering the evapotranspiration effect in a LWS, caution must be taken in their design to obtain the highest efficiency possible from a VGS.

Furthermore, the optimal configuration shown in the previous Table gives the maximum reduction of the heat flux and therefore, energy savings. This energy savings are considerable as shown in Table 7.4, and compare the energy demands of a fully optimized VGS in a building with a concrete building used as a reference model. The influence of climate conditions

	Living Wall System		Green Façade	
	CDC	HDC	CDC	HDC
Albedo	0.21	0.09	0.21	0.09
LAD	1.50	1.00	1.50,0.50 ⁶	0.50
LAI	4.00	4.00	4.00	4.00
Substrate thickness [m]	0.30	0.30	-	-
Moisture content [%]	19.5	19.50	-	-

Table 7.3: Optimal parameter configuration for living wall systems for different climate conditions

in the performance of the VGS is clearly observed for both types of VGS, indicating a higher efficiency in hot and humid climate conditions (Singapore) followed by hot and dry (Phoenix), caused by the higher release of moisture due to the evapotranspiration process, and finally cold and humid (Amsterdam). Although there are energy savings provided by the VGS in cold climates, they are 3 to 4 times lower than their warm weather counterparts indicating a lower efficiency of the VGS in urban environments. Furthermore, the heat resistance of a LWS is higher than in a GF due to the presence of a substrate layer which can increase the energy savings by up to two to three times. This shows the promise of using VGS as an alternative to modern insulation materials with a higher environmental footprint. Nevertheless, this comparison has been done between buildings without any type of insulation materials in the façade which indicates the potential of these systems for a sustainable energy renovation of existing buildings. Buildings already insulated with artificial materials such as rock wool, might have a lower increase in their energy efficiency if a VGS is added although more research is needed to indicate the extent of the reduction of heat transmission that a VGS could have in these well insulated buildings.

Additionally, based on Susorova's thermal model[81], the heat resistance of VGS can be calculated, which can be used to compare their performance with common insulating materials. For instance, when considering the heat resistance of each VGS, a conversion to an equivalent thickness of Rockwool⁷ can take place. The value shown in Table 7.4 represents the layer of artificial insulating material required to obtain the same benefits as the VGS providing a comparison with common building materials.

		Energy savings [%]	Eq. Rockwool thickness [cm]
Singapore	LWS	56.49	22.48
	GF	24.23	5.54
Phoenix	LWS	46.87	15.28
	GF	17.74	3.74
Amsterdam	LWS	13.57	2.72
	GF	7.87	1.48

Table 7.4: Energy savings caused by the reduction in transmissive heat transfer and equivalent performance offered by a single Rockwool layer for an optimized vertical green system in each climate condition

Even if VGS can provide the same insulation levels as artificial materials, they take a larger space which can be used for other purposes, such as larger usable building footprints. Therefore, every benefit provided by VGS described in Chapter 4 should be taken into consideration and an economic analysis is required to evaluate its feasibility in different construction projects.

7.5.1. Economic feasibility of vertical green systems

For any construction project, material selection highly depends on its functionality, availability, access and in most cases, cost. The return on investment should be attractive enough for

⁷Common insulation material taken as a reference with a $\lambda = 0.04$ W/mK

investors to carry out a project. However, in the case of building integrated vegetation, the wide array of benefits they provide are not exclusive to a single building. These additional effects should be taken into consideration when performing a financial case. Information regarding the economic sustainability of green envelopes is still scarce [53], even though their environmental benefits have been widely researched. Perini and Rosasco performed a cost-benefit analysis for GF and LWS in 2013 [64], where many aspects including personal costs and benefits, initial investment, maintenance, disposal, property value, energy savings, longevity, social costs and benefits⁸ were included⁹.

The different components of a VGS define the evaluation of a cost-benefit analysis. Additional materials, such as supporting elements for indirect green façades, can significantly increase the investment costs of the systems countering all the personal and social benefits they can provide [64]. Perini's study analyzed four different types of VGS: direct green façade, an indirect green façade with HDPE mesh support, an indirect green façade combined with planter boxes and a living wall system. The study concluded that only a green façade can achieve a positive net present value with a pay back period of 16 years. The rest of the analyzed cases showed a negative net present value with a pay back period of 35 years for the HDPE indirect green façade and over 50 years for both the living wall system and the indirect green façade with planter boxes. Therefore, the only fully economically sustainable alternative is the direct green façade, as the supporting system in the indirect façade has a substantial contribution in the costs component of a cost-benefit analysis. The living wall system was not considered economically sustainable due to much higher installation and maintenance costs. Nonetheless, the study considered only a reduction of 10-20% of the cooling demands due to the VGS. As seen in Table 7.4, the energy savings provided by a VGS can be significantly higher than the ones assumed for Perini and Rosasco's study which can potentially turn the cost-benefit analysis around and make other systems such as the LWS, economically feasible. Nevertheless, an in-depth study is required which extends out of the scope of this research. Furthermore, these results match the LCA research performed by Ottélé et al. [58]. The LCA focused on the environmental impact of several VGS, concluding that the environmental impact from the system is highly related to its supporting structure. Consequently, direct greening systems have a minimal environmental footprint and, in the case of indirect greening systems, favoring materials such as hard wood, HDPE or coated steel over stainless steel can significantly reduce their environmental burden. Additionally, the choice for growing mediums in LWS is dominant in its environmental footprint, where planter boxes showed the best outcome. All in all, it is the opinion of this author that the implementation of any VGS can become both economic and environmentally sustainable as long as there is an optimal design and proper incentives to provide environmental benefits on both micro and macro urban scales.

7.5.2. Plant layer parametrization

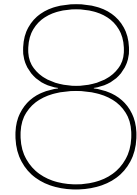
Besides the cost analysis, the botanical component in a VGS is crucial. Plant and leaf morphology define the behavior of a VGS. Leaves control photosynthetic, respiration and transpiration rates [76] and are indispensable in the evapotranspiration process. Therefore, the actual vegetation present in a building define the efficiency of the systems. The numerical analysis performed in this research involves a mathematical representation of the leaf and the configuration of the canopy. Nevertheless, in order to accurately represent reality, the exact biological equivalent is required. This is no easy task as growth patterns, leaf distribution, phyllotaxis, and several other plant parameters vary significantly between plant species. Identifying, categorizing and documenting the LAI, LAD and albedo of each plant species, is a considerable task and to the knowledge of the author, no such database exists. This is a critical limitation in the implementation of optimal greenery systems, nevertheless, the principles shown in the research apply and rules of thumb can be developed to implement in real life projects.

⁸Includes air quality improvement, carbon reduction, habitat creation, aesthetics, and UHI

⁹Tax reductions, although fairly common, are not considered in the study due to the location it took place.

7.6. Summary

A discussion of the results obtained from the optimization study is performed which analyzes the effects of both LWS and GF in the heat transmission of a façade. The behavior of each parameter was identified showing the rules of thumb to optimize a VGS. First, regarding the LAI, there is a high dependency on the relative humidity of the environment and on the stomatal resistance, therefore no general rule can be derived. Second, the LAD showed a high dependency on the geographical location where horizontal and vertical leaf orientation showed the optimal results with low zenith angles, while no preference was found for locations with high solar zenith angles. Third, a minor effect was found caused by the leaf surface albedo, where higher values lower the heat transmission in warm climate conditions while the opposite takes place in cold climate conditions. Fourth, the substrate properties showed that higher substrate thickness and moisture content increase the insulation potential of the VGS. Finally, the reduction on the heat transmission is higher in LWS than in GF, with larger effects in Singapore followed by Phoenix and lastly by Amsterdam.



Impact of Vertical Green Systems on an Urban Setting

This chapter will present the results obtained from the optimization study regarding their influence on an urban area in each of the three climate conditions defined in Chapter 6 for the optimized VGS configuration obtained from Chapter 7.

8.1. Introduction

The benefits of vertical green systems extend way beyond the reduction of heating or cooling demands in a building. After all, as described in Chapter 4, they possess a wide array of benefits to its environment; for example, an increase in aesthetics, biodiversity, air quality, the mitigation of the urban heat island effect among others. Therefore, building integrated vegetation can directly counter the negative effects associated with an urban environment. The capacity of a vegetation layer to mitigate negative urban effects associated the UHI effect is detailed in this section¹.

To further understand the behavior of a vertical green system (VGS), a refined model was constructed to simulate their effects in an urban setting while taking into account the optimal configuration obtained in the previous chapter (See Table 7.3). As the implementation of a VGS depends solely in the benefits it can provide to an individual building, to portray a more realistic scenario, the optimal configuration of the VGS is used to measure the effects of building integrated vegetation in its surroundings. In other words, this analysis evaluates the effects of a VGS optimized to reduce heat transmission through a façade, in the temperature of its surroundings. Overall, this section attempts to identify the potential of VGS as a mitigation strategy of the UHI effect, by evaluating wind, ambient temperature, reflected short wave and emitted long wave radiation from a vegetated building, providing a first step into the evaluation of large scale implementation of optimized building integrated vegetation.

8.2. Wind speed

As one of the main mechanisms of heat transfer, convection relies heavily on the movement of the particles within a medium. When the medium is air, the velocity of the wind defines the rate of heat transfer. When dealing with building physics, it is a well known fact that there is an increase of heat resistance in a wall due to the presence of a stagnant air layer in both the outer and inner surface of a wall caused by the reduction of the wind flow. Due to the inclusion of a vegetation layer in a buildings façade, the air flow pattern is modified as an irregular surface is replacing the usually smooth and straight surface seen in a building's façade. Subsequently, wind is reduced which in turn decreases the convective heat transfer increasing the performance of the VGS as an insulating material. As the wind speed

¹Complete simulation results are shown in Appendix C

decreases, a stagnant air layer is formed both within the vegetation layer and in the exterior surface of the façade.

For this particular research scenario, there is an initial N-S wind orientation², which creates wind alleys in the east and western façades of the buildings, where its speed is at its maximum. In the east and west alleys of the urban street canyon, a decreased wind speed is found which is commonly seen in these types of configurations [78], due to their perpendicular orientation to the wind direction. In contrast, the north and south façades of the buildings show a mixture of orientations and reduced speed due to the turbulent air flow caused by conflicting wind directions. As the configuration of the urban street canyon and the wind behavior is symmetrical, in order to simplify the analysis only the effects of the vegetation layer on the south and west façades will be considered for the wind analyses.

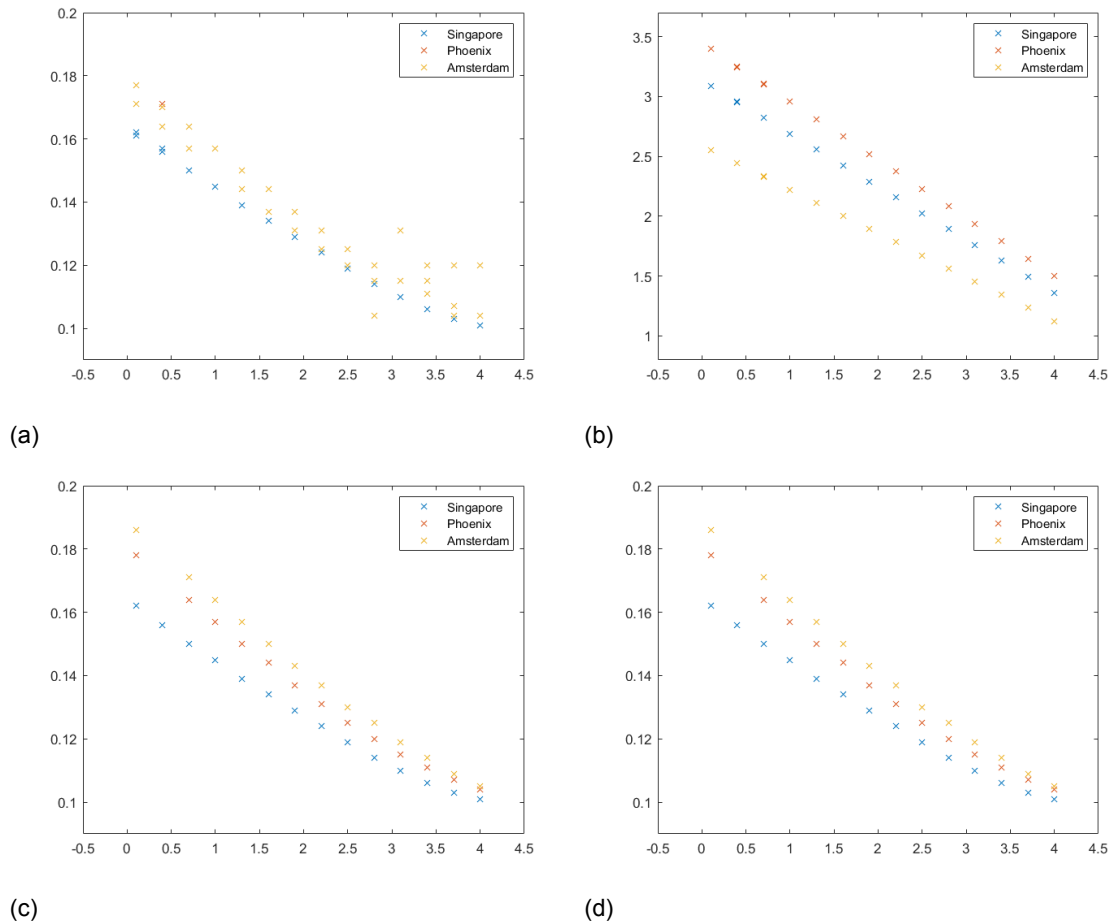


Figure 8.1: Wind speed as a function of LAI in each climate group and vector direction. (a) Living wall system south, (b) Living wall system west, (c) Green façade south, (d) Green façade west

Unlike the correlations shown in Table 7.1, the effects of the vegetation layer on the wind speed in front of the façade are significantly higher. Regardless of the climate conditions, all simulations showed a correlation of approximately -1.0 for the leaf area index (LAI) and the wind speed in front of the façade, indicating that the larger the canopy density, the lower this wind speed, while the albedo and leaf angle distribution (LAD) had a minimum to negligible impact in the wind speed. This negative correlation is shown in Figure 8.1, confirming the inversely proportional relation between the foliage density and the wind speed for different climate conditions and wind orientation. It should be noted that the reduction of wind speed is taking place regardless of the wind and façade orientation, whether the wind is parallel or perpendicular to the façade, a similar reduction is seen. A similar research was performed

²Figures displaying the detailed wind orientation for all weather groups are shown in Appendix C

by Perini and Grabowiecki [32, 65], which concluded with the same relation between LAI and wind speed, nevertheless, to the knowledge of the author, no analytic relationship exists between the LAI and the wind speed parallel to the façade.

Due to the considerable effect that the reduction of wind speed can have in the convective heat transfer in a buildings façade through the creation of a semi-stagnant air layer, and in the comfort of the people in its surroundings, an expression was developed to link the LAI with the wind speed as a function of the initial velocity. The values of wind speed for the west and south façade were normalized as a function of the highest value, in order to share the same frame of reference. Thus, Figure 8.2 shows the normalized values of the wind speed characterized by wind orientation parallel to both west and south façades.

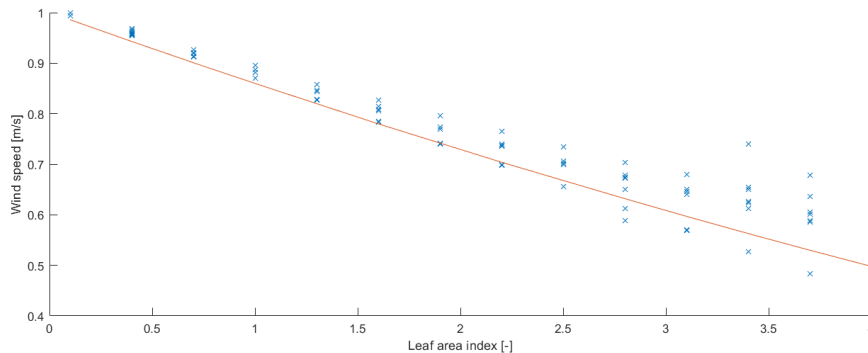


Figure 8.2: Polynomial regression between initial wind speed and leaf area index for a VGS

By analyzing the whole data set, the polynomial regression seen in Figure 8.2 was developed to establish the relationship between the LAI and the wind speed as a function of the initial wind speed represented by Eq. 8.1 with a correlation coefficient R^2 of 0.92. The expression shows that dense vegetation layers can lead to a decrease of up to 50% of the original wind speed, which gives way to a large amount of application within the urban environment.

$$V_w = V_0 * (0.0049 * LAI^2 - 0.1451 * LAI + 1) \tag{8.1}$$

Where V_w is the decreased wind speed, V_0 the initial wind speed and LAI the leaf area index for LAI between 0.1 and 4.

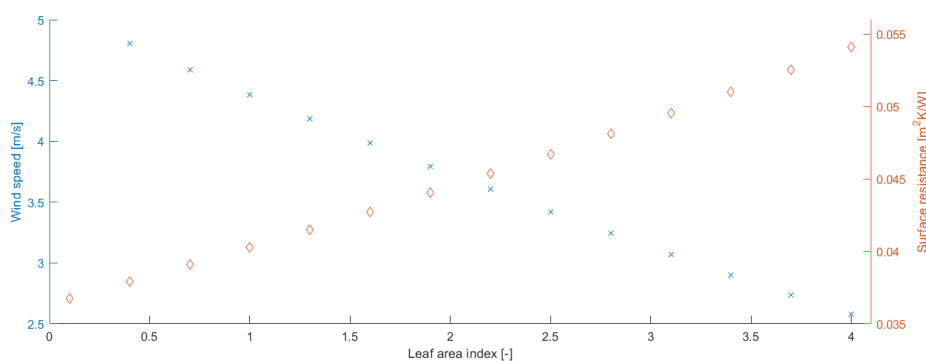


Figure 8.3: Effects of LAI in wind speed and surface heat resistance in a VGS

The impact of wind speed reduction in terms of convective heat transfer, is considered by analyzing the additional insulation it provides to the façade. According to NEN-EN-ISO 6946:2017, there is an exterior surface resistance associated with an air layer equal to 0.04 m^2K/W . However, with decreasing wind speeds, this "free" resistance is increased. Assuming a gentle breeze, with a wind speed of 5 m/s, the decrease and associated heat transfer

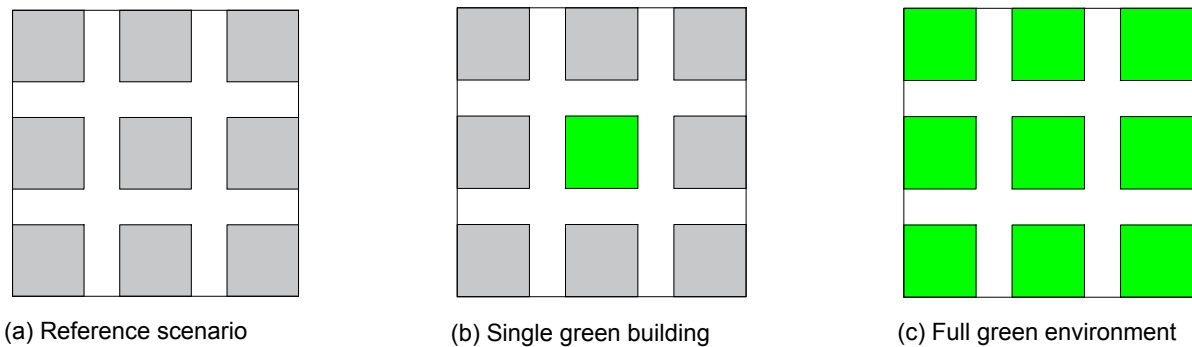


Figure 8.4: Cases for evaluation of the ambient temperature in varying urban conditions

resistance³ change as seen on Figure 8.3. Although theoretically the heat transfer resistance tends to infinity when wind speed approaches zero due to non turbulent heat transfer processes, a practical limitation of $V_{min} = 0.5m/s$ has been set by the Joint Research Center of the European Commission which means to create a more realistic representation of this phenomena .

Whereas the LAI has an considerable effect in the wind speed, the LAD and surface albedo have shown no effect on the speed of wind parallel to the façade, as there was no significant difference on the results with the variation of these parameters.

8.3. Ambient temperature

The ambient temperature of an urban environment is directly involved in the perception of comfort and behavioral patterns of its inhabitants, as well as the energy performance of buildings. As the population strives to achieve adequate levels of comfort, changes in their clothing or levels of activity can take place to counter the effects of extreme temperatures. Especially inside buildings, thermal comfort must be at allowable levels which can be achieved through a number of ways as shown in Figure 5.1. Nevertheless, little to no attention is placed on the quality of the outdoor environment and people's response to it during the design of a building. Due to the rapid growth of cities during the last decades, a large amount of problems have arisen as a consequence, as adequate environmental measures were often replaced by faster construction practices. Among the urban problems described in Chapter 2, the UHI effect stands out. The increase of the surface temperature in urban areas due to the configuration and surface material of the urban street canyons, has led to extreme temperatures conditions forcing changes in the behavior of both people and buildings to cope with them. Therefore, this section will analyze the effects of building integrated vegetation in the ambient temperature and as a possible mitigation strategy for the UHI effect. As stated before, the impacts of a fully optimized VGS, for the reduction of heat transmissivity obtained in Chapter 7, will be tested based on three individual cases, shown in Figure 8.4. Case A is used as a reference scenario which considers an urban environment covered with common urban surfaces, i.e. concrete for the buildings and asphalt for roads. Case B replaces the façade surfaces of the central building by a VGS to test the effects of a single green building in its environment, and Case C considers a fully greened environment which replaces every concrete façade by a VGS to evaluate the cooperation of independent vegetation layers in the same environment.

8.3.1. Living wall systems

The higher complexity of a LWS showed that it has a higher performance when reducing the heat flux through a façade when compared to a GF. Nevertheless, its potential effects on the ambient temperature are still in question. As seen before, the performance of any VGS is highly dependent of the weather conditions and for this analysis, it is no exception. Therefore, Figures 8.5 through 8.7 show the effects of the implementation of a LWS in cases B and C indicating the wide range of effects of LWS in the temperature of its environment. For

³Conversion from wind speed to heat transfer resistance is based on values published by NEN-EN-ISO 6946:2017

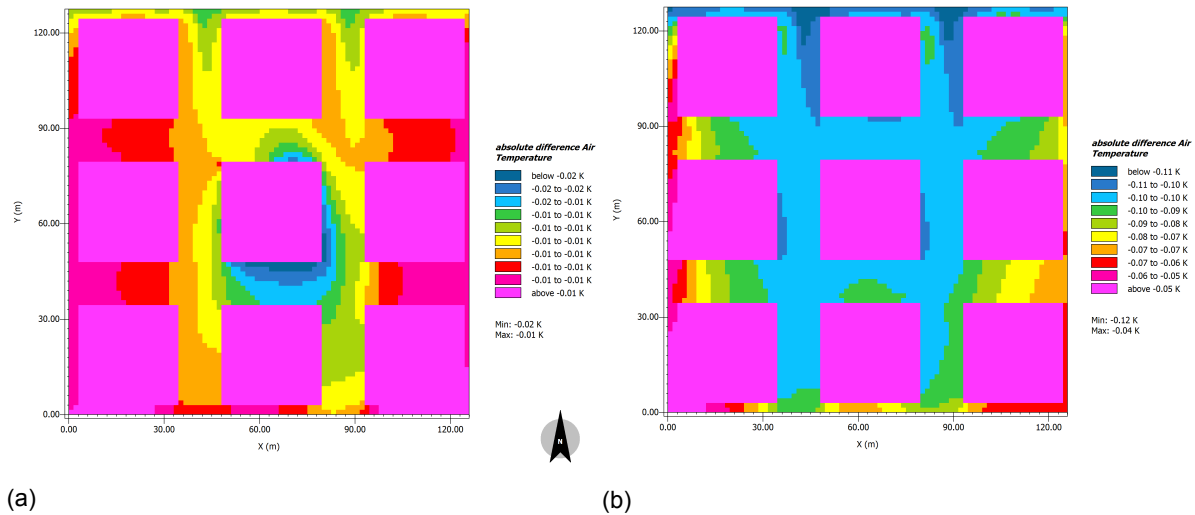


Figure 8.5: Effects of the implementation of a LWS on (a) single and (b) multiple buildings during an hour period in Singapore

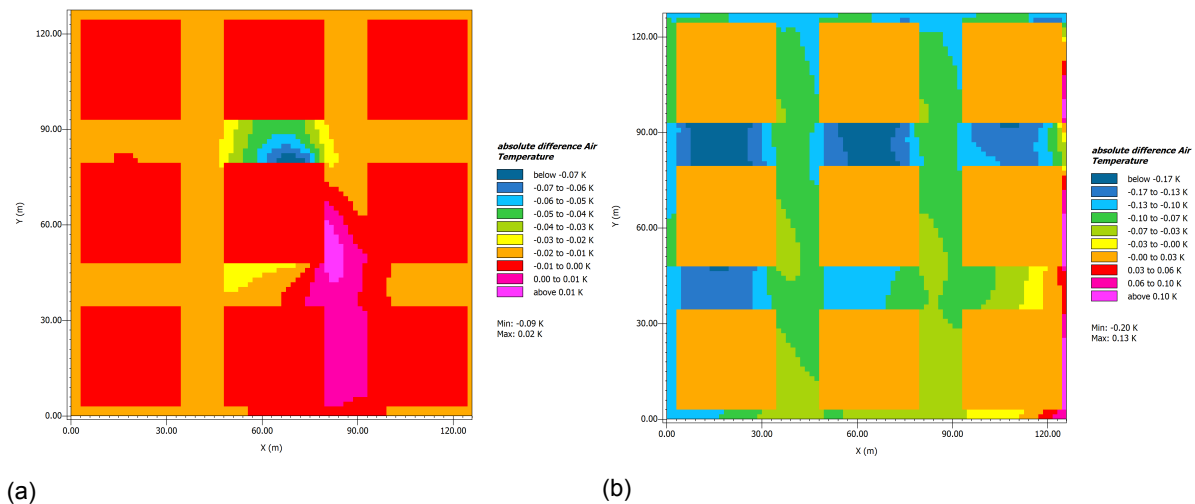


Figure 8.6: Effects of the implementation of LWS on (a) single and (b) multiple buildings during an hour period in Phoenix, Az

all three climate conditions, the magnitude and distribution of the ambient temperature is modified by the inclusion of a LWS, when comparing to the initial conditions seen in Appendix C. Additionally, all cases show a decrease in the temperature of the environment caused by the latent heat released associated with the evapotranspiration process within the VGS.

First, the results from Case A, seen in Figures 8.5a, 8.6a and 8.7a, will be interpreted to evaluate the effects of a single vegetated building. As expected, the maximum changes in the ambient temperature take place in close proximity to the façade up to a distance of 1.50 meters. In farther distances, the intensity of the temperature change decreases proportionally to the distance. Furthermore, each climate group showed different changes in temperature. In the case of Group A and B, Singapore showed a maximum decrease of 0.02 K while Phoenix a decrease of 0.07 K. Although this is barely perceptible for humans, the cooling effect from the vegetation is taking place improving the outdoor temperature conditions. This increase of 250% between Group A and B is caused by the greater evapotranspiration rate and associated higher VPD as seen in Figure 7.1. Therefore, there is a larger amount of moisture being released from the vegetation and substrate layer to compensate the lack of moisture in the ambient air. In the case of Group C, the sub-zero temperatures in Amsterdam are further decreased by a maximum of 0.11 K as seen on Figure 8.7a. As a result, the implementation of a LWS in this type of climate conditions can be detrimental to the environment in its sur-

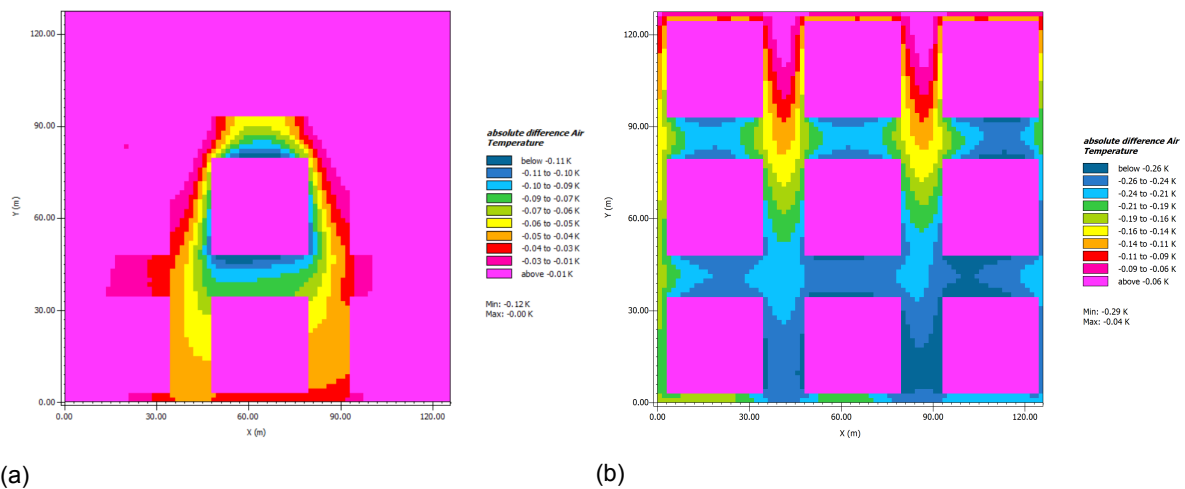


Figure 8.7: Effects of the implementation of LWS on (a) single and (b) multiple buildings during an hour period in Amsterdam

roundings, as it reduces the efficiency of any measure to reduce the thermal demands of a building.

Next, the results for the analysis of the fully greened environment depicted in Case C are shown in Figures 8.5b, 8.6b and 8.7b. The inclusion of additional LWS significantly increases the magnitude of the cooling effect seen in Case B, as well as creating a more uniform distribution. The maximum cooling effect of Singapore and Phoenix raise to 0.11 K and 0.17 K respectively, increasing them by 450% and 142.86% from Case B. On the other hand, Amsterdam presents a temperature drop of 0.26 K, a 136.36% increase from Case B. The collaboration between all LWS in the urban setting is evident as it amplifies the cooling effects in every climate condition. Nevertheless, based on the simulation results, it can be argued that LWS have a more significant effect in warm conditions such as the ones falling under climate types similar to Group B due to the increased rate of moisture release from the LWS.

Furthermore, the influence of wind speed and orientation has a fundamental role in the distribution of cooling effects. For the reference scenario, a N-S wind orientation is predominant in the main streets⁴ which remains similar in Case B and C. The influence of the cooling in Case B, see Figures 8.5a, 8.6a and 8.7a, follows the wind paths created by the configuration of the urban street canyons, with a higher effect in the leeward side of the central building than in the windward side. This fact matches the areas around the building with lower wind speeds, thus displaying the inversely proportional relation between temperature fluctuations and wind speed. As the foliage density of the canopy layer greatly influences the wind speed (See Section 8.2), the addition of a LWS can decrease the wind speed in front of the façade thus increasing the cooling effects in the ambient air. Even though the decrease in wind speed can increase the thermal effects of a LWS, the addition of a dense vegetation canopy can be detrimental as it reduces the effective range of cooling effect due to its reliance on wind velocity, limiting the influence of the system.

8.3.2. Green façades

Compared to LWS, GF have a simple configuration which consists of a single vegetation layer in front of the façade. As there is no substrate layer, the evapotranspiration process is governed mainly by the transpiration rate and aerodynamic resistance of the vegetation layer, which defines its potential to reduce temperature extremes.

The effects of a GF on the surroundings of a building are shown in Figures 8.8 thru 8.10. When analyzing Case B, GF showed a similar behavior to the one seen for LWS for hot climate conditions as a cooling of the environment is taking place. Nevertheless, the inclusion of a GF in a cold environment further decreases the temperature due to the shading effect of the

⁴See Figures C.2, C.5, C.8 in Appendix C

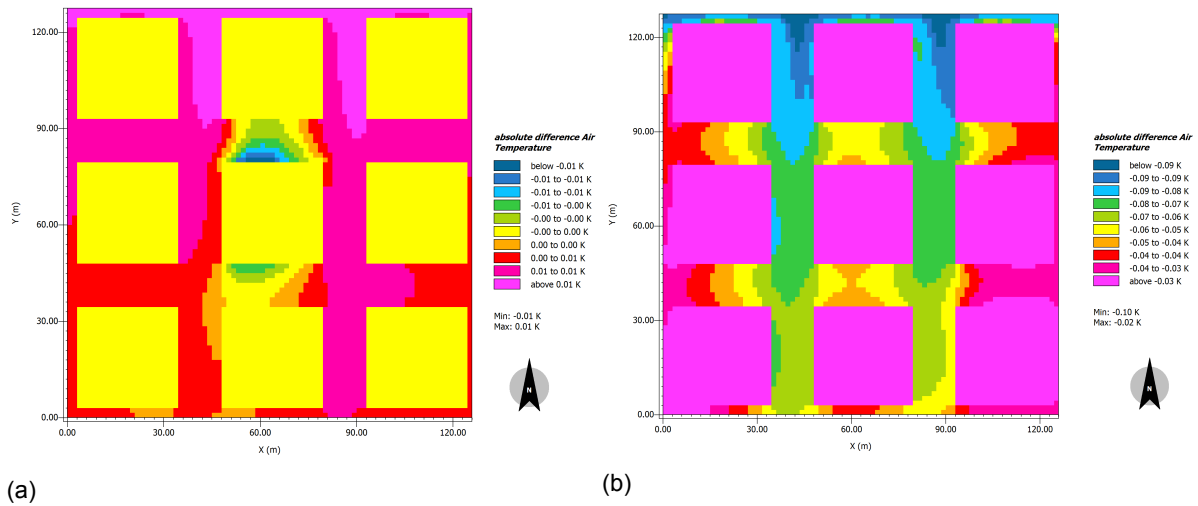


Figure 8.8: Effects of the implementation of a GF on (a) single and (b) multiple buildings during an hour period in Singapore

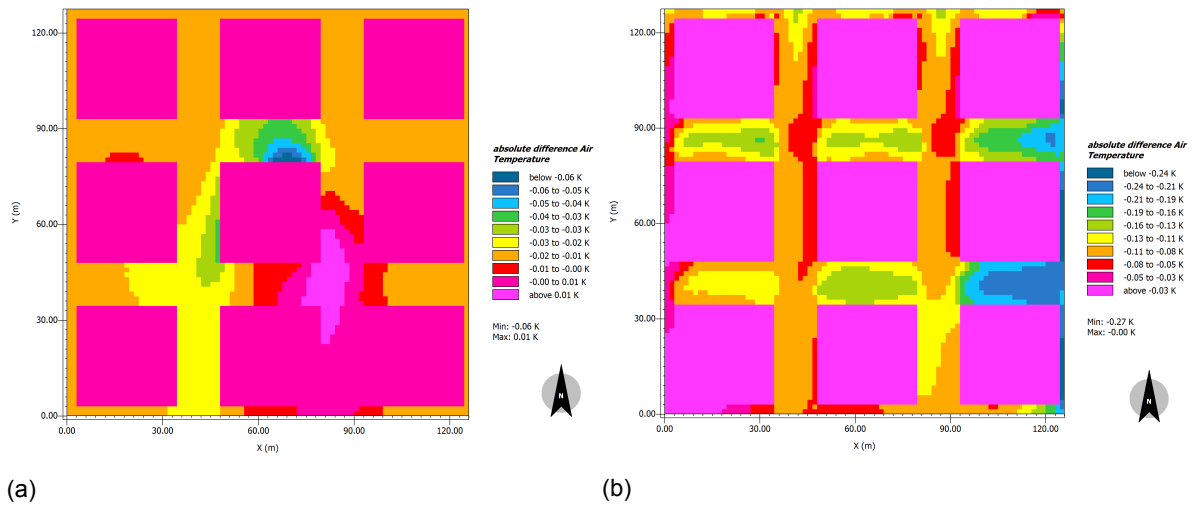


Figure 8.9: Effects of the implementation of a GF on (a) single and (b) multiple buildings during an hour period in Phoenix, Az

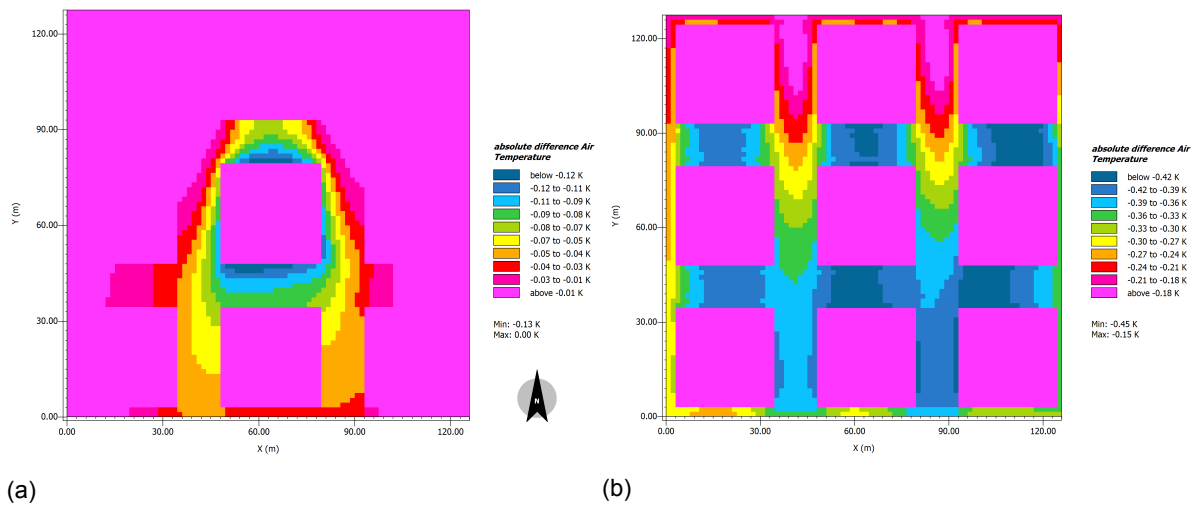


Figure 8.10: Effects of the implementation of a GF on (a) single and (b) multiple buildings during an hour period in Amsterdam

vegetation layer. Although there is a clear drop in the ambient temperature, the magnitude of this effect is considerably lower than the one shown for a LWS. In the case of Singapore, there is a decrease of temperature of 0.01 K in north and south façades, where low wind speeds are found, while a slight increase can be seen in the east and west ones. However, this minimal change in the temperature leads to the realization that a single optimal GF has a negligible effect in this type of weather conditions, and can even raise temperatures during the hottest moment of the day. Phoenix on the other hand, has a significantly stronger cooling effect up to 0.06 K which represents an increase of 500% when compared with the GF in Singapore, but a decrease of almost 17% when compared with the temperature reduction obtained by a LWS. Finally, the effect of a GF in cold climate conditions, i.e. Amsterdam, decreases the temperature by up to 0.12 K. This temperature decrease is detrimental for this particular case, as the GF has a cools the already cold environment caused by the reduction of short wave radiation incident in the façade. As seen in Figure 5.4, the amount of sunlight allowed through a vegetation layer with a LAI of 4.0, can be decreased more than 70% of its original value⁵, greatly diminishing the amount of energy that can be stored in a building.

For Case C, the effects of full scale implementation of a GF can be seen in Figures 8.8b thru 8.10b. Like in the case of a LWS, the effects of the vegetation layer on the environment are magnified. Nevertheless, due to the significant reduction of absorbed short wave radiation, for climate types in Group A, there is a decrease in temperature of 400% compared to the maximum cooling obtained for a single building. For climate types in Group B an increased cooling effect was also seen, reaching lower temperature drops of up to 0.24 K, an increase of performance of 300% and 42% when compared to the single GF and the fully greened LWS environment respectively. Due to the absence of a substrate layer, the lower amount of stored energy leads to a larger decrease of the ambient temperature, showing the higher cooling potential of a GF when used as a large scale counter measure for the UHI effect. Nevertheless, in cold temperatures a higher temperature reduction is seen in Case C than in Case B. The further decrease of the ambient temperature cools down the environment by 0.42 K, an increase of 250% when compared to Case B. This undesirable behavior completely undermines the useful effect seen in Chapter 7 regarding the heat transmission through the system, which can lead to negative consequences to the environment. As more resources are required to keep a comfortable indoor temperature, to compensate for this additional temperature drop.

Furthermore, the influence of wind speed is still noticeable in the distribution of the cooling effect. Higher velocities transport cool air reducing the temperature in that direction. However, the largest cooling effect is still observed in the immediate surroundings of the buildings.

8.3.3. Observations regarding the ambient temperature

Due to the model scale and the short analysis period, the influence of the VGS on the ambient temperature is still limited. Nevertheless, it clearly shows the potential of VGS in altering the temperature of its environment. Although a positive effect is seen in climate types fitting the description of Group A and B, LWS and GF can be detrimental to climates like the ones in Group C, as it reduces the amount of radiation that can be absorbed by the urban canopy. However, deciduous plant species can counter this detrimental behavior as they can shed off leaves during winter leaving the surface of the façade exposed to short wave radiation. Nevertheless, there is a loss of the additional insulation provided by this vegetation systems. Ultimately, a larger effect can be obtained when an integrated system is used, with vegetation covering urban surfaces in a large scale, proving its potential as a UHI mitigation strategy and the reduction of hazardous health effects for the population.

8.4. Reflected short wave and emitted long wave radiation

The effects of both short wave and long wave radiation on urban surfaces are widely considered as one of the main causes of the UHI effect. Due to the propagation of short wave

⁵With a fixed LAI, the decrease in sunlight transmissivity through the vegetation layer depends solely on the solar zenith angle and leaf angle distribution χ

radiation in the built environment, energy is stored and reflected due to the material properties of a building's surface. The light path created by the propagation of solar radiation causes more energy to be stored in materials with high thermal admittance, which can be later released as long wave radiation into the environment [46]. However, changes in the heat capacity and surface albedo of urban surfaces effectively alters the amount of energy stored in a city.

As seen in Chapter 7, the optimized LWS has an albedo of 0.21 for cooling dominated climates and 0.09⁶ for heating dominated ones; therefore, the reduction of 30% and 70% in the surface albedo for cooling and heating dominated climates respectively, decreases the total amount of radiation incident in the façade which depends on the intensity of solar radiation represented by the angle of incidence [34]. Depending on the LAD, the reflected and absorbed solar radiation can significantly change. For both VGS, the intensity of the solar radiation depends on the optimal leaf orientation seen in Table 7.3 and the solar zenith angles shown in Table 8.1⁷. A horizontal leaf orientation ($\chi = 1.50$) gives a maximum sunlight intensity of 99.79% for Singapore, 95.84% in Phoenix and 26.20% for Amsterdam, while a vertical orientation ($\chi = 0.5$) gives a maximum of 95.61% in Singapore, 96.61% in Phoenix and 99.28% in Amsterdam⁸. The variation in the intensity of incoming solar radiation caused by the orientation of the vegetation surface defines, in part, the performance of a VGS. The following sections show the changes in the reflected short wave radiation and emitted long wave radiation for both the green façade and living wall systems.

Time	7:00	8:00	9:00	10:00	11:00	12:00
Singapore	-	-	61.99	47.04	32.11	17.27
Phoenix	75.04	62.66	50.16	37.81	26.23	17.36
Amsterdam	-	-	-	83.13	78.31	75.46

Time	13:00	14:00	15:00	16:00	17:00	18:00
Singapore	3.73	13.35	28.13	43.05	58.00	72.95
Phoenix	16.58	24.69	36.07	48.36	60.87	73.30
Amsterdam	74.81	76.45	80.20	-	-	-

Table 8.1: Solar Zenith angles for Singapore, Phoenix and Amsterdam weather condition

8.4.1. Living wall systems

Figures 8.11 to 8.13 show the reflected short wave radiation and emitted long wave radiation of the vegetated models in comparison to the un-vegetated reference model. The change in surface albedo significantly decreases the total amount of energy stored in the system. In the case of cooling dominated climates such as Singapore and Phoenix, there is a reduction of 61.81% and 72.02% respectively from the original value. The 10.21% difference in reflectivity between Singapore and Phoenix is caused by the higher absorption of short wave radiation due to a increase of sunlight intensity in Singapore. Considering the horizontal leaf orientation for this system ($\chi = 1.5$), and the zenith angles, the additional absorbed sunlight in Singapore is stored in the substrate layer and leads to the increased emitted long wave radiation seen in Figure 8.11 and Figure 8.12. Due to the higher absorption in Group A, the total amount of absorbed radiation throughout the day increases by 10.24% while in Group B, the reduction in sunlight intensity reflects most of the short wave radiation increasing the total amount of emitted long wave radiation only by 9.14%.

⁶Albedo value for heavyweight concrete used in the benchmark model in ENVI_met is 0.30

⁷A visual representation of the solar zenith angles for each climate condition can be seen in Figure 6.9

⁸Maximum intensity level is obtained from the angle of incidence on the leaves surfaces considering the time of day where the solar zenith angle is lowest on a fully horizontal leaf orientation or when the zenith angle is highest on a vertical leaf orientation

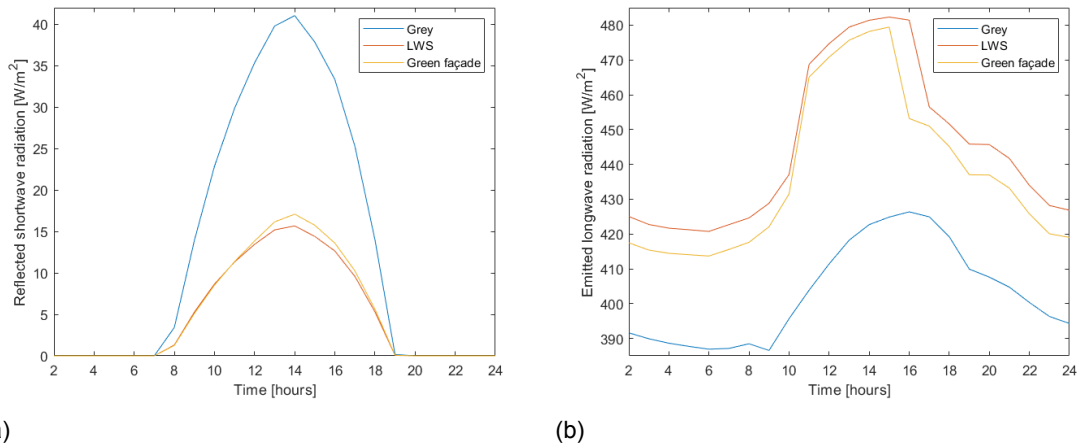


Figure 8.11: (a) Reflected short wave radiation and (b) emitted long wave radiation for vertical wall systems during April 1st 1989 for Singapore

On the other hand, in the cold weather conditions of Group C: Amsterdam, seen in Figure 8.13, there is a 90.54% reduction in the reflection of the short wave radiation and a decrease of 2.55% in the total emitted long wave radiation throughout the day. Under cold weather conditions, a LWS has a lower heat capacity and is unable to store as much heat as its grey counterpart. As most of the short wave radiation is reflected, there is little energy left to be stored and due to the thermal effusivity, and a lower activity level of the vegetation⁹, there is a lower thermal exchange with its environment. Additionally, Figure 8.13 shows how the difference in emitted radiation shrinks during the last hours of the day, indicating the capacity of the system to reduce extreme values and maintain constant temperatures. However, as thermal energy storage is a dynamic process, more research is needed to understand the full effects of living wall system as thermal mass.

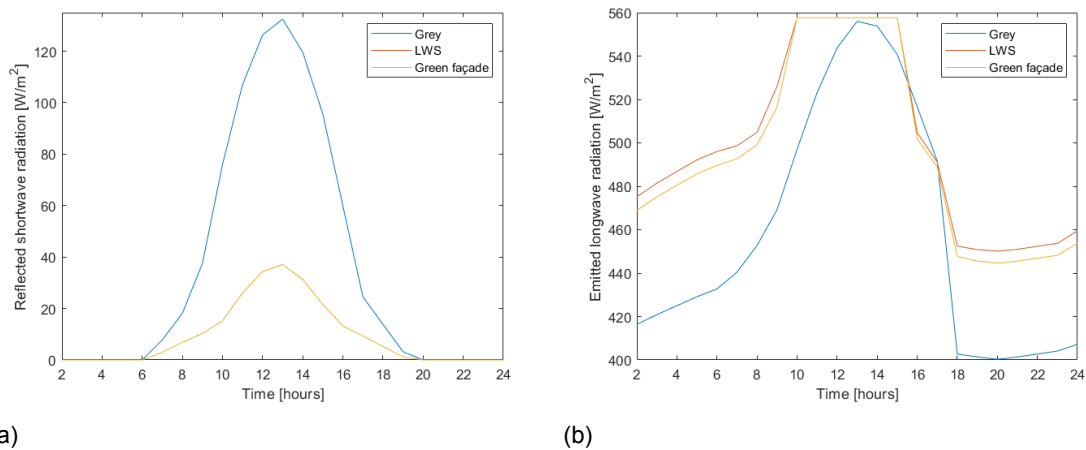


Figure 8.12: (a) Reflected short wave radiation and (b) emitted long wave radiation for vertical wall systems during August 1st 1988 for Phoenix

8.4.2. Green façades

In the case of cooling dominated climate conditions, the reflected and emitted radiation for a green façade show the same behavior as a living wall system. However, the reduction in reflected short wave radiation decreases by 58.36% for Singapore and 72.04% for Phoenix. Therefore, there is little to no influence of vertical or horizontal leaf angle orientations in the

⁹In general, plant leaf effusivity is much lower than other materials commonly found in urban areas, with values ranging from 675 to 750 $Ws^{1/2}/(m^2K)$ [44] which depends on the plant species, while concrete can reach values up to 1250 $Ws^{1/2}/(m^2K)$ [39]

reflected short wave radiation due to the large density of the vegetation layer as similar drops were found in the case of a LWS. Nevertheless, Figure 8.12 shows that even though a similar behaviour is seen, an increase in the emitted long wave radiation of the building of 8.39% for Singapore and 8.21% for Phoenix is spotted. Although the GF still has a some heat storage capacity, it is decreased in comparison to the living wall system by 1.85% and 0.93% for Singapore and Phoenix respectively, as there is no longer a substrate layer serving as thermal mass. Since the vegetation canopy is very dense, the amount of radiation coming through it is minimal, reducing the effective energy incoming to any material acting as thermal storage.

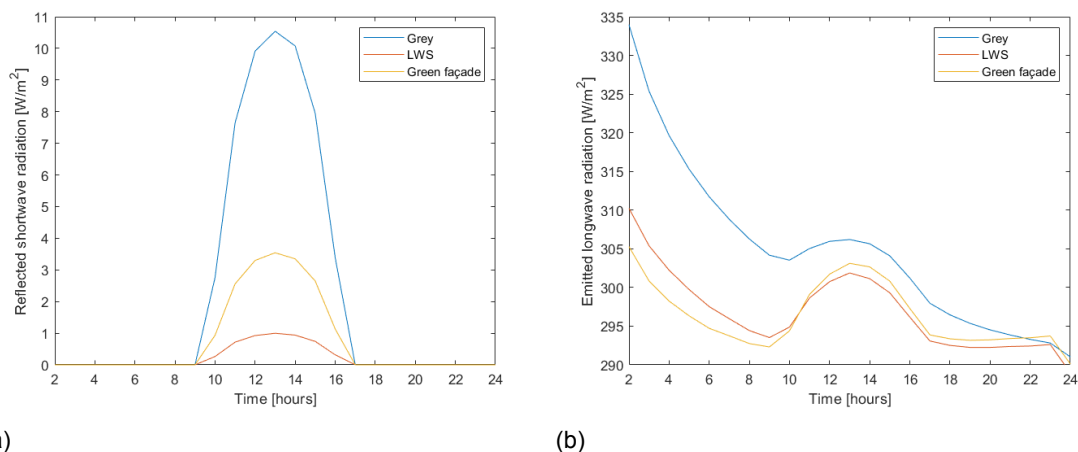


Figure 8.13: (a) Reflected short wave radiation and (b) emitted long wave radiation for vertical wall systems during January 6th 1988 for Amsterdam

In the case of Amsterdam, Figure 8.13, the reflected short wave radiation is reduced by 66.41% compared to the benchmark model, as the predominant vertical leaf orientation ($\chi = 0.5$) has a higher angle of incidence. The leaf orientation, combined with large zenith angles, increases the intensity of sunlight, therefore increasing the heat stored in leaves, as seen in Figure 8.13. The 24.13% difference between vertical and horizontal leaf orientations, in GF and LWS respectively, alters the total amount of energy stored in the VGS and the effective long wave radiation it can emit. Although there is an apparent increase in the heat released from the system, the GF has a lower total emitted radiation throughout the day in comparison with the LWS, caused by the absence of a substrate layer. Nevertheless, due to the dense foliage, its influence is small as a tiny amount of radiation manages to get through the canopy.

8.5. Mitigation of the urban heat island effect

The urban heat island effect is a modern day problem that arose due to unregulated city growth, expansion and minimally controlled industrial practices. It has had dire consequences in the living conditions of many cities worldwide causing a deterioration of the living environment, an increase in energy consumption, elevation in ground-level ozone and larger mortality rates [72]. Consequently, these problems are a matter of concern due to the larger risk posed with changes in climate patterns that have taken place in the last decades, giving less time for any city, and its population, to adapt.

The implementation of greenery systems in cities has been proven to be a suitable solution to counter the UHI effect [57, 72]. Furthermore, the evaluation of VGS in an urban setting on both temperature, reflected short wave and emitted long wave radiation showed the potential for mitigation of the UHI effect, and its positive effect on the environment. In general, the changes of the surface albedo, the shading effect caused by large foliage densities and the latent heat release associated with the evapotranspiration process can be attributed with the drop in the ambient temperature.

Focusing on warm climate conditions, i.e. Singapore and Phoenix, the amount of shading provided by the vegetation significantly reduces the amount of reflected short wave radiation

		Total incoming short wave radiation [W/m ²]	Reduction [%]
Singapore	Ref. model	296.908	-
	GF	118.669	60.03
	LWS	112.884	61.98
Phoenix	Ref. model	821.837	-
	GF	214.372	73.92
	LWS	214.573	73.89
Amsterdam	Ref. model	52.267	-
	GF	17.462	66.59
	LWS	4.897	90.63

Table 8.2: Decrease of incoming short wave radiation due to shading effect caused by the vegetation layer

as seen in Table 8.2. Additionally, the moisture released by the evapotranspiration process cools down the environment storing heat in the water molecules¹⁰. This cooling effect highly depends the wind speed and orientation based on the configuration of the urban environment which indicates the potential for further design and optimization of an urban space. Subsequently, with an adequate configuration of an urban street canyon thermal conditions can be improved, reducing temperature peaks and creating a more stable environment.

All in all, choosing the appropriate VGS for an urban setting depends highly on the requirements of the project and its objectives, as the energy saving benefits provided by a LWS for example, might not compensate the environmental impact of their implementation due to its associated material use and maintenance costs as shown in Section 7.5.1.

8.6. Summary

An evaluation of the effects of VGS in an urban setting was performed. The analysis focused on the effects on wind speed, ambient temperature, short wave and emitted long wave radiation. The implementation of VGS regarding wind revealed an inversely proportional relation between the LAI and the wind speed leading to higher surface resistance in the façade. Furthermore, there is a cooling effect provided by the evapotranspiration process from the vegetation layer. This leads into cooler temperatures in the surroundings of the vegetated buildings, although a significant increase was seen under fully greened environments, indicating the potential of VGS to decrease ambient temperatures when they are applied on a large scale. Furthermore, due to the shading provided by the vegetation, the short wave radiation incident in the façade is decreased lowering the total energy incoming and therefore kept within the system.

¹⁰In order to guarantee a continuous cooling effect due to the evapotranspiration process, the amount of moisture in the growing medium, e.g. the substrate layer, should be constantly replenished to compensate for the amount that has been released into the environment

9

Conclusion

This thesis project aims to understand the potential use of vertical green systems in a large scale and to create general guidelines for their optimal design in an urban setting. Moreover, it focuses on the thermal aspects of VGS, primarily on the heat transmission through a façade and as a strategy for the mitigation of the UHI effect. To do so, a computational work flow was developed by combining several independent software packages which allowed the testing of the performance of green façades and living walls system in a large number of configurations. Consequently, a deeper understanding of the physical processes led to the definition of the optimal configuration of these systems to increase the energy efficiency of a single building and the analysis of the conditions in its surroundings. The analyses were performed under three different climate groups. Group A consists of a fully humid equatorial rainforest climate, Group B of a desert climate, and Group C of a warm, temperate, fully humid climate in winter conditions.

9.1. Conclusions

This research project tackles some of the uncertainty associated with VGS in an urban environment. To do so, the research questions stated in Chapter 3 are answered based on the results and discussion presented throughout this report:

How can vertical green systems be optimized to improve the performance of a building for different climate types?

Vertical green systems can be optimized by tackling each one of the following four mechanisms: external sun-shading, thermal insulation, evaporative cooling through evapotranspiration and barrier effect for wind. Due to their innate integrated behavior, both vertical green systems were parametrized and each parameter analyzed independently to understand its relevance in the overall behavior of the system. The optimization of these systems can be summarized in Table 9.1, which show design guidelines that can be applied in future projects on different geographical locations or climate conditions.

Climate Conditions Latitude	LWS			GF		
	Group A Low	Group B Mid	Group C High	Group A Low	Group B Mid	Group C High
Leaf area index	+/-	+/-	+/-	+/-	+	+
Leaf angle distribution	H/V	H/V	n/a ¹	H/V	H/V	n/a
Leaf surface albedo	+	+	-	+	+	-
Moisture content	+	+	+	n/a	n/a	n/a
Substrate thickness	+	+	+	n/a	n/a	n/a

Table 9.1: Design strategies for vertical green systems

The parametrization of the system showed that the following strategies should be used in order to optimize the systems:

- Leaf area index: there is no general rule applicable to this parameter as its influence depends highly on the relative humidity of the environment and on the stomatal resistance of the vegetation layer. Due to the collaboration of the aerodynamic and bulk surface resistances, the evapotranspiration rate can vary significantly based on the vapor pressure deficit of the ambient air. Therefore, an individual analysis should be performed for each case to understand the rate of moisture release into the atmosphere based on the weather conditions and plant species. However, they show the largest potential in reducing the heat transmission through the façade and therefore maximize energy savings. It should be noted that in the case of climates groups B and C, with green façades, there is a negligible contribution from the bulk surface resistance. This suggests that higher values of leaf area index and therefore, higher foliage density and aerodynamic resistance, lead to an increase in the efficiency of the system.
- Leaf angle distribution: this parameter showed no correlation with the characteristics of each climate group, but showed a high one with the solar zenith angle associated with the geographical location of the system. In locations with low and mid latitudes, i.e. low solar zenith angles, an increase in the performance was observed when horizontal or vertical leaf orientations were present. Nevertheless, in high latitudes, i.e. high solar zenith angles, the leaf angle distribution had a negligible effect on the performance of the system.
- Leaf surface albedo: for both vertical green systems, similar findings were obtained. In climate types A and B, the higher the albedo the larger the reflectivity of the surface which reduces the amount of energy stored in the system. Thus, decreasing the temperature difference between the indoor air and the vertical green system. On the other hand, in climate type C, the opposite was found. A lower albedo increases the absorption of short wave radiation, thus increasing the temperature of the system and therefore decreasing the heat flux through it.
- Moisture content²: the amount of moisture present in the substrate layer is directly responsible for the rate of evapotranspiration and its effects represented mostly by the influence of the leaf area index. Nevertheless, an increase on the thermal insulation provided by the substrate can be obtained with larger moisture levels in the soil.
- Substrate thickness²: besides providing a growth medium for the vegetation layer, in general, the larger the thickness the better its performance to reduce heat transmission.

Furthermore, a number of sub-research questions were developed based on the main research question, with the following answers:

Which are the parameters with the highest influence on the performance of vertical green systems?

In the case of living wall systems, the leaf area index has the highest influence in the performance of the system, followed by the substrate thickness, the leaf angle distribution, the leaf surface albedo and finally by the moisture content of the substrate layer. This applies to climate types A and B, while for climate type C the leaf angle distribution has the lowest influence in the performance of the system.

On the other hand, regarding a green façade, the leaf area index has the highest influence same as the living wall system, followed by the albedo and lastly by the leaf angle orientation in all climate conditions.

To what extent is evapotranspiration capable of reducing a building's energy demand?

The rate of the evapotranspiration process is controlled by the contribution of both aerodynamic resistance and surface bulk resistance of a vertical green system. These resistances

²Applicable only to living wall systems and for all climate groups

are directly related to the foliage density of the vegetation represented by the leaf area index. Therefore, the extent of the evapotranspiration process, assuming a constant moisture source, is controlled by the influence of the leaf area index. The total contribution of the vertical green system in the reduction of the heat transmission can be seen in Table 7.4, where savings from 8% to 50% can be obtained. While the decrease of heat transmission due to the optimal choice of leaf area index LAI ranges from 5% to 16% as seen on Table 9.2³.

Climate Conditions	LWS			GF		
	Group A	Group B	Group C	Group A	Group B	Group C
Leaf area index	9.91	11.25	4.97	7.28	15.35	6.00

Table 9.2: Percentual reduction of heat transmission due to the leaf area index

How large is the influence of the soil substrate layer for the performance of the system?

The increase in the performance of the vertical green system, two different aspects must be analyzed. First, a direct effect is seen since a resistance to heat flux is introduced which comes from the thickness and the moisture content of the substrate layer as seen in Table 9.3⁴. Second, indirectly, it serves as a growing medium for the vegetation layer allowing the cooling effect through the evapotranspiration process takes place, as well as the use in heights that green façades cannot reach.

Climate Conditions	LWS		
	Group A	Group B	Group C
Substrate Thickness	6.89	1.71	3.49
Moisture content	0.25	3.27	0.63

Table 9.3: Percentual reduction of heat transmission due to the thickness and moisture content of the substrate layer

How does a vertical green system respond under the urban heat island effect in an urban environment?

The inclusion of a vertical green system in an urban environment leads to a drop in the ambient temperature of its surroundings. Due to the change in the surface albedo and the cooling effect caused by evapotranspiration process, there is a measurable temperature drop which depends on the amount of reflected short wave radiation, wind patterns, and vapor pressure deficit in the atmosphere. The temperature drop is highest in weather conditions with lower relative humidity, i.e. Group B, although it is still in order of magnitude of less than 0.2 °C. Furthermore, the change of surface albedo can significantly alter the reflected short wave radiation which reduces the total amount of energy received and stored in the urban canopy.

How does the leaf area index influence wind velocity in the surroundings of the vegetation layer?

The foliage density, represented by the leaf area index, has an inversely proportional relation of the wind speed in front of the façade. The denser the foliage layer, the higher the decrease of the wind speed. A polynomial regression was obtained based on the normalized values of wind speed for different façades in different climate conditions, where large values of leaf area index, i.e. 4.0; a decrease of up to 50% of the original wind speed was seen. Additionally, this effect can further increase the cooling of the ambient temperature, proving

³Values are based on the regression obtained from the simulation results as seen in Chapter 7 considering the leaf area index that leads to the maximum and minimum heat transmission

⁴Values indicate the percentual change of the thermal demands due to an increase from 15 to 30cm of the soil substrate and from 11.7 to 19.5% of the moisture content based on polynomial regressions

the potential of vertical green systems as a strategy for the mitigation of the urban heat island effect and improving the conditions for pedestrians in the vicinity of the vegetated buildings.

9.2. Limitations

While this research aimed to reduce the uncertainty of the design of VGS, the conceived mathematical model is limited regarding the representation of all the phenomena involved in the micro-climate simulations done in ENVI_met. Therefore, the following limitations were found in the study:

- The study is based on a 24 hour period which limits possible variations from weather conditions. The long term effects of building integrated vegetation were not analyzed which can create deviations in the observed performance in particular when dealing with the urban effects of vertical green systems.
- The amount of moisture in the substrate layer was assumed constant during the analysis periods, i.e. there is no decrease due to the release of moisture. The constant moisture content keeps both the magnitude of the insulation provided by the substrate and the rate of evapotranspiration constant which is not an accurate representation of reality. A decreased effect could be seen in a real setting due to decrease of moisture over time.
- The optimization study was based on a stationary analysis. Therefore, no time dependent effects were considered in the simulation work flow.
- The results regarding the environmental effects of vertical green systems highly depend on the geometrical configuration of the urban setting. Therefore, these findings serve merely as guidelines but careful consideration must be taken in their application, in particular where different wind patterns are present in the analyzed area.
- The design guidelines are applicable for weather conditions similar to the ones presented in this research and extrapolation of the results can be performed with a high degree of accuracy. Nevertheless, due to the use of different plant species and their corresponding stomatal resistance, an in depth analysis should be performed whenever plant species do not match the properties assumed for the vegetation layer or when significantly different solar zenith angles, temperature and relative humidity conditions are present.
- The mathematical interpretation of the performance of vertical green systems is limited to any practical implications associated with the adequate selection of plant species, construction process and maintenance of the systems. The conceptual representation of the vegetation layer was simplified, thus, there is a lower reliability if they were to be compared with actual measurements. Nonetheless, they provide a solid reference to estimate the performance of VGS and conceive an optimal design.

9.3. Recommendations & Future work

Due to the large scope of this project, many topics were not fully taken into consideration. Therefore, more research regarding the following topics is needed to continue the learning process and to quantify the performance of a vertical green system. They are shown in the following list:

- An in depth analysis of the contribution of the stomatal resistance and its dependency on the soil moisture content, as it defines the contribution of the bulk surface resistance and aerodynamic resistance.
- An analysis of the influence of the leaf area index and leaf angle distribution regarding the wind speed and orientation on turbulent wind conditions due to irregular urban configurations.

- The identification of the full extent of the cooling effects provided by the vertical green systems regarding their distribution in space and their optimization potential on different urban configurations and climate conditions.
- A calculation of the total amount of moisture that is being released into the environment due to the cooling effect as well as the amount of water required to maintain optimal levels of moisture and prevent a decrease in the evapotranspiration rate.
- Additional work is required regarding the practical implications of this research. A database consisting of the categorization of plant species based on their leaf area index, leaf angle distribution and leaf surface albedo at different stages of plant growth is required. This database could be used to pair up the mathematical results from the simulations with real plants species to have a fitting design with the one obtained in the model, to achieve all the environmental benefits described throughout this document.
- Finally, larger flexibility of the Grasshopper model to interpret the data from ENVI_met is needed. Since the developed workflow allows for an immediate and automatic extraction of specific data regarding ambient air temperature, wind speed, and thermal demands, additional functionality is required to have easier access to the large amount of results that are provided by the software.

Bibliography

- [1] N.H. Abu-Hamdeh. Thermal properties of soils as affected by density and water content. *Biosystems engineering*, 86(1):97–102, 2003.
- [2] N.H. Abu-Hamdeh and R.C. Reeder. Soil thermal conductivity effects of density, moisture, salt concentration, and organic matter. *Soil science society of America Journal*, 64(4):1285–1290, 2000.
- [3] H. Akbari, D. Kurn, S.E. Bretz, and J.W. Hanford. Peak power and cooling energy savings of shade trees. *Energy and buildings*, 25(2):139–148, 1997.
- [4] A.A. Alvey. Promoting and preserving biodiversity in the urban forest. *Urban Forestry & Urban Greening*, 5(4):195–201, 2006.
- [5] Ansglobal. Living wall case study, marks & spencer newcastle, 2019. URL <https://www.ansgroupglobal.com/living-wall/case-studies/marks-spencer-newcastle>. Accessed on: 03-04-2019.
- [6] Z. Azkorra, G. Pérez, J. Coma, L.F. Cabeza, S. Burés, J.E. Álvaro, A. Erkoreka, and M. Urrestarazu. Evaluation of green walls as a passive acoustic insulation system for buildings. *Applied Acoustics*, 89:46–56, 2015.
- [7] A. Baklanov, L.T. Molina, and M. Gauss. Megacities, air quality and climate. *Atmospheric Environment*, 126:235–249, 2016.
- [8] L. Bragança, S.M. Vieira, and J.B. Andrade. Early stage design decisions: The way to achieve sustainable buildings at lower costs. *The scientific world journal*, 2014, 2014.
- [9] Green Building. A guide to using plants on roofs, walls and pavements. *Mayor of London. Greater London Authority*, 2004.
- [10] G.S. Campbell and J.M. Norman. *An introduction to environmental biophysics*. Springer Science & Business Media, 2012.
- [11] H.F. Castleton, V. Stovin, S. Beck, and J.B. Davison. Green roofs; building energy savings and the potential for retrofit. *Energy and buildings*, 42(10):1582–1591, 2010.
- [12] CLEX. Reading envi_met files, 2018. URL <https://climate-cms.org/2018/04/24/reading-envi-met.html>. Accessed on: 08-06-2019.
- [13] J.A. Coakley. Reflectance and albedo, surface. *Encyclopedia of Atmospheric Sciences*, page 1914–1923, 2003.
- [14] J. Coma, G. Pérez, A. de Gracia, S. Burés, M. Urrestarazu, and L.F. Cabeza. Vertical greenery systems for energy savings in buildings: A comparative study between green walls and green facades. *Building and environment*, 111:228–237, 2017.
- [15] European Commission. Energy performance of buildings, 2019. URL <https://ec.europa.eu/energy/en/topics/energy-efficiency/energy-performance-of-buildings>. Accessed on: 22-03-2019.
- [16] Conceptcon. Bioclimatic design principles, 2011. URL <http://www.conceptcon.gr/eng/bioclimatic.html>. Accessed on: 20-12-2018.
- [17] F. Convertino, G. Vox, and E. Schettini. Heat transfer mechanisms in vertical green systems and energy balance equations. *International Journal of Design & Nature and Ecodynamics*, 14(1):7–18, 2019.

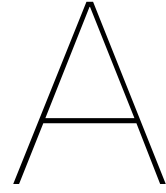
- [18] W. Curtis. *Le Corbusier: ideas and forms*. Phaidon Oxford, 1986.
- [19] H. da Costa Silva, L.S. Kinsel, and S.T. Garcia. Paper 601: Climate analysis and strategies for bioclimatic design purposes. In *Conference on passive and low energy architecture*. PLEA, 2008.
- [20] S. Dalley. *The mystery of the Hanging Garden of Babylon: an elusive world wonder traced*. OUP Oxford, 2013.
- [21] M.J.M. Davis, M. Tenpierik, F.R. Ramírez, and M.E. Perez. More than just a green facade: The sound absorption properties of a vertical garden with and without plants. *Building and Environment*, 116:64–72, 2017.
- [22] C. Diakaki, E. Grigoroudis, and D. Kolokotsa. Towards a multi-objective optimization approach for improving energy efficiency in buildings. *Energy and Buildings*, 40(2008): 1747–1754, 2008.
- [23] R. Djedjig, R. Belarbi, and E. Bozonnet. Green wall impacts inside and outside buildings: experimental study. *Energy Procedia*, 139:578–583, 2017.
- [24] A.M. Dzhambov and D.D. Dimitrova. Urban green spaces' effectiveness as a psychological buffer for the negative health impact of noise pollution: a systematic review. *Noise and Health*, 16(70):157, 2014.
- [25] enHEALTH. The health effects of environmental noise, 2018.
- [26] Executive Agency for small and medium-sized enterprises. High energy performing buildings: Support for innovation and market uptake under horizon 2020 energy efficiency. *European Commission*, 2018.
- [27] FAO. Crop evapotranspiration - guidelines for computing crop water requirements - fao irrigation and drainage paper 56, 1998. URL [http://www.fao.org/3/X0490E/x0490e06.htm#aerodynamic%20resistance%20\(ra\)](http://www.fao.org/3/X0490E/x0490e06.htm#aerodynamic%20resistance%20(ra)). Accessed on: 02-02-2019.
- [28] S.E. Gill, J.F. Handley, A.R. Ennos, and S. Pauleit. Adapting cities for climate change: the role of the green infrastructure. *Built environment*, 33(1):115–133, 2007.
- [29] C. Gimenez. Plant-water relations. *Encyclopedia of Soils in the Environment*, pages 231–238, 2005.
- [30] E. Giouri. Zero energy potential of a high rise office building in a mediterranean climate. Msc. thesis, Delft University of Technology, 2017.
- [31] M.A. Goddard, A.J. Dougill, and T.G. Benton. Scaling up from gardens: biodiversity conservation in urban environments. *Trends in ecology & evolution*, 25(2):90–98, 2010.
- [32] K. Grabowiecki, A. Jaworski, T. Niewczas, and A. Belleri. Green solutions-climbing vegetation impact on building–energy balance element. *Energy Procedia*, 111:377–386, 2017.
- [33] Vertical Green. Maintain your greens! vertical garden & landscape maintenance, 2018. URL <https://verticalgreen.co.id/blog/maintain-greens-vertical-garden-landscape-maintenance/>. Accessed on: 16-02-2019.
- [34] H. Gunerhan and A. Hepbasli. Determination of the optimum tilt angle of solar collectors for building applications. *Building and Environment*, 42(2):779–783, 2007.
- [35] Y. He, H. Yu, A. Ozaki, N. Dong, and S. Zheng. Influence of plant and soil layer on energy balance and thermal performance of green roof system. *Energy*, 141:1285–1299, 2017.
- [36] Healthwise Staff. Harmful noise levels, 2018. URL <https://www.healthlinkbc.ca/health-topics/tf4173>. Accessed on: 14-02-2019.

- [37] M. Hostetler, W. Allen, and C. Meurk. Conserving urban biodiversity? creating green infrastructure is only the first step. *Landscape and Urban Planning*, 100(4):369–371, 2011.
- [38] A. Hoyano. Climatological uses of plants for solar control and the effects on the thermal environment of a building. *Energy and buildings*, 11(1-3):181–199, 1988.
- [39] Thermtest Instruments. Material thermal properties database, 2018. URL <https://thermtest.com/materials-database>. Accessed on: 16-06-2019.
- [40] H. Ising and B. Kruppa. Health effects caused by noise: evidence in the literature from the past 25 years. *Noise and Health*, 6(22):5, 2004.
- [41] Itaca. Part 1: Solar astronomy, 2011. URL <https://www.itacanet.org/the-sun-as-a-source-of-energy/part-1-solar-astronomy/>. Accessed on: 08-04-2019.
- [42] W. Jabi. *Parametric Design for Architecture*. Laurence King Publishing, London, England, 2013.
- [43] M.Z. Jacobson. Review of solutions to global warming, air pollution, and energy security. *Energy & Environmental Science*, 2(2):148–173, 2009.
- [44] M.S. Jayalakshmy and J. Philip. Thermophysical properties of plant leaves and their influence on the environment temperature. *International journal of Thermophysics*, 31(11-12):2295–2304, 2010.
- [45] A. Kirby. Human consumption of earth’s natural resources has tripled in 40 years, 2016. URL <https://www.ecowatch.com/humans-consumption-of-earths-natural-resources-tripled-in-40-years-/1943126747.html>. Accessed on: 10-01-2019.
- [46] L. Kleerekoper, M. Van Esch, and T.B. Salcedo. How to make a city climate-proof, addressing the urban heat island effect. *Resources, Conservation and Recycling*, 64:30–38, 2012.
- [47] V. Larasati. Bioclimatic architecture in cambodia, 2015. URL <http://www.asiagreenbuildings.com/10308/bioclimatic-architecture-in-cambodia/>. Accessed on: 25-01-2019.
- [48] G. Mangione. *Performative microforests: Investigating the potential benefits of integrating spatial vegetation environments into buildings, in regards to the performance of buildings, their occupants + local ecosystems*. PhD dissertation, Delft University of Technology, 2015.
- [49] M. Manso and J. Castro-Gomes. Green wall systems: a review of their characteristics. *Renewable and Sustainable Energy Reviews*, 41:863–871, 2015.
- [50] F. Manzano-Agugliaro, F.G. Montoya, A. Sabio-Ortega, and A. Garcia-Cruz. Review of bioclimatic architecture strategies for achieving thermal comfort. *Renewable and Sustainable Energy Reviews*, 49:736–755, 2015.
- [51] C. Marugg. Vertical forests, the impact of green balconies on the microclimate by solar shading, evapotranspiration and wind flow change. Msc. thesis, Delft University of Technology, 2019.
- [52] E. McPherson, L. Herrington, and G. Heisler. Impacts of vegetation on residential heating and cooling. *Energy and Buildings*, 12(1):41–51, 1988.
- [53] A. Medl, R. Stangl, and F. Florineth. Vertical greening systems—a review on recent technologies and research advancement. *Building and Environment*, 125:227–239, 2017.

- [54] M. Nunez and T.R. Oke. The energy balance of an urban canyon. *Journal of Applied Meteorology*, 16(1):11–19, 1977.
- [55] E. Oberndorfer, J. Lundholm, B. Bass, R.R. Coffman, H. Doshi, N. Dunnett, S. Gaffin, M. Köhler, K. Liu, and B. Rowe. Green roofs as urban ecosystems: ecological structures, functions, and services. *BioScience*, 57(10):823–833, 2007.
- [56] B. Offerle, I. Eliasson, C.S.B. Grimmond, and B. Holmer. Surface heating in relation to air temperature, wind and turbulence in an urban street canyon. *Boundary-Layer Meteorology*, 122(2):273–292, 2007.
- [57] M. Ottelé. *Green building envelope, vertical greening*. PhD dissertation, Delft University of Technology, 2011.
- [58] M. Ottelé, K. Perini, A.L.A. Fraaij, E.M. Haas, and R. Raiteri. Comparative life cycle analysis for green façades and living wall systems. *Energy and Buildings*, 43:3419–3429, 2011.
- [59] A.J.D. Pask, J. Pietragalla, D.M. Mullan, and M.P. Reynolds. *Physiological breeding II: a field guide to wheat phenotyping*. CIMMYT, 2012.
- [60] S.W. Peck, C. Callaghan, M.E. Kuhn, and B. Bass. *Greenbacks from green roofs: forging a new industry in Canada*. Citeseer, 1999.
- [61] G. Perez, L. Rincon, A. Vila, J.M. Gonzalez, and L.F. Cabeza. Green vertical systems for buildings as passive systems for energy savings. *Applied energy*, 88(12):4854–4859, 2011.
- [62] G. Pérez, J. Coma, I. Martorell, and L.F. Cabeza. Vertical greenery systems (vgs) for energy saving in buildings: A review. *Renewable and Sustainable Energy Reviews*, 39: 139–165, 2014.
- [63] G. Pérez, J. Coma, S. Sol, and L.F. Cabeza. Green facade for energy savings in buildings: The influence of leaf area index and facade orientation on the shadow effect. *Applied energy*, 187:424–437, 2017.
- [64] K. Perini and P. Rosasco. Cost–benefit analysis for green façades and living wall systems. *Building and Environment*, 70:110–121, 2013.
- [65] K. Perini, M. Ottelé, A. Fraaij, E. Haas, and R. Raiteri. Vertical greening systems and the effect on air flow and temperature on the building envelope. *Building and Environment*, 46(11):2287–2294, 2011.
- [66] L. Pitts. Monitoring soil moisture for optimal plant growth, 2016. URL <https://observant.zendesk.com/hc/en-us/articles/208067926-Monitoring-Soil-Moisture-for-Optimal-Crop-Growth#conclusion>. Accessed on: 01-05-2019.
- [67] D. Powers. About balconies, 2017. URL <https://homesteady.com/about-4709844-balconies.html>. Accessed on: 17-02-2019.
- [68] M.A. Rahman. Cpython plugin for rhino-grasshopper, 2019. URL https://github.com/MahmoudAbdelRahman/GH_CPython. Accessed on: 16-03-2019.
- [69] B. Raji, M. Tenpierik, and A. van Dobbelen. The impact of greening systems on building energy performance: A literature review. *Renewable and Sustainable Energy Reviews*, 45(2015):610–623, 2015.
- [70] B. Raji, M. Tenpierik, and A. van den Dobbelen. An assessment of energy-saving solutions for the envelope design of high-rise buildings in temperate climates: A case study in the Netherlands. *Energy and Buildings*, 124:210–221, 2016.

- [71] B. Raji, M. Tenpierik, and A. van den Dobbelsteen. Early-stage design considerations for the energy-efficiency of high-rise office buildings. *Sustainability*, 9(4):623, 2017.
- [72] A.M. Rizwan, L. Dennis, and L. Chunho. A review on the generation, determination and mitigation of urban heat island. *Journal of Environmental Sciences*, 20(1):120–128, 2008.
- [73] M. Santamouris. *Energy and climate in the urban built environment*. Routledge, 2013.
- [74] M. Santamouris. Cooling the cities—a review of reflective and green roof mitigation technologies to fight heat island and improve comfort in urban environments. *Solar energy*, 103:682–703, 2014.
- [75] O. Schweitzer and E. Erell. Evaluation of the energy performance and irrigation requirements of extensive green roofs in a water-scarce mediterranean climate. *Energy and Buildings*, 68:25–32, 2014.
- [76] A. Shipunov. *Introduction to botany*. Minot State University, 2018.
- [77] H. Simon, L. Kissel, and M. Bruse. Evaluation of envi-met’s multiple-node model and estimation of indoor climate. *Design to thrive*, 2017.
- [78] L. Soulhac, R.J. Perkins, and P. Salizzoni. Flow in a street canyon for any external wind direction. *Boundary-Layer Meteorology*, 126(3):365–388, 2008.
- [79] W. Speer. Why are lohas interested in green buildings?, 2019. URL <https://colliers-one.com/why-are-lohas-interested-in-green-buildings/>. Accessed on: 03-04-2019.
- [80] T. Susca, S. Gaffin, and GR. Dell’Osso. Positive effects of vegetation: Urban heat island and green roofs. *Environmental pollution*, 159(8-9):2119–2126, 2011.
- [81] I. Susorova, M.a Angulo, P. Bahrami, and B. Stephens. A model of vegetated exterior facades for evaluation of wall thermal performance. *Building and Environment*, 67:1–13, 2013.
- [82] P.Y. Tan, J. Wang, and A. Sia. Perspectives on five decades of the urban greening of singapore. *Cities*, 32:24–32, 2013.
- [83] The Editors of Encyclopaedia Britannica. Stephan boltzmann law, 2019. URL <https://www.britannica.com/science/Stefan-Boltzmann-law>. Accessed on: 06-05-2019.
- [84] H. Tundrea and M. Budescu. Bioclimatic architecture, a sensible and logical approach towards the future of building development. *Buletinul Institutului Politehnic din Iasi. Sectia Constructii, Arhitectura*, 59(6):109, 2013.
- [85] Cornell University. Competency area 2: Soil hydrology aem, 2010. URL <https://nrcca.cals.cornell.edu/soil/CA2/CA0212.1-3.php>. Accessed on: 20-03-2019.
- [86] A.C. van der Linden, P. Erdtsieck, Kuijpers-van L. Gaalen, and A. Zeegers. *Building Physics*. ThiemeMeulenhoff, 2013.
- [87] S. Vardoulakis, B. Fisher, K. Pericleous, and N. Gonzalez-Flesca. Modelling air quality in street canyons: a review. *Atmospheric environment*, 37(2):155–182, 2003.
- [88] B. Vidrih and S. Medved. The effects of changes in the climate on the energy demands of buildings. *International Journal of Energy Research*, 32(11):1016–1029, 2008.
- [89] S. Wagner and P. Mellblom. The next generation of energy efficient building design: where are we and where should we be going? In *Building Enclosure Science and Technology, BEST Conference, June*, pages 10–12, 2008.

-
- [90] E. White and B. Gatersleben. Greenery on residential buildings: Does it affect preferences and perceptions of beauty? *Journal of environmental psychology*, 31(1):89–98, 2011.
- [91] N.H. Wong, Y. Chen, C.L. Ong, and A. Sia. Investigation of thermal benefits of rooftop garden in the tropical environment. *Building and environment*, 38(2):261–270, 2003.
- [92] T. Wortmann, C. Waibel, G. Nannicini, R. Evins, T. Schroepfer, and J. Carmeliet. Are genetic algorithms really the best choice for building energy optimization? In *Proceedings of the Symposium on Simulation for Architecture & Urban Design*. Toronto, CA, 2017.
- [93] J. Yang, J. McBride, J. Zhou, and Z. Sun. The urban forest in beijing and its role in air pollution reduction. *Urban forestry & urban greening*, 3(2):65–78, 2005.



Grid Size Study

ENVI_met is used as the main engine to run the simulations which includes the analysis of the micro-climate of the defined environment. This sort of simulations carry a heavy toll on computational time due to the large amount of calculations required. As a DOE and optimization procedure is intended and this takes a large number of simulations, a computational time study was performed to reduce computational time with a minimal reduction of accuracy in the results. To do so, the grid size used in the simulations was modified and tested to obtain the optimal value for the DOE and optimization simulations.

The study consisted on varying the grid size and measuring the change of the air temperature value in the southwest corner of the main building. A model with a grid size of 2 meters was taken as a reference to evaluate the accuracy of the different grid sizes ranging from 3 to 10. Table A.1, provides detailed information regarding the total time required for each simulation. As seen on Figure A.1, there is an exponential decay in time with larger grid sizes. This leads to an optima with a grid size of 5 meters, which does not only presents an acceptable computational time but has an accuracy decrease of less than 3% which is considered as an acceptable level as seen on Table A.2. Additionally, when comparing the model resolutions, Figure A.2, it can be seen that a grid size of 5 meters provides a more accurate representation, geometrically speaking, of the initial model defined for this research; which does not take place with larger grid sizes as the ENVI_met software adjusts the buildings shape to fit the sizes of each cell in the grid.

Grid Size [m]	2	3	5	6	7	10
Cells in Z	15	10	7	5	5	3
Initialization time [s]	234	76	30	23	23	25
Simulation time [min]	156.9	51.5	20.65	24	12.55	12.08
Total time [min]	160.8	52.77	21.15	16.06	12.93	12.5
Time variation	-	-67.18%	-86.85%	-90.01%	-91.96%	-92.23%

Table A.1: Computational time required for grid size alternatives

As no significant time savings or accuracy decrease are obtained with a grid size larger than 5 meters, and with its capacity of maintaining the most accurate representation of the base geometry, a grid size of 5 meters is used for the design exploration and optimization procedure.

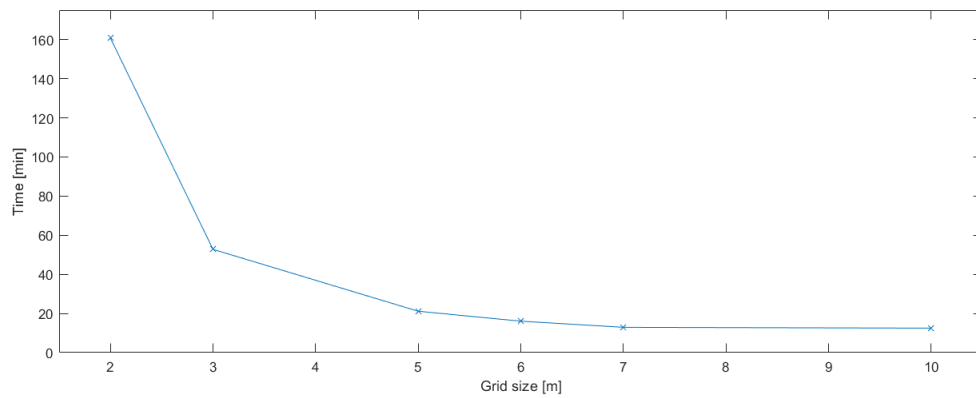


Figure A.1: Computational time trend

Time	GS = 2m	GS = 3m	GS = 5m	GS = 6m	GS = 7m	GS = 10m
06.00.00	15.039	15.016	15.043	14.961	14.925	15.018
07.00.00	15.607	15.606	15.593	15.5	15.519	15.548
08.00.00	16.413	16.437	16.326	16.192	16.239	16.351
09.00.00	17.023	17.017	16.883	16.703	16.823	16.993
10.00.00	17.853	17.883	17.651	17.492	17.639	17.584
11.00.00	18.512	18.632	18.304	18.124	18.211	18.08
12.00.00	19.435	19.538	19.069	18.875	18.995	18.985
13.00.00	19.888	19.83	19.506	19.227	19.238	19.272
14.00.00	19.551	19.617	19.219	18.919	19.057	19.137
15.00.00	19.648	19.736	19.291	19.044	19.183	19.014
16.00.00	18.96	18.942	18.722	18.514	18.667	18.446
17.00.00	18.471	18.423	18.22	17.964	18.074	18.241
18.00.00	17.583	17.49	17.502	17.229	17.249	17.443
19.00.00	16.413	16.271	16.389	16.125	16.135	16.194
20.00.00	15.285	15.076	15.27	15.032	14.964	15.057
21.00.00	14.723	14.499	14.723	14.528	14.454	14.524
22.00.00	13.826	13.533	13.81	13.607	13.502	13.534
23.00.00	13.234	12.917	13.207	13.01	12.895	12.9
00.00.00	14.34	14.195	14.35	14.248	14.211	14.237
01.00.00	14.442	14.304	14.456	14.361	14.324	14.346
02.00.00	14.424	14.293	14.441	14.354	14.318	14.334
03.00.00	14.397	14.273	14.419	14.339	14.305	14.316
04.00.00	14.311	14.186	14.335	14.257	14.223	14.228
05.00.00	14.279	14.161	14.306	14.234	14.202	14.203

Table A.2: Results for Air Temperature [°C] at SW corner of central building

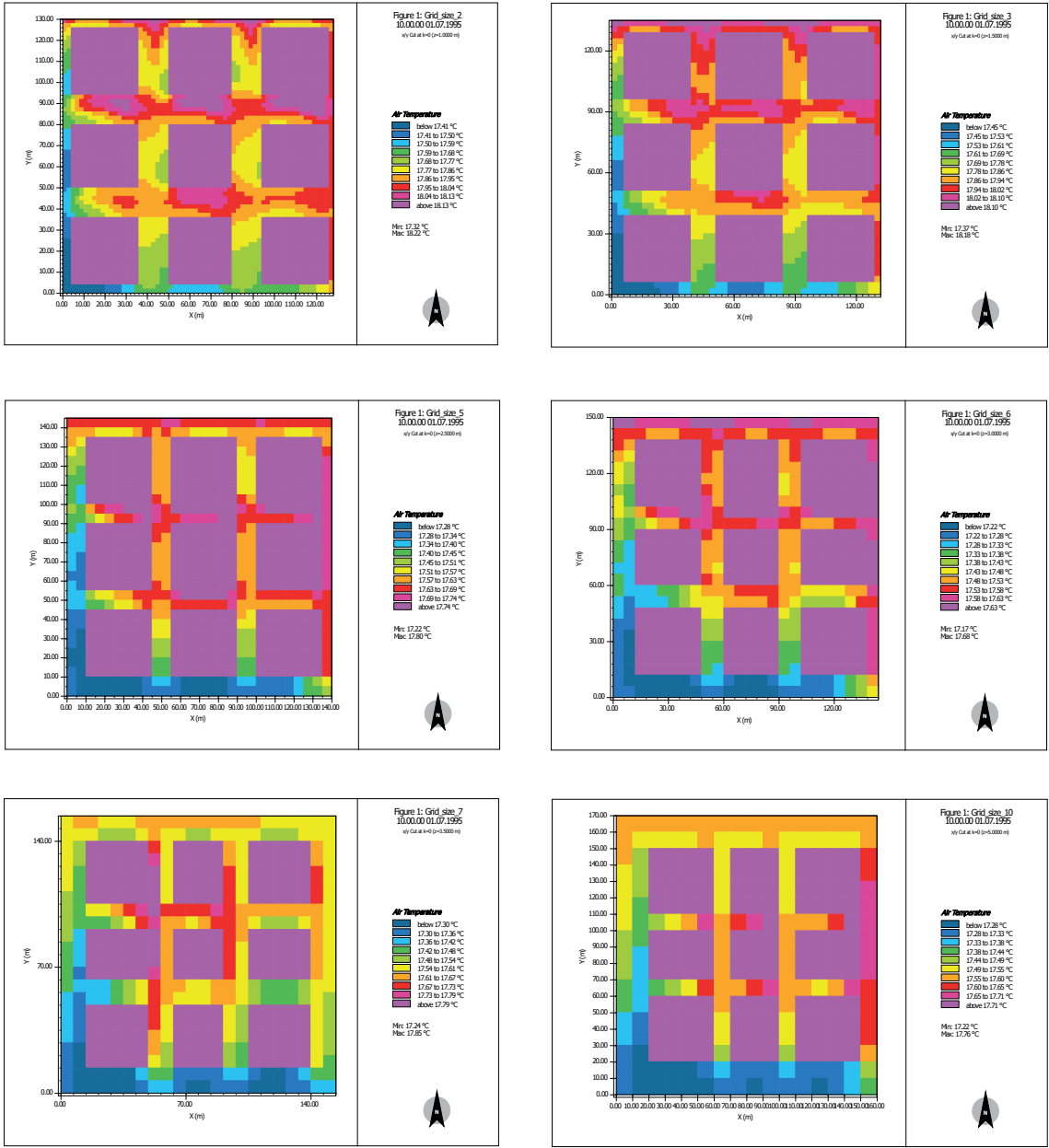
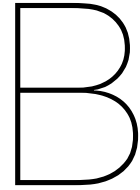


Figure A.2: Geometrical configuration of the base model with different grid sizes. From Top left to bottom right: 2m, 3m, 5m, 6m, 7m, 10m



Computational Optimization Process

This appendix presents an overview of the optimization process, the algorithms considered for the analysis of the greenery models and the work-flow definition in modeFRONTIER.

B.1. Optimization algorithms

A design optimization process aims to find the best solution to a problem considering a pre-defined criteria, it can be divided in the following steps:

1. Preliminary design exploration
2. Rough optimization using global search algorithms
3. Refinement of the Pareto optimal set using deterministic algorithms

When deciding on a particular optimization algorithm, its robustness, accuracy and convergence rates must be analyzed. It is the trade-off between these three aspects that define the efficiency of an algorithm, allowing to find the global optima no matter where in the design landscape the analysis begins after as little evaluations as possible without significantly reducing accuracy in the results. Therefore, a full optimization process might not be suitable nor pragmatic due to the large amount of resources required to achieve it. Therefore, the simulation model was simplified as much as possible, limiting the amount of variables, their range and objectives to further speed up the optimization process.

The search for the most adequate optimization algorithm has led to the development of many alternatives which can be optimal for a particular problem. As this research uses optimization algorithms as a tool, only black-box optimization methods are being considered. In order to understand them, a brief overview of the existing alternatives is presented [92].

B.1.1. Direct search

Deterministic and sequential. They have proven convergence properties and generally superior performance on (convex, non-convex, smooth and non-smooth) benchmark problems in comparison with Metaheuristic methods. There are local and global methods.

Algorithms

- SUBPLEX
- DIRECT

B.1.2. Metaheuristics

Often lack proven convergence properties and often draw their motivation from physical and biological phenomena. Nevertheless, they are mostly used for BEO due to their ease of implementation and availability.

Algorithms

- Genetic algorithms (GA): evolve a population of good solutions through crossover and recombination of individual solutions which allow larger jumps across the fitness landscape to avoid entrapment in local optima. Mutation facilitates gradual changes. Results converge on a set of good, often similar, solutions.
- Particle swarm optimization (PSO): swarm particles represent a population of solutions. Particles move on a direction weighted randomly between the best solution encountered by itself and the best solution overall. The swarm converges gradually in a good region of the landscape. A broad initial distribution of particles, prevents entrapment by local optima.
- Simulated annealing (SA): considers a single solution. It gradually shifts from exploration to exploitation.

B.1.3. Model-based methods

Uses machine-learning methods such as Neural Networks, Support Vector Machines and Radial Basis Functions to approximate the unknown fitness landscape. It uses a surrogate model which produces less accurate but much faster results. Once the fitness landscape is approximated, the algorithm searches the model deterministically, randomly or with a metaheuristic method. Not very used for sustainable building design.

Local model-based methods, a.k.a. Trust region methods also use surrogate models, but are limited to simple models. They work best for fitness landscapes without multiple optima.

Algorithms

- Trust region methods
 - COBYLA: linear model
 - BOBYQA: quadratic model
- Global model-based method: interpolates the surrogate model with Radial Basis Functions and a GA to search it.

In order to achieve the best results with the optimization process, it was decided to use a hybrid algorithm due to their robustness and good results in similar projects.

B.2. Tools

modeFRONTIER can be used for post-processing since it allows sophisticated statistical analysis and data visualization [30]. It allows for an automatic work-flow allowing to test dozens of different configurations to perform either a single objective optimization process as well as a multi-objective one. Each case will be simulated based on the expected outcomes. In the case of Groups A: Singapore and B: Phoenix, the high ambient temperatures will lead to a cooling load throughout the year suitable for a single objective optimization. While Group C: Amsterdam with a more temperate climate will present heating loads during winter. modeFRONTIER will be used to run the simulations with a design of experiments (DOE) sequence followed by the hybrid optimization algorithm pilOPT.

Design of experiment Allows for a random, uniformly distributed creation of input variables to test the design space and provide the initial step for an optimization algorithm. Based on the Latin Hypercube sampling.

Optimization algorithm pilOPT is a hybrid multi-strategy self-adapting algorithm that combines the advantages of a local search and a global search algorithm and it adjusts the ratio of real and RSM-based design evaluations based on their performance. Due to its performance, accessibility and simple implementation, the blackbox algorithm pilOPT, included in modeFRONTIER was chosen to be suitable for the level of research and accuracy required due to the accuracy and lower computational times reported in similar projects.

C

Optimization and Urban Study Results

C.1. Reference grey model

C.1.1. Group A: Singapore

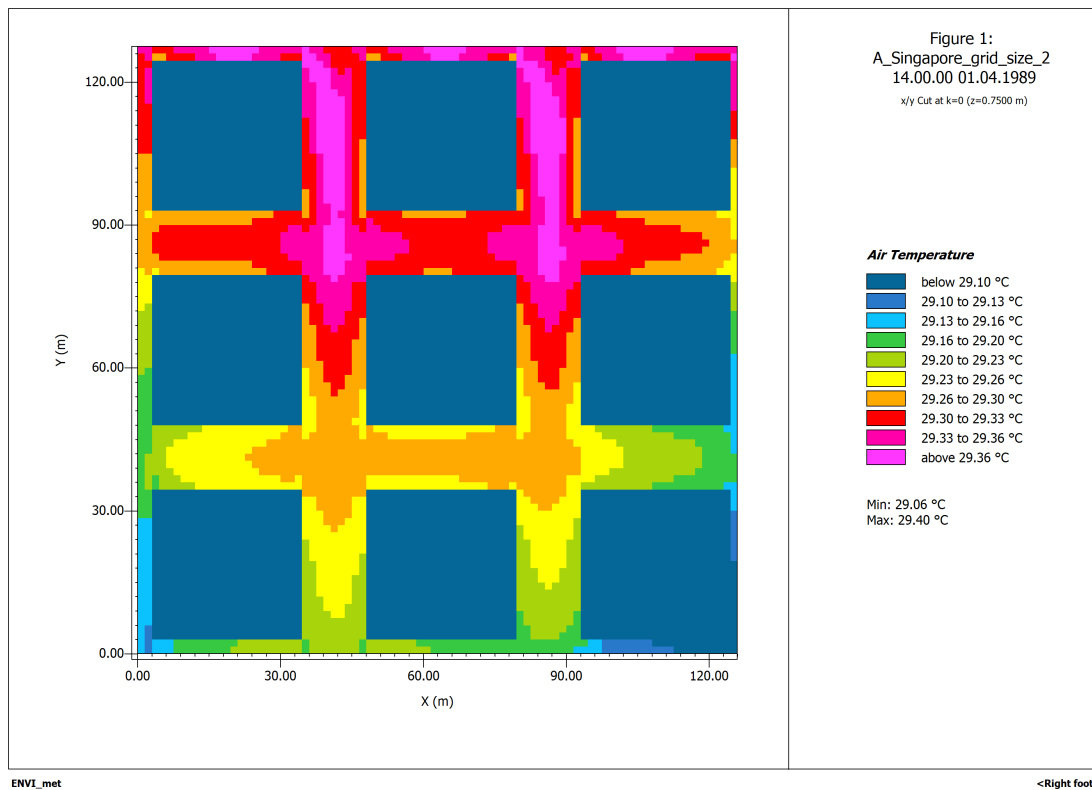


Figure C.1: Air temperature at 14:00 on April 1st 1989, for Singapore grey model

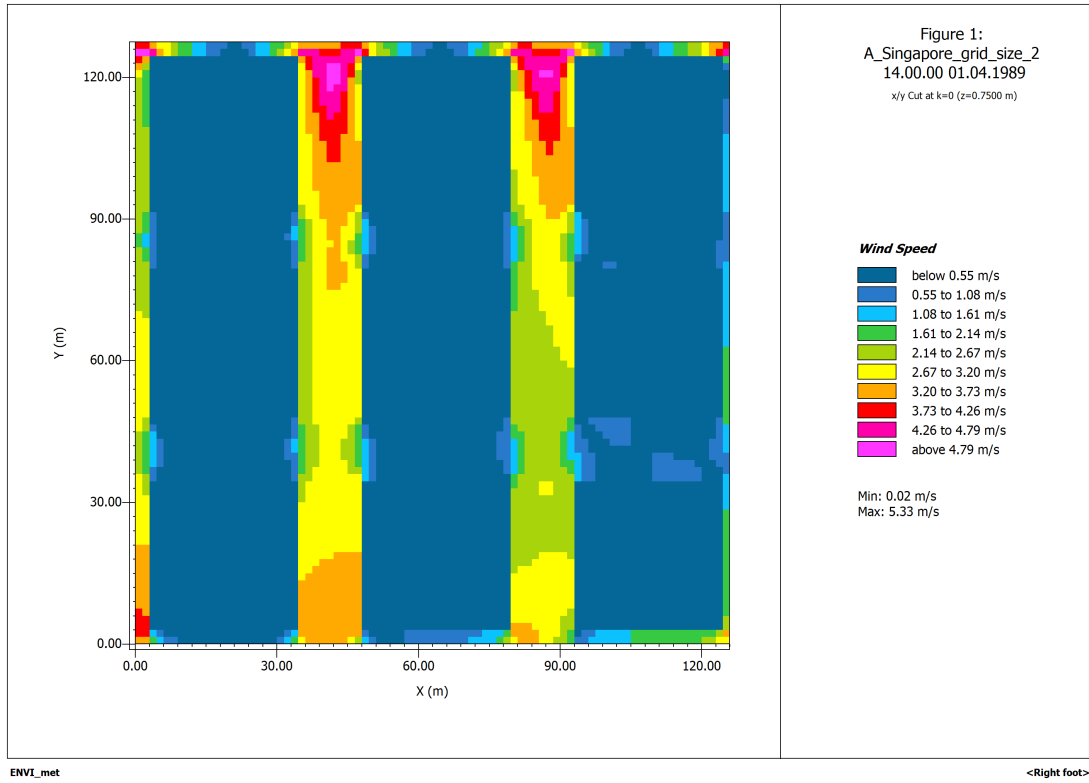


Figure C.2: Wind speed at 14:00 on April 1st 1989 for Singapore grey model

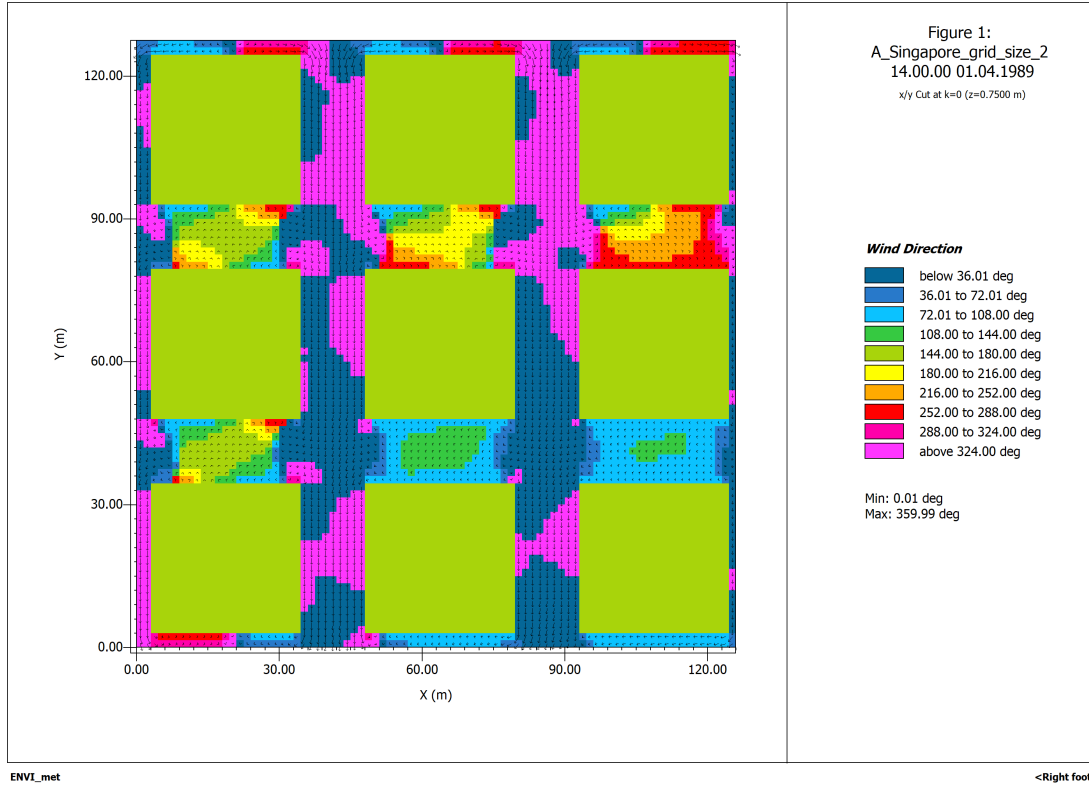


Figure C.3: Wind orientation at 14:00 on April 1st 1989 for Singapore grey model

C.1.2. Group B: Phoenix

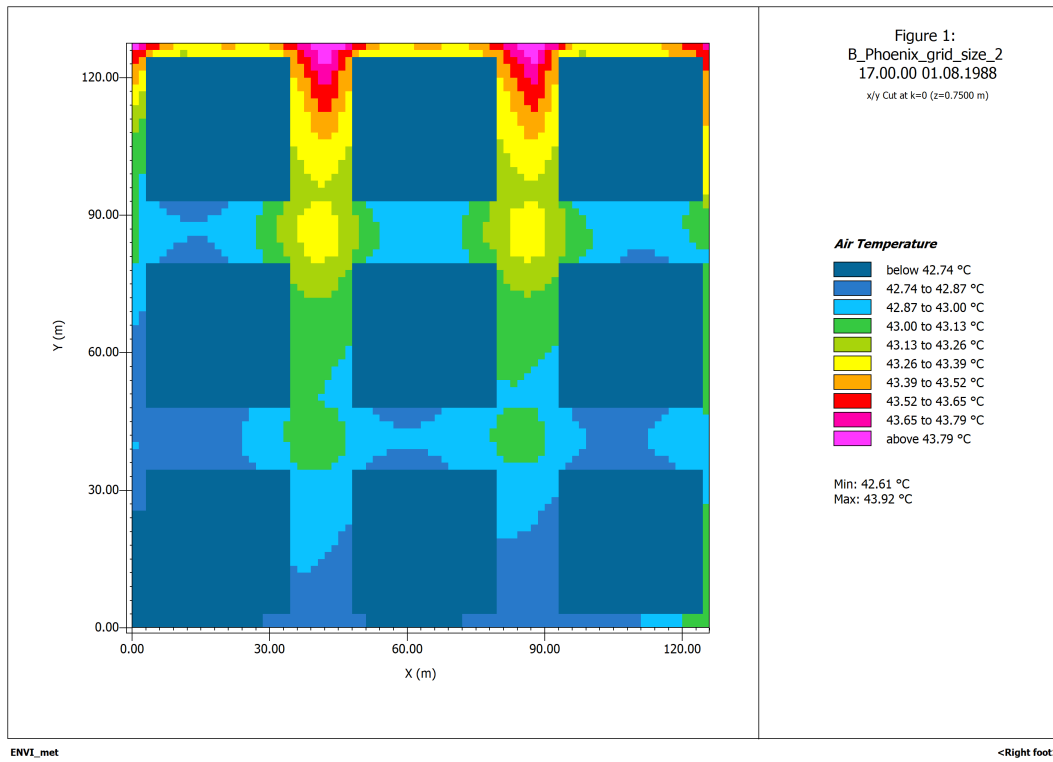


Figure C.4: Air temperature at 17:00 on August 1st 1988, for Phoenix grey model

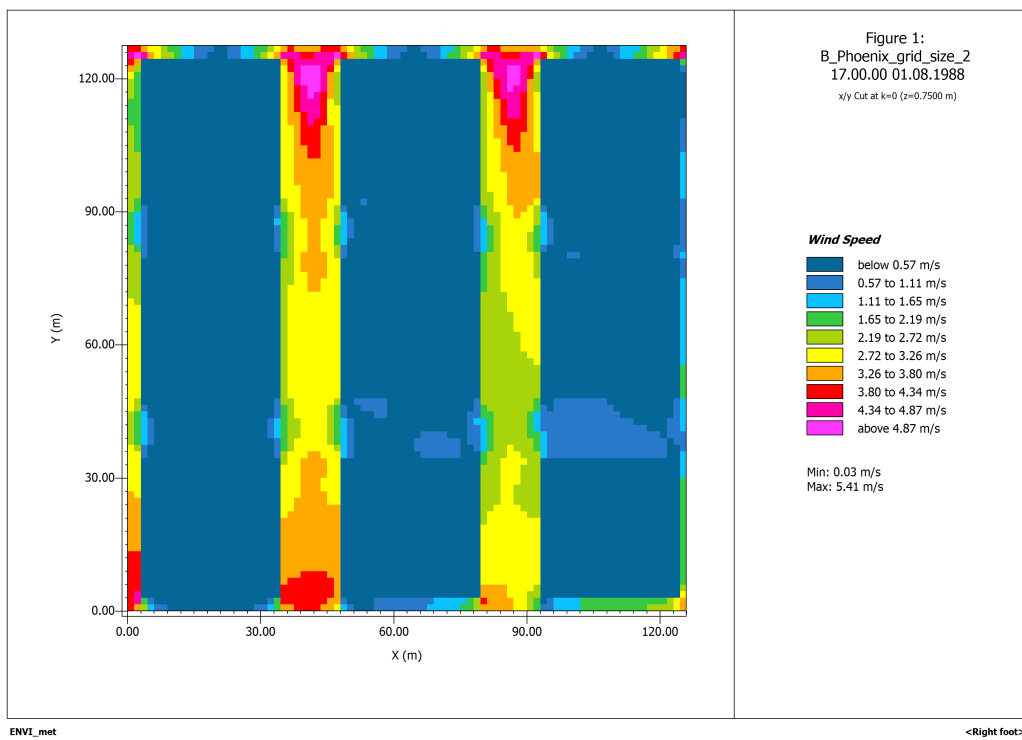


Figure C.5: Wind speed at 17:00 on August 1st 1988, for Phoenix grey model

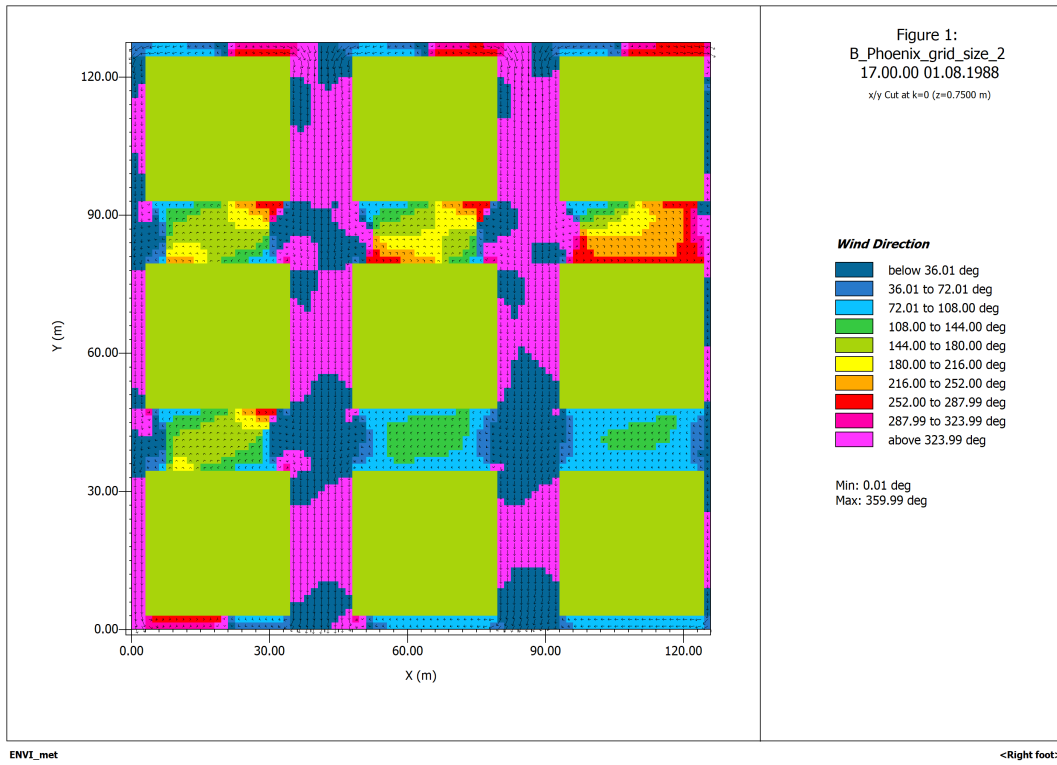


Figure C.6: Wind orientation at 17:00 on August 1st 1988, for Phoenix grey model

C.1.3. Group C: Amsterdam

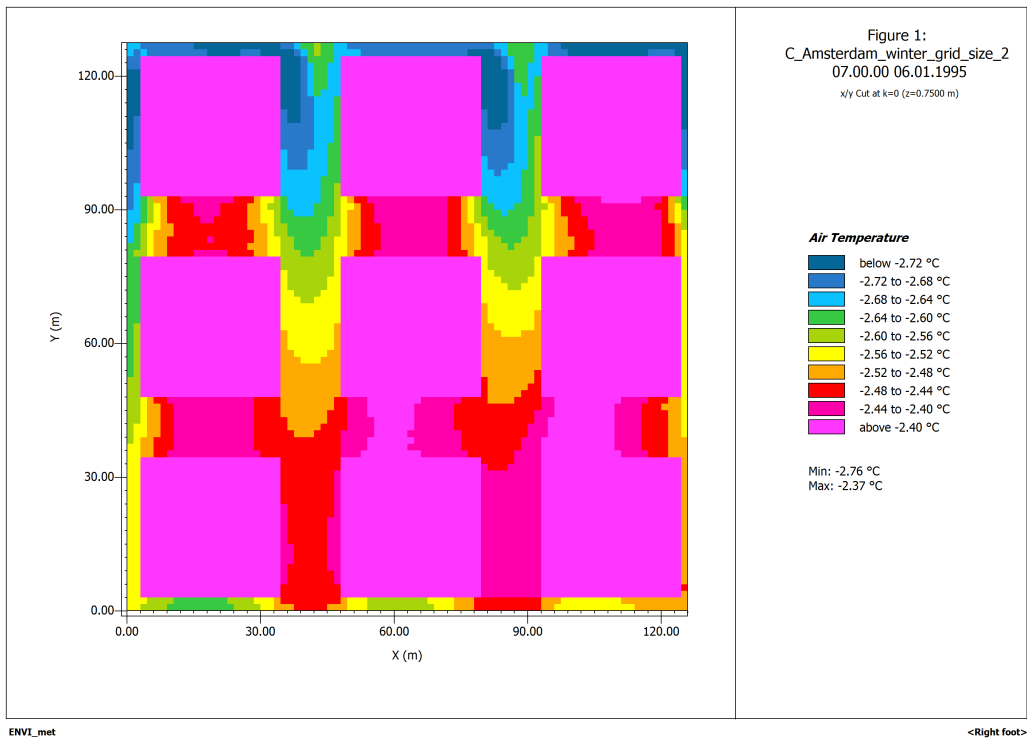


Figure C.7: Air temperature at 7:00 on January 6th 1995, for Amsterdam grey model

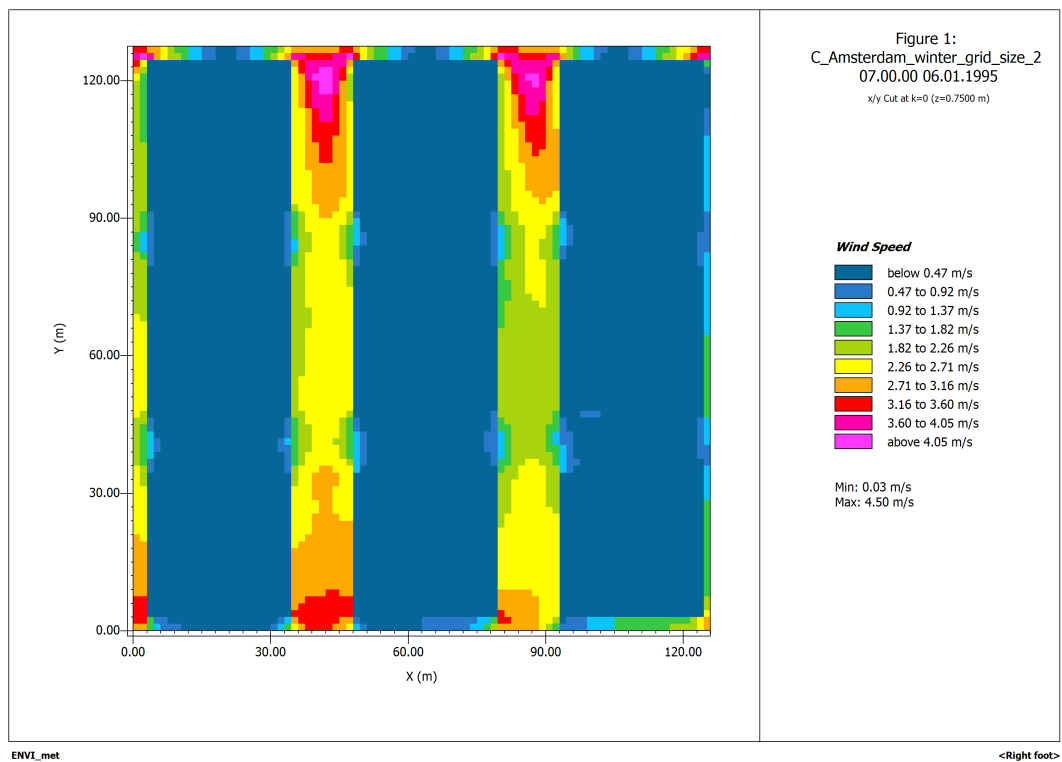


Figure C.8: Wind speed at 7:00 on January 6th 1995, for Amsterdam grey model

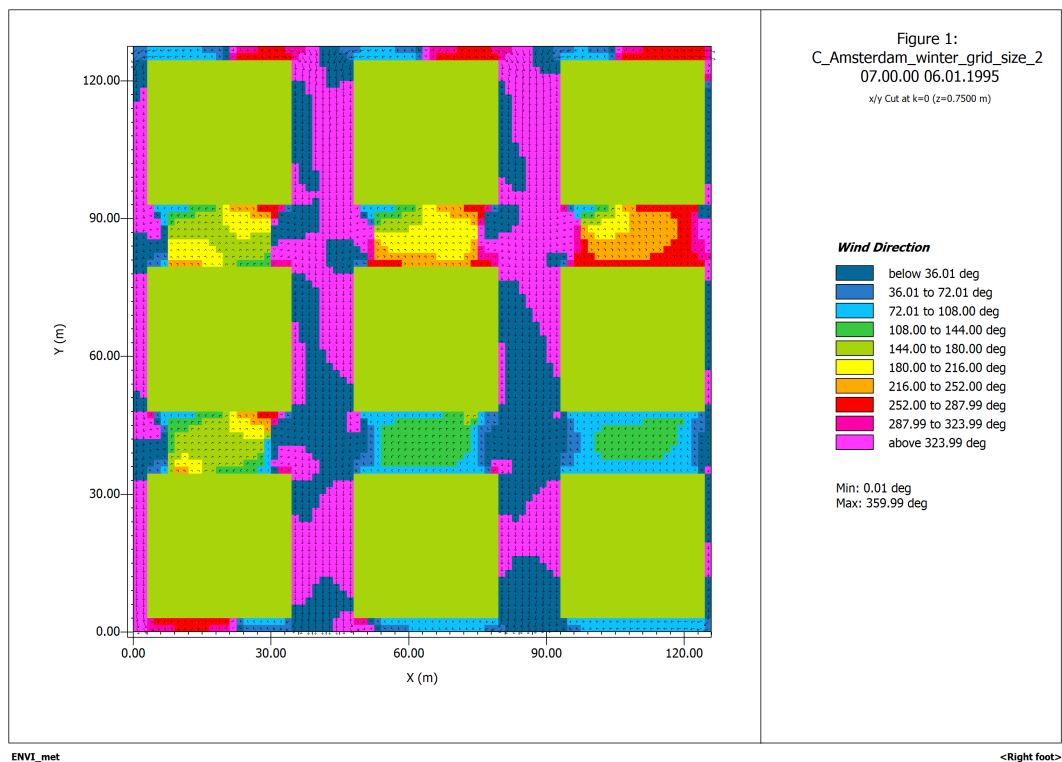


Figure C.9: Wind orientation at 7:00 on January 6th 1995, for Amsterdam grey model

C.2. Optimization results living wall system

C.2.1. Group A: Singapore

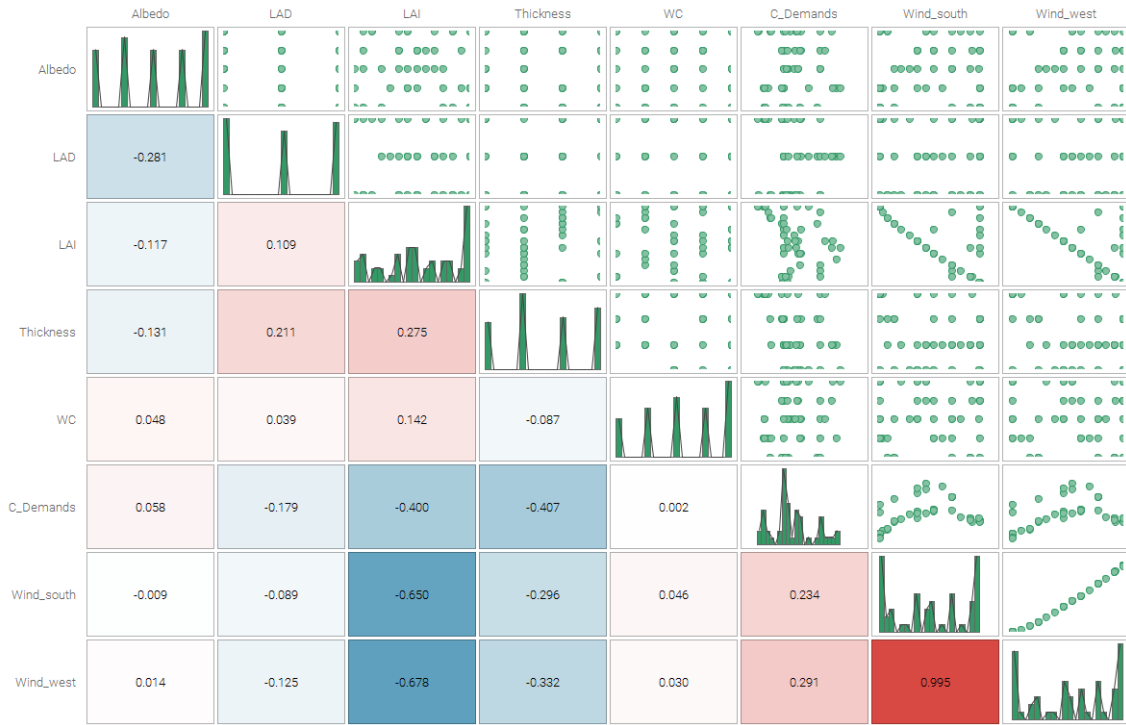


Figure C.10: Correlation matrix for all parameters analyzed in the optimization for Group A: Singapore

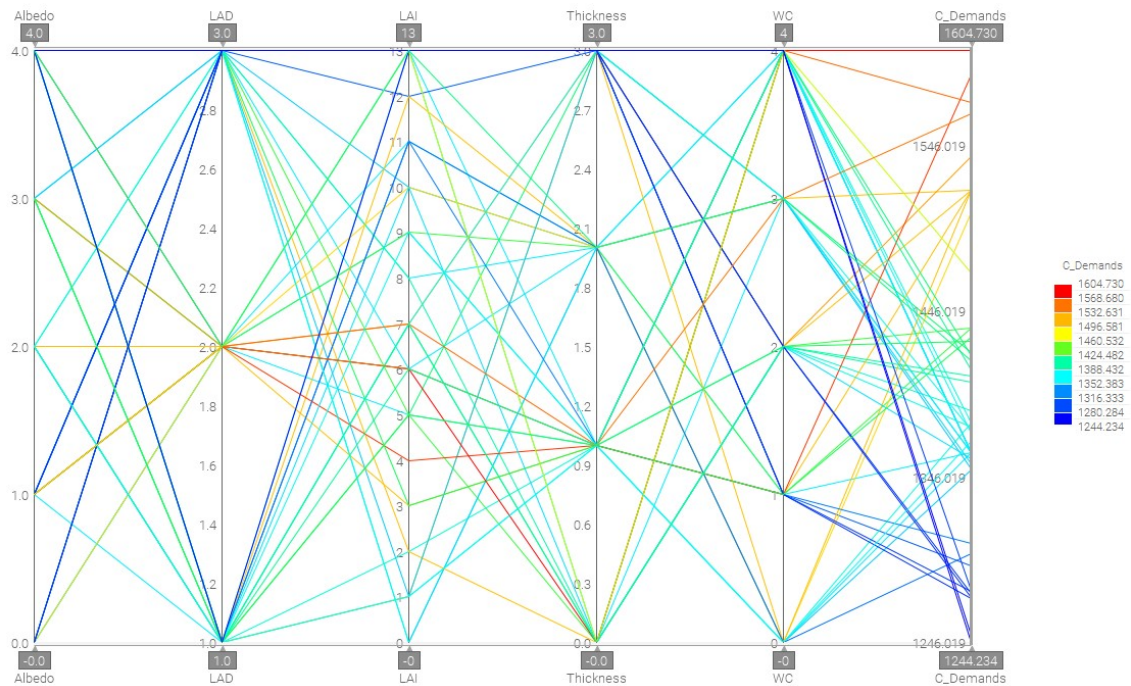


Figure C.11: Parallel coordinates from optimization study for Group A: Singapore

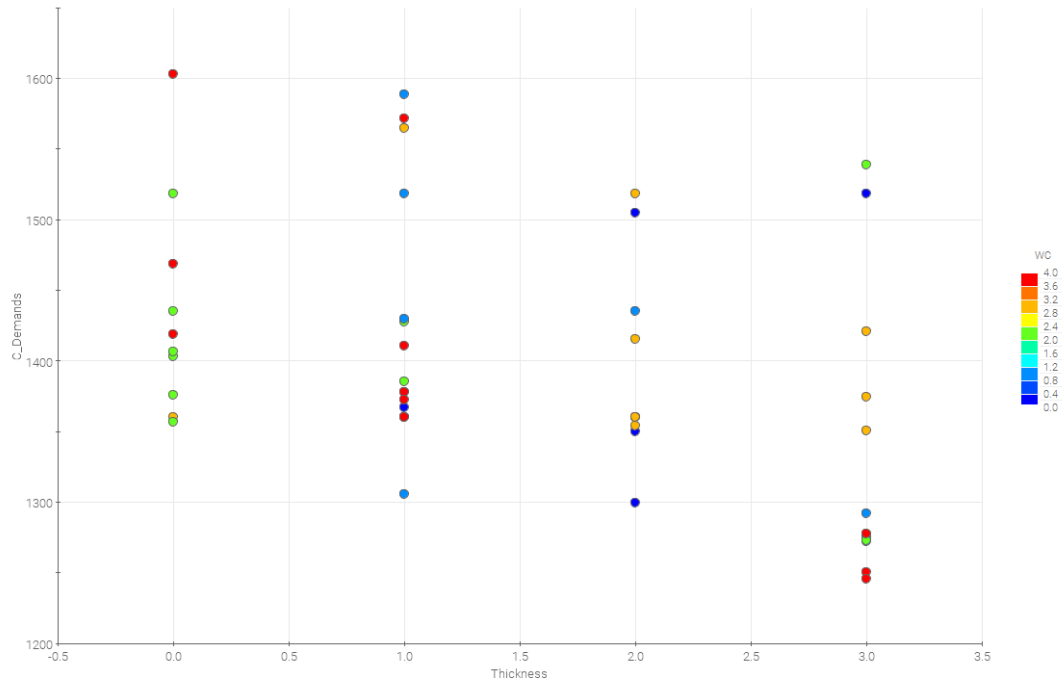


Figure C.12: Bubble plot showing the relation between substrate thickness, water coefficient and cooling demands for Group A: Singapore

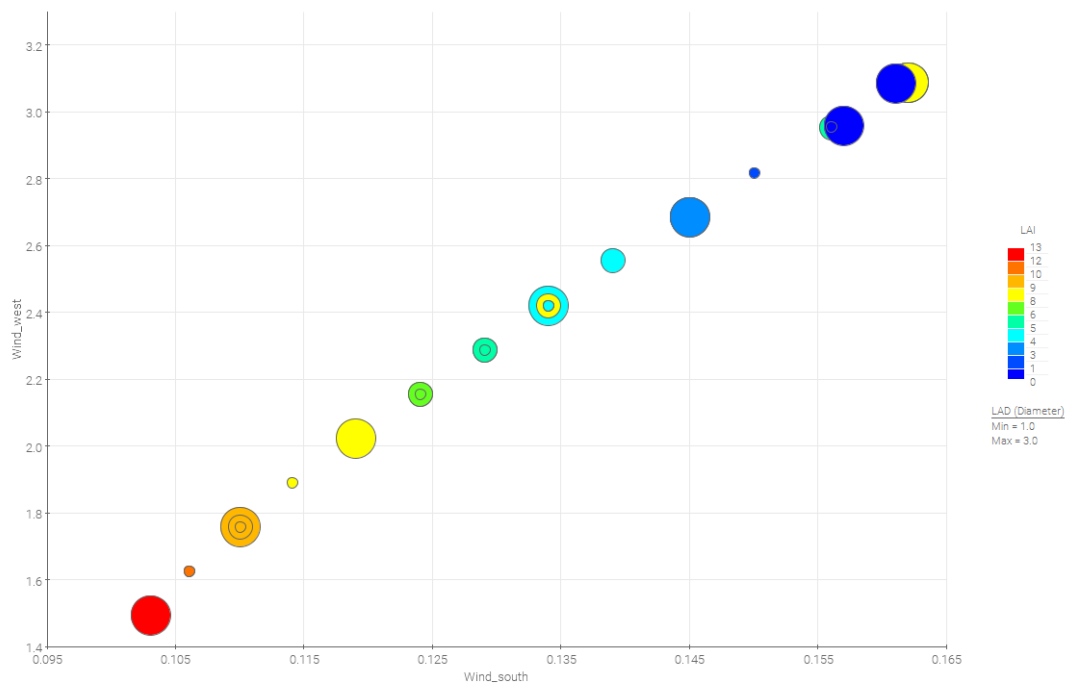


Figure C.13: Bubble plot showing the relation between LAI, χ_i and wind speed in south and west directions in Singapore

C.2.2. Group B: Phoenix

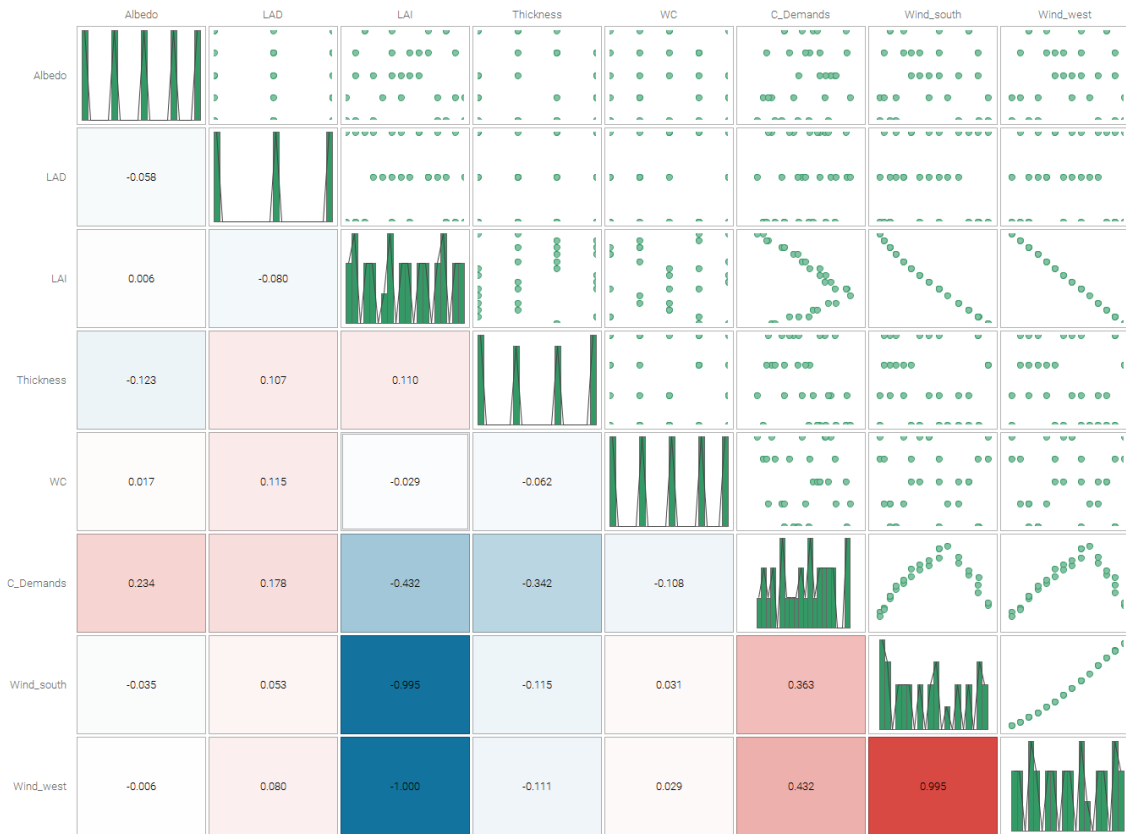


Figure C.14: Correlation matrix for all parameters analyzed in the optimization for Group B: Phoenix

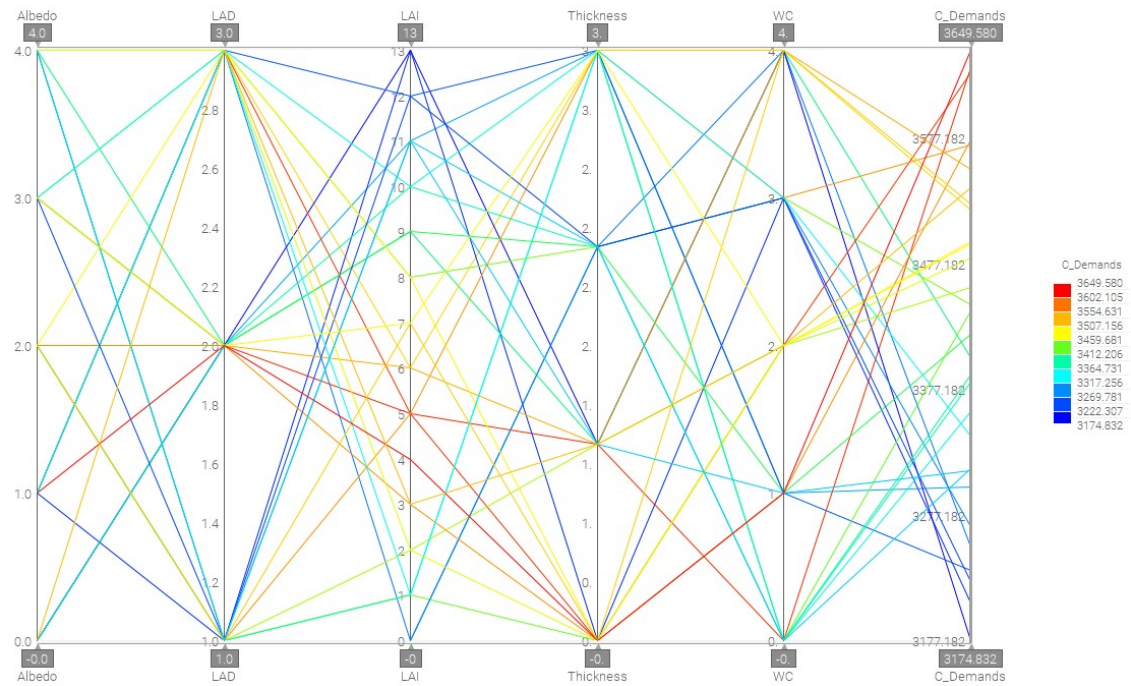


Figure C.15: Parallel coordinates from optimization study for Group B: Phoenix

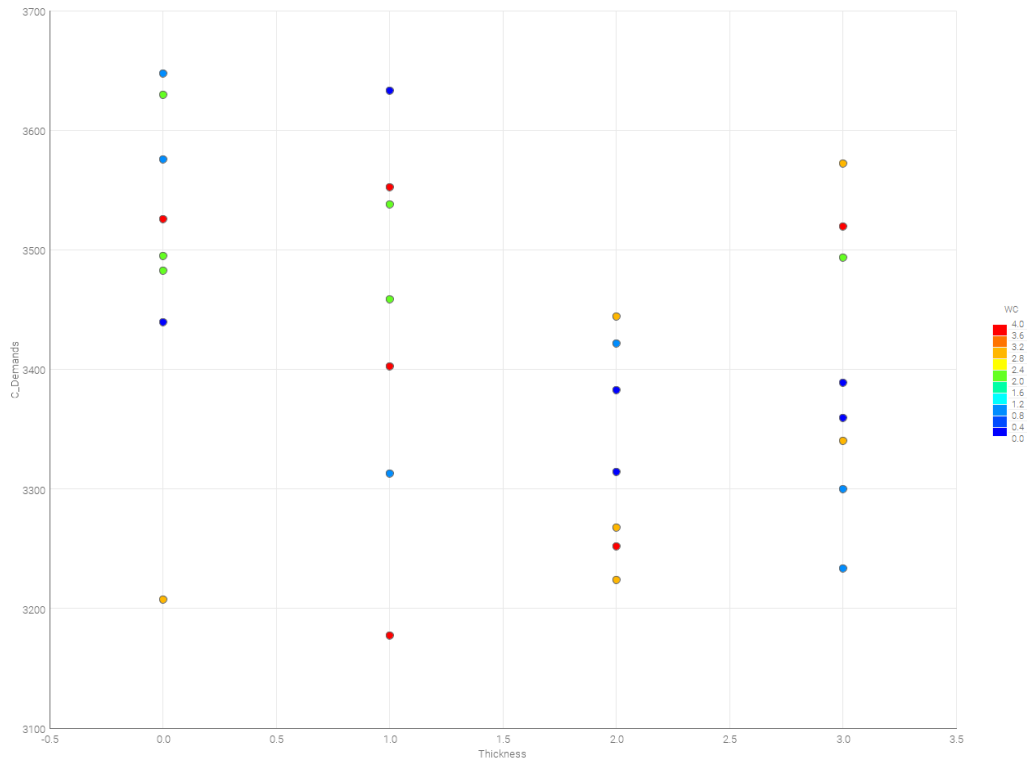


Figure C.16: Bubble plot showing the relation between substrate thickness, water coefficient and cooling demands for Group B: Phoenix

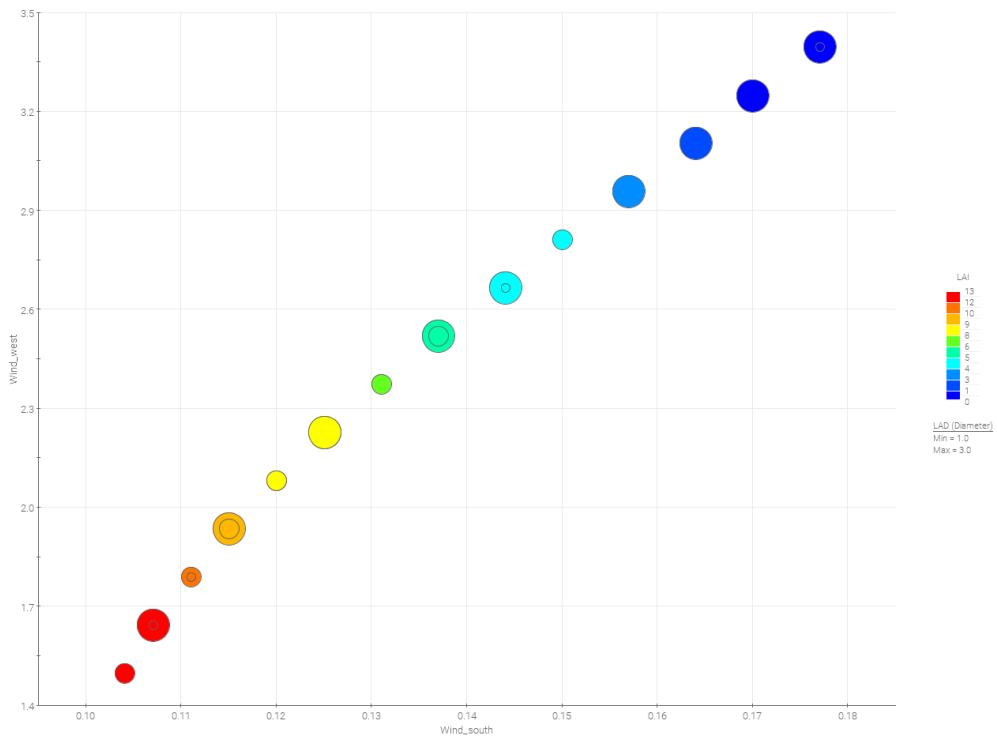


Figure C.17: Bubble plot showing the relation between LAI, χ_i and wind speed in south and west directions in Phoenix, AZ

C.2.3. Group C: Amsterdam

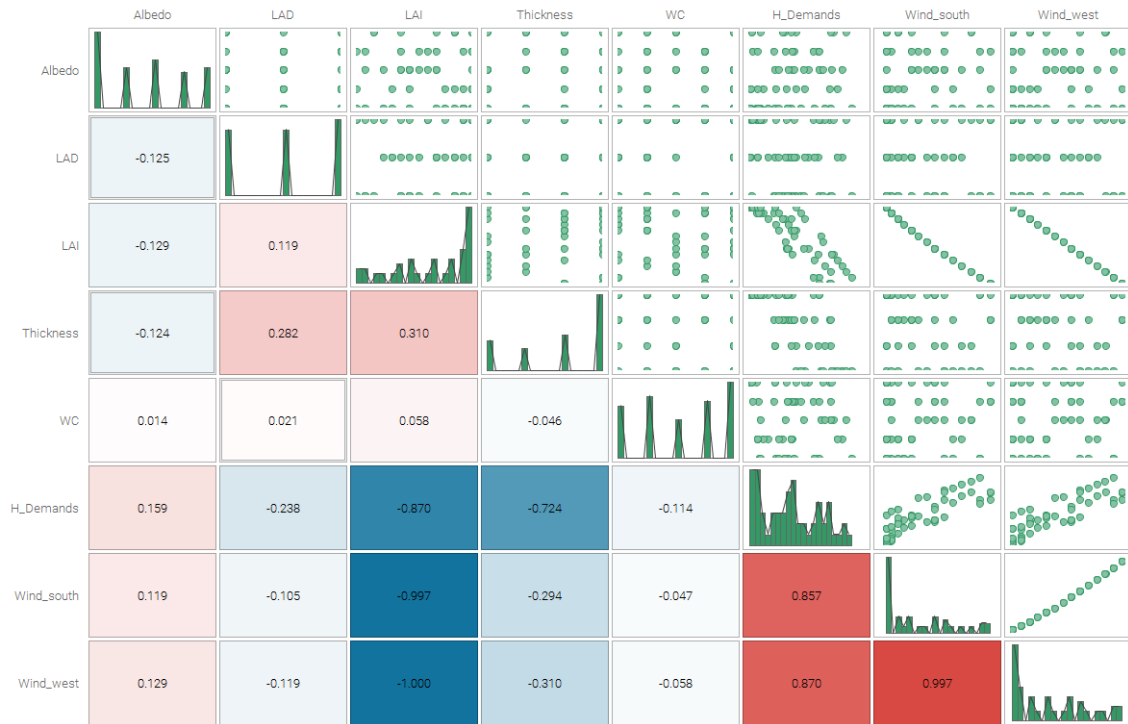


Figure C.18: Correlation matrix for all parameters analyzed in the optimization for Group C: Amsterdam

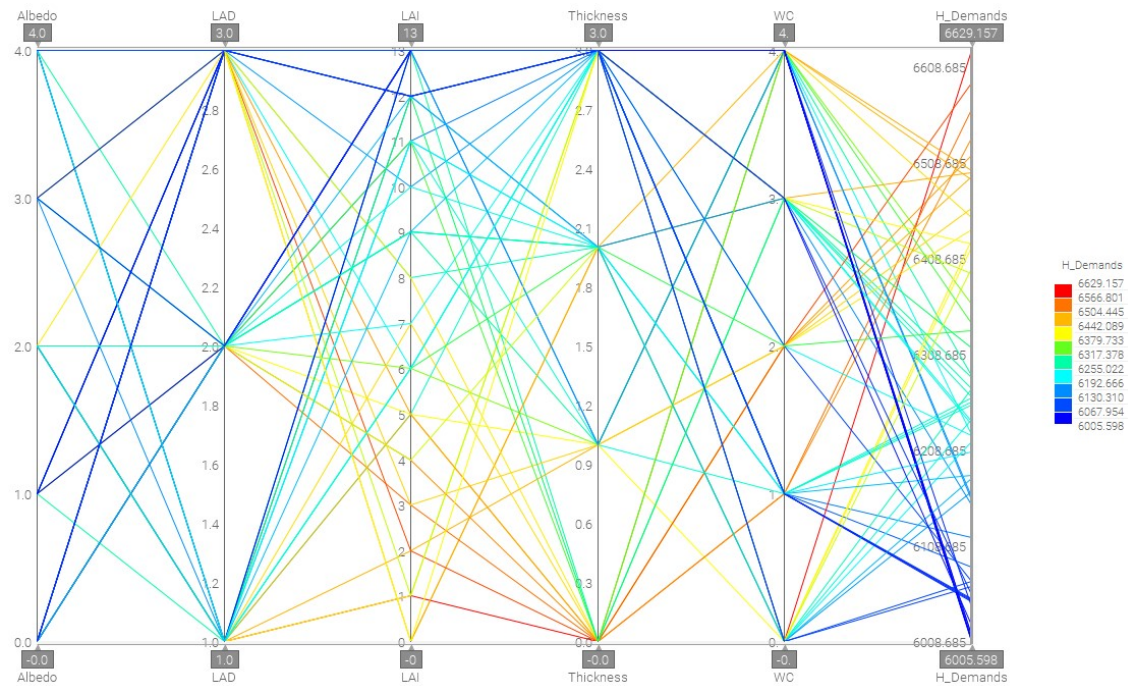


Figure C.19: Parallel coordinates from optimization study for Group C: Amsterdam

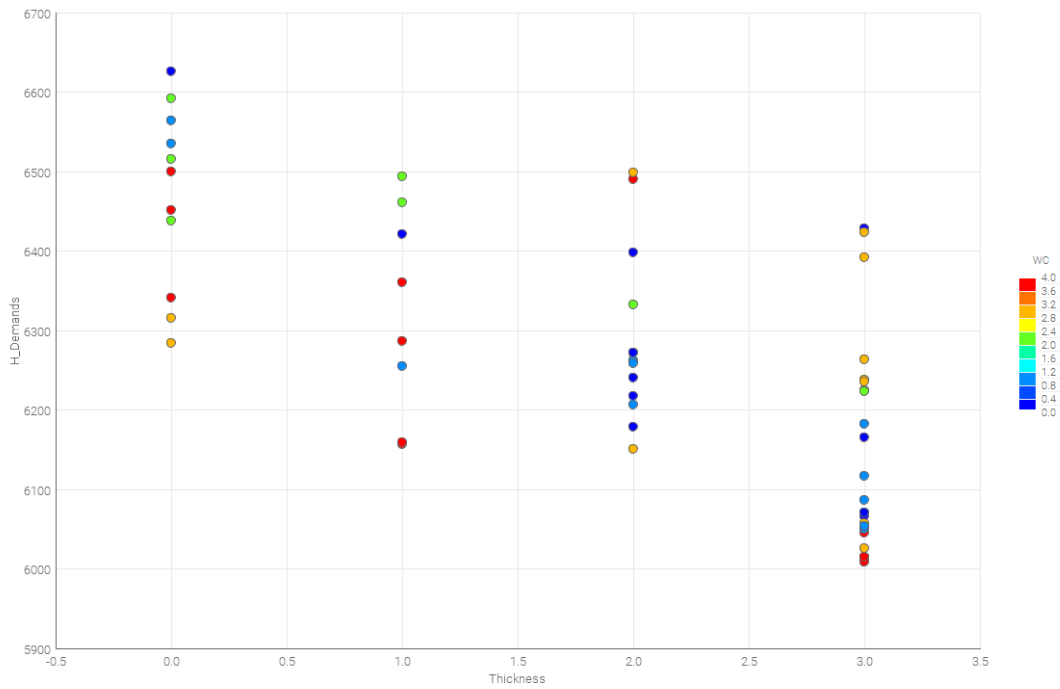


Figure C.20: Bubble plot showing the relation between substrate thickness, water coefficient and cooling demands for Group C: Amsterdam

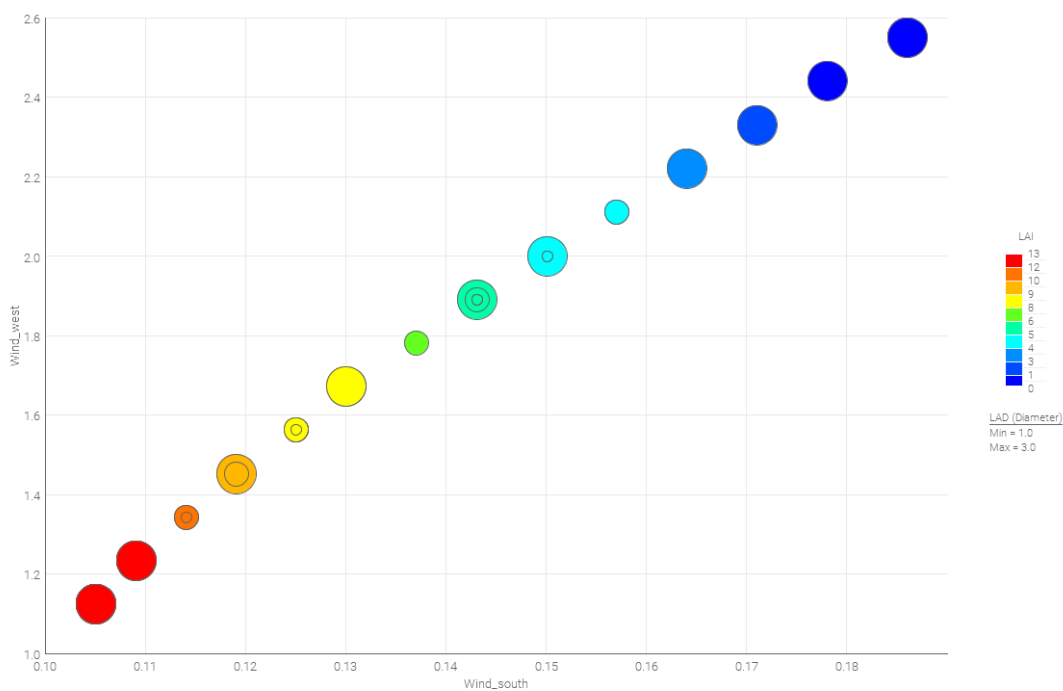


Figure C.21: Bubble plot showing the relation between LAI, χ_i and wind speed in south and west directions in Amsterdam

C.3. Optimization results green façade

C.3.1. Group A: Singapore

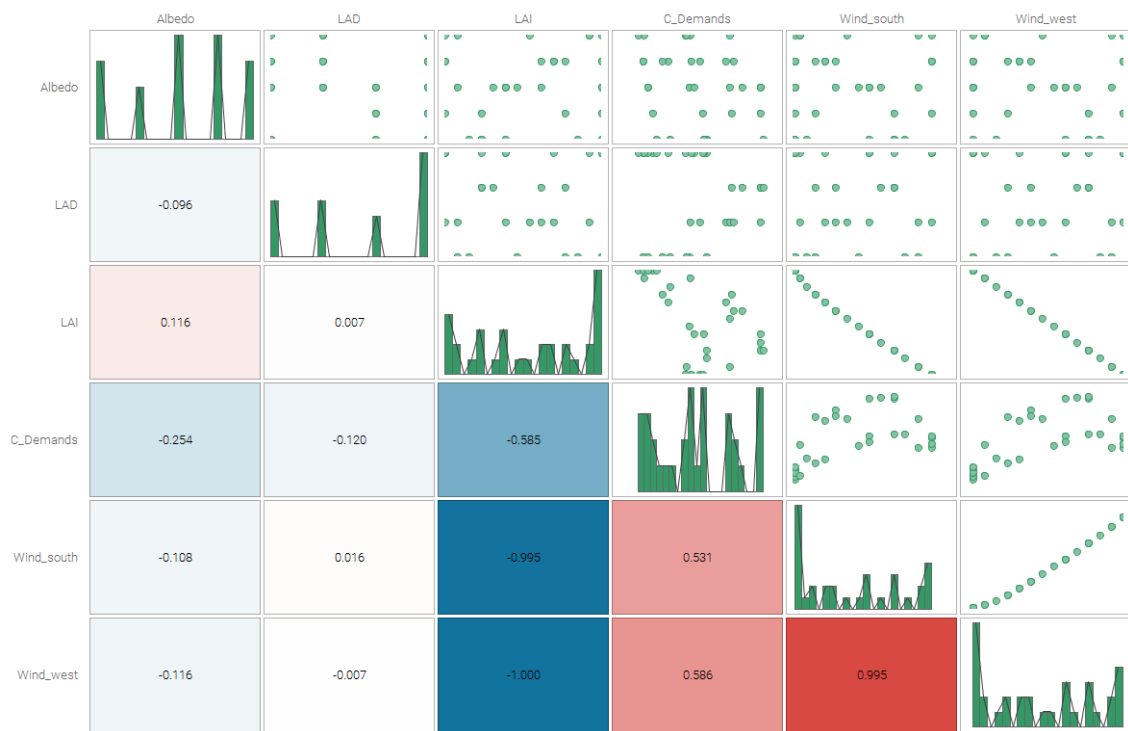


Figure C.22: Correlation matrix for all parameters analyzed in the optimization for Group A: Singapore

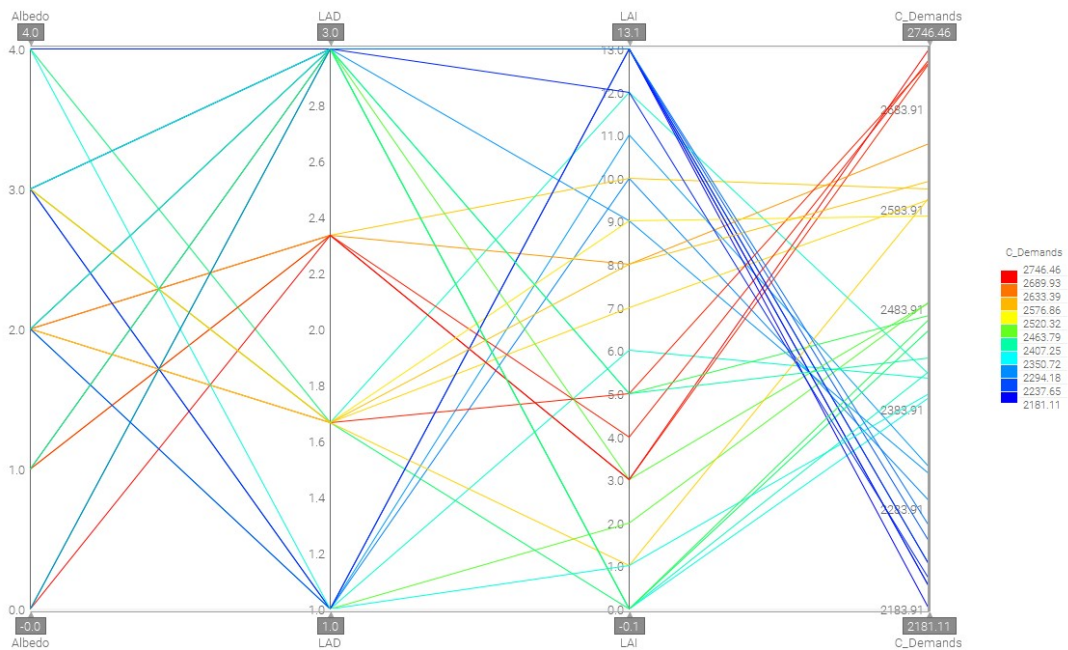


Figure C.23: Parallel coordinates from optimization study for Group A: Singapore

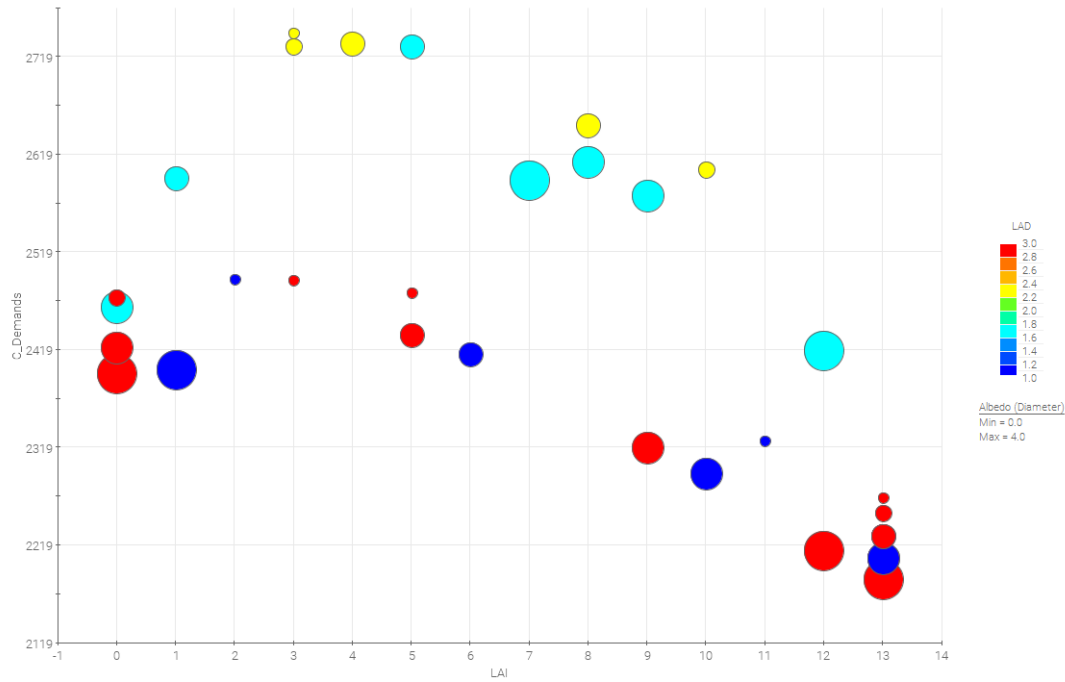


Figure C.24: Bubble plot showing the relation between LAI, cooling demands, *chi* and Albedo in Singapore

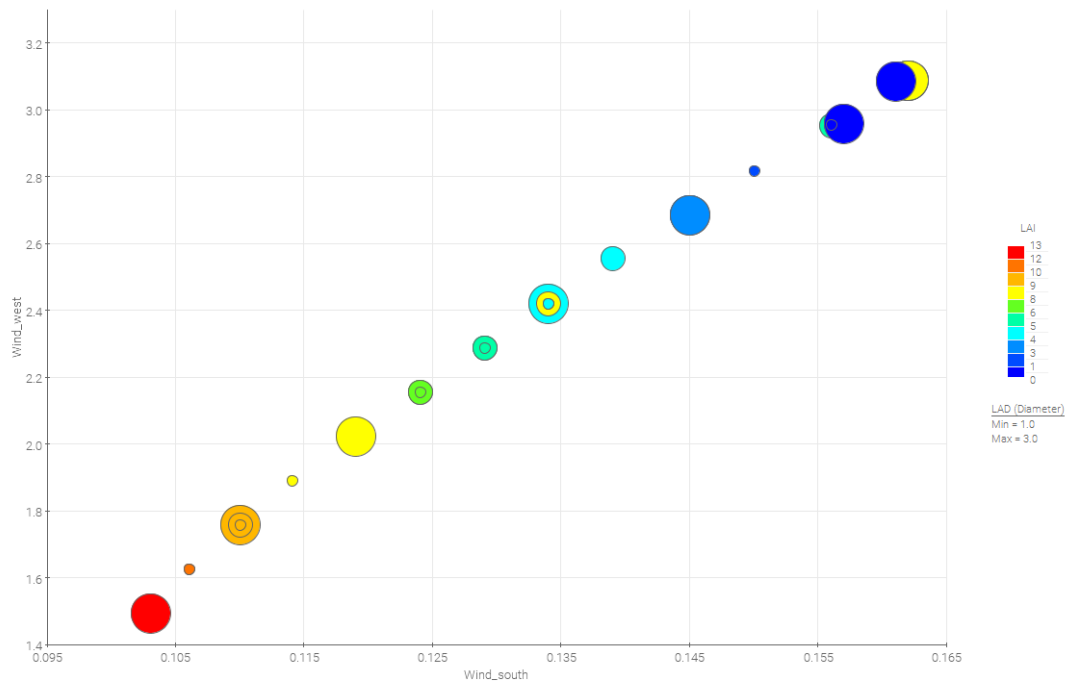


Figure C.25: Bubble plot showing the relation between LAI, *chi* and wind speed in south and west directions in Singapore

C.3.2. Group B: Phoenix

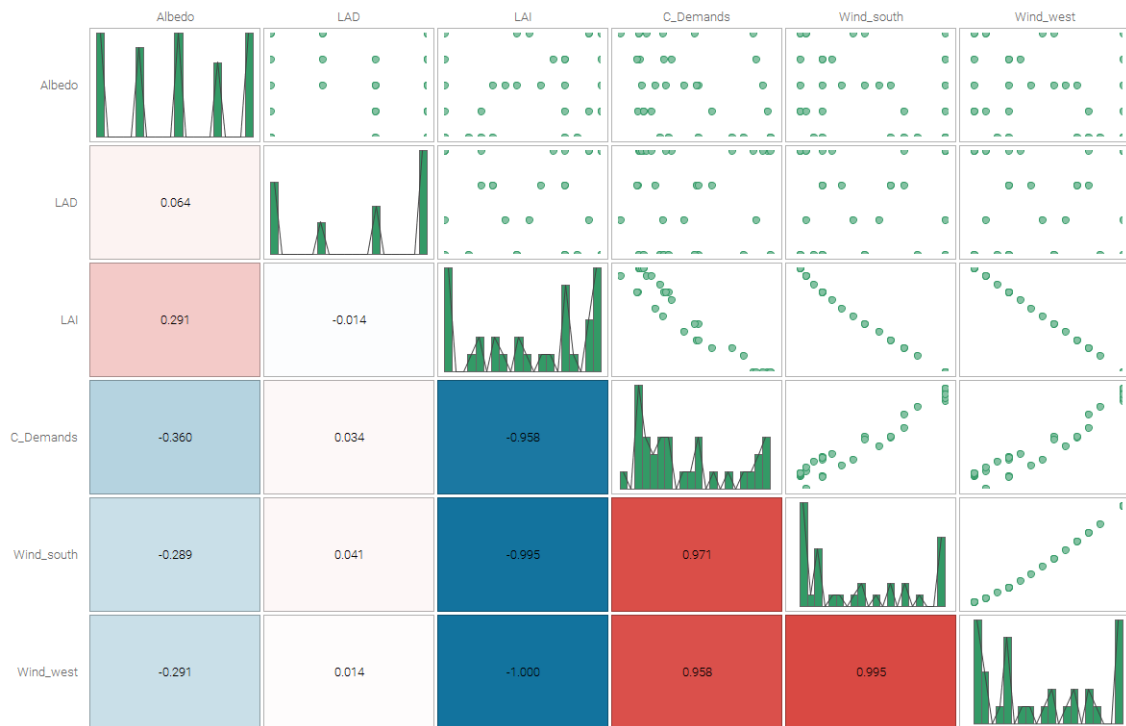


Figure C.26: Correlation matrix for all parameters analyzed in the optimization for Group B: Phoenix

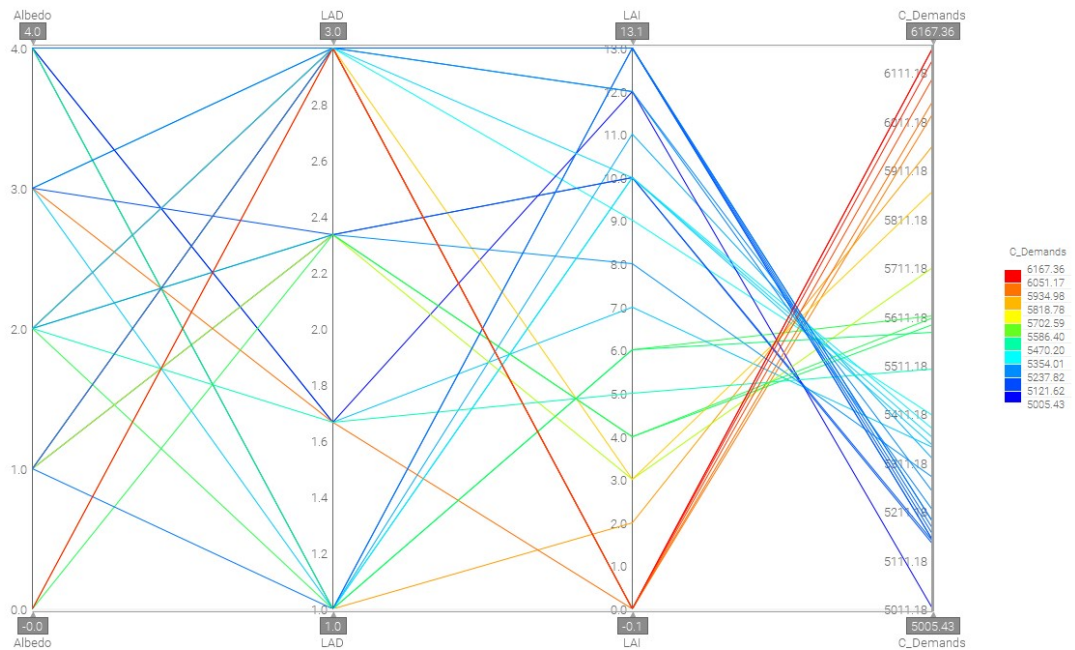


Figure C.27: Parallel coordinates from optimization study for Group B: Phoenix

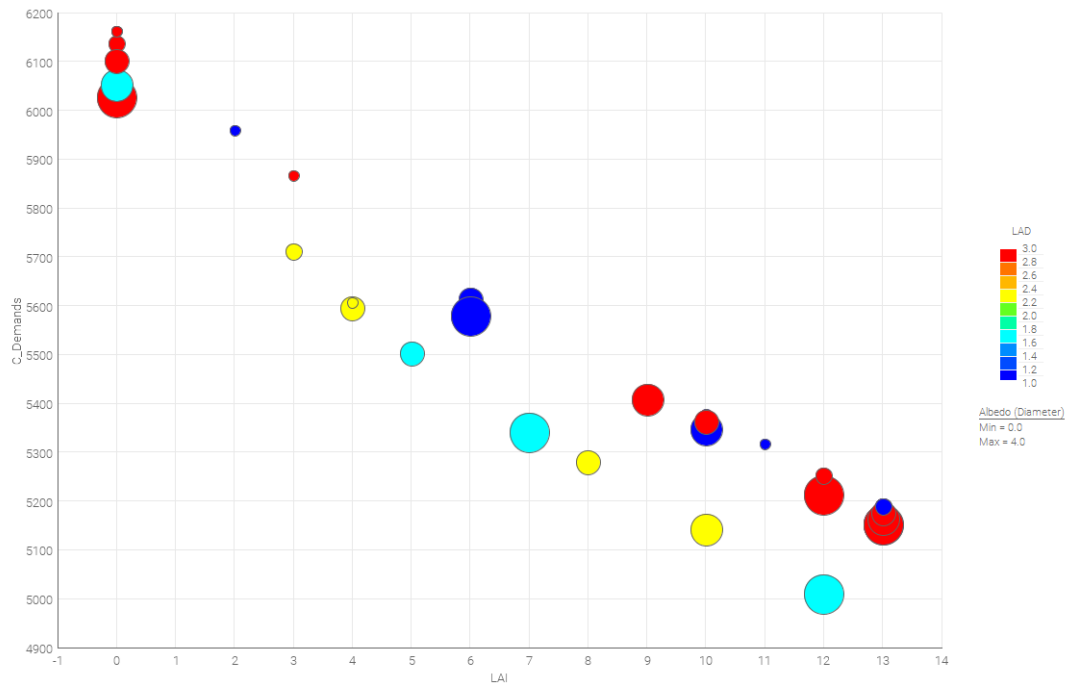


Figure C.28: Bubble plot showing the relation between LAI, cooling demands, *chi* and Albedo in Phoenix

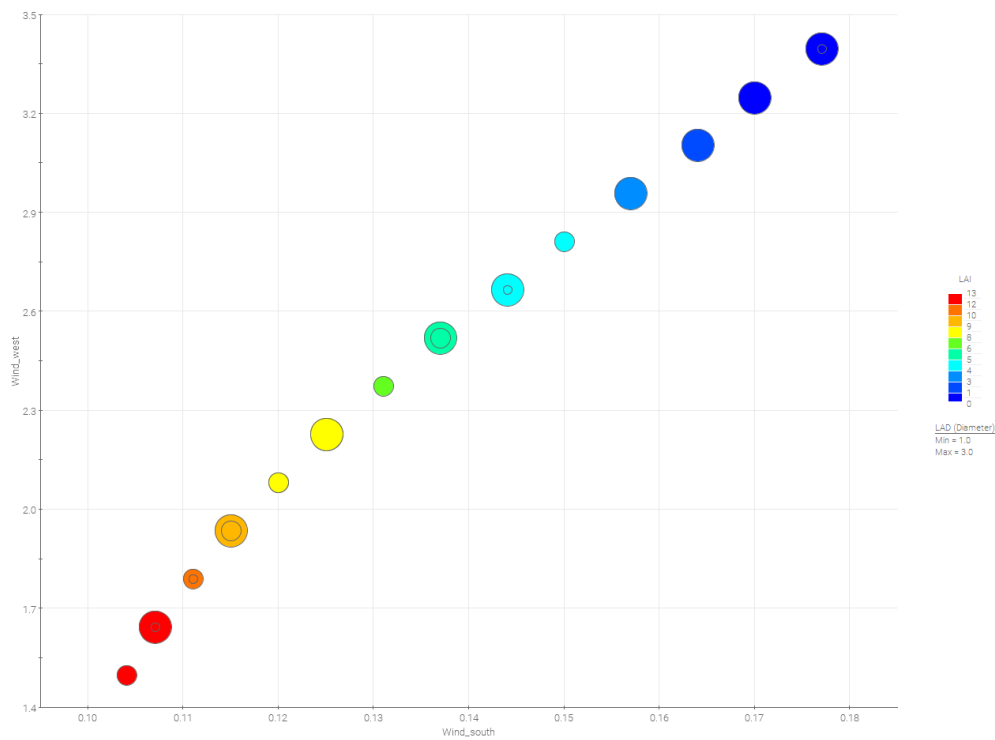


Figure C.29: Bubble plot showing the relation between LAI, *chi* and wind speed in south and west directions in Phoenix, AZ

C.3.3. Group C: Amsterdam

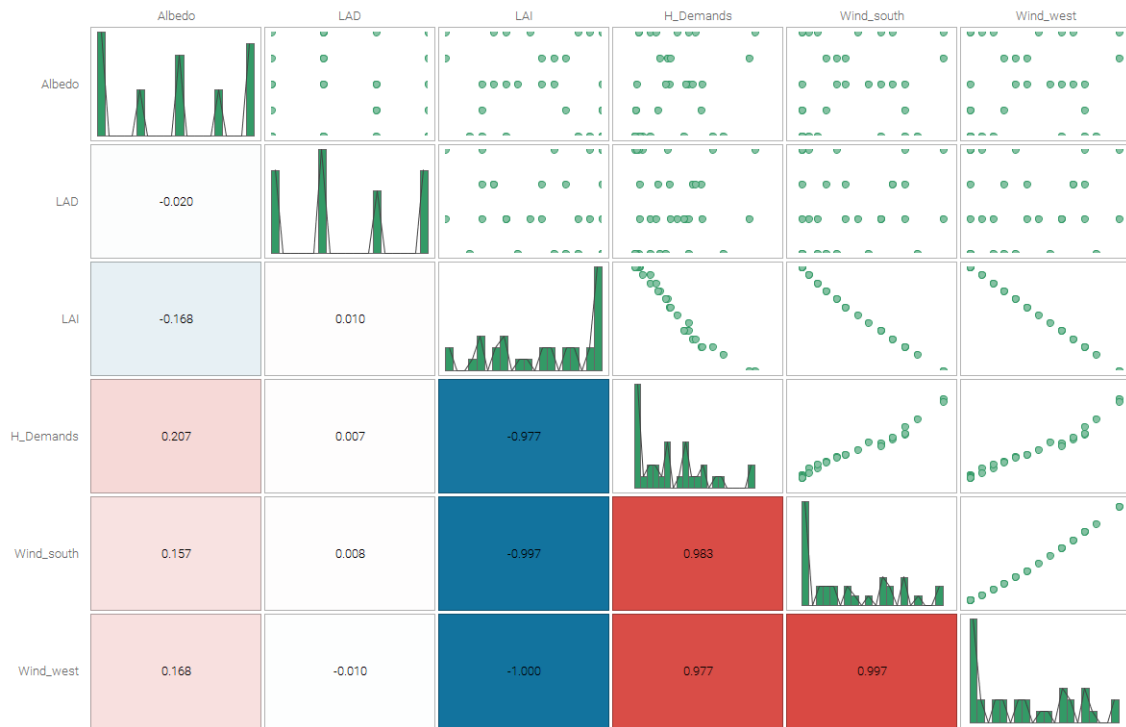


Figure C.30: Correlation matrix for all parameters analyzed in the optimization for Group C: Amsterdam

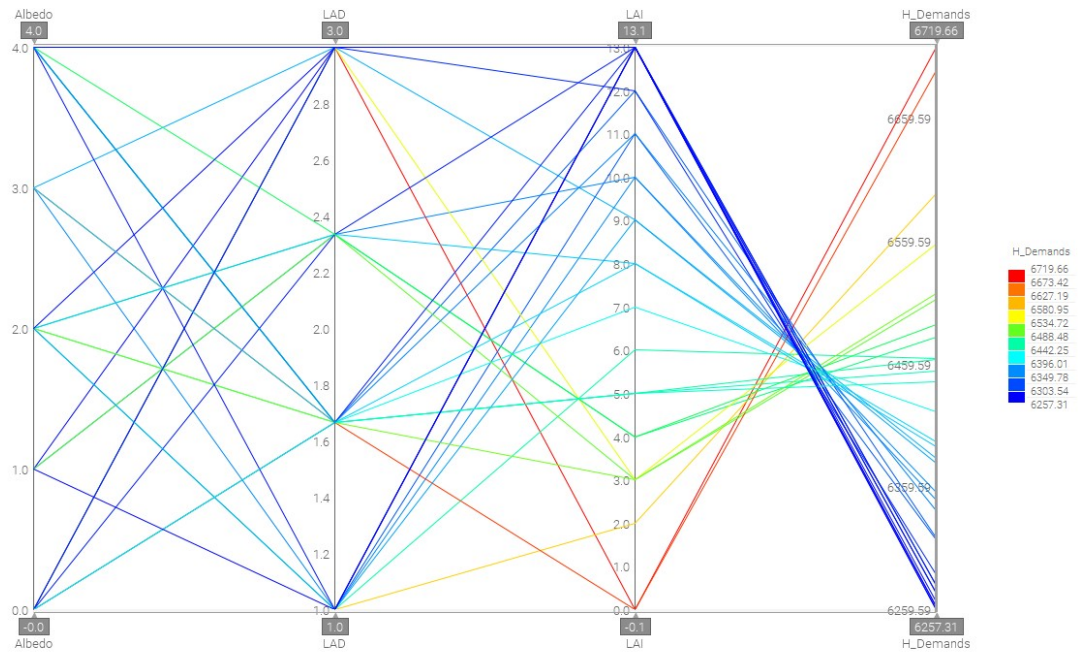


Figure C.31: Parallel coordinates from optimization study for Group C: Amsterdam

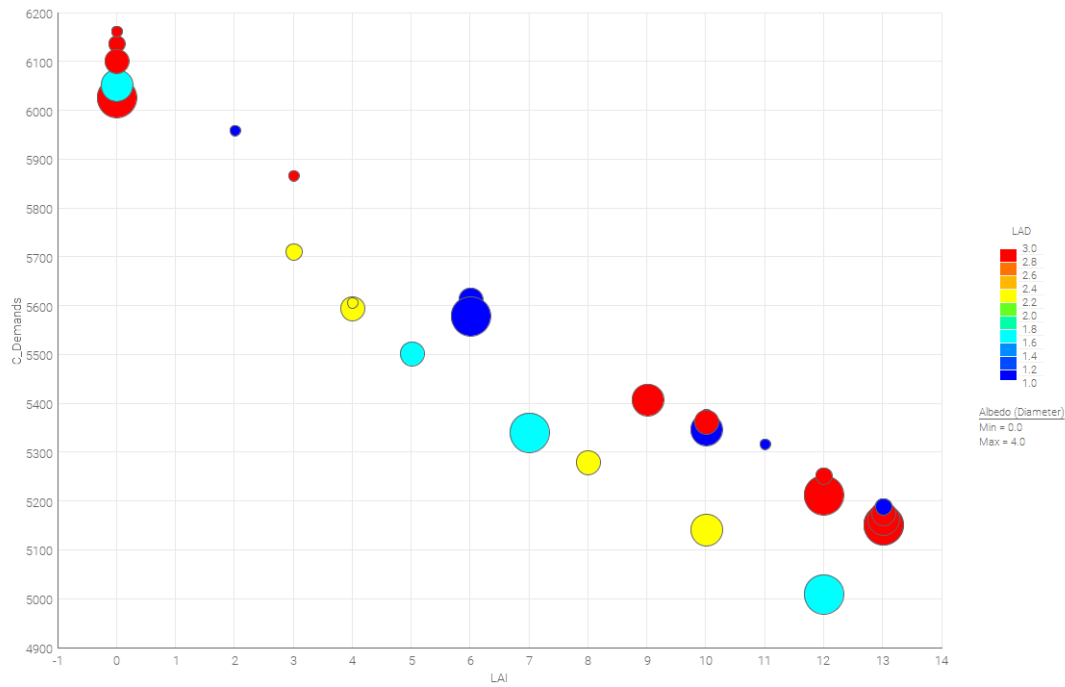


Figure C.32: Bubble plot showing the relation between LAI, cooling demands, *chi* and Albedo in Amsterdam

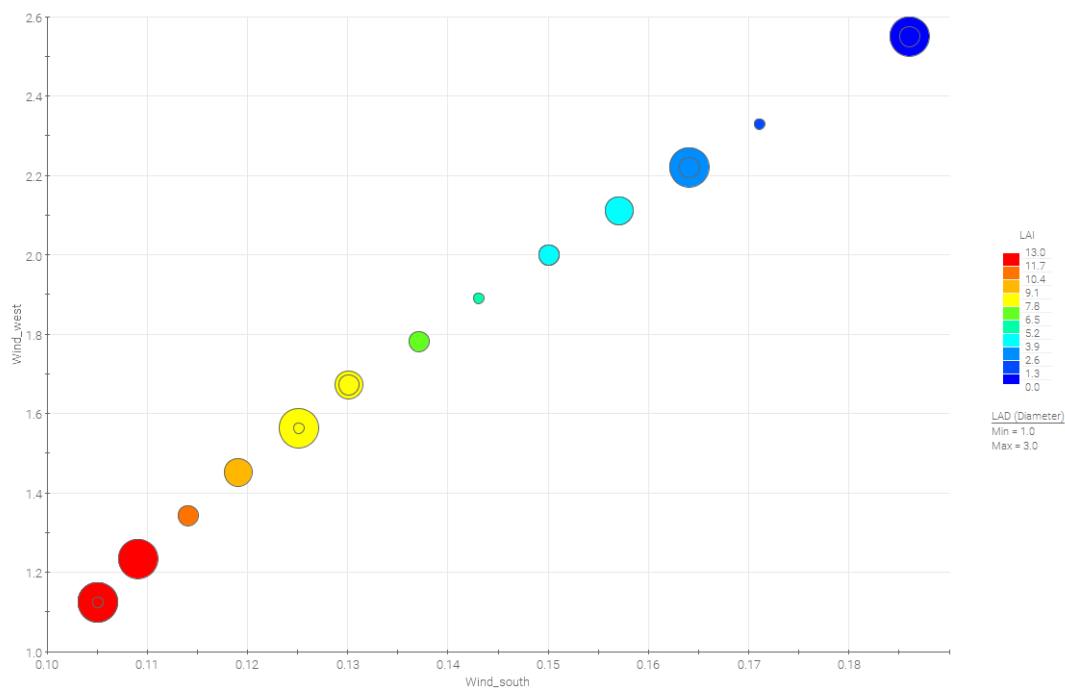


Figure C.33: Bubble plot showing the relation between LAI, *chi* and wind speed in south and west directions in Amsterdam

C.4. Optimized single green building model

C.4.1. Singapore

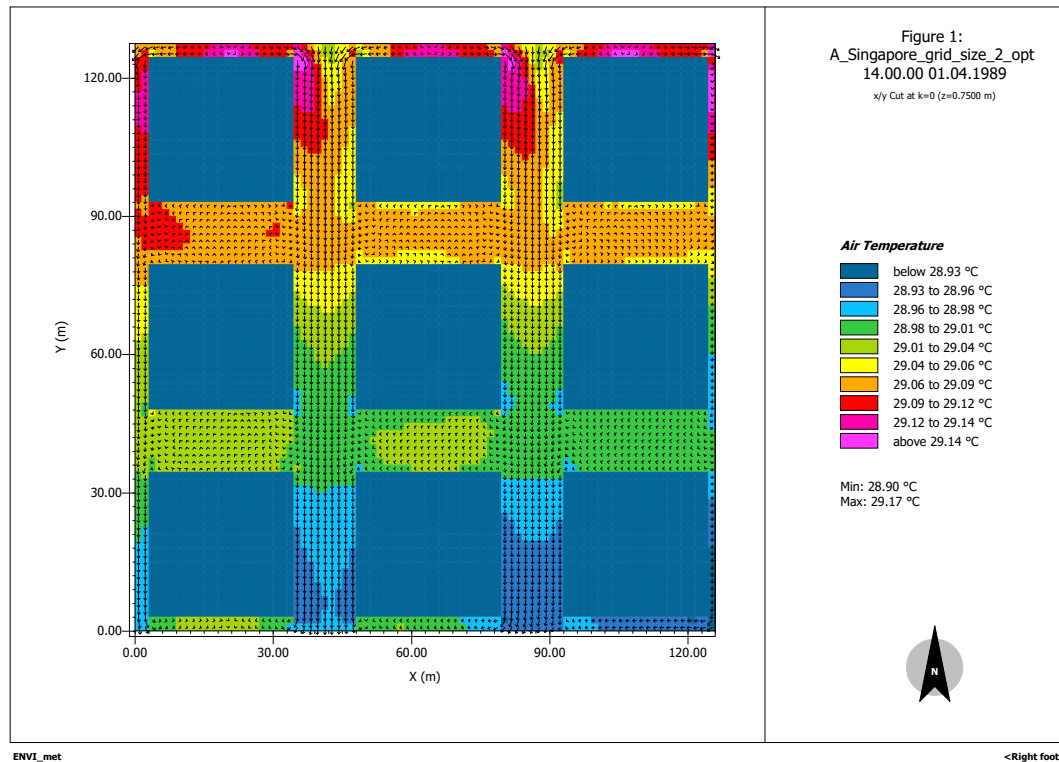


Figure C.34: Air temperature at 14:00 on April 1st 1989, for Singapore single green building model

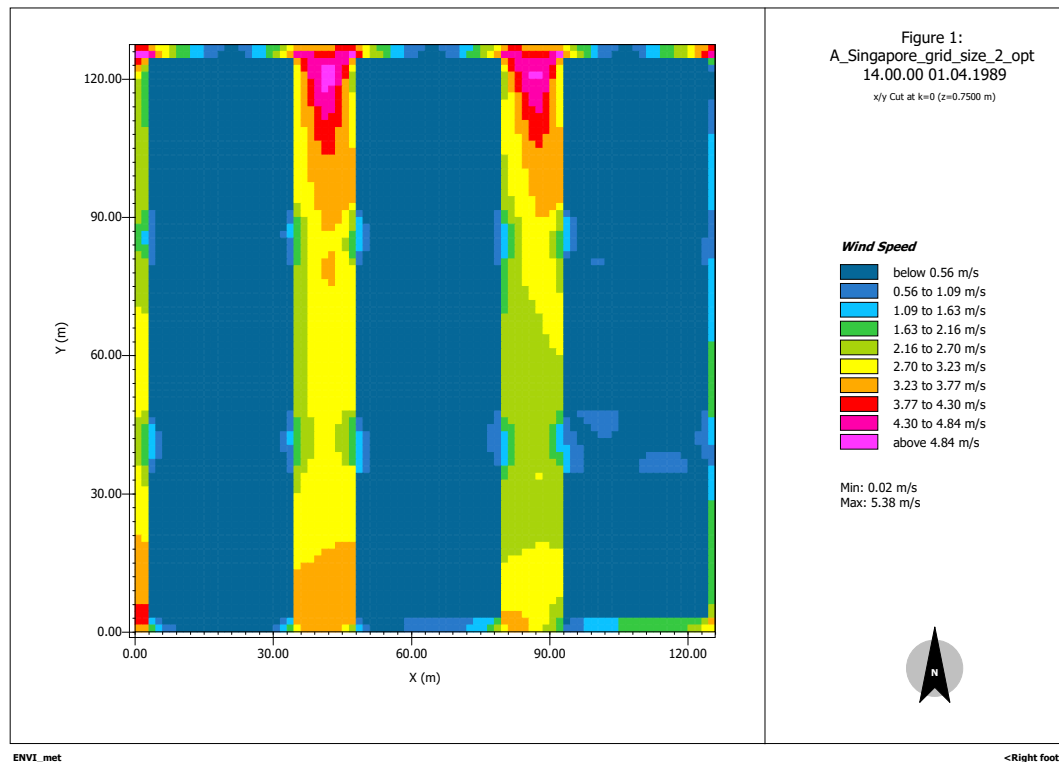


Figure C.35: Wind speed at 14:00 on April 1st 1989 for Singapore single green building model

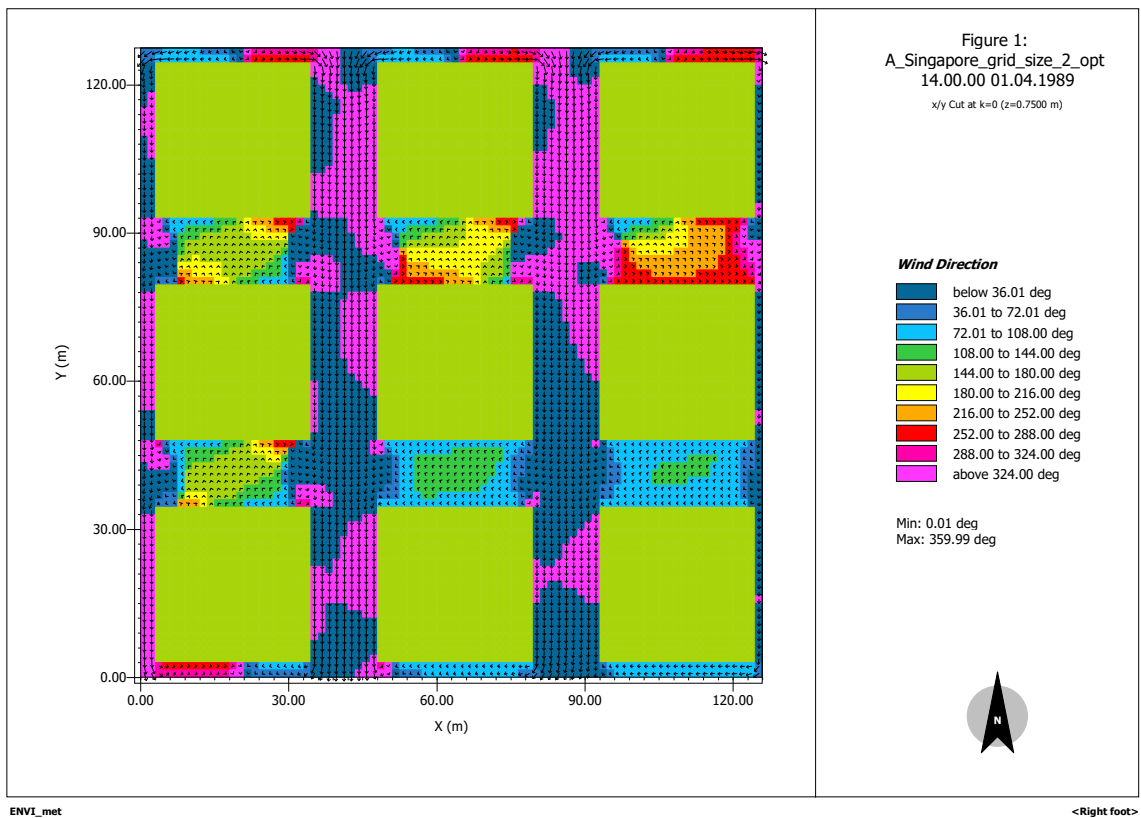


Figure C.36: Wind orientation at 14:00 on April 1st 1989 for Singapore single green building model

C.4.2. Group B: Phoenix

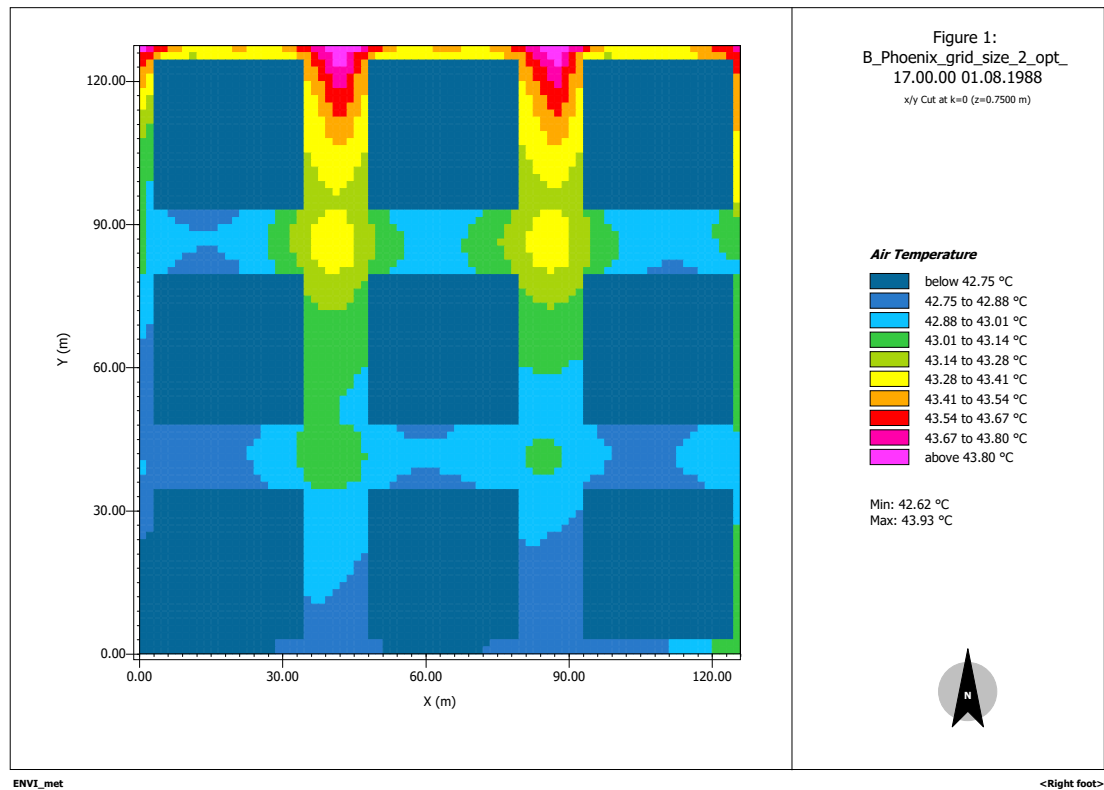


Figure C.37: Air temperature at 17:00 on August 1st 1988, for Phoenix single green building model

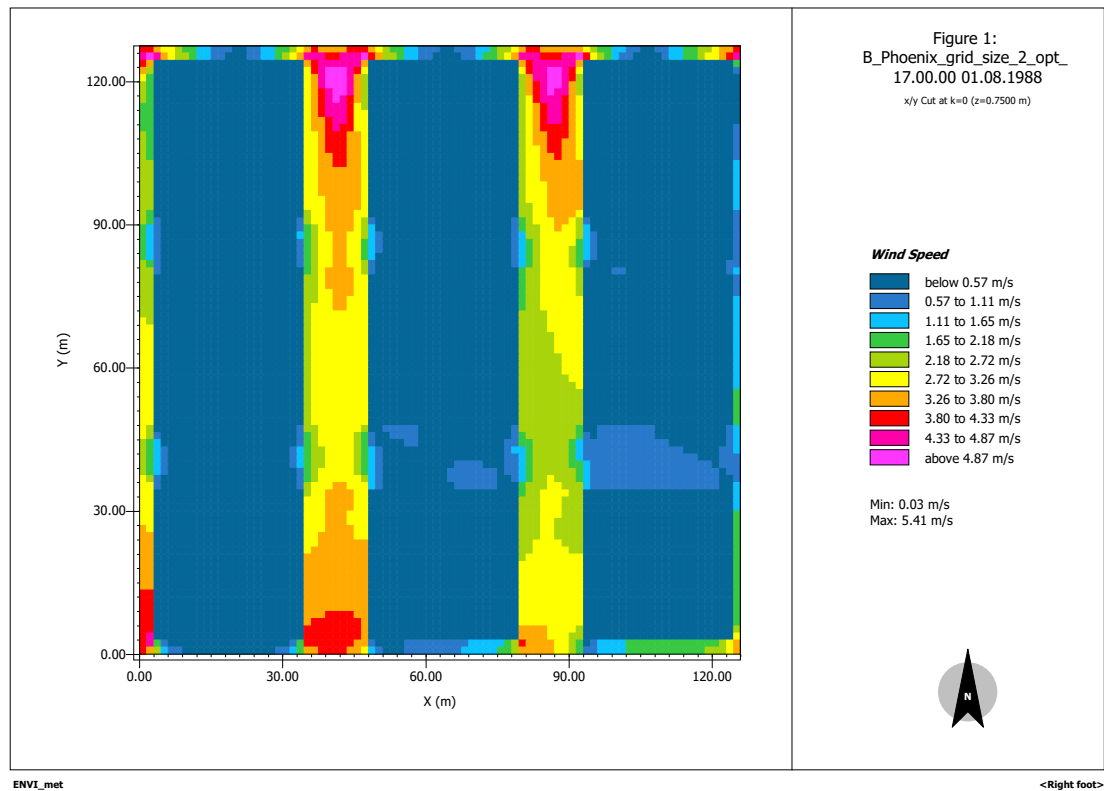


Figure C.38: Wind speed at 17:00 on August 1st 1988, for Phoenix single green building model

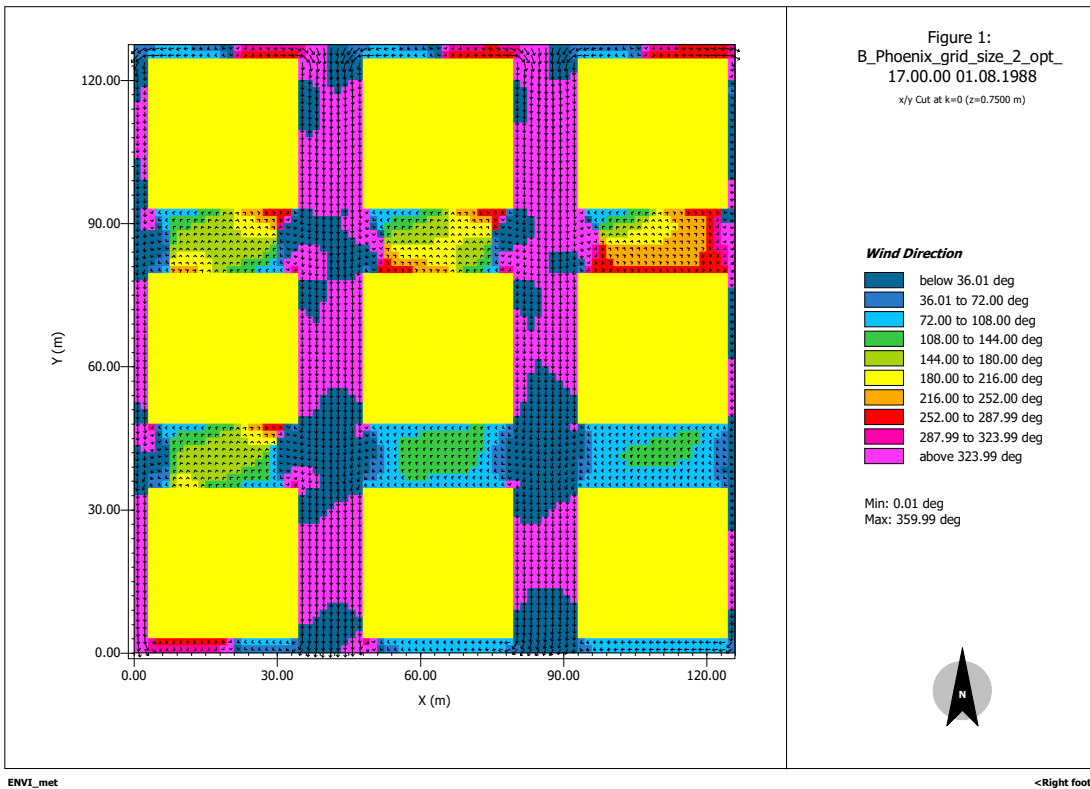


Figure C.39: Wind orientation at 17:00 on August 1st 1988, for Phoenix single green building model

C.4.3. Group C: Amsterdam

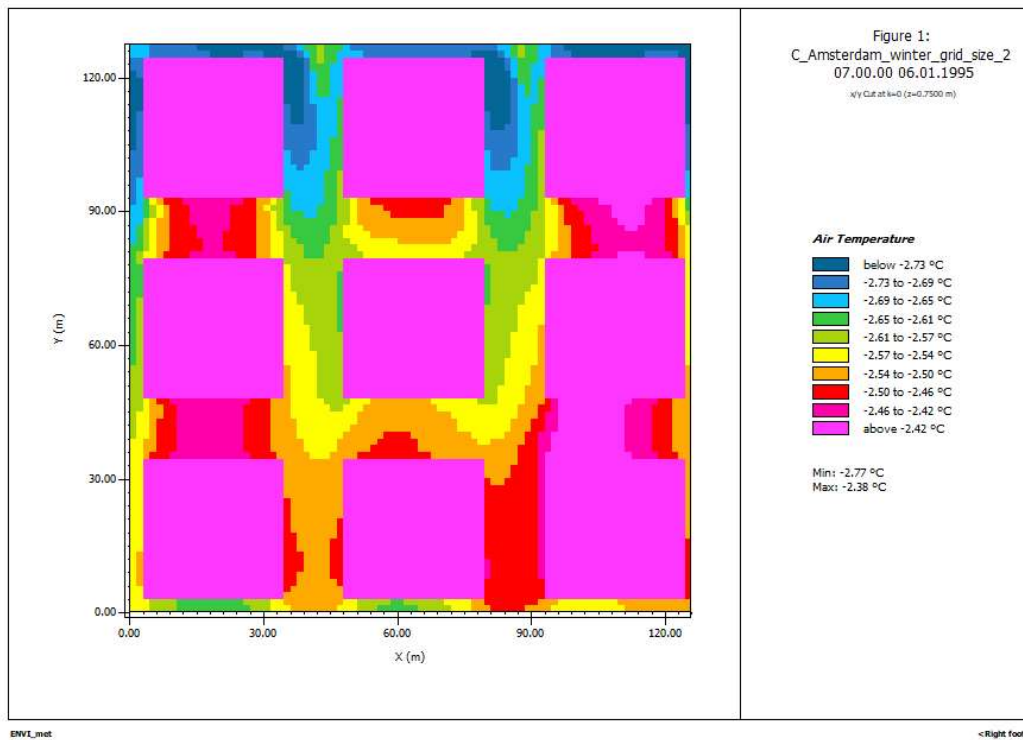


Figure C.40: Air temperature at 7:00 on January 6th 1995, for Amsterdam single green building model

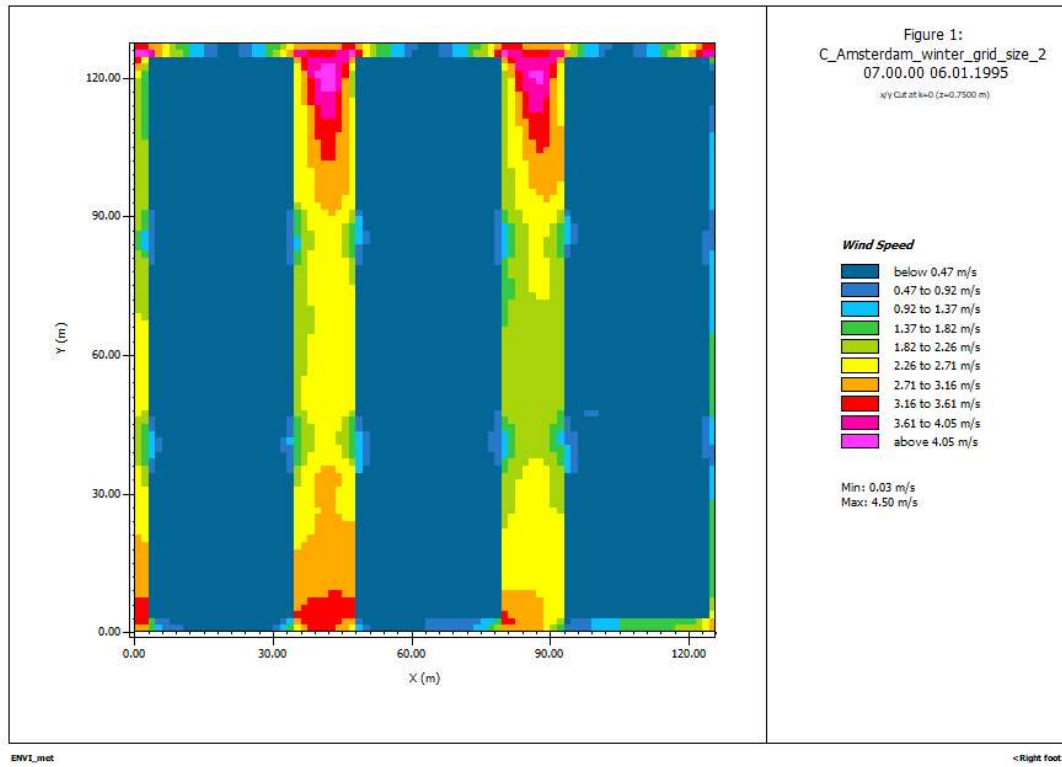


Figure C.41: Wind speed at 7:00 on January 6th 1995, for Amsterdam single green building model

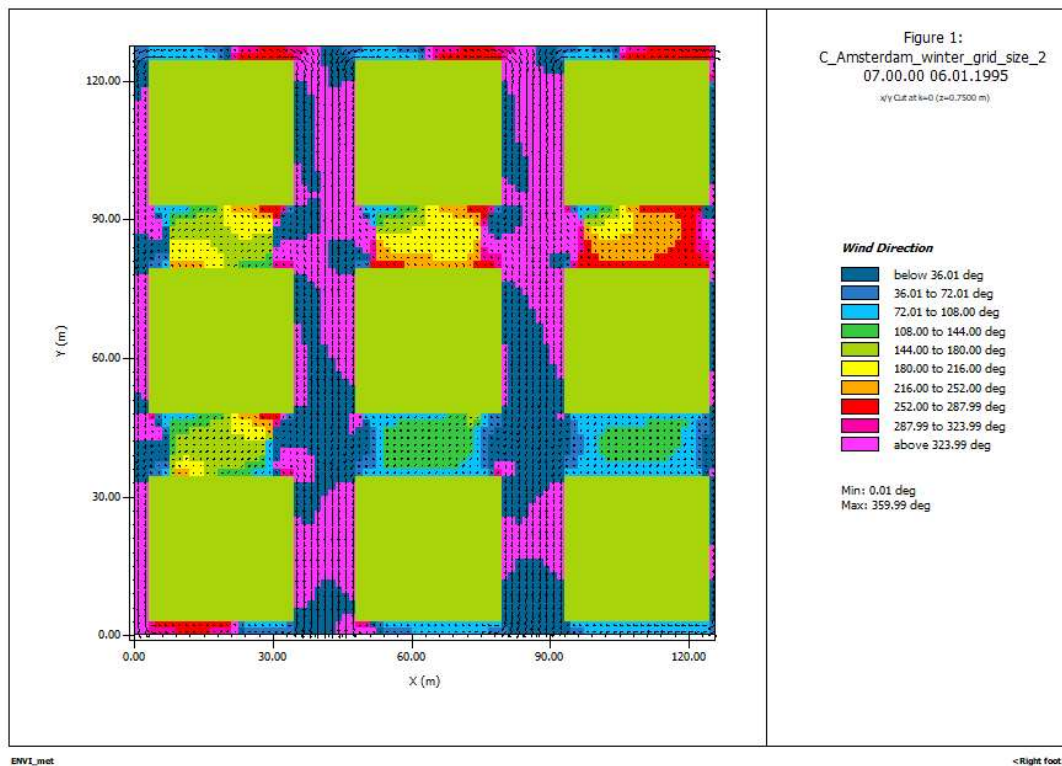


Figure C.42: Wind orientation at 7:00 on January 6th 1995, for Amsterdam single green building model

C.5. Optimized full green building model

C.5.1. Singapore

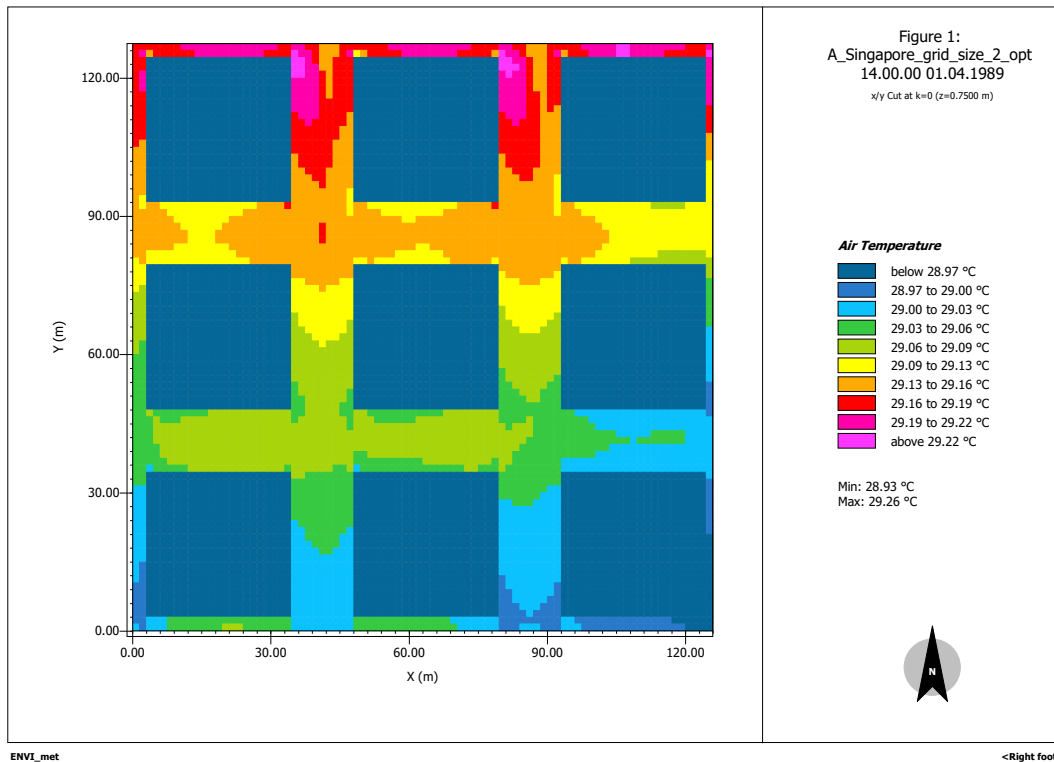


Figure C.43: Air temperature at 14:00 on April 1st 1989, for Singapore full green building model

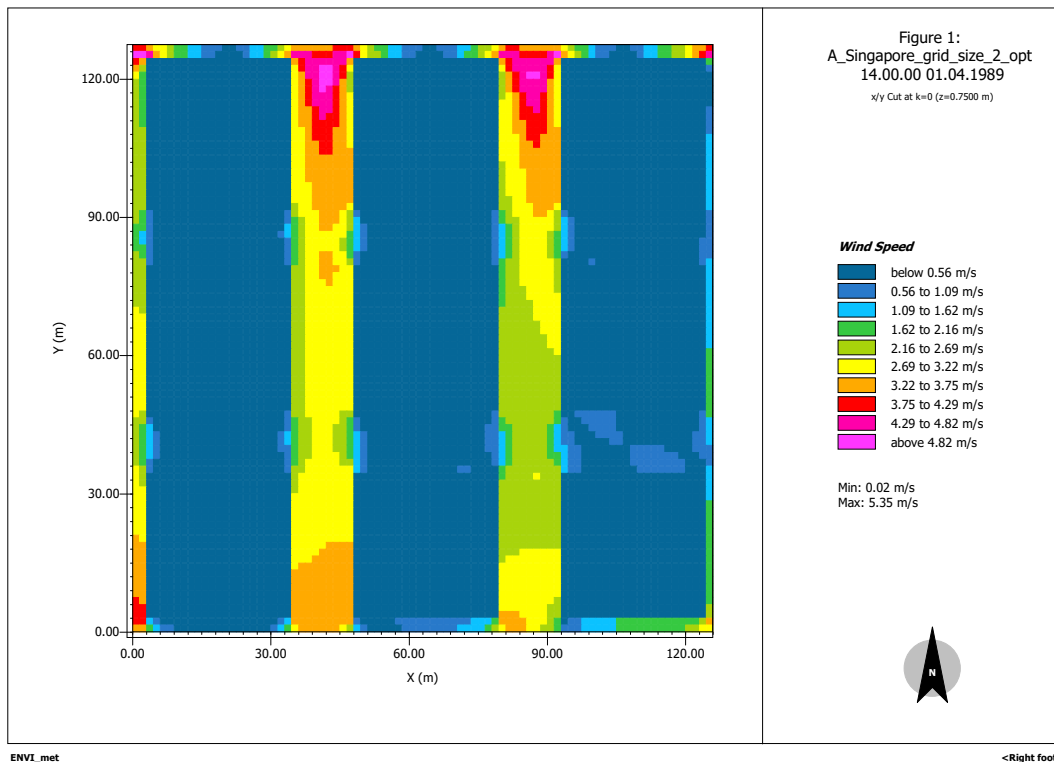


Figure C.44: Wind speed at 14:00 on April 1st 1989 for Singapore full green building model

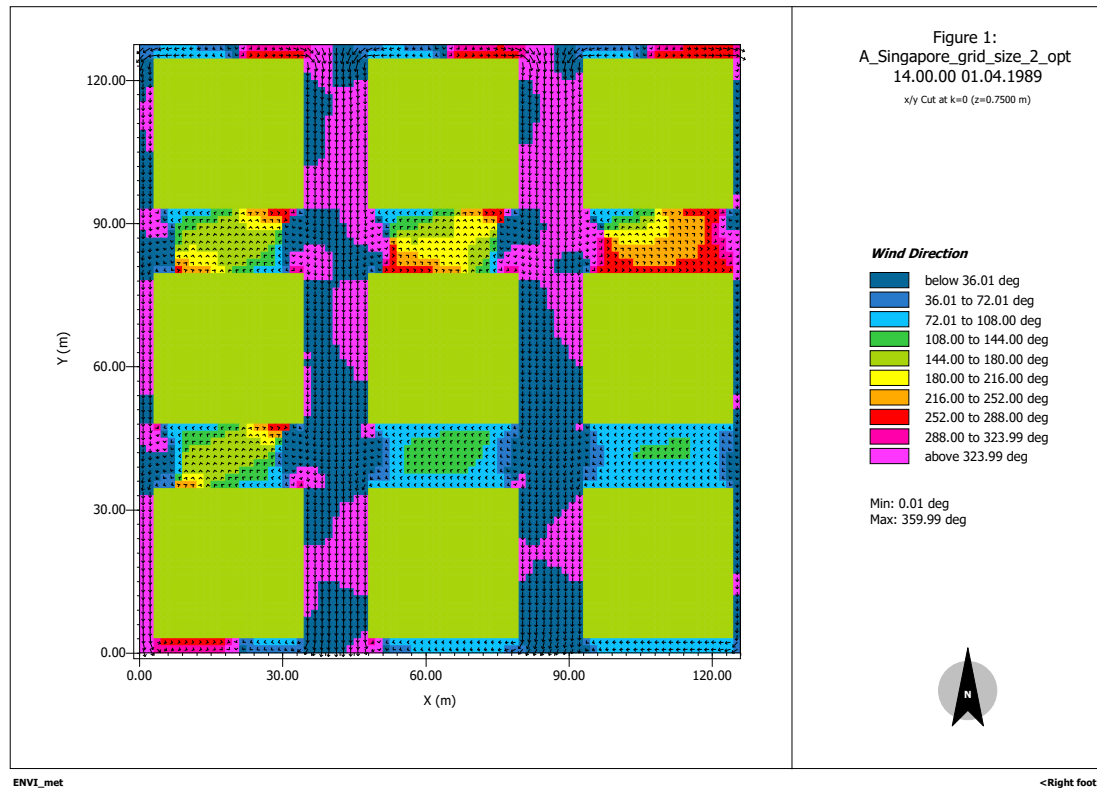


Figure C.45: Wind orientation at 14:00 on April 1st 1989 for Singapore full green building model

C.5.2. Group B: Phoenix

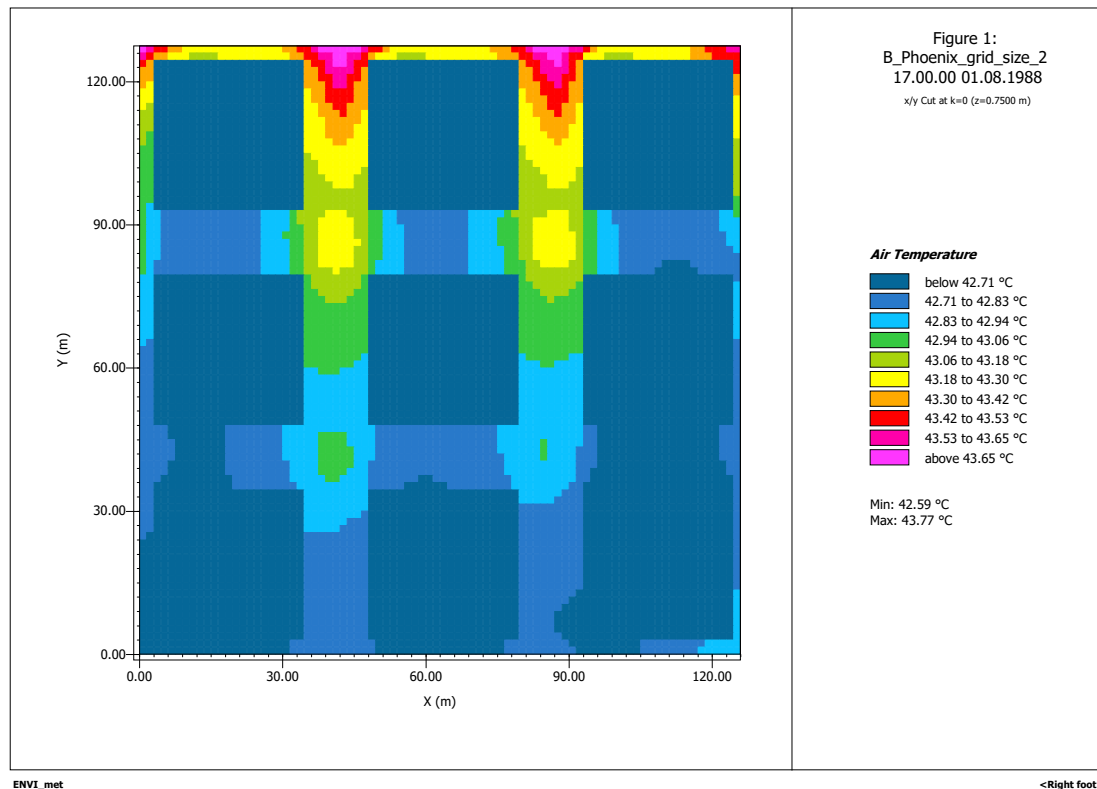


Figure C.46: Air temperature at 17:00 on August 1st 1988, for Phoenix full green building model

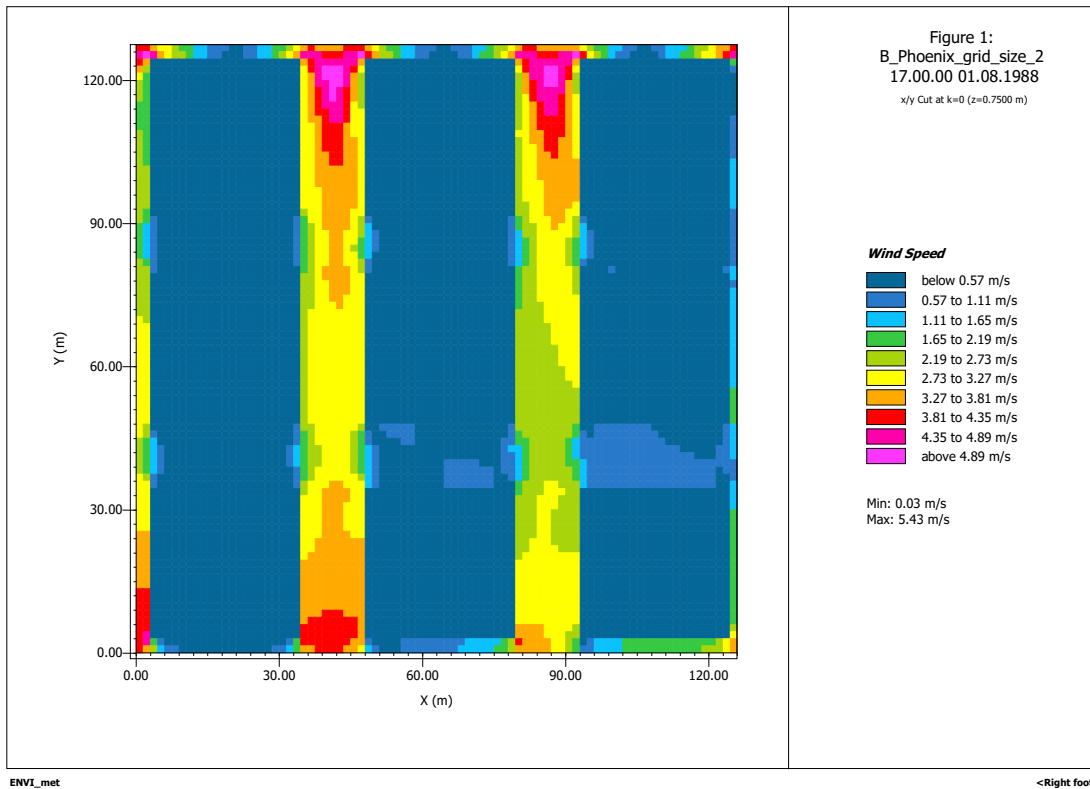


Figure C.47: Wind speed at 17:00 on August 1st 1988, for Phoenix full green building model

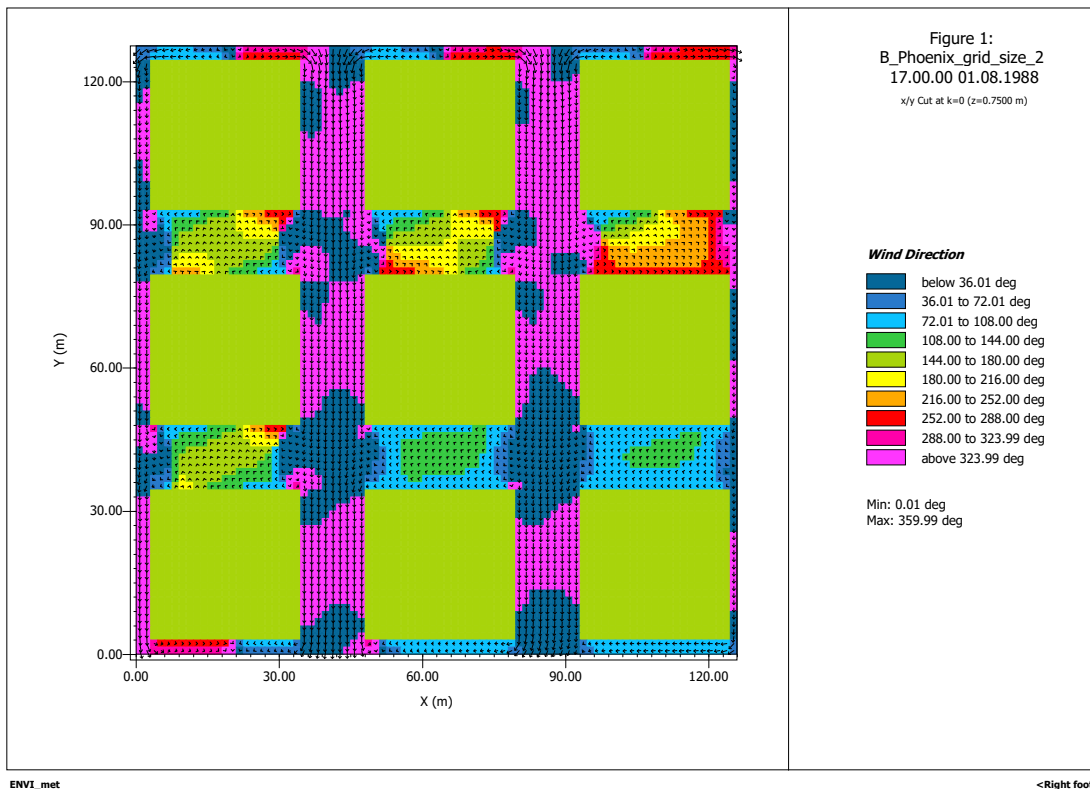


Figure C.48: Wind orientation at 17:00 on August 1st 1988, for Phoenix full green building model

C.5.3. Group C: Amsterdam

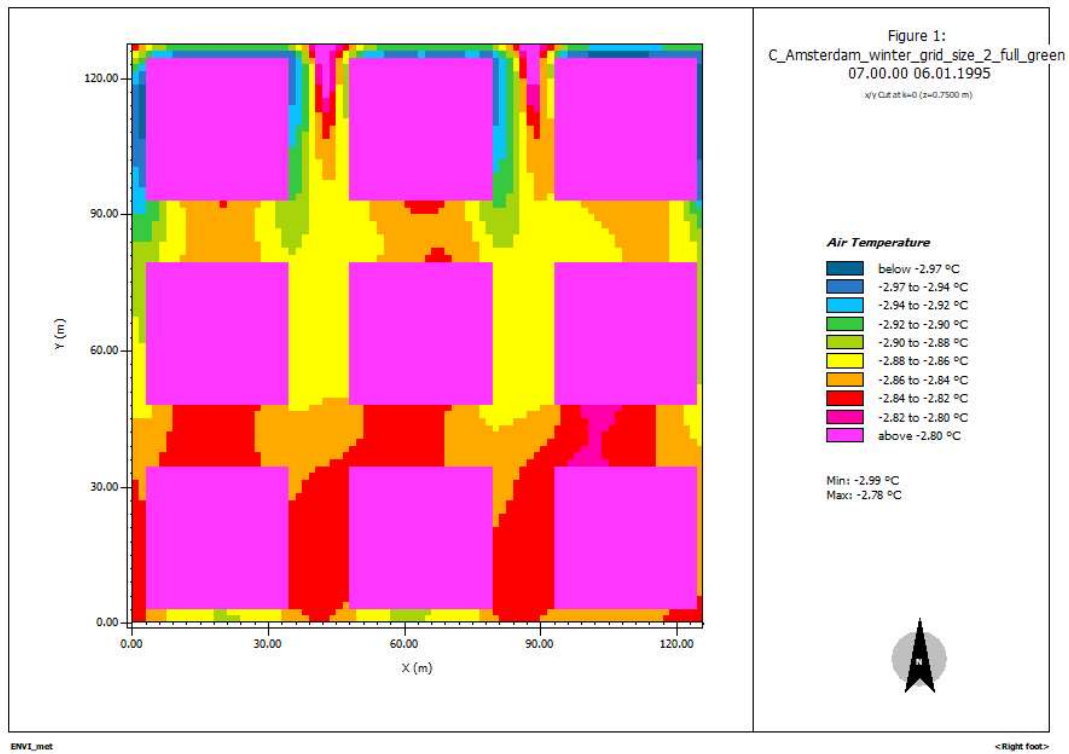


Figure C.49: Air temperature at 7:00 on January 6th 1995, for Amsterdam full green building model

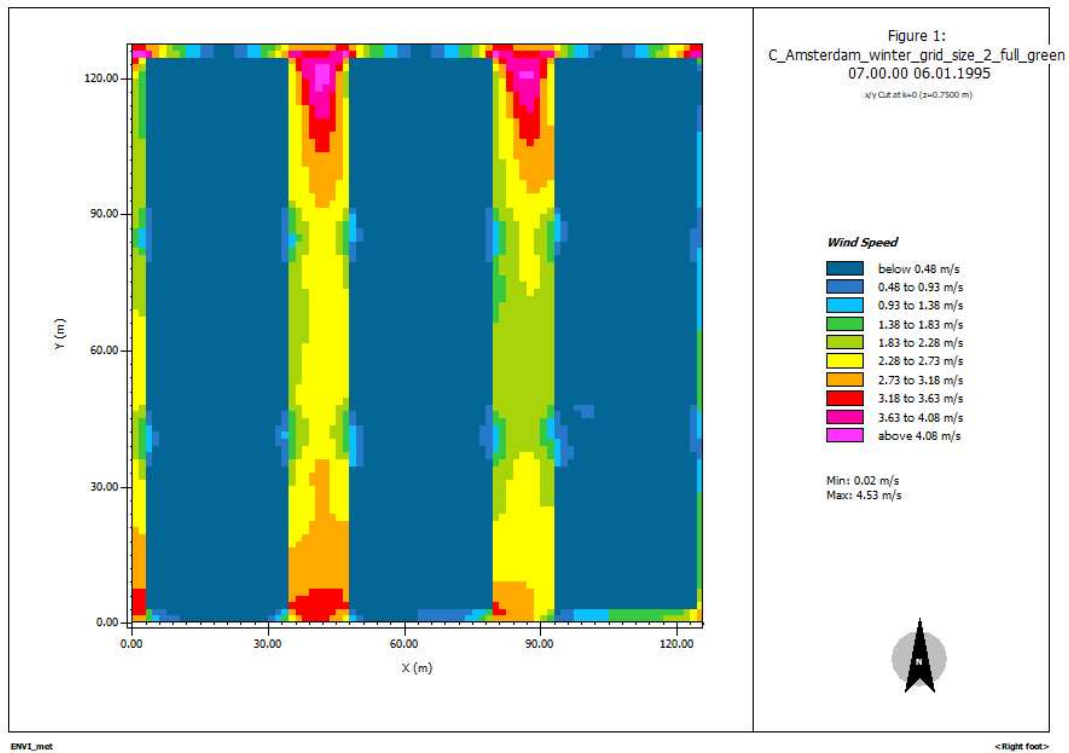


Figure C.50: Wind speed at 7:00 on January 6th 1995, for Amsterdam full green building model

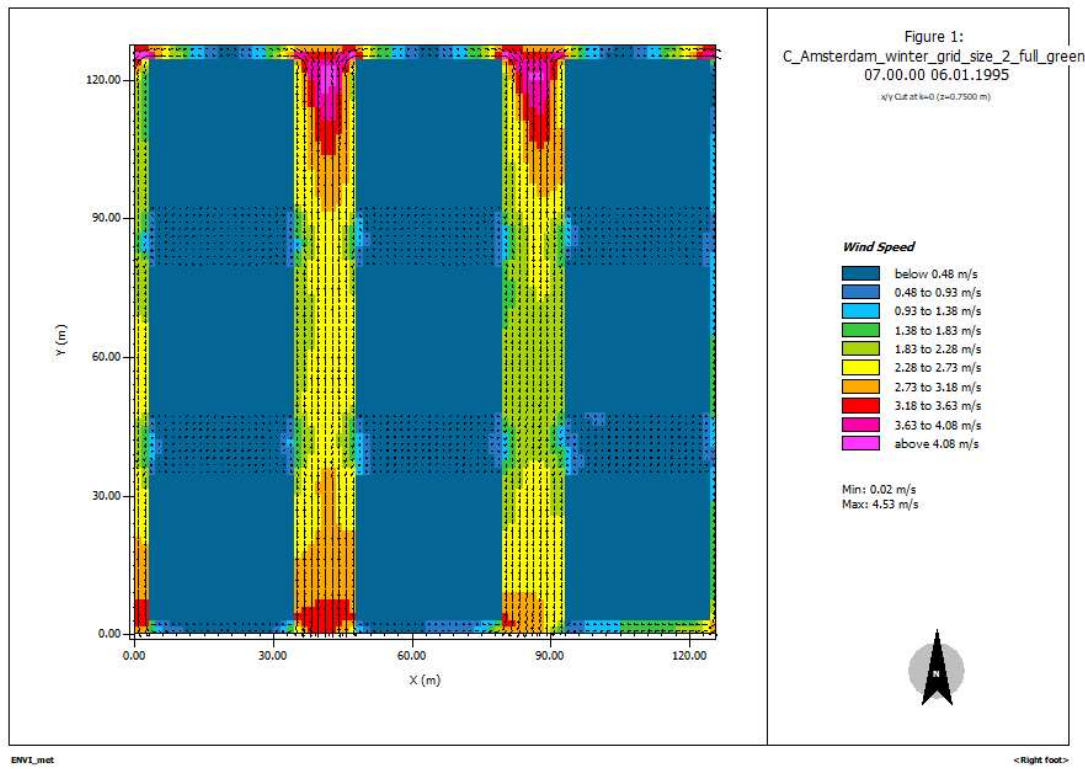
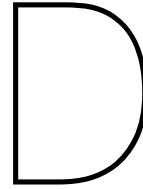


Figure C.51: Wind orientation at 7:00 on January 6th 1995, for Amsterdam full green building model



Grasshopper Component Scripts

D.1. Adding input to ENVI_met database

```
import rhinoscriptsyntax as rs
import os
import math
import datetime as dt

# Open the file and delete all information after a specific line (index)
index_value = 117957
file = "C:\ENVI\met4\sys.basedata\database.edb"
temp_file = "C:\ENVI\met4\sys.basedata\database_temp.edb"

actualfile = open(file,"r") # Opens the file
infile = actualfile.readlines() # Reads all information in the file and
    stores it into a variable
with open(temp_file,"w+") as outfile:
    for index,line in enumerate(infile):
        if index < index_value:
            outfile.write(line[0:1000]) # Writes the information in a new
                file after the specified index. 1000 refers to the amount
                    of charaters copied in that line

#tau = round(math.exp(-(k*LAI)),3)

f = open(temp_file,"a+") # Add new information in the bottom part of the
    file
f.write(" <PLANT>")
f.write("\n    <ID> " + Plant_ID + " </ID>")
f.write("\n    <Description> " + Plant_Name + " </Description>")
f.write("\n    <AlternativeName> (None) </AlternativeName>")
f.write("\n    <Planttype> 0 </Planttype>")
f.write("\n    <Leaftype> 1 </Leaftype>")
f.write("\n    <Albedo> " + str(Alb) + " </Albedo>")
f.write("\n    <Transmittance> 0.3000 </Transmittance>")
f.write("\n    <rs_min> 200.00000 </rs_min>")
f.write("\n    <Height> 0.25000 </Height>")
f.write("\n    <Depth> 0.50000 </Depth>")
f.write("\n    <LAD-Profile> 0.15000,0.15000,...,0.15000,0.15000 </LAD-
    Profile >")
```



```

f.write("\n      <RAD-Profile > 0.10000,0.10000,...,0.10000,0.00000 </RAD-
Profile >")
f.write("\n      <Season-Profile > 1.00000,1.00000...,1.00000,1.00000 </
Season-Profile >")
f.write("\n      <Group> Facade Greening plants </Group>")
f.write("\n      <Color> 7642716 </Color>")
f.write("\n    </PLANT>")
f.write("\n    <GREENING>")
f.write("\n      <ID> " + Green_Wall_ID + " </ID>")
f.write("\n      <Name> " + Green_Wall_Name + " </Name>")
f.write("\n      <HasSubstrate> 1 </HasSubstrate>")
f.write("\n      <SoilID> " + Soil_ID + ", " + Soil_ID + ", " + Soil_ID + "
</SoilID >")
f.write("\n      <ThicknessLayers> " + str(round(d/3,2)) + ", " + str(round(
d/3,2)) + ", " + str(round(d/3,2)) + " </ThicknessLayers >")
f.write("\n      <subEmissivity> 0.95000 </subEmissivity >")
f.write("\n      <subAlbedo> 0.30000 </subAlbedo >")
f.write("\n      <subWaterCoeff> " + str(Water_coefficient) + " </
subWaterCoeff >")
f.write("\n      <SimplePlantID> " + Plant_ID + " </SimplePlantID >")
f.write("\n      <LAI> " + str(LAI) + " </LAI >")
f.write("\n      <SimplePlantThickness> 0.30000 </SimplePlantThickness >")
f.write("\n      <LeafAngleDistribution> " + str(LAD) + " </
LeafAngleDistribution >")
f.write("\n      <AirGap> 0.10000 </AirGap >")
f.write("\n      <Color> 7642716 </Color >")
f.write("\n      <Group> Default Greenings with air gap </Group >")
f.write("\n      <AddValue1> 0.00000 </AddValue1 >")
f.write("\n      <AddValue2> 0.00000 </AddValue2 >")
f.write("\n    </GREENING >")
f.write("\n</ENVI-MET_Datafile >")
f.close()

```

```
actualfile.close()
```

```
# Rename new file to original file name
```

```
if os.path.exists(file) == True:
```

```
    os.remove(file)
```

```
os.rename(temp_file, file)
```

```
# Show information as output of the component
```

```
Plant_Properties = "Name: " + str(Plant_Name) + "\nID: " + str(Plant_ID) +
"\nAlbedo: " + str(Alb)
```

```
Green_Wall_Properties = "Name: " + str(Green_Wall_Name) + "\nID: " + str(
Green_Wall_ID) + "\nLAI: " + str(LAI) + "\nLAD: " + str(LAD)
```

```
Soil_Properties = "Soil ID: " + str(Soil_ID) + "\nMoisture Content: " +
str(Moisture_content) + "%\nThickness: " + str(d) + " m"
```

```
Green_Wall_ID = Green_Wall_ID
```

```
#Checks if the output folder exists, and if it doesn't it creates it
```

```
if os.path.exists(Path) == False:
```

```
    os.mkdir(Path)
```

```
# Log creation
```

```
if Create_log == True:
```

```
    lst = [0,0,0,0,0]
```

```

# Creates log
log_path = Path + "\simulation_log_" + Log_name + ".txt"

log = open(log_path,"a+")
print "Log path: " + log_path

# Checks if there is a change in the variables used for each
simulation
if lst[0] != Alb or lst[1] != LAI or lst[2] != LAD or lst[3] !=
Water_coefficient or lst[4] != d:

    # Set simulation number
    data = open(log_path).read()
    count = data.count('Simulation') + 1

    # Write data input for each simulation
    log.write("Simulation number " + str(count) + ", starting at " +
str(dt.datetime.now()))
    log.write("\nPlant Properties\n")
    log.write("Albedo: " + str(Alb) + "\n\n")
    log.write("Green Wall Properties\n")
    log.write("LAI: " + str(LAI) + "\nLAD: " + str(LAD) + "\n\n")
    log.write("Soil Properties\n")
    log.write("Moisture Content: " + str(Moisture_content) + "%\
nThickness: " + str(d) + " m" + "\n\n")
    log.close()

else:
    log.write("Simulation input has not changed.")

lst[0] = Alb
lst[1] = LAI
lst[2] = LAD
lst[3] = Water_coefficient
lst[4] = d

else:
    print "No log created"

```

D.2. Checking model completion for data processing

```

import os
import datetime
import psutil
import pathlib
import time
from pathlib import Path

#filename in the parantheses has to be replaced by the path to the file if
script is not in same folder
def modification_date(filename):
    t = os.path.getmtime(filename)
    return datetime.datetime.fromtimestamp(t)

#returns true when the simulation is already finished with that file ,
false otherwise

```



```

        filenames.append(filename_part1 + str(n) + filename_part2)

for n in range(0, 2):
    filenames.append(filename_part1 + '0' + str(n) +
        filename_part3)

for filename in filenames:
    # Check for each file if its timestamp is later than the last
    file
    print(filename + "\n")

last = filenames[-1]
print(last)
print("\n2")

if os.path.isfile(last): #which means we are NOT in the first run
    of the simulation

    for filename in filenames:
        # Check for each file if its timestamp is later than the
        last file
        print("\nChecking file " + filename + "\n")
        if(filename == last):
            print("Checking last file ")

            #get path of current directory
            while simulation_finished(last) == False:
                if panic_error_handling(Pnc_path):
                    Process_data = False
                    break
                time.sleep(time_delay)

            print("Loop break")

            time.sleep(time_end_simulation) # Add delay to let
            simulation finish

            print("Process data = " + str(Process_data))

        else:
            last_timestamp = modification_date(last)
            current_timestamp = modification_date(filename)

            while(current_timestamp < last_timestamp):
                if panic_error_handling(Pnc_path):
                    Process_data = False
                    break
                time.sleep(time_delay)
                current_timestamp = modification_date(filename)

    else: #which means we are in the first run and all files are just
    created

    print("New creation")

    while os.path.isfile(last) == False:

```

```

    if panic_error_handling(Pnc_path):
        Process_data = False
        break
    time.sleep(time_delay)

#get path of current directory, might become unnecessary later
while simulation_finished(last) == False:
    if panic_error_handling(Pnc_path):
        Process_data = False
        print("Process data after PNC check in new creation")
        break
    time.sleep(time_delay)

time.sleep(time_end_simulation) # add delay to let simulation
finish
print("Proces data = " + str(Process_data))

```

D.3. ENVI_met data processing

Script based on CLEX reading ENVI_met files [12].

```

import os
import pandas as pd
import numpy
import xarray
import xml.etree.ElementTree as ET
from pathlib import Path

```

```
"""
```

```

[desc]
ENVI_met results reader
[/desc]

```

RETURN:

```

<out>
    Max_Temperature : Maximum temperature during analysis period [°C]
</out>
<out>
    Min_Temperature : Minimum temperature during analysis period [°C]
</out>
<out>
    Average_Temperature : Average temperature during analysis period [
    °C]
</out>
<out>
    Heating_Demands : Total heating demands from the façade during the
    analysis period [kWh]
</out>
<out>
    Cooling_Demands : Total cooling demands from the façade during the
    analysis period [kWh]
</out>
<out>
    HC_Demands : Total sum of heating and cooling demands from the
    façade during the analysis period [kWh]
</out>
<out>

```

```

    Av_Wind_Speed_South : Average wind speed in the south façade [m/s]
</out>
<out>
    Av_Wind_Speed_West : Average wind speed in the west façade [m/s]
</out>
"""
# Read, convert and retain useful information from the Building.DAT file
def building_DAT(file_name, file_content):
    index_value = 0
    temp_file = Path(Output_folder_path) / "buildings" / "dynamic" / "temp
.DAT"
    print(temp_file)
    file_content[0] = file_content[0][2:]
    # Open the file and delete all information after a specific line (
    index)
    with open(temp_file, "w+") as outfile:
        for index, line in enumerate(file_content):
            if index == index_value:
                outfile.write(file_content[0])
            if index > index_value:
                outfile.write(line[:]) # Writes the information in a new
                file after the specified index. 1000 refers to the
                amount of charaters copied in that line

    # Rename new file to original file name
    if os.path.exists(file_name) == True:
        os.remove(file_name)
        os.rename(temp_file, file_name)

def open_edx_AT(filename):
    # Open a EDX/EDT dataset, returns an xarray dataset

    # Parse the metadata file
    parser = ET.XMLParser(encoding='ISO-8859-1')
    meta = ET.parse(filename, parser=parser).getroot()

    variable_names = meta.find('variables/name_variables').text.strip().
        split(',')
    variable_selection = ['Objects ( )', 'Flow u (m/s)', 'Flow v (m/s)', '
    Flow w (m/s)', 'Wind Speed (m/s)', 'Wind Speed Change (%)', 'Wind
    Direction (deg)', 'Pressure Perturbation (Diff)', 'Air Temperature
    (C)', 'Air Temperature Delta (K)', 'Air Temperature Change (K/h)',
    'Spec. Humidity (g/kg)', 'Relative Humidity (%)']

    nr_xdata = int(meta.find('datadescription/nr_xdata').text)
    nr_ydata = int(meta.find('datadescription/nr_ydata').text)
    nr_zdata = int(meta.find('datadescription/nr_zdata').text)
    nr_ndata = int(meta.find('variables/Data_per_variable').text)

    date = meta.find('modeldescription/simulation_date').text.strip()
    time = meta.find('modeldescription/simulation_time').text.strip()

    # Get the time
    t = pd.to_datetime(date+' '+time, format='%d.%m%Y %H.%M%S')

    # Read the data file

```

```

data = numpy.fromfile(os.path.splitext(filename)[0]+'.EDT', '<f4 ')
cube = data.reshape((len(variable_names), nr_zdata, nr_ydata, nr_xdata
, nr_ndata, 1))

# Create a dataset
dataset = xarray.Dataset({name: ([ 'z', 'y', 'x', 'n', 'time' ], cube[idx
, :, :, :, :])
                           for idx, name in enumerate(
                               variable_selection)},
                           coords={'time': [t]},)

return dataset

def open_edx_EF(filename):
# Open a EDX/EDT dataset, returns an xarray dataset

# Parse the metadata file
parser = ET.XMLParser(encoding='ISO-8859-1')
meta = ET.parse(filename, parser=parser).getroot()

variable_names = meta.find('variables/name_variables').text.strip().
split(',')
variable_selection = ['Wall shading flag ()', 'Wall: Temperature Node
1/ outside (°C)', 'Wall: Temperature Node 2 (°C)', 'Wall:
Temperature Node 3 (°C)', 'Wall: Temperature Node 4 (°C)', 'Wall:
Temperature Node 5 (°C)', 'Wall: Temperature Node 6 (°C)', 'Wall
: Temperature Node 7/ inside (°C)', 'Building: Sum Humidity Flux
at facade (g/s*m3)', 'Wall: Longwave radiation emitted by facade
(W/m2)', 'Wall: Wind Speed in front of facade (m/s)', 'Wall: Air
Temperature in front of facade (°C)', 'Wall: Shortwave radiation
received at facade (W/m2)', 'Wall: Absorbed direct shortwave
radiation (W/m2)', 'Wall: Incoming longwave radiation (W/m2)', '
Wall: Reflected shortwave radiation facade (W/m2)', 'Wall:
Sensible Heat transmission coefficient outside (W/m2K)', 'Wall:
Longwave Energy Balance (W/m2)', 'N.N. ()', 'Building: Temperature
of building (inside) (°C)', 'Building: Reflected shortwave
radiation (W/m2)', 'Building: Longwave radiation emitted (W/m2)',
'Greening: Temperature Leafs (°C)', 'Greening: Air Temperature
Canopy (°C)', 'Greening: Air Humidity Canopy (g/kg)', 'Greening:
Longwave radiation emitted (two-side) (W/m2)', 'Greening: Wind
Speed in front of greening (m/s)', 'Greening: Air Temperature in
front of greening (°C)', 'Greening: Shortwave radiation received
at greening (W/m2)', 'Greening: Incoming longwave radiation (two-
side) (W/m2)', 'Greening: Reflected shortwave radiation (W/m2)',
'Greening: Transpiration Flux (g/s*m3)', 'Greening: Stomata
Resistance (s/m)', 'Greening: Water access factor ()', 'Substrate
: Temperature Node 1/ outside (°C)', 'Substrate: Temperature Node
2 (°C)', 'Substrate: Temperature Node 3 (°C)', 'Substrate:
Temperature Node 4 (°C)', 'Substrate: Temperature Node 5 (°C)', '
Substrate: Temperature Node 6 (°C)', 'Substrate: Temperature Node
7/ inside (°C)', 'Substrate: Surface humidity (g/kg)', 'Substrate
: Humidity Flux at substrate (g/s*m3)', 'Substrate: Longwave
radiation emitted by substrate (W/m2)', 'Substrate: Wind Speed in
front of substrate (m/s)', 'Substrate: Air Temperature in front of
substrate (°C)', 'Substrate: Shortwave radiation received at
substrate (W/m2)', 'Substrate: Absorbed direct shortwave radiation

```

```

        (W/m2) ', 'Substrate: Incoming longwave radiation (W/m2) ', '
        Substrate: Reflected shortwave radiation substrate (W/m2) '])

nr_xdata = int(meta.find('datadescription/nr_xdata').text)
nr_ydata = int(meta.find('datadescription/nr_ydata').text)
nr_zdata = int(meta.find('datadescription/nr_zdata').text)
nr_ndata = int(meta.find('variables/Data_per_variable').text)

date = meta.find('modeldescription/simulation_date').text.strip()
time = meta.find('modeldescription/simulation_time').text.strip()

# Get the time
t = pd.to_datetime(date + ' ' + time, format='%d.%m.%Y %H.%M.%S')

# Read the data file
data = numpy.fromfile(os.path.splitext(filename)[0]+'.EDT', '<f4')
initial_useless_data = nr_zdata * nr_ydata * nr_xdata
data2 = data[initial_useless_data:]

global cube
cube = data2.reshape((len(variable_names), nr_zdata, nr_ydata,
                    nr_xdata, nr_ndata))
#print(cube[1,0,11,11,1])

# Create a dataset
dataset = xarray.Dataset({name: ([ 'z', 'y', 'x', 'n'], cube[idx, :, :, :])
                          for idx, name in enumerate(variable_names)}, coords={'time': [t]})

return dataset

if __name__ == '__main__':

    if Run == True:
        """
        Get temperature results
        """

        # Grids of interest for analysis of temperature in the
        # surroundings of the building for a Grid Size of 5m
        i = [10, 11, 12, 13, 14, 15, 16, 17, 18, 10, 11, 12, 13, 14, 15,
            16, 17, 18, 10, 10, 10, 10, 10, 10, 10, 18, 18, 18, 18, 18, 18,
            18, 10, 11, 12, 13, 14, 15, 16, 17, 18, 10, 11, 12, 13, 14,
            15, 16, 17, 18, 10, 10, 10, 10, 10, 10, 10, 18, 18, 18, 18, 18,
            18, 18, 10, 11, 12, 13, 14, 15, 16, 17, 18, 10, 11, 12, 13,
            14, 15, 16, 17, 18, 10, 10, 10, 10, 10, 10, 10, 18, 18, 18, 18,
            18, 18, 18, 10, 11, 12, 13, 14, 15, 16, 17, 18, 10, 11, 12,
            13, 14, 15, 16, 17, 18, 10, 11, 12, 13, 14, 15, 16, 17, 18, 10,
            11, 12, 13, 14, 15, 16, 17, 18, 10, 11, 12, 13, 14, 15, 16,
            17, 18, 10, 11, 12, 13, 14, 15, 16, 17, 18, 10, 11, 12, 13, 14,
            15, 16, 17, 18, 10, 11, 12, 13, 14, 15, 16, 17, 18, 10, 11,
            12, 13, 14, 15, 16, 17, 18]
        j = [10, 10, 10, 10, 10, 10, 10, 10, 18, 18, 18, 18, 18, 18,
            18, 18, 18, 11, 12, 13, 14, 15, 16, 17, 11, 12, 13, 14, 15, 16,
            17, 10, 10, 10, 10, 10, 10, 10, 10, 18, 18, 18, 18, 18,
            18, 18, 18, 18, 11, 12, 13, 14, 15, 16, 17, 11, 12, 13, 14, 15,
            16, 17, 10, 10, 10, 10, 10, 10, 10, 10, 10, 18, 18, 18, 18,

```



```

18, 18, 18, 18, 18, 11, 12, 13, 14, 15, 16, 17, 11, 12, 13, 14,
15, 16, 17, 10, 10, 10, 10, 10, 10, 10, 10, 10, 10, 11, 11, 11,
11, 11, 11, 11, 11, 11, 12, 12, 12, 12, 12, 12, 12, 12, 12, 13,
13, 13, 13, 13, 13, 13, 13, 13, 13, 14, 14, 14, 14, 14, 14, 14,
14, 14, 15, 15, 15, 15, 15, 15, 15, 15, 15, 15, 16, 16, 16, 16, 16,
16, 16, 16, 16, 17, 17, 17, 17, 17, 17, 17, 17, 17, 17, 18, 18,
18, 18, 18, 18, 18, 18, 18]
k = [0, 0, 0, 0, 0, 0, 0, 0, 0, 0, 0, 0, 0, 0, 0, 0, 0, 0, 0, 0,
0, 0, 0, 0, 0, 0, 0, 0, 0, 0, 0, 0, 0, 1, 1, 1, 1, 1, 1, 1, 1, 1,
1, 1, 1, 1, 1, 1, 1, 1, 1, 1, 1, 1, 1, 1, 1, 1, 1, 1, 1, 1,
1, 1, 2, 2, 2, 2, 2, 2, 2, 2, 2, 2, 2, 2, 2, 2, 2, 2, 2, 2, 2, 2,
2, 2, 2, 2, 2, 2, 2, 2, 2, 2, 2, 2, 2, 2, 3, 3, 3, 3, 3, 3, 3, 3,
3, 3, 3, 3, 3, 3, 3, 3, 3, 3, 3, 3, 3, 3, 3, 3, 3, 3, 3, 3,
3, 3, 3, 3, 3, 3, 3, 3, 3, 3, 3, 3, 3, 3, 3, 3, 3, 3, 3, 3,
3, 3, 3, 3, 3, 3, 3, 3, 3, 3, 3, 3, 3, 3, 3, 3, 3, 3, 3, 3,
3, 3, 3, 3, 3, 3, 3, 3, 3, 3, 3, 3, 3, 3, 3, 3, 3, 3, 3, 3]
lst = []

sample_1 = range(0, len(i))

# Reads file names from atmosphere results from output folder

T_filename_part0 = Path(Output_folder_path) / "atmosphere" /
Sim_name
T_filename_part1 = str(T_filename_part0) + "_AT_"
T_filename_part2 = ".00.00 0" + str(Analysis_day) + ".0" + str(
Analysis_month) + "." + str(Analysis_year) + ".EDX"
T_filename_part3 = ".00.00 0" + str(Analysis_day + 1) + ".0" + str
(Analysis_month) + "." + str(Analysis_year) + ".EDX"

datasets = []

for n in range(2, 24):

    if n < 10:
        x = str(T_filename_part1) + '0' + str(n) + str(
            T_filename_part2)
        datasets.append(open_edx_AT(x))

    else:
        x = str(T_filename_part1) + str(n) + str(T_filename_part2)
        datasets.append(open_edx_AT(x))

for n in range(0, 2):
    x = str(T_filename_part1) + '0' + str(n) + str(
        T_filename_part3)
    datasets.append(open_edx_AT(x))

ds = xarray.concat(datasets, dim='time')

different_grids = []

# Appends values from all grid cells of interest in the same file
for r in sample_1:
    single_grid = ds.isel(x=i[r], y=j[r], z=k[r], n=0)

```

```

different_grids.append(single_grid)

# Creates an .xls file with all the temperature results of the
# grid cells of interest
df = xarray.concat(different_grids, dim='time').to_dataframe() #
# muchas muchas <3
open(Path(Output_folder_path) / "Atmospheric_results.xls", 'a').
close()
df.to_excel(Path(Output_folder_path) / "Atmospheric_results.xls")

max_temp = round(df.loc[:, 'Air Temperature (C)'].max(), 3)
min_temp = round(df.loc[:, 'Air Temperature (C)'].min(), 3)
av_temp = round(df.loc[:, 'Air Temperature (C)'].mean(), 3)

print("Maximum temperature: " + str(max_temp) + "°C")
print("Minimum temperature: " + str(min_temp) + "°C")
print("Average temperature: " + str(av_temp) + "°C")

Max_Temperature = max_temp
Min_Temperature = min_temp
Average_Temperature = av_temp

"""
Get energy flux through the façade
"""

# Grids of interest for analysis of energy flux through the façade
i = [11, 12, 13, 14, 15, 16, 17, 11, 12, 13, 14, 15, 16, 17, 11,
     12, 13, 14, 15, 16, 17, 11, 12, 13, 14, 15, 16, 17, 11, 12, 13,
     14, 15, 16, 17, 11, 12, 13, 14, 15, 16, 17, 11, 11, 11, 11,
     11, 11, 11, 11, 11, 11, 11, 11, 11, 11, 11, 11, 11, 11, 18, 18,
     18, 18, 18, 18, 18, 18, 18, 18, 18, 18, 18, 18, 18, 18,
     18, 18, 18, 18]
j = [11, 11, 11, 11, 11, 11, 11, 11, 11, 11, 11, 11, 11, 11, 11,
     11, 11, 11, 11, 11, 11, 18, 18, 18, 18, 18, 18, 18, 18, 18, 18,
     18, 18, 18, 18, 18, 18, 18, 18, 18, 18, 12, 13, 14, 15,
     16, 17, 12, 13, 14, 15, 16, 17, 12, 13, 14, 15, 16, 17, 11, 12,
     13, 14, 15, 16, 17, 11, 12, 13, 14, 15, 16, 17, 11, 12, 13,
     14, 15, 16, 17]
k = [0, 0, 0, 0, 0, 0, 0, 0, 1, 1, 1, 1, 1, 1, 1, 1, 2, 2, 2, 2, 2, 2,
     2, 0, 0, 0, 0, 0, 0, 0, 0, 1, 1, 1, 1, 1, 1, 1, 1, 2, 2, 2, 2, 2, 2,
     2, 0, 0, 0, 0, 0, 0, 0, 1, 1, 1, 1, 1, 1, 1, 2, 2, 2, 2, 2, 2, 0, 0,
     0, 0, 0, 0, 0, 1, 1, 1, 1, 1, 1, 1, 1, 2, 2, 2, 2, 2, 2, 2]
lst = []

sample_2 = range(0, len(i))

# Reads file names from atmosphere results from output folder
E_filename_part0 = Path(Output_folder_path) / "buildings" / "
dynamic" / Sim_name
E_filename_part1 = str(E_filename_part0) + "_BLDG_"
E_filename_part2 = ".00.00 0" + str(Analysis_day) + ".0" + str(
Analysis_month) + "." + str(Analysis_year) + ".EDX"
E_filename_part3 = ".00.00 0" + str(Analysis_day + 1) + ".0" + str
(Analysis_month) + "." + str(Analysis_year) + ".EDX"

```

```

datasets = []

heating_demands = []
cooling_demands = []

for n in range(2, 24):
    if n < 10:
        y = str(E_filename_part1) + '0' + str(n) + str(
            E_filename_part2)
        datasets.append(open_edx_EF(y))

    else:
        y = str(E_filename_part1) + str(n) + str(E_filename_part2)
        datasets.append(open_edx_EF(y))

for n in range(0, 2):
    y = str(E_filename_part1) + '0' + str(n) + str(
        E_filename_part3)
    datasets.append(open_edx_EF(y))

ds = xarray.concat(datasets, dim='time')

Grid_area = Grid_size**2

energy_transmission = []
heating_demands = []
cooling_demands = []

different_grids = []

# Appends values from all grid cells of interest in the same file
for r in sample_2:
    single_grid = ds.isel(x=i[r],y=j[r],z=k[r])
    different_grids.append(single_grid)

# Creates an .xls file with all the temperature results of the
# grid cells of interest
df = xarray.concat(different_grids, dim='time').to_dataframe()
#muchas muchas <3

# Calculate heating and cooling demands
#df['Variable'][Axis: x = 0, y = 1, z = 2][Time (starting from
# zero)]
for axis in range(0,2):
    for hour in range(0, 24):
        # Q_transmission = U * A * (To - Tin)/1000 [kWh]
        energy_transmission = (Thermal_conductivity/
            Wall_thickness * Grid_area * ((df['Wall:
            Temperature Node 1/ outside (°C)'][axis][hour]) - (
            df['Building: Temperature of building (inside) (°C)
            ')[axis][hour])))/1000
        if energy_transmission < 0:
            heating_demands.append(energy_transmission)
        else:
            cooling_demands.append(energy_transmission)

```

```

for r in sample_2:
    single_grid = ds.isel(x=i[r],y=j[r],z=k[r])
    different_grids.append(single_grid)

open(Path(Output_folder_path) / "Building_results.xls", 'a+').
    close()
df.to_excel(Path(Output_folder_path) / "Building_results.xls")

Heating_Demands = abs(round(sum(heating_demands),3))
Cooling_Demands = round(sum(cooling_demands),3)
total_demands = Heating_Demands + Cooling_Demands

print("")
print("Total heating demands: " + str(Heating_Demands) + " kWh")
print("Total cooling demands: " + str(Cooling_Demands) + " kWh")
print("Total demands: " + str(total_demands) + " kWh")

HC_Demands = total_demands

"""
Get façade wind speed
"""

# Grids of interest for wind speed in South façade
i_s = [11, 12, 13, 14, 15, 16, 17, 11, 12, 13, 14, 15, 16, 17, 11,
        12, 13, 14, 15, 16, 17]
j_s = [11, 11, 11, 11, 11, 11, 11, 11, 11, 11, 11, 11, 11, 11, 11, 11,
        11, 11, 11, 11, 11, 11]
k_s = [0, 0, 0, 0, 0, 0, 0, 0, 1, 1, 1, 1, 1, 1, 1, 1, 2, 2, 2, 2, 2, 2,
        2]
lst_s = []

sample_3 = range(0,len(i_s))

wind_speed_south_data = []
single_grid = []
different_grids = []

# Appends values from all grid cells of interest in the same file
for r in sample_3:
    single_grid = ds.isel(x=i_s[r],y=j_s[r],z=k_s[r])
    #print(single_grid['Wall: Wind Speed in front of facade (m/s)
    '][0][0])
    different_grids.append(single_grid)

# Creates an .xls file with all the temperature results of the
grid cells of interest
df = xarray.concat(different_grids, dim='time').to_dataframe()
#muchas muchas <3

# Get wind speed in front of the façade
#df['Variable'][Axis: x = 0, y = 1, z = 2][Time (starting from
zero)]
for hour in range(0, 24):

```

```

wind_speed_south = df['Wall: Wind Speed in front of facade
(m/s) '][1][hour+(r*24)]
if wind_speed_south == -999:
    pass
else:
    wind_speed_south_data.append(wind_speed_south)
wind_speed_south_data

Av_wind_speed_south = sum(wind_speed_south_data)/len(
wind_speed_south_data)

print("")

print("Av wind speed south façade: " + str(Av_wind_speed_south) +
" m/s")

Av_Wind_Speed_South = round(Av_wind_speed_south,3)

# Grids of interest for wind speed in West façade
i_w = [11, 11, 11, 11, 11, 11, 11, 11, 11, 11, 11, 11, 11, 11, 11,
11, 11, 11, 11, 11]
j_w = [11, 12, 13, 14, 15, 16, 17, 11, 12, 13, 14, 15, 16, 17, 11,
12, 13, 14, 15, 16, 17]
k_w = [0, 0, 0, 0, 0, 0, 0, 1, 1, 1, 1, 1, 1, 1, 2, 2, 2, 2, 2, 2,
2]
lst_w = []

sample_4 = range(0,len(i_w))

wind_speed_west_data = []
single_grid = []
different_grids = []

# Appends values from all grid cells of interest in the same file
for r in sample_3:
    single_grid = ds.isel(x=i_w[r],y=j_w[r],z=k_w[r])
    #print(single_grid['Wall: Wind Speed in front of facade (m/s)
'][0][0])
    different_grids.append(single_grid)

# Creates an .xls file with all the temperature results of the
grid cells of interest
df = xarray.concat(different_grids , dim='time').to_dataframe()
#muchas muchas <3

# Get wind speed in front of the façade
#df['Variable '][Axis: x = 0, y = 1, z = 2][Time (starting from
zero)]
for hour in range(0, 24):
    wind_speed_west = df['Wall: Wind Speed in front of facade
(m/s) '][0][hour+(r*24)]
    if wind_speed_west == -999:
        pass
    else:
        wind_speed_west_data.append(wind_speed_west)

```

```

Av_wind_speed_west = sum(wind_speed_west_data)/len(
    wind_speed_west_data)

print("Av wind speed west façade: " + str(Av_wind_speed_west) + "
    m/s")

Av_Wind_Speed_West = round(Av_wind_speed_west,3)

print("")

# Update simulation log
log_file = "simulation_log_" + str(Log_name) + ".txt"
log_path = Path(Output_folder_path) / log_file
f = open(log_path,"a+")

f.write("Results")
f.write("\nMax Temperature: " + str(Max_Temperature) + "°C")
f.write("\nAv. Temperature: " + str(Average_Temperature) + "°C")
f.write("\nMin Temperature: " + str(Min_Temperature) + "°C")
f.write("\nHeating Demands: " + str(Heating_Demands) + "kWh")
f.write("\nCooling Demands: " + str(Cooling_Demands) + "kWh")
f.write("\nAv. Wind Speed South Façade: " + str(
    Av_Wind_Speed_South) + "m/s")
f.write("\nAv. Wind Speed West Façade: " + str(Av_Wind_Speed_West)
    + "m/s")
f.write("\n\n
    _____\n
    n\n")

f.close()

elif Run == False:
    Max_Temperature = -999
    Average_Temperature = -999
    Min_Temperature = -999
    Heating_Demands = -999
    Cooling_Demands = -999
    HC_Demands = -999
    Av_Wind_Speed_South = -999
    Av_Wind_Speed_West = -999

# Delete the PANIC file in the model path
Pnc_path = Path(Output_folder_path) / 'atmosphere'

for x in os.listdir(Pnc_path):
    if str(x).find('PANIC') != -1:
        del_pnc_file = Pnc_path / x
        if os.path.exists(del_pnc_file):
            os.remove(del_pnc_file)

num_pnc_files = sum(1 for x in Pnc_path.glob("*PANIC*"))
if num_pnc_files == 0:
    print("There are no PANIC files")
else:
    print("Check for PANIC files")

```

```
# Update simulation log
log_file = "simulation_log_" + str(Log_name) + ".txt"
log_path = Path(Output_folder_path) / log_file
f = open(log_path,"a+")

f.write("\n\nSimulation failed due to PANIC error")
f.write("\n\n
_____ \
n\n")

f.close()
```